THE ROLE OF HSP70 AND NEK6 IN CENTROSOME CLUSTERING IN CANCER CELLS

Thesis submitted for the degree of

Doctor of Philosophy

at the University of Leicester

by

Iosifina Sampson MSc (Hons) (Leicester)

Department of Molecular and Cell Biology

University of Leicester

November 2017

DECLARATION

The accompanying thesis submitted for the degree of Doctor of Philosophy, entitled "Targeting centrosome clustering pathways in human cancers" is based on work conducted by the author in the Department of Molecular and Cell Biology at the University of Leicester mainly during the period between October 2013 and July 2017. All the work recorded in this thesis is original unless otherwise acknowledged in the text or by references. None of the work has been submitted for another degree in this or any other University.

Signed:

Date:

Department of Molecular and Cell biology

University of Leicester

Lancaster Road

Leicester

LE1 9HN

TARGETING CENTROSOME CLUSTERING PATHWAYS IN HUMAN CANCERS

IOSIFINA SAMPSON

SUMMARY

Mitosis is an important process for the generation of two genetically identical daughter cells. Formation of a bipolar mitotic spindle requires the presence of two centrosomes as these are required to form each pole of the spindle. However, cancer cells, frequently possess extra centrosomes. Therefore, they have developed mechanisms to cluster them into two poles to enable mitotic pseudo-spindle formation and cell survival. Inhibiting centrosome clustering offers a unique and attractive therapeutic approach to selectively kill cells with amplified centrosomes by promoting formation of multipolar spindle poles and mitotic catastrophe. Centrosome clustering mechanisms include proteins with specific roles in microtubule dynamics, microtubule attachments to centrosomes, kinetochores and the cell cortex, as well as the spindle assembly checkpoint. Here, we identify a new pathway that contributes to centrosome clustering and involves the Nek6 kinase and Hsp72 chaperone. Nek6, as well as its upstream activators Plk1 and Aurora-A, targets Hsp72 to the poles of cells with amplified centrosomes. Blocking Hsp72 or Nek6 activity leads to formation of multipolar spindles with poles that always contain centrosomes, whereas other centrosome de-clustering agents trigger formation of acentrosomal poles. Indeed, inhibition of Hsp72 in ALL cells led to an increase of multipolar spindle frequency that correlated with centrosome amplification. Dynein/dynactin and phospho-Hsp72 colocalise to kinetochores and we suggest that they are required for proper attachment of microtubules to kinetochores to facilitate a stable bipolar mitotic spindle and potentially centrosome clustering. Additionally, loss of Hsp72 or Nek6 function did not disrupt either mitotic spindle formation or mitotic progression in non-cancer derived cells versus cancer cells. Hence, the Nek6-Hsp72 pathway, and its potential downstream target dynein, may act as a novel pathway of centrosome clustering that reveals a new opportunity for targeting centrosome clustering and mitotic progression in cancer cells.

ACKNOLEDGEMENTS

First and foremost, I would like to thank my supervisor Prof. Andrew Fry for giving me the opportunity to work on this project and in his laboratory. He was always there when I needed support and his advices were very helpful throughout my project. I was always amazed by his enthusiasm and extended knowledge into this work, which were true inspiration to me to complete my PhD and made me become a “fan” of centrosome research.! I would also like to thank my co-supervisors Prof. Martin Dyer and Prof. Richard Bayliss for their useful suggestions and discussions. Many thanks to my committee members Dr. Salvador Macip and Dr. Ildiko Gyory for their useful discussion and advises throughout my project. I would like to thank my sponsors Hope Against Cancer and the Medical Research Council (MRC) whose grants made my work possible.

A big thank also to Dr. Kees Straatman for all of his support and guidance with the microscope imaging facility. I wish to say a big thank you to Dr. Sandrine Jayne and Dr. Ildiko Gyory who kindly provided me with acute lymphoblastic leukemic cell lines. Of course, a massive thank you to all the past and present members of the Fry lab, who have been very supportive and helpful throughout my project. To my lab buddies and friends, Karolin, Sarah, Rozi, Tammy, Jess, Anita and Sukrat, who lab life would not be fun and entertaining without them and mostly for their big support and encouragement that they gave me throughout my project.

And last big thank you to all of my friends in Leicester and Cyprus for their extra support and stress relief that they gave me, especially Yiota, Giannis, Theodosia, Charis and Styliana. A big thank you to a special person, Michele, who believed in me and supported me, especially the last couple of months of my PhD. Last but not least, an enormous thank you goes to my family for supporting me all of these years even miles away from home.!

CONTENTS

Chapter 2 Materials and Methods

ABBREVIATIONS

aa	amino acid
ab	antibody
A	Absorbance
ALL	Acute lymphoblastic leukaemia
AML	Acute myeloid leukaemia
APC/C	Anaphase promoting complex/cyclosome
APS	Ammonium persulfate
BL	Burkitt's lymphoma
BI-2536	Polo like kinase 1 inhibitor
BSA	Bovine serum albumin
Cdk	Cyclin-dependent kinase
CIN	Chromosomal instability
CKI	Cdk inhibitor
CLL	Chronic lymphocytic leukaemia
CML	Chronic myeloid leukaemia
CO_2	Carbon dioxide
DCIS	Ductal carcinoma *in-situ*
DDR	DNA damage response
DLCBCL	Diffuse large B-cell lymphoma
DMEM	Dulbecco's Modified Eagle's Media
DMSO	dimethylsulfoxide

DNA	deoxyribonucleic acid
EDTA	ethylene diamine tetraacetic acid
EGTA	ethylene glycol tetraacetic acid
FACS	fluorescence-activated cell sorting
FBS	foetal bovine serum
FL	Follicular lymphoma
γ-TuRC	γ -tubulin ring complex
GFP	Green fluorescent protein
GF	Griseofulvin
HBL-100	Human breast milk cell line
HeLa	Human cervix adenocarcinoma cell line
HNSCC	Head and neck squamous cell carcinomas
HPV	Human papillomavirus
Hrs	Hours
HRP	horseradish peroxidase
HSP	Heat shock protein
hTERT-RPE1	telomerase-immunortalized human retinal pigment epithelial
IF	Immunofluorescence microscopy
IFT	Intraflagellar transport
IDC	Invasive ductal carcinoma
IP	Immunoprecipitation
IHC	Immunohistochemistry
kDa	kilo Daltons

LSCM	Laser scanning confocal microscope
M	Molar
MAP	Microtubule associate protein
MCL	Mantle cell lymphoma
μg	micro-gram
μl	micro-litre
μM	micro-molar
μm	micro-meter
μl	microliter
mg	milli-gram
ml	milli-litre
mM	milli-molar
mRNA	messenger ribonucleic acid
MDA-MB-231	human breast adenocarcinoma cell line
MLN-8054	Aurora-A inhibitor
MMP-2	Matrix metalloproteinase-2
MT	microtubule
MTOC	microtubule organising center
MS	Mass spectrometry
min	minutes
ng	nano-gram
nM	nano-molar
nm	nano-meter

MZBCL	Marginal zone B-cell lymphoma
N-	amino
Nek	NIMA-related kinase
NIE-115	mouse neuroblastoma cell line
NIMA	never in mitosis A
NP-40	nonidet P-40
Noc	nocodazole
OD_{650}	Optimal Density (absorbance) at 650 nm
PBL	Primary B-lymphocytes
PBS	phosphate buffered saline
PCM	pericentriolar material
Pen/Strep	penicillin/streptomycin
pH3	phospho-histone H3
Plk	Polo-like kinase
PI	propidium iodide
PIC	Protease inhibitor cocktail
PKD	Polycystic kidney disease
Rb	Retinoblastoma protein
RIPA	RadioImmuno Precipitation Assay Buffer
RNA	ribonucleic acid
RNAi	RNA interference
ROI	Region of interest
rpm	revolutions per minute

SAC	spindle assembly checkpoint
SD	standard deviation
SDS	sodium dodecyl sulfate
siRNA	small interfering RNA
SPB	spindle pole body
TEMED	N, N, N, N,-tetramethylethyleneediamine
TBS	tris-buffered saline
Tris	Tris (hydroxymethyl) aminomethane
v/v	volume per volume ratio
V	Volts
VER-155008	Adenosine-derived inhibitor of Heat Shock protein 70
w/v	weight per volume ratio
U	Unit
UPS	Ubiquitin-proteasome system
UV	Ultraviolet
WT	wild-type

TABLES AND FIGURES

Chapter 1

Introduction

1.1 Cell cycle control

1.1.1 Cell cycle phases and mitosis

The cell cycle is separated into four phases: Gap1 (G_1), Synthesis (S), Gap2 (G_2) and the mitotic phase (M). In an additional fifth phase, known as quiescense (G_0), cells exit the cell cycle and remain in a resting phase due to lack of growth factors or differentiation (Schafer, 1998). During G_1, S and G_2 phases, the cell grows and prepares for mitosis. The G_1, S and G_2 phases are together known as interphase. Specifically, in G_1 phase, the cell prepares for DNA replication by synthesising proteins and organelles. At this stage, the cell determines whether its intracellular and extracellular environment is suitable to proceed for cell division. If the conditions are appropriate, the cell passes the restriction point (R point) and enters into S phase, in which each chromosome is precisely duplicated generating a pair of identical copy, known as sister chromatids. DNA replication is followed by a continuing period of cell growth and synthesis of proteins essential for mitosis in a stage known as G_2. Finally, the cell with duplicated DNA enters the stage to generate two identical daughter cells, known as M-phase (Nigg, 2001) (Figure 1.1).

The M-phase is composed of two main events, mitosis and cytokinesis. Mitosis is a fundamental process that ensures the equal segregation of duplicated sister chromatids into two identical daughter cells. Mitosis is divided into 5 distinct stages: prophase, prometaphase, metaphase, anaphase and telophase (Figure 1.2). At the beginning of mitosis, the cell enters a stage called prophase during which sister chromatids are organized into highly condensed structures for their later separation. At this time, the cell already has duplicated centrosomes, microtubule organising centres (MTOC), from where microtubules are nucleated for the formation of the mitotic spindle. At prometaphase, the mitotic spindle begins to form, the nuclear envelope collapses and microtubules capture chromosomes at specialised structures called kinetochores. During metaphase, microtubules from opposite spindle poles attach to chromosomes and as a result of bi-polar tension these align on the metaphase plate.

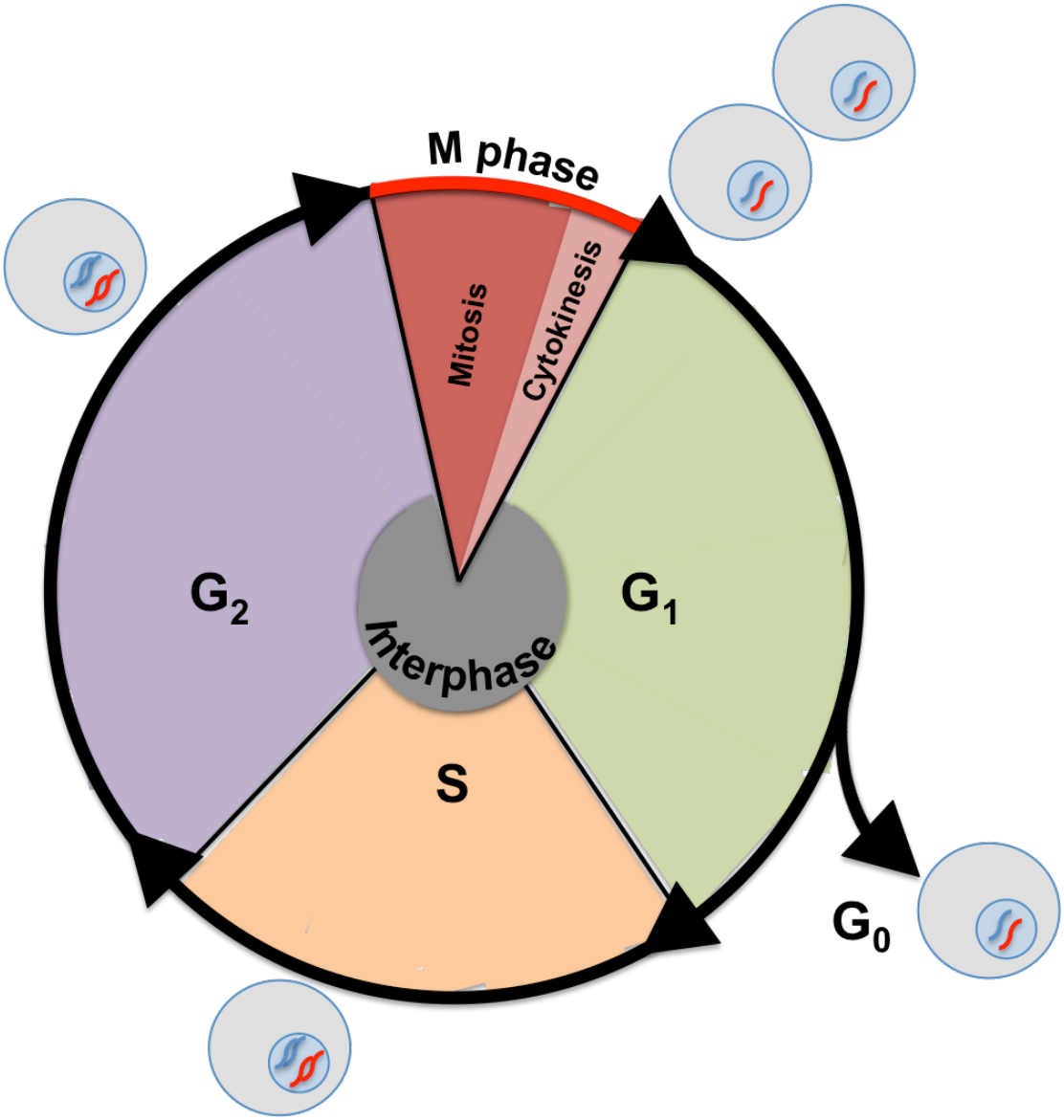

Figure 1.1 The eukaryotic cell cycle

The eukaryotic cell cycle is divided into interphase and M-phase. Interphase consists of growth stages (G_1 and G_2) and a DNA replication as "synthesis" stage (S). M-phase is composed of mitosis and cytokinesis, where two identical daughter cells are generated. Absence of growth factors cause cells to exit the cell cycle into an extra stage, G_0 (quiescence). The cartoon shows an identical typloid cell with two copies of a single chromosome. Adapted from Nigg (2001).

At anaphase, the sister chromatids are pulled apart by the microtubules to either ends of the cell. At telophase, the nuclear envelope re-forms and chromosomes de-condense and soon after, the cytoplasm is divided in a process called cytokinesis (Janssen and Medema, 2011). A contractile ring is a characteristic feature of cytokinesis; this is made of myosin and actin proteins, and pinches the two cells apart through constriction of the plasma membrane (Figure 1.2).

1.1.2 Cell cycle checkpoints

In all stages of the cell cycle, essential checkpoint pathways ensure conditions are appropriate before entry to the next stage and a number of proteins are implicated in those checkpoints. Importantly, checkpoint proteins are frequently mutated in various cancers allowing abnormal proliferation and accumulation of DNA damage (Nigg, 2001). It is not surprising then that checkpoint proteins are attractive targets for cancer therapy in combination with more traditional therapies, such as chemotherapy and radiotherapy.

There are five main checkpoints in the cell cycle: midway through $G_{1,}$ at the G_1/S transition, S-phase, G_2/M transition and during mitosis (Nurse, 2000). In G_1 phase, the extracellular and intracellular environments are monitored to decide whether the cell should itself continue the cell cycle or enter into G_0 (quiescence) phase. This point is known as the restriction (R) point in animal cells. Signals for progression past the R-point induce expression of cyclin D and reduce expression of p16. This activates Cdk4 and Cdk6 proteins, which in turn phosphorylate the retinoblastoma (Rb) tumour suppressor protein. The non-phosphorylated Rb binds and inhibits the activity of E2F transcription factors, HDACs and chromatin remodelling factors and thus, preventing progression into S-phase. However, in the presence of mitogenic signals, the phosphorylated Rb dissociates from E2F factors allowing transcription of genes important for cell cycle progression, including cyclin E and A (Cobrinik, 2005; Malumbres and Barbacid, 2005).

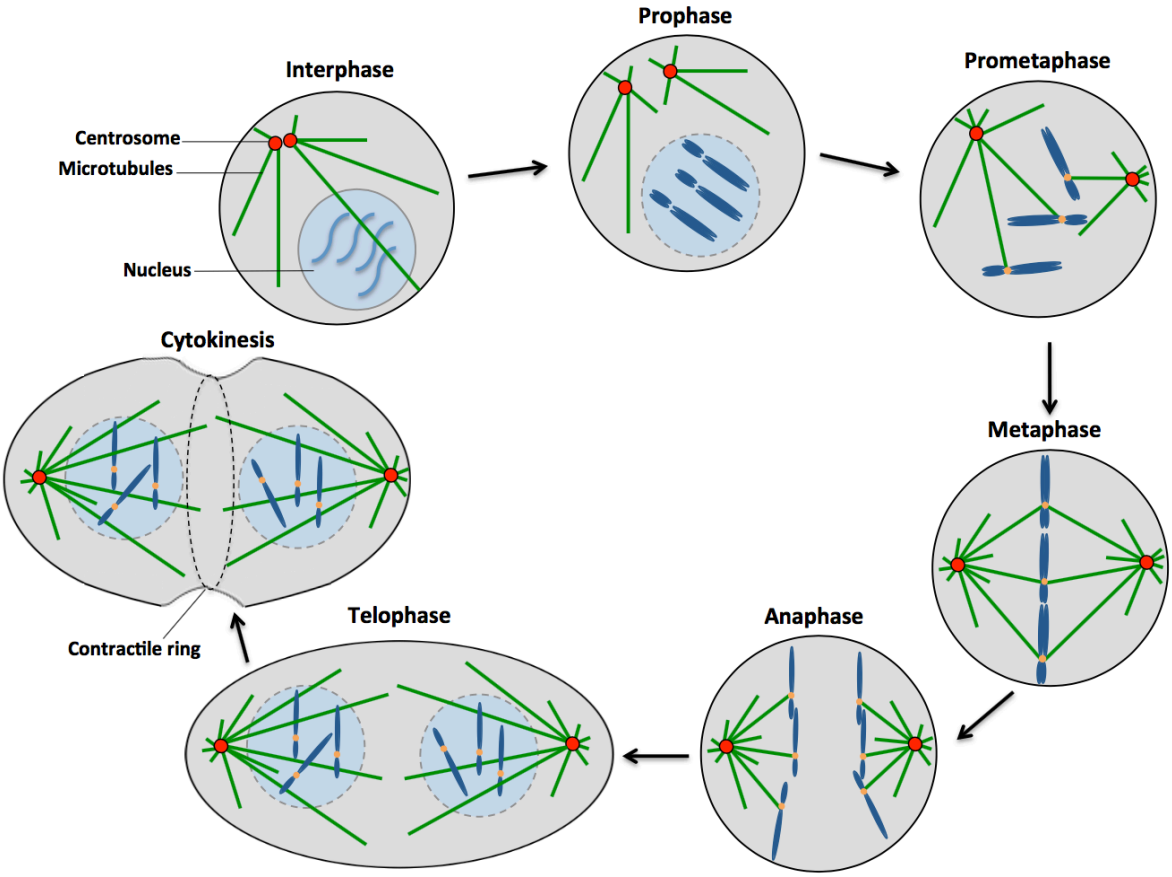

Figure 1.2 The stages of M-phase

The M-phase consists of mitosis and cytokinesis. Mitosis is composed of different stages known as prophase, prometaphase, metaphase, anaphase and telophase. At the end of mitosis, the cytoplasm is divided by forming a contractile ring generating two identical daughter cells in a separate process known as cytokinesis. Adapted from Walczak et al (2010).

At the beginning of S phase, DNA replication is initiated by activation of Ckd2/cyclin E complex. Once DNA replication begins, the levels of cyclin E are significantly reduced leading to inactivation of the Ckd2/cylcin E complex to prevent re-replication of DNA (Hwang & Clurman, 2005). Once the cell goes into S phase, activation of Cdk2/cyclin A reinforces the inactivation by phosphorylation of pRb, as well as phosphorylating proteins important for initiating DNA replication (Hwang and Clurman, 2005). Ckd1/cyclin A is also important for completion of S-phase and entry into G_2 phase (Figure 1.3). The presence of DNA damage or stalled replication forks activates the DNA damage response (DDR) to deal with these errors. DDR involves a series of cellular events, including proteins that act as sensors of DNA damage followed by activation and amplification of signals that will cause a range of responses such as cell cycle arrest, transcription initiation, DNA repair and apoptosis (Jackson & Bartek, 2009). At G1/S transition, cells rely on p53-p21 pathway that prevents initation of DNA replication. In the presense of genotoxic insult, ATM/ATR (ataxia telangiectasia) and Chk1/Chk2 kinases are activated and phosphorylate p53, which in turn, it leads to transcription of p21 that leads to inactivation of Cdk2/cyclin E complex resulting to cell cycle arrest (Figure 1.3) (Deckbar et al., 2010; el-Deiry et al., 1993). In response to the intra-S DNA damage checkpoint, the ATM/ATR phosphorylates and activates Chk1 kinase, reduces the levels of Cdc25A protein and thus, keeping Cdk2/cyclinA inactive (Deckbar et al., 2011).

In late G_2, accumulation of cyclin B promotes activation of Cdk1 leading to entry into mitosis. The activation state of Cdk1/cyclin B is controlled by a number of proteins, including the Cdk-activating kinase (CAK) that phosphorylates Cdk1 at Thr161. However, the Cdk1/cyclin B complex remains inactive at this time due to phosphorylation of Thr14 and Tyr15 by Myt1 and Wee1 kinases. Once a cell has checked that it has error-free DNA and completed DNA replication, those inhibitory phosphate groups are removed by Cdc25 allowing entry into mitosis (Figure 1.3) (Cobrinik, 2005).

After the cell enters mitosis, there is one other checkpoint that plays an important role to ensure the proper segregation of sister chromatids. The spindle assembly checkpoint

(SAC) blocks the metaphase to anaphase transition until proper bipolar attachment of microtubules to kinetochores of all sister chromatids has been achieved thereby ensuring error-free segregation in anaphase (Musacchio, 2015; Janssen and Medema, 2011). Key players of the SAC include Bub1, Bub3, Mps1, Mad1, Mad2 and BubR1. These SAC proteins are localised to unattached kinetochores during prometaphase and monitor attachment of microtubules to kinetochores before allowing sister chromatid segregation. The mechanism through which the SAC operates is to control the activity of the APC/C (anaphase-promoting complex/cyclosome), an E3 ubiquitin ligase. Specifically, upon bipolar attachment of microtubules to kinetochores during metaphase, the SAC is inactivated leading to APC/C activation, which in turn leads to degradation of cyclin B and securin. These promote mitotic exit and sister chromatid separation, respectively (Musacchio, 2015). Hence, the SAC is fundamental for the fidelity of chromatid segregation during mitosis, and maintenance of genome stability.

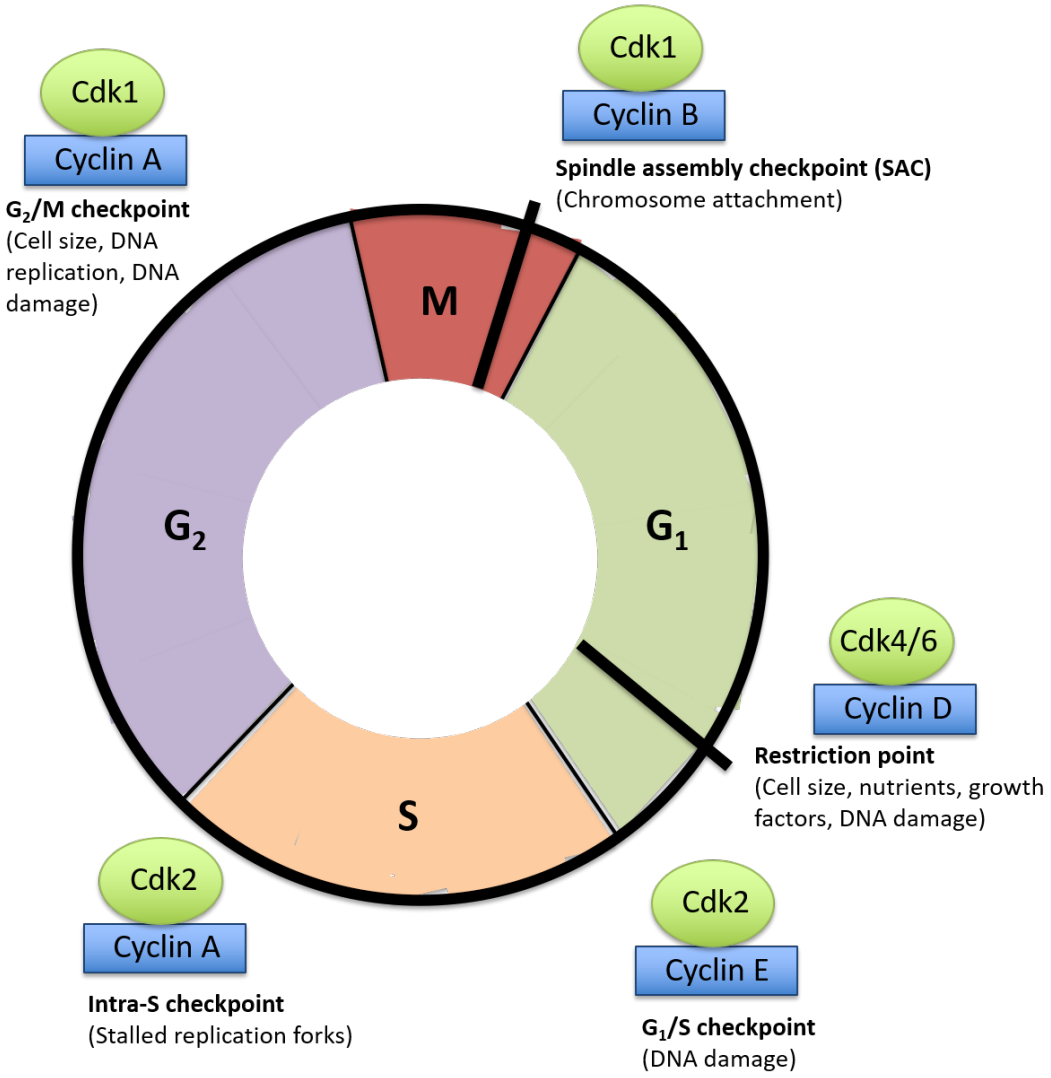

Figure 1.3 Cell cycle checkpoints

Cell cycle progression is heavily depended on the activity of cyclin-dependent kinases (Cdks) and cyclins. In each stage of cell cycle, a heterodimer of Cdk/cyclin has key roles in cell cycle progression. At G_1 phase, phosphorylation of Rb by Cdk4/6-cyclin D allows progression of the R-point in the presence of mitogenic signals. At G_1-S transition, Cdk2/cyclin A and cyclin E monitor errors in DNA replication. Cdk1/cyclin A control completion of S-phase and entry into G_2 phase. Cdk1/cyclin B activity allows entry into mitosis. Adapted from Gabrielli et al (2012).

1.2 Microtubule organizing centres

Microtubules are essential structures required for many cellular processes, including organelle positioning and trafficking, cell shape, cell polarity and mobility, and cell division (Meunier and Vernos, 2012). They are highly dynamic structures formed by α- and β-tubulin heterodimers that are assembled head to tail fashion into a protofilament structure (Akhmanova and Steinmetz, 2015). Microtubule structure is formed by the lateral assembly of thirteen protofilaments generating a hollow cylindrical structure of ~25 nm in diameter. As the cell enters into mitosis, microtubule arrays undergo distinct reorganisation, in such way as to form the spindle apparatus.

In animal cells, microtubules tend to be nucleated mainly from a small number of sites, known as microtubule organising centres (MTOCs). The centrosome is the primary MTOC in dividing animal cells. It consists of a pair of centrioles surrounded by an ordered assembly of proteins, known as the pericentriolar material (PCM). In yeast, the primary MTOC is a multi-layered disc-like structure embedded in the nuclear envelope, known as the spindle pole body (SPB) (Jaspersen and Winey, 2004). On the other hand, plant cells have no centrosomes or SPB, but principally nucleate microtubule arrays from the cell cortex (Murata et al., 2007). Hence, there are different types of MTOC in different organisms. However, many individual protein components important for microtubule nucleation, such as γ-tubulin, are conserved in eukaryotic cells.

1.2.1 The centrosome

In the majority of animal cells, centrosomes are the major microtubule organizing centres. The centrosome is an organelle of approximately 1 μm in diameter that consists of a pair of centrioles surrounded by pericentriolar matrix material (PCM), a matrix rich in proteins that contribute to microtubule nucleation (Figure 1.4A) (Bornens, 2012). Centrosomes dictate the microtubule array structure necessary for bipolar spindle formation during cell division, as well as cell motility, polarity and shape (Conduit et al.,

2015). A number of small granules, known as centriolar satellites, associate more peripherally with centrosomes and contain various proteins that have roles in centrosome maintenance (Tollenaere et al., 2015). However, the precise functions of centriolar satellites and how they are organised are not yet understood.

Centrioles are short barrel-shaped cylinders, approximately 400-450 nm long and 150-200 nm in diameter, of nine triplet microtubules organised into a pinwheel structure (Paintrand et al., 1992; Bornens, 2012). The two centrioles are not identical. The older one is referred to as the ‘‘mother’’ centriole and is characterised by distinctive distal and subdistal appendages, which are missing in the younger ‘‘daughter’’ centriole (Paintrand et al., 1992; Nigg and Stearns, 2011). The two centrioles are held in close proximity in interphase by a physical inter-centriolar linker that extends between the proximal ends. This linker consists of various proteins, including C-Nap1/Cep250, rootletin, Cep68, centlein, LRRC45 and β-catenin (Bahe et al., 2005; Bahmanyar et al., 2008; Fry et al., 1998a; Fang et al., 2014; Graser et al., 2007b; Yang et al., 2006; He et al., 2013). Proteins, such as ninein and dynactin, localise to the mother centriole appendages and are important for microtubule anchoring (Doxsey, 2001).

The PCM is one of the main functional parts of the centrosome as it organises and nucleates microtubules. However, this matrix also contains various proteins involved in cell signalling and cell cycle regulation (Alves-Cruzeiro et al., 2014; Arquint et al., 2014). It was previously thought that the PCM is an amorphous cloud of proteins, however, recent super-resolution microscopy analysis has revealed a structural order to the PCM that provides a better understanding of how microtubule nucleation is regulated and how proteins contribute to this process. The PCM is assembled into distinct layers, with the proximal layer consisting of pericentrin and Cep152 filament proteins that are closely attached to the centriole, as well as a population of Cdk5Rap2 and Cep192 proteins (Woodruff et al., 2014; Mennella et al., 2014). A second population of Cep192 and Cdk5Rap2 are present further out in the PCM proximal layer (Sonnen et al., 2013). These PCM proteins anchor to γ-TuRCs, which in turn, organise tubulin polymerisation and formation of microtubules (Kollman et al., 2011). Additionally, many of the proximal layer PCM components, including Cep152, pericentrin and Cdk5Rap2, as well as ch-TOG

and TPX2 proteins, can directly bind to α/β-tubulin dimers and contribute to microtubule nucleation independent of γ-tubulin (Woodruff et al., 2017). During mitosis, the PCM is expanded in size through recruitment of additional PCM components, including pericentrin, Cdk5Rap and Cep192. This recruitment is heavily depended on phosphorylation by the Plk1 kinase, in a process known as centrosome maturation (Figure 1.4B) (Lee et al., 2011; Woodruff et al., 2015).

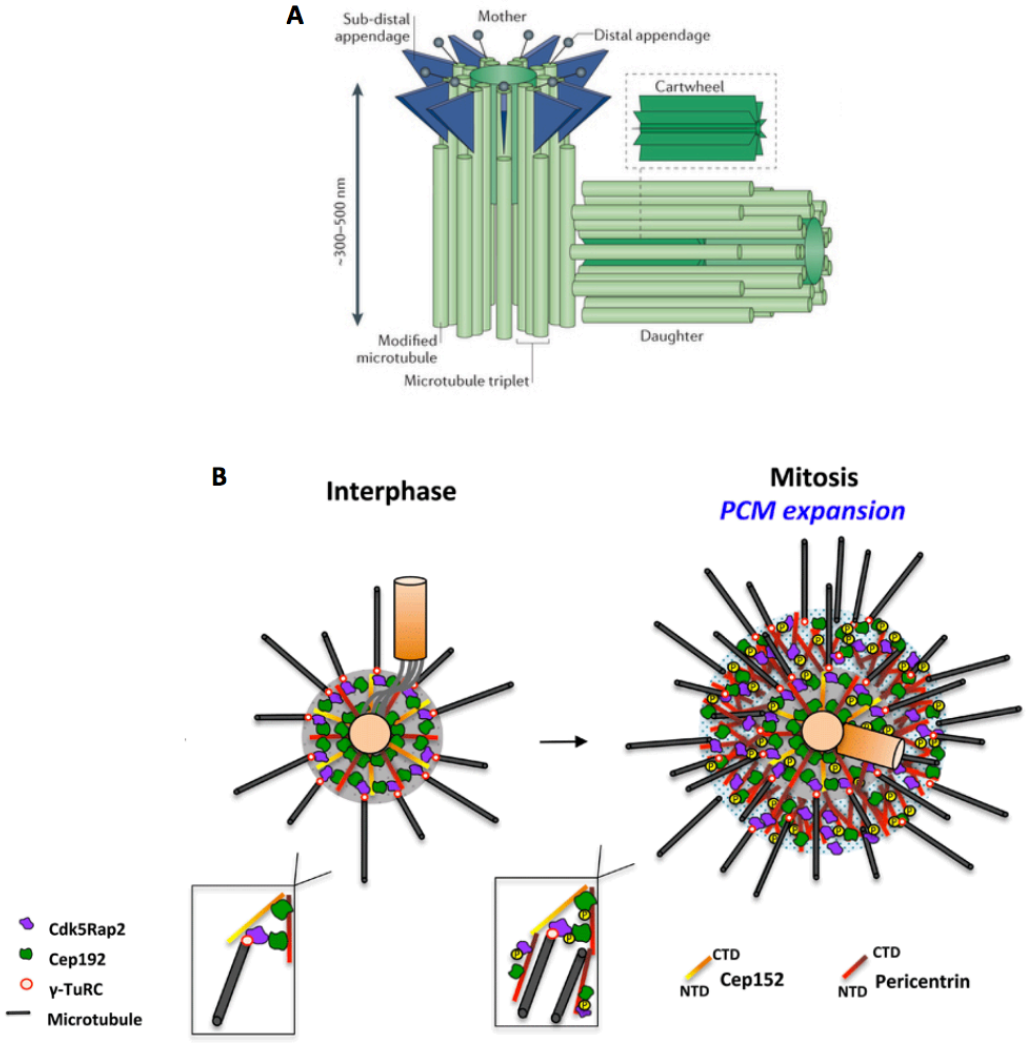

Figure 1.4 The structure of the centrosome

The centrosome consists of a pair of centrioles, the ‘‘mother’’ and ‘‘daughter’’, and the pericentriolar material (PCM). **A.** In most vertebrate cells, each centriole comprises of nine triplet microtubules that form a central cartwheel structure. The mother centriole is decorated with distal and sub-distal appendages, whilst these are missing in the daughter. Adapted from Conduit et al (2015). **B.** The organization of PCM in interphase and mitosis. During interphase, the two centrioles are linked at their proximal ends by a fibrous linker while the two filament proteins, pericentrin and Cep152, generate a proximal layer of the PCM. This layer also contains other proteins, including Ckd5Rap2 and Cep192, which create a matrix for recruitment of γ-TuRCs. A second Cep192 population is concentrated at the centriole surface. In mitosis, phosphorylation of various PCM components expands the PCM creating an outer layer that in turn increases the number of γ-TuRCs to allow increased microtubule nucleation. From Fry et al (2017).

1.2.2 The role of the centrosome in spindle assembly

In most animal cells, one of the major functions of the centrosome is to act as a microtubule organising centre (MTOC) during mitosis. Microtubules are principally nucleated from centrosomes, specifically from the γ-tubulin ring complexes (γ-TuRC). In contrast, higher plant cells and oocytes of many animals are able to form mitotic spindles without centrosomes (Rappaport, 1961; Dumont and Desai, 2012). Experimentally, it was observed that somatic cells were able to form functional bipolar spindles even after removal of centrosomes by microsurgery (Khodjakov and Rieder, 2001). The absence of centrioles due to mutations in *Drosophila* and *Chlamydomonas* species had no affect on cell viability (Basto et al., 2006). Similarly, *Xenopus laevis* egg extracts lacking centrosomes were able to assemble mitotic spindles around DNA-coated beads (Heald et al., 1996). Although centrioles are not necessary during oogenesis, centriolar and PCM components still remain in the cytoplasm of oocytes (Manahdhar et al., 2005). Meanwhile, in some invertebrates, such as the planarian flatworm *Schmidtea mediterranea*, centrioles contribute to cilia formation to achieve motility, but are not present in cells involved in development of its head, tail and gut (Azimzadeh et al., 2012). Hence, it became clear that cells with or without centrosomes are able to form bipolar spindles, suggesting that centrosomes are not the only key drivers in this process.

Several other non-centrosomal related pathways and molecular motors cooperate to nucleate and stabilize microtubules during mitosis. For example, the chromatin-mediated microtubule nucleation pathway allows assembly of microtubules around chromatin in mitosis (Karsenti and Vernos, 2001). RCC1, a chromatin-bound nucleotide-exchange factor for Ran, concentrates RanGTP around chromosomes, which in turn promotes formation of microtubules by displaying imports from spindle-associated factors, such as TPX2 (Gruss and Vernos, 2004). The augmin complex pathway also contributes to formation of new microtubules without the need of centrosomes. Specifically, this pathway allows nucleation of microtubules from pre-existing microtubules (Goshima et al., 2008; Goshima and Kimura, 2010). Additionally, acentriolar MTOC nucleation of microtubules can occur, in which some PCM

components form foci without centrioles but retain the ability to microtubules (Kleylein-Sohn et al., 2012; Baumbach et al., 2015). All these mechanisms can act in the presence of centrosomes thereby enhancing spindle assembly during mitosis.

1.2.3 The role of the centrosome in cilia and flagella formation

Cilia and flagella are slim antennae-like microtubule-based organelles that project out from the plasma membrane of vertebrate cells. Cilia are dynamic organelles made from an insoluble microtubule based structure called the axoneme. They assemble when cells enter quiescence (G_0) where the centriole pair moves to the cell surface. Cilia are directly nucleated from the basal body of the mother centriole, while at the same time remain tethered to the daughter centriole (Beisson and Wright, 2003). Cilia are divided into two categories: primary and motile cilia. Most mammalian cell types have primary cilia, which exists as a single copy organelle that develops from the mother centriole (Goetz and Anderson, 2010). In contrast, motile cilia are found in multiple copies on the epithelial surfaces of the trachea and oviduct; their rhythimic beating pattern moves fluid over their surface (Ishikawa and Marshall, 2011). Flagella are mainly present on sperm and single-celled protista.

Ciliogenesis is the process in which cell generates a cilium. It involves migration of the centriole pair to the cell surface where they are converted to basal bodies, elongation of the ciliary axoneme with the aid of intraflagellar transport (IFT), and generation of accessory structures that help anchor the basal bodies and create a gated barrier to the cilium (Ishikawa and Marshall, 2011). IFT is an important process for cilia formation that controls the transport of various ciliary proteins between the ciliary base and tip via anterograde and retrograde transport along the microtubule axoneme (Hao and Scholey, 2009). A number of microtubule motors are involved in IFT, including kinesin-2 and cytoplasmic dynein 2 (Signor et al., 1999; Hou et al., 2004; Evans et al., 2006). This type of movement contributes to cilia morphology and function, as well maintaining cilia length.

Cilia have a wide range of functions as they are important not only for motility, but also for development and sensory perception. Importantly, motile cilia aid the movement of eggs along oviducts, clear the mucus out of airways and contribute to embryo development by controlling left-right asymmetry of the viscera (Nonaka et al., 1998; Ishikawa and Marshall, 2011). Motile flagella are also essential for sperm movement. However, the ciliary membrane is also rich in receptors and channels allowing it to act as a chemical and mechanical sensor. For example, in the kidney, cilia are able to sense the flow of urine modulating morphogenesis of the duct (Berbari et al., 2009), while more generally cilia control hedgehog signalling contributing to skeletal development in the embryo (Huangfu et al., 2003).

The wide range of ciliary functions makes this organelle very important in multicellular as well as single celled organisms and it is not surprising that a range of human diseases, collectively known as ciliopathies, are strongly associated with defective cilia (Nigg and Raff, 2009). Abnormal ciliary functions have a major impact on many organs of the body, such as cartilage and bone development with polydactyly common in patients with Bardet-Biedl syndrome (BBS) and Meckel syndrome (Toriello and Parisi, 2009). Cilia loss also causes ataxia due to cerebellar hypoplasia in patients with a Joubert syndrome-like disorder (Brancati et al., 2009), and infertility in patients with ciliopathies due to abnormal sperm flagella and motile oviduct cilia (Mykytyn et al., 2004). Additionally, cilia abnormalities are strongly associated with cyst formation in the kidneys, liver, biliary duct and pancreas (Nishio et al., 2010). Defects in cilia sensory functions give rise to inherited forms of polycystic kidney disease (PKD) and nephronophthisis (Sun et al., 2004).

1.2.4 The centrosome cycle

The centrosome cycle describes the series of structural and numerical changes that occur at the centrosome during the cell cycle. Centrosomes duplicate once every cell cycle; this occurs in parallel with DNA replication during S phase such that only cells containing accurately duplicated DNA and two centrosomes enter into mitosis (Nigg and

Stearns, 2011). The centrosome cycle is characterised by four major stages: centriole disengagement, centriole duplication, centrosome disjunction and centrosome maturation (Figure 1.5). Each step of the centrosome cycle is tightly controlled by multiple enzymes, including Nek2, Plk1, Plk4 and Aurora-A (Table 1.1) (Nigg and Stearns, 2011). In metaphase, each spindle pole contains a pair of centrioles that are in a close perpedicular association. However, by the end of mitosis, this association between the two centrioles is lost (Nigg and Stearns, 2011). This loss of the orthogonal, perpendicular arrangement of the centriole pair is known as centriole disengagement and acts a licensing step for centriole duplication in the subsequent cell cycle. Nevertheless, during G_1 phase, the centriole pair remains more loosely connected by an intercentriolar linkage that is assembled in early G_1. Now the centrioles are found approximately 1-2 µm apart and form their own pericentriolar material. At the G_1 to S transition, centriole duplication begins as procentrioles begin to form in a perpendicular manner at the proximal ends of the two existing centrioles, a process which is under the control of Plk4 kinase (Puklowski et al., 2011). Procentrioles elongate throughout S and G_2 phase; reaching full-length around the start of mitosis (Schmidt et al., 2009; Azimzadeh et al., 2009; Singla et al., 2010). In late G_2 phase, centrosome maturation occurs, in which several PCM proteins, including Cep152, Cep192, pericentrin and Cdk5Rap2 are recruited to enrich PCM capacity and anchor additional γ-TuRCs for enhanced microtubule nucleation once the cell enters mitosis (Table 1.1) (Conduit et al., 2015).

Throughout interphase, the two parental centrioles remain connected via the intercentriolar linker enabling the centrosome to function as a single MTOC. Proteins, such as C-Nap1, rootletin, Cdk5Rap2 and Cep68 are components of this linker (Mayor et al., 2000; Graser et al., 2007b). In late G_2, at the same time as centrosome maturation, the Nek2 kinase phosphorylates C-Nap1 and rootletin components to promote disassembly of the linker; this separate process is termed centrosome disjunction (Fry et al., 1998a; Fry et al., 1998b; Helps et al., 2000). Subsequently, microtubule based motor proteins, such as Eg5, complete the separation of the two centriole pairs allowing formation of spindle poles (Bertan et al., 2011; Mardin et al., 2011).

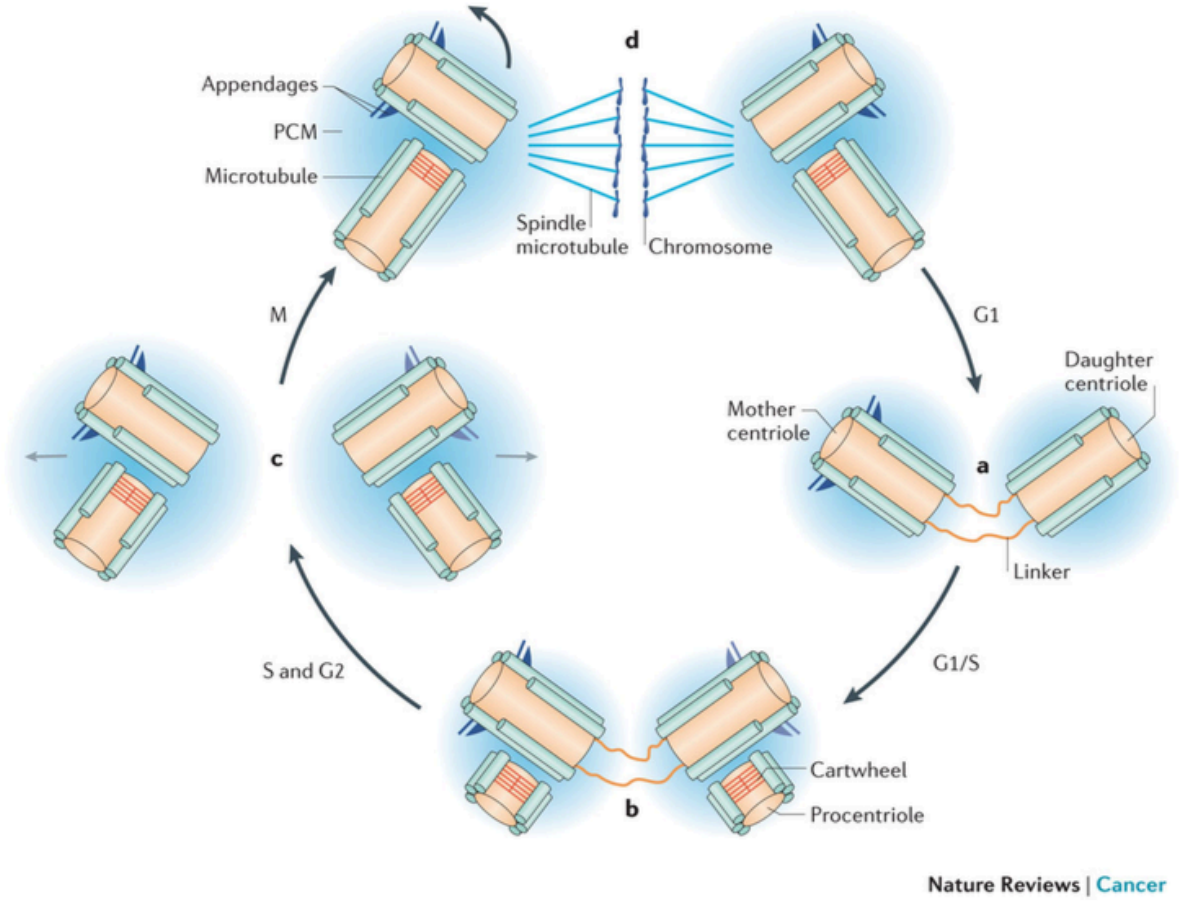

Figure 1.5 The centrosome cycle

The centrosome cycle consists of four stages. **a.** During G_1 phase, centrioles are loosely connected by an inter-centriolar linker and each one recruits its own pericentriolar material (blue shading). **b.** During S phase, procentrioles start to form at the proximal ends of each existing centriole in a process known as centriole duplication. These procentrioles are elongated during S and G_2 phases. **c.** In late G_2 phase, centrosomes undergo maturation and the PCM is expanded. The intercentriolar linker is also removed and the two centrosomes complete the process of disjunction. **d.** In mitosis, the duplicated centrosomes separate to form the two poles of the bipolar spindle. From Gonczy (2015).

Centrosome proteins	Centrosomal function
PLK4/SAK	The master regulator of centriole duplication (Bettencourt-Dias et al., 2005; Habedanck et al., 2005)
SAS6	Protein involved in the symmetry of the 9-fold cartwheel of the procentriole and required at the early stages of duplication (Leidel et al., 2005; Kitagawa et al., 2011)
SAS4/CPAP	Centrosome protein important to attach microtubules to centrioles after their assembly (Pelletier et al., 2006)
SAS5/Ana2/STIL	Centriolar proteins required at early stages of centriole duplication. Interacts with SAS6 and SAS4 (Goshima et al., 2007; Arquint et al., 2012)
ASL/CEP152	Centriole protein important for centriole duplication and PCM recruitment (Blachon et al., 2008; Hatch et al., 2010)
CEP192	PCM protein that regulates function and formation of mitotic spindle. Recruits other centrosomal proteins and stimulates nucleation of microtubules (Gomez-Ferreria et al., 2007)
CP110	Centrosomal protein that controls length of procentrioles, localises to the distal end of the procentriole (Kleylein-Sohn et al., 2007; Chen et al., 2002)
Nek2	Centrosomal kinase that regulates centrosome separation and the establishment of mitotic spindle (Fry et al., 1998).
CDK5Rap2	PCM protein required for centrosome cohesion and anchorage to mitotic spindle (Barr et al., 2010; Lucas and Raff, 2007)
PCNT/PLP	PCM protein that maintains the integrity of the poles of the mitotic spindle (Rauch et al., 2008)

Table 1.1 Centrosomal proteins and their functions

The table highlights the function of few of the key proteins involved in centriole duplication and spindle pole integrity. Adapted from Marthiens et al (2012).

1.3 Centrosome defects in cancer

In the majority of animal cells, centrosomes have fundamental roles in many different cellular processes and through its function in assembly of the primary cilium, it also contribute to signalling and motility, and tissue development. It has been long debated whether centrosome functions are essential for mitosis with studies in *Drosophila* and vertebrate DT40 cells showing that centrosome absence leads to chromosome instability and aneuploidy (Sir et al., 2013; Debec, 1978). Hence, it is not suprising that abnormalities in centrosome structure or function lead to diverse diseases, including cancer. Centrosome defects are strongly associated with tumour progression. Centrosome aberrations have been identified in several human cancers, such as breast, prostate, colon and ovarian (Pihan et al., 1998; Lingle et al., 1998; Hsu et al., 2005; Chan, 2011).

1.3.1 Numerical centrosome defects

The most common centrosome abnormality detected in human cancers is numerical defects with the presence of extra centrosomes, more than two, usually referred to as centrosome amplification. It was over a century ago when Boveri first proposed the presence of extra centrosomes in cancer. Boveri also reported that dispermic eggs possessing extra centrosomes form multipolar spindles and generate aneuploid progeny (Boveri, 2008). However, for many years, researchers were sceptical about whether centrosome abnormalities might contribute to cancer progression. A key study by Fukasawa et al. (1996) reawakened the defects which they identified centrosome amplification upon loss of the tumour suppressor p53 in cancer cells. Since then, extensive studies have identified and verified the presence of extra centrosomes using a range of antibodies to detect centriolar and pericentriolar components.

Extensive studies have identified a number of mechanisms important for the origins of centrosome amplification in cancer cells. These include errors in centriole duplication,

failure of cytokinesis, *de novo* centriole assembly and cell-cell fusion (Godinho and Pellman, 2014). A number of oncogenes and tumours suppressor proteins are implicated in those mechanisms causing centrosome amplification (Fukasawa, 2007).

Deregulation of the centrosome duplication cycle is one of the most common causes of centrosome amplification. A number of proteins regulate the centrosome cycle and prevent re-duplication of centrioles (Brownlee and Rogers, 2013). Altered expression or activity of these proteins can trigger centrosome amplification (Fukasawa, 2007). A critical regulator is the Plk4 kinase, which promotes centriole duplication during S phase (Habedanck et al., 2005). Loss of Plk4 activity reduces centriole numbers, whilst overexpression of Plk4 increases centrioles numbers (Kleylein-Sohn et al., 2007; Habedanck et al., 2005). Plk4 levels are controlled by the ubiquitin ligase, $SCF^{\beta TrCP}$, as well as by autophosphorylation (Cunha-Ferreira et al., 2009; Rogers et al., 2009; Guderian et al., 2010). In addition, overexpression of the HPV-16 viral E6 and E7 oncoproteins increases the levels of Plk4 leading to centrosome amplification (Korzeniewski et al., 2011). Overexpression of HsSAS-6, a key protein for procentriole formation, promotes centriole overduplication leading to formation of extra centrosomes (Leidel et al., 2005). Similarly, p53 regulates Plk4 levels through the activity of HDAC (histone deacetylases) repressors (Li et al., 2005), suggesting a direct mechanism for how p53 could promote centrosome amplification.

Loss of p53 activity also helps cell survival following the mitotic defects of cells with centrosome amplification (Holland et al., 2012). Plk4 controls its expression levels by itself, but loss of this autoregulation rapidly increases centrosome amplification followed by block of proliferation in a p53-dependent manner. However, loss of p53 functions allow cell proliferation, suggesting that absence of p53 may allow centrosome amplification (Holland et al., 2012). Conversely, centrosome amplification in tetraploid cells stabilise p53 through the Hippo tumour suppressor pathway, favouring the elimination of those cells (Ganem et al., 2014). Other studies have shown that loss of p53 in mouse embryonic fibroblasts (MEFs) is sufficient to induce centrosome

amplification (Fukasawa et al., 1996). Further analysis is needed to determine whether loss of p53 directly induces centrosome amplification or simply allows survival of cells with amplified centrosomes.

Defects in cytokinesis, cell-cell fusion or mitotic slippage are able to generate tetraploid cells and centrosome amplification (Ganem et al., 2007). Tetraploid cells with no p53 activity exhibited centrosome amplification, which promoted tumorigenesis (Fujiwara et al. 2005). In contrast, cytokinesis failure in cells with intact p53 induced centrosome amplification, but cells subsequently lost their extra centrosomes (Krzywicka-Racka et al., 2011). It is therefore believed that while cytokinesis failure induces formation of extra centrosomes, other factors, such as cell type or genetic mutations, are needed to maintain centrosome amplification.

De novo centriole synthesis is another possible mechanism that leads to centrosome amplification (Nigg, 2002). Normally, the mother centriole enriches the PCM with factors that allow centriole biogenesis, as well as it concentrates the PCM to regulate the formation of the procentrioles (Loncarek et al., 2008). However, cells that lack centrosomes, which they destroyed by laser ablation, were able to form centrioles *de novo*, suggesting that activation of *de novo* centriole synthesis can increase centrosome numbers in cancer cells (Khodjakov et al., 2006). Interestingly, the Red-Br-nos, a noscapinoid member, induced robust *de novo* centrosome formation scattered throughout in the cytoplasm by altering Plk4 and cdk2 levels and causing an override of the centriolar biogenesis pathway (Pannu et al., 2012).

Overexpression of PCM components, such as pericentrin, is also enough to generate formation of extra centrosomes (Loncarek et al., 2008). Similarly, increased levels of γ-tubulin upon loss of the tumour suppressor BRCA1 led to centrosome amplification (Starita et al., 2004). Prolonged G_2 arrest allows centriole reduplication with the help of Plk1 kinase (Loncarek et al., 2010). Consistently, in the presence of DNA-damage-induced

cell cycle arrest, Plk1 and APC/C promote early centriole disengagement leading to centrosome amplification (Prosser et al., 2012). Hence, the presence of DNA damage may allow cells to remain in G_2 phase favouring centrosome amplification.

Centrosome amplification can be fatal for the survival of cells, however it is surprising how this defect is one of the main characteristic of several cancers. It is likely that suppression of pro-survival pathways, such as Hippo or p53, allows cells with amplified centrosomes to proliferate in cancer. Centrosome amplification is considered to be a key driver of chromosomal instability (CIN) promoting tumour initiation and evolution. It is not surprising then that centrosome amplification contributes to tumour heterogeneity and it is frequently found in advanced and aggressive cancers (McBride et al., 2015).

1.3.2 Structural centrosome defects

Extensive analysis of abnormal centrosomes in human cancers classified them into two major types: structural and numerical defects. The most common types of structural defects are associated with centriole structure and PCM integrity (Nigg, 2006; Godinho and Pellman, 2014). Abnormal size is one of the most common structural defects of centrioles detected in various cancers. Up or down regulation of centrosomal components can potentially increase the centriole length, although it is not clear how these alterations occur. Overexpression of centriolar proteins, such as CPAP/SAS-4 and CP110, cause abnormally long centrioles, which for the same reason lead to multipolar spindles and cytokinesis defects (Kohlmaier et al., 2009; Schmidt et al., 2009). Additionally, abnormal large PCM size is also a structural centrosome defect seen in various cancers. The increased PCM size could result from either amplified centrosomes that cluster during interphase or overexpression of PCM components (D'Assoro et al., 2002). Despite the recent progress in understanding structural centrosome abnormalities, development of more advanced methods is needed to understand the origins of these structural centrosome defects.

1.3.3 Centrosome defects and CIN

Chromosomal instability is a key characteristic of cancer cells, in which cells acquire multiple segregation errors during cell division leading to genetic instability (Vitre and Cleveland, 2012). The presence of amplified centrosomes promotes genome instability, cancer survival and progression (Vitre and Cleveland, 2012). Centrosome amplification causes defects in chromosome segregation and asymmetric cell division. Live cell imaging studies have shown that cancer cells with extra centrosomes form transient multipolar spindles that favour generation of merotelic microtubule-chromosome attachments; in turn these contribute to CIN and aneuploidy (Ganem et al., 2009; Cimini et al., 2001; Cimini, 2008). Experimental studies in Drosophila have shown that centrosome aberrations are able to form tumours (Basto et al., 2008). Additionally, centrosome amplification can initiate tumour in a mouse model of intestinal neoplasia and promote spontaneous tumour development in multiple tissues (Levine et al., 2017). In some mouse models, aneuploidy is able to promote tumorigenesis, whilst in others the presence of elevated aneuploidy acts as a tumour suppressor (Schvartzman et al., 2010). *Drosophila* studies have shown that transplantation of neuroblasts with amplified centrosomes into adult flies is sufficient to generate tumours with minimal levels of aneuploidy and kill the recipient host, but aneuploidy is unable to induce tumours on itself in this model (Basto et al., 2008; Castellanos et al., 2008).

The presence of CIN allows cancer cells to continuously evolve leading to intratumor heterogeneity (ITH). This is a key part of the progression to an aggressive and therapy-resistant cancer (McBride et al., 2015). Additionally, the frequent presence of micronuclei due to lagging chromosomes leads to DNA damage and abnormal DNA replication (Crasta et al., 2012). Chromothripsis is a process in which chromosomes are cropped into multiple fragments and some of these fragments are stitched together randomly (Stephens et al., 2011). Potential causes of chromothripsis include radiation, micronuclei formation, escaped from apoptosis and breakage-fusion-bridge cycles (Forment et al., 2012). Centrosome amplification is another factor that is likely to contribute to CIN through chromothripsis (McBride et al., 2015).

Centrosome amplification can be a potential prognostic biomarker for cancer detection. Centrosome amplification is rarely detected in normal or benign tissues from breast, prostate, lung, cervix, head and neck, and ovary (Chan, 2011). In some rare cases, centrosome abnormalities have been found in benign breast lesions (Guo et al., 2007). Non-malignant tumours from pancreatic adenoma and soft tissue can also possess extra centrosomes without promoting aggressiveness of the disease (Sato et al., 1999; Perucca-Lostanlen et al., 2004). In contrast, other studies suggest that centrosome amplification is a key driver of CIN and thus the ITH in high-grade metastatic cancers (McBrider et al., 2015). These evidences support the idea that centrosome amplification can be used as a prognostic marker and in combination with other biomarkers can provide powerful information for a more personalized cancer therapy (Chan, 2011; McBride et al., 2015).

1.3.4 Centrosome defects in breast and other solid cancers

Breast cancer is associated strongly with centrosome aberrations, including excess number and volume of centrosomes, supernumerary centrioles and increased PCM. This leads to formation of multiple MTOCs and abnormal cell polarity (Lingle et al., 1999). The presence of extra centrosomes is partially associated with late stage and high grade breast cancers (Denu et al., 2016). Centrosome amplification is also strongly related to lymph node metastasis in breast cancer (D'Assoro et al., 2002; Guo et al., 2007). Indeed, centrosome amplification significantly alters cytoskeleton morphology and promotes cell invasion through Rac1 activity (Godinho et al., 2014). Loss of the tumour suppressor p53 is another key event that may play a critical role in the formation of extra centrosomes in breast cancer cells by causing loss of control at the G1/S cell cycle checkpoint (D'Assoro et al., 2004). Loss of BRCA1 or overexpression of Aurora-A promotes centrosome amplification in breast cancer cells (Zhou et al., 1998; Starita et al., 2004). Overexpression of Aurora-A is frequently detected in ductal carcinoma *in-situ* (DCIS), but not in invasive ductal carcinoma (IDC). On the other hand, overexpression of Nek2 is found in DCIS and IDC and promotes centrosome amplification via cytokinesis failure (Hayward et al., 2004). The majority of these breast cancers exhibited high levels of CIN,

but some had low levels of CIN, suggesting a complex relationship between centrosome amplification and chromosome segregation that may reflect efficiency of centrosome clustering mechanisms that protect cancer cells from lethal mitoses.

Similar to breast cancer, excess components of the PCM, such as pericentrin, and loss of tumour suppressor proteins, such as p53, promote centrosome amplification and spindle defects in prostate cancer cell lines (Pihan et al., 2001; Ouyang et al., 2001). The human papillomavirus (HPV) E7 oncoprotein promotes formation of extra centrosomes leading to high-grade cervical dysplasia and invasive cervical malignancies (Riley et al., 2003). Furthermore, overexpression of Aurora-A was detected in primary ovarian tumour cells, but not in testicular germ cell tumours (Mayer et al., 2003). In lung cancer, loss of pRb, overexpression of E2F1 and cyclin E correlate with centrosome amplification (Koutsami et al., 2006). In other types of solid cancer, such as squamous cell carcinomas of the head and neck (HNSCC), centrosome amplification is detected at high levels and associates with tumour stage, size, metastasis and overall survival (Gustafson et al., 2000; Reiter et al., 2009).

1.3.5 Centrosome abnormalities in haematological malignancies

Apart from solid cancers, centrosome abnormalities have also been detected in several haematological malignancies, including acute and chronic myeloid leukaemias, non-Hodgkin lymphoma and multiple myelomas (Kramer et al., 2005; Giehl et al., 2005; Kramer et al., 2011). Leukaemia and lymphomas represent approximately 10% of all cancers worldwide (Stewart and Wild, 2014). Leukeamia arise from the abnormal production of white blood cells in the bone marrow. Under normal conditions, the bone marrow produces blood stem cells that have the ability to differentiate into lymphoid blast, myeloid blast, erythoblast, and megakaryoblast cells (Figure 1.6). The lymphoid

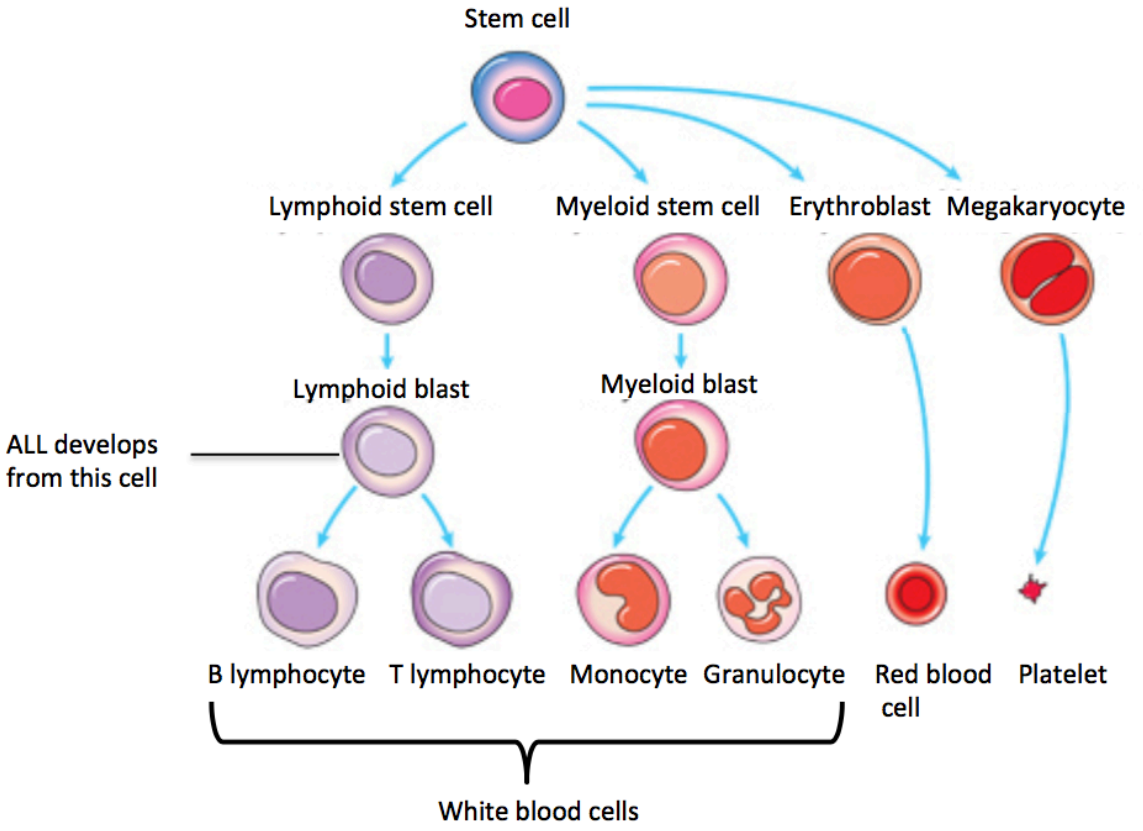

Figure 1.6 Blood stem cell development

Bone marrow produces blood stem cells that differentiate into lymphoid and myeloid stem cells, platelets and megakaryocyte. B and T lymphocytes are derived from lymphoid stem cells and have essential functions for the organism. B-lymphocytes produce antibodies to fight infections and T-lymphocytes help them in this process. These types of cells belong to the group of white blood cells that are frequently overproduced in leukeamic patients. ALL develops from accumulation of lymphoid blasts. Adapted from Cancer Research UK.

blast produces B and T lymphocytes, whereas the myeloid blast generates monocytes and granulocytes. However, in leukaemia, this differentiation process can go wrong at different stages, leading to overduplication of particular blood cells with improper functions. There are several types of lymphoid-based or myeloid-based leukaemias, including acute and chronic myeloid leukaemia (AML or CML, respectively), B and T-cell acute and chronic lymphoblastic leukeamia's (ALL and CLL), Hodgkin's and non Hodgkin's lymphomas, and multiple myeloma (Greaves, 2016). Chromosomal translocations are a frequent characteristic of cancer cells in patients with leukaemia. At the beginning of 1960s, a major breakthrough in cancer biology was the identification of the Philadelphia (Ph) chromosome, which is formed from the reciprocal translocation of chromosome 9 and 22 and encodes the bcr-abl fusion protein, in chronic myeloid leukaemia (CML) (Nowell and Hungerford, 1960; Rowley, 2001; Konopka et al., 1984). As in solid cancers, centrosome defects have been frequently found in haematological malignancies, including Hodgkin's and non-Hodgkin's lymphomas, AML and CML, CLL and multiple myeloma (Kramer et al., 2005). Haematological malignancies have classified into two major groups based on their origin, the myeloid and lymphoid malignancies.

Centrosome abnormalities have also been detected in several myeloid malignancies, including AML, aplasic anemias and myelodysplastic syndromes (Neben et al., 2003; Kearns et al., 2004). Analysis of 48 AML samples detected structural and numerical centrosome defects that they were correlated with the chromosomal changes and cytogenetic risk profile (Neben et al., 2003). In addition, fluorescence in situ hybridization identified centrosome abnormalities that were correlated to the amount of numerical centrosome abnormalities in 5 out of 25 myelodyplastic syndrome and aplastic anemia samples (Kearns et al., 2004). cDNA-based microarrays identified 18 genes that exhibit high levels of expressions correlated to ploidy status and centrosome aberrations in AML samples (Neben et al., 2004). These genes include those encoding centrosome proteins, such as pericentrin and NUMA (Neben et al., 2004). One study showed that centrosome amplification in BCR-ABL1-positive cells occurs at early stages of CML development, and that high levels of centrosome amplification were found in

cells at blast crisis (BC) rather than in chronic phase (CP) (Giehl et al., 2005; Patel and Gordon, 2009). AML cells exhibit a high degree of numerical and structural centrosome defects that correlate with high CIN, as well as overexpression of centrosome-associated proteins, such as centrin (Neben et al., 2003). Similarly, centrosome amplification was detected in 25 patients with hematopoietic bone marrow failure disorders that had a risk for development into AML (Kearns et al., 2004).

In addition, several patients with lymphoid malignancies also exhibit centrosome abnormalities (Kramer et al., 2005; Chan, 2011). Several subtypes of B-cell lineage NHL including diffuse large B-cell lymphoma (DLCBCL), mantle cell lymphoma (MCL), follicular lymphoma (FL), Burkitt's lymphoma (BL) and marginal zone B-cell lymphomas (MZBCL) possess centrosome defects (Hensel et al., 2007). Specifically, forms of aggressive lymphomas, such as DLCBCL, BL and MCL exhibit more severe centrosome abnormalities than FL and MZBCL. In FL, centrosome amplification was correlated with histological grading and in MCL, numerical centrosome abnormality was correlated with a high frequency of near-tetraploid chromosome numbers (Kramer et al., 2003). In a single case of Burkitt's lymphoma, centrosome abnormalities were observed in approximately 30-50% of cells (Duensing et al., 2003). Furthermore, centrosome aberrations were also detected in ALK- positive anaplastic large cell lymphoma (ALCL) (Ventura et al., 2004). Furthermore, centrosome amplification correlates with aggressiveness of CLL time, while the vast majority of CLL cases showed approximately 50% centrosome amplification (Hensel et al., 2007). Aurora-A kinase overexpression and chromosome abnormalities were detected in 28 CLL patients suggesting a link between genomic instability and centrosome amplification (Inamdar et al., 2008). A recent study showed numerical and structural centrosome aberrations in 36 out of 50 CLL cases (Kerketta et al., 2017). On the other hand, little is known about the centrosome amplification frequency and B-precursor acute lymphoblastic leukaemia (ALL).

1.4 Centrosome clustering during mitosis

The majority of cancer cells with extra centrosomes would be expected to form multipolar spindles leading to chaotic cell divisions and cell death (Ganem et al., 2009; Milunovic-Jevtic et al., 2016). Cancer cells solve these detrimental consequences of a multipolar mitosis by either inactivation of extra centrosomes, centrosome loss or centrosome clustering (Godinho et al., 2009). The inactivation of extra centrosomes is one of the mechanisms that cancer cells may use to survive and divide. Studies in *Drosophila* showed that cells inactivate extra centrosomes by reducing the PCM levels in the scattered spindle poles and decreasing the numbers of the extra microtubule asters (Basto et al., 2008). Centrosome loss can therefore be considered as a mechanism that cancer cells use to avoid lethal multipolar mitoses (Mikeladze-Dvali et al., 2012). The mechanisms of centrosome loss or inactivation still remain elusive. Centrosome clustering is the best-described mechanism for dealing with centrosome amplification in mitosis (Gergely and Basto, 2008; Kwon et al., 2008).

1.4.1 Mechanisms of centrosome clustering

Cancer cells with amplified centrosomes have the ability to survive lethal multipolar mitoses by clustering their extra centrosomes in a bipolar manner (Kwon et al., 2008; Ganem et al., 2009; Basto et al, 2008). Centrosome clustering was first observed in mouse neuroblastoma NIE-115 cells, in which extra centrosomes were able to cluster in both interphase and mitosis (Ring et al., 1982). An extensive amount of work over the last two decades have identified a number of mechanisms implicated to centrosome clustering (Godinho and Pellman, 2014).

A number of microtubule-based processes, including microtubule dynamics, motor protein activity and microtubule attachments to the centrosome, chromosomes and cell cortex are important for centrosome clustering (Leber et al., 2010; Kwon et al., 2008). Dynein, a minus-end directed motor protein, was the first protein identified to be

necessary for centrosome clustering (Quintyne et al., 2005). The role of dynein in centrosome clustering was confirmed by Leber et al. (2010), in a genome-wide RNA interference screen. However, other studies have suggested that dynein is not necessary for clustering of extra centrosomes in HPV16 E7 transfected human keratinocytes and fibroblasts (Nguyen et al., 2008). Similarly, depletion of dynein does not block centrosome clustering in *Drosophila* S2 cells (Goshima et al., 2005). Hence, these experiments suggest that dynein may not be required for centrosome clustering in all cell types.

Dynein regulates the length and position of the mitotic spindle, controls centrosome assembly and localisation, and participates in microtubule-kinetochore attachments and spindle assembly checkpoint (SAC) silencing (Bader and Vaughan, 2010). Based on dynein functions and its potential involvement in centrosome clustering, two models were proposed. The first model suggests that dynein, and its adaptor dynactin, move towards the cell cortex walking along astral microtubules pulling centrosomes and the spindle towards the cellular periphery (Moore et al., 2009; Sommi et al., 2011). The centrosome position is achieved with the aid of other motors, such as myosins which direct forces outward, and this balances with the inward motors, such as HSET (Dujardin and Vallee, 2002; Sommi et al., 2011). Hence, its believed that a balance of a net force on centrosomes contributes to centrosome clustering in cancer cells (Ogden et al., 2012).

HSET/KIFC1, a minus-end directed motor protein, also contributes to centrosome clustering by crosslinking antiparallel microtubules between adjacent centrosomes (Kwon et al., 2008). HSET protein localises between adjacent microtubules within the mitotic spindle (Mountain et al., 1999). Indeed, loss of HSET induced formation of multipolar spindles with both centrosomal or acentrosomal poles in cancer cells (Kleylein-Sohn et al., 2012; Kwon et al., 2008). HSET interacts with Cep215, known also as Cdk5Rap2, promoting centrosome clustering and allowing survival of cancer cells (Chavali et al., 2016). Interestingly, HSET inhibition did not affect cell viability in human

BJ fibroblasts that do not possess amplified centrosomes (Loffler et al., 2007), on mouse NIE-3T3 fibroblast and human MCF-7 cell lines that have low levels of centrosome amplification (Kwon et al., 2008).

Other microtubule-associated proteins (MAPs), such as ch-TOG and TACC3, contribute to centrosome clustering potentially via the integrin-linked kinase (ILK) (Fielding et al., 2008a; Fielding et al., 2011). ILK has important functions in regulation of the actin cytoskeleton and mitotic spindle organisation (Fielding et al., 2008b). ILK regulates TACC3 and ch-TOG interactions during mitosis and its inhibition induces multipolar mitoses via loss of TACC3/ch-TOG complex from the spindle (Fielding et al., 2008a). The TACC3 homolog is also important for centrosome clustering in *Drosophila* S2 cells (Kwon et al., 2008). In human, there are three TACC proteins, with evidence so far that it is the TACC3 protein that is important for centrosome clustering in human breast BT549 and prostate cancer PC3 cell lines (Fielding et al., 2011). ch-TOG is a microtubule plus-end protein that forms a complex with TACC3 providing stability to K-fibres (Peset and Vernos, 2008). The role of ch-TOG in centrosome clustering was again confirmed by the genome wide-screen RNA interference screen (Leber et al., 2010).

A robust spindle assembly checkpoint (SAC) also supports survival of cancer cells with amplified centrosomes during mitosis (Leber et al., 2010; Ogden et al., 2012). The SAC is a checkpoint mechanism that controls the metaphase to anaphase transition by monitoring proper kinetochore-microtubule attachment of chromosomes before segregation (Musacchio and Salmon, 2007). Specifically, the SAC stops chromosome segregation by maintaining the anaphase-promoting complex/cyclosome (APC/C) in an inactive state (Acquaviva and Pines, 2006). Cancer cells with amplified centrosomes require longer time in mitosis due to the formation of transient multipolar spindles, in which incorrect microtubule-kinetochore attachments delay the normal bipolar orientation of chromosomes (Godinho and Pellman, 2014). Loss of SAC proteins, including Mad2, BubR1 and CENP-E, accelerates mitosis and so prevents the time required for centrosome clustering (Kwon et al., 2008; Yang et al., 2008). The importance

of the SAC in centrosome clustering was also confirmed in *Drosophila* model organism (Basto et al., 2008). Interestingly, loss of the APC/C also specifically increases the levels of the Eg5 motor kinesin disrupting the balance of forces on the mitotic spindle and thus potentially leading to centrosome clustering (Drosopoulos et al., 2014).

A number of proteins with important roles in microtubule attachments to kinetochores, centrosomes and the cell cortex are also implicated in centrosome clustering (Kwon et al., 2008; Leber et al., 2010). Specifically, proteins of the chromosome passenger complex (CPC), sister chromatid cohesion, augmin complex and in kinetochore-microtubule attachments have been identified as important players in centrosome clustering (Leber et al., 2010). The CPC complex regulates chromosome-microtubule interactions and spindle tension at the kinetochores during metaphase and cytokinesis (Ruchaud et al., 2007). Genome wide-siRNA screens identified a number of CPC proteins, including Aurora-B, INCENP, survivin and borealin, that are important for centrosome clustering in cancer UPCI: SCC114 cells (Leber et al., 2010). Knockdown of the CPC proteins disrupts microtubule-kinetochore attachments leading to spindle multipolarity in cancer cells (Leber et al., 2010). In addition, the Ndc80 complex is also required for centrosome clustering (Leber et al., 2010). The Ndc80 complex consists of HEC1, SPC24, SPC25 and Nuf2 and localises at the outer kinetochore domain where it acts as a platform for kinetochore-microtubule attachments (Wei et al., 2007). Loss of three components of the Ndc80 complex, HEC1, SPC24 and SPC25, promote spindle multipolarity (Leber et al., 2010). Similar to Ndc80 depletion, knockdown of CENP-T, a kinetochore protein, also induces spindle multipolarity (Leber et al., 2010). This suggests that CPC and Ndc80 proteins control spindle tension favouring centrosome clustering in cancer cells with amplified centrosomes, while loss of these proteins induces spindle multipolarity.

Proteins important for sister chromatid cohesion are also required for centrosome clustering in cancer cells. Both shugoshin (SGOL1) and sororin provide tension between chromosomes (Salic et al., 2004), and their depletion leads to spindle multipolarity with

mitotic arrest (Leber et al., 2010). Cep164, a centrosomal protein localised at the distal appendages of mature centrioles (Graser et al., 2007a), favours centrosome clustering (Leber et al., 2010). Depletion of Cep164 led to spindle multipolarity in cancer and normal cells, suggesting that Cep164 is important for spindle pole integrity (Leber et al., 2010). Therefore, both sister chromatid and centrosome-microtubule tension are important factors for centrosome clustering (Figure 1.7).

The augmin complex is composed of eight proteins, and is important for microtubule-based microtubule generation within the spindle by recruiting γ-tubulin ring complexes to spindle microtubules (Uehara et al., 2009). Loss of the augmin complex fails to localise γ-tubulin to the spindle activating the SAC via loss of kinetochore microtubules and reduction of tension at kinetochores (Lawo et al., 2009). Genome wide siRNA screens identified three members of the Augmin complex, FAM29A, HEI-C and HAUS3, as important for centrosome clustering (Leber et al., 2010). These data suggest that tension at spindle poles and at microtubule-kinetochore connecting points are necessary for clustering of extra centrosomes (Figure 1.7). Similarly, the Ran GTPase effector and microtubule-associated protein HURP regulates microtubule-kinetochore attachment and stability of k-fibres, but loss of HURP leads to formation of multipolar spindles in cancer cells (Breuer et al., 2010).

Furthermore, the use of adhesive contacts on micropatterned coverslips has revealed the importance of extracellular conditions with the microenvironment for centrosome clustering (Kwon et al., 2008). Importantly, the actin organisation allows cell shape and adhesion influencing centrosome positioning via forces applied on astral microtubules. Myo10 is another important candidate protein involved in centrosome clustering by controlling the organisation of cortical actin forces on astral microtubules (Kwon et al., 2008). During mitosis, cells become rounded-up and retraction fibres connect the cell cortex to the adjacent surface promoting spindle orientation (Thery et al., 2005). The presence of strong cortical attachments determines whether cancer cells are able to cluster their amplified centrosomes and therefore their survival (Kwon et al., 2008).

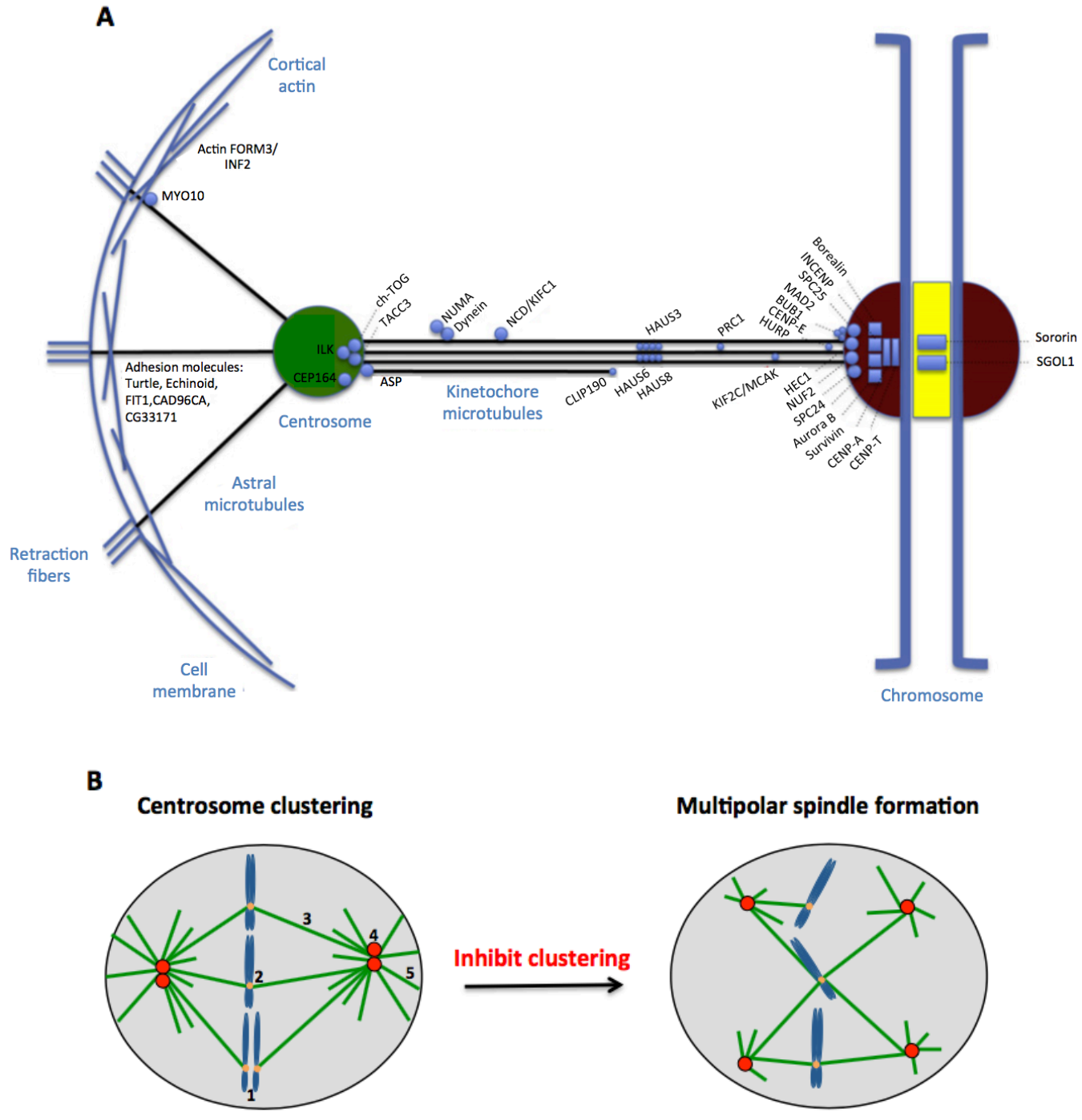

Figure 1.7 Centrosome clustering mechanisms

A. In this schematic model, five distinct mechanisms are illustrated, with multiple proteins involved in each mechanism. **1.** Centrosome clustering is brought about by the tension between sister chromatids that is controlled by SGOL1 and sororin. **2.** Microtubule-kinetochore attachments provide spindle tension brought by CENP-T, CPC and Ndc80 complexes, and thus favouring clustering of extra centrosomes **3.** Microtubule-associated proteins (MAPs), such as dynein, the augmin complex, HSET and ch-TOG, promote spindle tension. **4.** Microtubule-centrosome attachments is another mechanism of centrosome clustering. **5.** Cortical attachments provide further spindle tension and polarity allowing clustering. From Leber et al (2010). **B.** This schematic figure provides a simplified overview of centrosomal clustering in cancer cells with amplified centrosomes. Inhibition of the centrosome clustering mechanisms leads to formation of multipolar spindles.

1.4.2 Amplified centrosomes as a therapeutic target in cancer

Apart from the potential of centrosome amplification as a prognostic biomarker, it can be also considered as a therapeutic target. The fact that centrosome amplification is frequently observed in several cancers but not in the majority of non-neoplastic tissues makes it an attractive target for development of selective cancer drugs. Two main aspects of centrosome biology are currently targets for cancer therapy: the centriole duplication and centrosome clustering mechanisms (Korzeniewski et al., 2013). In this section, I will mainly focus on the identification of potential targets of centrosome clustering during mitosis.

A number of proteins have important roles in the centrosome duplication cycle. Plk1 is a kinase required for centriole disengagement (Schockel et al., 2011). Loss of Plk1 prevents centriole disengagement and subsequent centriole duplication; however, this effect seen to be less severe in normal cells compared to cancer cells (Liu et al., 2006). Recent progress on development of Plk1 inhibitors, such as Volasertib, has shown important anti-tumour activity and some of them are currently in clinical trials (Lapenna and Giordano, 2009; Gutteridge et al., 2016). Plk4 is another kinase essential for centriole duplication; loss of Plk4 blocks centriole duplication and its overexpression promotes formation of extra centrioles (Habedanck et al., 2005). The development of small molecule inhibitors against Plk4 may be beneficial against cancers with centrosome amplification, as they could block centriole duplication and inhibit cell proliferation (Wong et al., 2015; Bedard et al., 2016; Korzenieswski et al., 2009). Cdk2, a cell cycle kinase, also promotes centriole duplication in interphase. Loss of Cdk2 activity blocks centriole overduplication, without affecting normal centriole duplication and cell cycle progression (Tetsu et al., 2003). Roscovitine, a Cdk2 inhibitor, inhibit centriole overduplication, promoting cell death in vitro (MacCallum et al., 2005). However, numerous cdk inhibitors did not respond well in clinical trials with disappointing results (Asghar et al., 2015).

Other proteins, including Nek2 and Eg5, are required for centrosome separation to form the bipolar mitotic spindle. Nek2, a centrosomal kinase, phosphorylates C-Nap1 and rootletin promoting centrosome separation. Eg5, a kinesin motor, is also required for centrosome separation and compensates for loss of Nek2 function (Mardin et al., 2010). Inhibiting the activity of those two proteins should block centrosome separation preventing formation of the bipolar mitotic spindle. Aurora-A and Plk1 also have key roles in centrosome maturation by recruiting γ-tubulin and other PCM components to the centrosome. Aurora-A is often overexpressed in several cancers and this is thought to promote centrosome amplification and polyploidy (Zhou et al., 1998). Inhibition of Aurora-A can lead to errors in chromosome segregation, mitotic catastrophe and cell death (Asteriti et al., 2011). A number of Aurora-A inhibitors, such as Alisertib (MLN8237) are in clinical trials giving promising results (Kollareddy et al., 2012; Bavetsias & Linardopoulos, 2015). The development of small molecule agents that will selectively target centrosome kinases may hold the promise for a beneficial therapy of cancers with centrosome amplification.

A big effort has been put for development of agents that block centrosome clustering in cancer cells. Centrosome clustering mechanisms not only allow survival of cancer cells with extra centrosomes but also propagate low levels of CIN (McBride et al., 2015). The wide variety of proteins involved in these mechanisms provides promising opportunities for development of more specific anti-cancer agents. The persistence of multipolar spindles in cancer cells with amplified centrosomes may arrest cells in mitosis and activate cell death through apoptotic mechanisms (Karna et al., 2011). Indeed, several compounds have been identified that block clustering and induce spindle multipolarity, including griseofulvin, phenenthrene-derived PARP inhibitors and noscarpinoids (Odgen et al., 2012; Castiel et al., 2011; Raab et al., 2012).

Griseofulvin is an antifungal agent that induces spindle multipolarity in human cancer cells in a dose-dependent manner (Rebacz et al., 2007). Griseofulvin was also found to

block centrosome clustering in both interphase and mitosis in the murine neuroblastoma NIE-115 cells (Pannu et al., 2014). Griseofulvin was proposed to have selective anticancer potential, since it inhibits proliferation of tumor cells but not healthy cells. A synthetic derivative of griseofulvin, GF-15, led to multipolarity in cancer cells with increased potency and reduced tumour growth in xenograft mouse models of human colon cancer and multiple myeloma (Raab et al., 2012). However, the exact mechanisms of griseofulvin action remain unknown. One hypothesis suggests that griseofulvin disrupt microtubule dynamics causing microtubule stabilisation, similar to taxol treatment (Panda et al., 2005; Chen et al., 2002). Indeed, griseofulvin is able to bind to tubulin and disrupt microtubule dynamics leading to multipolar spindles, misaligned chromosomes and mitotic arrest in MCF-7 cells that have normal centrosome numbers (Rathinasamy et al., 2010). The reason for this is that griseofulvin induces spindle multipolarity not only by blocking centrosome clustering but also via formation of acentrosomal spindle poles, in which MTOCs are generated that lack a bona fide centrosome, as judged by centriole staining (Rebacz et al., 2007; Rathinasamy et al., 2010).

In addition to griseofulvin, noscapinoids are another type of centrosome declustering agent. Bromonoscapine, known also as EM011, is a derivative of the poppy-derived antifussive that disrupts microtubule dynamics (Karna et al., 2011). Similar to griseofulvin, bromonoscapine induces mitotic arrest followed by apoptotic cell death (Karna et al., 2011). The molecular mechanism of how bromonoscapine affects microtubule dynamicity without causing stabilisation or depolymerisation is still under investigation, although bromonoscapine potentially disrupts the binding of the plus-end microtubule associated proteins, EB1 and CLIP-170 (Karna et al., 2011; Ogden et al., 2012).

Phenanthrene-derived compound that were originally developed as inhibitors of the DNA repair enzyme, poly-ADP-ribose polymerase (PARP), also led to formation of multipolar spindles in cancer cells with amplified centrosomes (Castiel et al., 2011). PARP-1 is overexpressed in several human cancers (Miwa and Masutani, 2007), whilst it

is down-regulated in others (Tong et al., 2007). PARP-1 is activated upon DNA damage and contributes to DNA repair by making the DNA more accessible to repair enzymes and transcription factors (Kraus, 2008). Suprisingly, a synthetic phenanthrene PARP inhibitor, known as PJ-34, was found to inhibit centrosome clustering promoting formation of multipolarity, mitotic catastrophe and cell death (Castiel et al., 2011). Homologs of PARP, tankyrase-1 and PARP-16, were identified as critical proteins for centrosome clustering in a *Drosophila* S2 screen, although why is entirely uknown (Kwon et al., 2008). However, a derived PARP inhibitor caused mitotic arrest in both healthy and cancer cell lines (Inbar-Rozensal et al., 2009).

Recently, a study by Kawamura et al. (2013) identified 14 small molecule inhibitors that induce spindle multipolarity in the breast BT-549 cancer cell line that harbours centrosome amplification. One of those compounds, the CCCI-01 (Centrosome Clustering Chemical Inhibitor-01), also known as N2-(3-pyridylmehtyl)-5-nitro-2-furamide, promoted spindle multipolarity and cell death selectively in cancer cells as compared to healthy breast and bone marrow hematopoietic progenitors (Kawamura et al., 2013). Furthermore, two other compounds, CP-673451 and crenolanib, that were originally developed for inhibition of platelet-derived growth factor receptor β (PDGFR-β), were reported to induce spindle multipolarity in cells with amplified centrosomes by activating cofillin, a key regulator of actin remodelling (Konotop et al., 2016).

Of most interest to date have been inhibitors developed against HSET/KifC1, a minus-end directed microtubule motor that is strongly associated with centrosome clustering and frequently overexpressed in many cancers (Kwon et al., 2008; Pannu et al., 2015; Mittal et al., 2016). A number of HSET/KifC1 inhibitors have been developed. AZ82 selectively promotes formation of multipolar spindles in breast BT-549 cancer cells with amplified centrosomes, but not in HeLa cells that do not exhibit centrosome amplification (Wu et al., 2013). Similarly, CW069, a second HSET/KifC1 inhibitor, promotes multipolarity in cancer cells with amplified centrosomes without altering bipolar spindle morphology in cells with normal centrosome numbers (Watts et al.,

2013). However, CW069 reduced proliferation not only of cancer cells with amplified centrosomes, but also MCF-7 cells that do not possess amplified centrosomes (Watts et al., 2013). Indeed, as seen with griseofulvin, depletion of HSET/KifC1 activity led to a significant increase of multipolar spindles with acentrosomal poles in BT-549 cells (Kleylein-Sohn et al., 2012).

Some process has therefore been made for developing inhibitors that selectively target cancer cells with amplified centrosomes without apparently affecting normal cells, such as hepatocytes, that still have the ability to divide (Gentric et al., 2012). However, the majority of these agents seen to work by disturbing microtubule dynamics and, above a certain dose, induce acentrosomal pole formation even in the absence of amplified centrosomes. Hence, they do not represent ideal agents.

1.5 Heat shock protein family

The majority of proteins must fold into a precise three-dimensional structure to become functionally active (Bartlett and Radford, 2009). Failure of protein folding can lead to loss of protein stability or solubility. Cells therefore ensure protein quality and function in a process called proteostasis (Powers et al., 2009). Errors in proteostasis frequently lead to disease, including neurodegeneration, cancer, type 2 diabetes and cardiovascular disease (Morimoto, 2008; Balch et al., 2008). Proteostasis is predominantly controlled by molecular chaperones and their regulators (Hartl et al., 2011). These molecular chaperones aid refolding and de novo folding of newly formed proteins, as well as promoting removal of misfolded proteins by the ubiquitin-proteasome system (UPS) and autophagy (Powers et al., 2009).

Molecular chaperones are often described as stress proteins or heat-shock proteins (HSPs). Chaperones are classified into families according to sequence and molecular weight. At least six HSP families have been identified so far: Hsp40, Hsp60, Hsp70,

Hsp90, Hsp100 and the small Hsps (Hartl et al., 2011). Heat shock proteins (HSPs) were first discovered as a set of proteins that rapidly increase their synthesis after induction of high temperatures in *Drosophila* larvae (Ritossa, 1962; Tissieres et al., 1974). These proteins rely on ATP and cofactors to aid the folding of protein, as well as to protect proteins from denaturation (Hartl et al., 2011). HSPs are also expressed in unstressed cells and important for normal growth (Hendrick and Hartl, 1995).

1.5.1 Hsp90 family

Hsp90 proteins are ubiquitously expressed in cells and comprise up 1-2% of cytosolic proteins. This molecular chaperone is responsible for correct folding of at least 200 different proteins and its activity is heavily dependent on ATP (Schopf et al., 2017). The structure of Hsp90 consists of three main regions: a (N)-terminal domain with an ATP-binding site and a hydrolysis pocket, a catalytic domain that allows binding of client proteins and a (C)-terminal domain that promotes Hsp90 dimerization (Taipale et al., 2010). In higher eukaryotes, two isoforms of Hsp90 are expressed in the cytoplasm and nucleus, Hsp90α and Hsp90β (Whitesell and Lindquist, 2005). Hsp90-related proteins are also found in chloroplasts, endoplasmic reticulum and mitochondria (Schopf et al., 2017). Loss of Hsp90 activity causes defects in development and differentiation (Lanneau et al., 2007). In *Drosophila* cells, point mutations of Hsp83, the homologue of Hsp90, are lethal (Yue et al., 1999). In mice, loss of Hsp90α did not affect placental development, but loss of Hsp90β activity was early embryonic lethal, suggesting an essential role for Hsp90β, but not Hsp90α, in placental development (Voss et al., 2000).

Apart from roles in general protein homeostasis, Hsp90 proteins have also more specific functions in cytoskeletal organisation and centrosome integrity (Liang and MacRae, 1997). Hsp90 may be involved in the recruitment and/or stabilisation of the PCM during centrosome maturation (Lane and Nigg, 1996). Similarly, loss of Hsp90 activity led to formation of abnormal mitotic spindles due to severely disrupted centrosomes suggesting that Hsp90 is required for maintaining centrosome integrity (Lange et al.,

2000). Studies in *Drosophila* and human cells showed an interaction between Hsp90 and the Plk1 kinase (de Carcer et al., 2001; Simizu and Osada, 2000). Loss of Hsp90 activity blocked cells in G_2 phase or at the metaphase to anaphase transition, and showed loss of Plk1 stability (de Carcer, 2004). Furthermore, Hsp90 interacts with cyclin B and the microtubule-associated protein (MAP) ch-TOG/XMAP215 (Basto et al., 2007). Importantly, Hsp90 is not involved in cyclin B or ch-TOG stability, but it is required for the localisation of those proteins at centrosomes and spindles suggesting that it affects their ability to interact with partner proteins (Basto et al., 2007). Inhibition of Hsp90 by geldanamycin led to reduced levels of nucleolin during mitosis (Wang et al., 2011). Similarly, inhibition of Hsp90 by 17-allylaminogeldanamycin (17-AAG) caused delocalisation of several kinetochore proteins including CENP-H and CENP-I, as well as misalignment of chromosomes and mitotic arrest (Niikura et al., 2006).

Hsp90 is overexpressed in cancer cells and favours their survival in response to different stresses, including proteotoxic stress, hypoxia and genomic instability (Neckers and Workman, 2012). Several Hsp90 client proteins are well characterised oncogenes, including HER2, EGFR, BCR-ABL and BRAF (Hong et al., 2013). These oncogenes have important roles in angiogenesis, apoptosis inhibition and metastasis (Hanahan and Weinberg, 2011). Hsp90 protects and maintains hypoxia-inducible factor-1α (HIF-1 alpha) and vascular endothelial growth factor receptor (VEGFR) and thus contributes to angiogenesis (Basso et al., 2002). Hsp90 also protects anti-apoptotic proteins, including AKT and survivin (Basso et al., 2002). Proteins involved in metastasis, such as matrix metalloproteinase-2 (MMP-2), are also protected by Hsp90 contributing to metastasis (Hong et al., 2013).

Based on the proven roles of Hsp90 in the survival of cancer cells, targeting Hsp90 offers a great promise for development of anti-cancer inhibitors (Mahalingam et al., 2009). Geldanamycin was the first Hsp90 inhibitor to be tested in tumour models; however, this drug showed high levels of hepatoxicity (Workman et al., 2007). Several other Hsp90 inhibitors, including tanespimycin, alverspimycin, IPI-493 and IPI-504 are in clinical trials,

although they still exhibit moderate or high levels of toxic-side effects (Li et al., 2009; Hong et al., 2013).

1.5.2 Hsp70 family

Another big family of heat shock proteins are the Hsp70 proteins. Members of Hsp70 family also have key roles in protein folding and proteostasis (Hartl et al., 2011). This HSP family is highly conserved among prokaryotes, eukaryotes and archaebacteria (Daugaard et al., 2007). In humans, the Hsp70 family consists of eight members characterised by differential gene expression, subcellular localisation and amino acid sequence (Table 1.2) (Daugaard et al., 2007). The majority of Hsp70 members are expressed mainly in the cytosol and nucleus, whereas the Hsc70-5 (Bip or Grp78) and the Hsp70-9 (mtHsp70 or Grp75) isoforms are restricted to the endoplasmic reticulum and mitochondrial matrix, respectively (Daugaard et al., 2007). Hsc70, encoded by *HSPA8* gene, is constitutively expressed in the cytoplasm and in most tissues with major housekeeping functions, whilst the Hsp72 isoform, encoded by the *HSPA1A* and *HSPA1B* genes is expressed at very low amounts in unstressed cells but is rapidly induced upon stress (Daugaard et al., 2007). The heat shock factor 1 (HSF1) transcription factor mediates the heat shock stress response pathway and is responsible for Hsp72 induction (de Billy et al., 2009). Hsp70 activity depends on ATP hydrolysis and the Hsp40 co-chaperones (Kampinga and Craig, 2010). The typical structure of Hsp70 consists of a N-terminal nucleotide-binding domain (NBD) that has ATPase activity, a peptide substrate-binding doimain (SBD) and a C-terminal domain, which ends with an EEVD motif that allows interaction with other co-chaperones (Brodsky and Chiosis, 2006).

Protein	Gene	Homology to Hsp70-1α (%)	Cellular localisation	Stress-Induced
Hsp70-1a/ Hsp72	*HSPA1A*	100	Cytosol, Nucleus, Lysosomes	Yes
Hsp70-1b / Hsp72	*HSPA1B*	99	Cytosol, Nucleus, Lysosomes	Yes
Hsp70-1t	*HSPA1L*	91	Cytosol, Nucleus	No
Hsc70	*HSPA8*	86	Cytosol, Nucleus	No
Hsp70-6	*HSPA6*	85	Cytosol, Nucleus	Yes
Hsp70-2	*HSPA2*	84	Cytosol, Nucleus	Yes
Hsp70-5	*HSPA5*	64	ER (endoplasmic reticulum)	No
Hsp70-9	*HSPA9*	52	Mitochondria	No

Table 1.2 The human Hsp70 family

The table shows the eight Hsp70 isoforms based on their gene nomenclature, subcellular localisation and whether the protein is expressed in response to stress. Adapted from Daugaard et al (2007).

1.5.3 Hsp70 proteins in mitosis

Apart from their general functions in protein homeostasis, Hsp70 proteins also have specific roles during mitosis. Early studies in xenopus eggs and embryos revealed potential roles of Hsp70 for microtubule and centrosome functions (Liang and MacRae, 1997). In normal cell growth conditions, Hsp70 localises to the centrosome and spindle poles (Wigley et al., 1999). Additionally, high levels of misfolded proteins leads to a rapid increase of Hsp70 at the centrosome (Wigley et al., 1999). Mortalin, also known as Grp75, localises to the centrosomes at G1 phase and may control centrosome duplication by promoting p53 dissociation from the centrosome (Ma et al., 2006). Very recently, depletion or inhibition of Hsp70 has been shown to disrupt the function of centrosomes, and impair microtubule nucleation from the spindle poles during mitosis (Fang et al., 2016). In the presence of excess heat, Hsp70 is rapidly recruited to mitotic centrosomes increasing dynamitin/p50 at those sites and protecting them from heat damage (Hut et al., 2005).

Hsp70 proteins also contribute to cytoskeleton organisation and mitotic spindle integrity (Liang and MacRae, 1997; O'Regan et al., 2015a). Hsp70 and the co-chaperone Hsp110 control spindle length during mitosis by regulating the kinesin-5 motor, Cin8 (Makhnevych and Houry, 2013). In a recent study carried out in our laboratory, the stress-inducible Hsp72 protein was found to be required for proper mitotic spindle formation to facilitate efficient chromosome congression and segregation (O'Regan et al., 2015b). Moreover, the Nek6 kinase was shown to phosphorylate Hsp72 and in turn the phosphorylated Hsp72 localised to the mitotic spindle. Specifically, depletion or inhibition of Hsp72 led to weak mitotic spindles due to reduced K-fibres. One explanation for this was that Hsp72 facilitates recruitment of the ch-TOG/TACC3 complex to spindle poles and spindle fibres (O'Regan et al., 2015). Additional data also suggested a potential role of Hsp72 in astral microtubule organisation and/or cortical attachment.

1.5.4 Hsp70 and cancer

It is well established that cancer cells rely on heat shock proteins, including Hsp90 and Hsp70, for proliferation, survival and invasion (Daugaard et al., 2007; Daugaard et al., 2005). For example, a recent study suggested an important role of the Hsp70 family member, mortalin (HSPA9), in the induction of the epithelial-to-mesenchymal transition (EMT) by upregulation of focal adhesion proteins and PI3K-Akt and JAK-STAT signalling (Na et al., 2016). The protective role of Hsp70 in response to several stresses, including irradiation, misfolded proteins and anti-cancer drugs, favours the survival of cancer cells. It is not surprising then that cancer cells have elevated expression of those chaperones (Garrido et al., 2006). Cancer cells exhibit elevated expressions of Hsp70-2 and Hsp72 (Hsp70-1A) proteins (Daugaard et al., 2005). Hsp70 proteins, including Hsp70-2, Hsc70 and Hsp72 promote cancer cell growth, whilst dual depletion of Hsc70 and Hsp70-2 led to cancer cell death (Rohde et al., 2005). Similarly, dual targeting of Hsc70 and Hsp72 induces G1 arrest, tumour-specific apoptosis and inhibits Hsp90 function (Powers et al., 2008). The high levels of Hsp70 proteins, particularly Hsp72, in cancers confer resistance to current cytotoxics (Sliutz et al., 1996).

The overexpression of Hsp70 can lead to its release with the severity upon detect of cancer cells and they may be used as a marker to discriminate cancer stages. The increased levels of serum Hsp27 and Hsp70 were detected in patients with non-small cell lung cancer (NSCLC) compared to healthy control cases, and significant differences in Hsp70 expression were also found between patients with early and advanced stage NSCLC (Zimmermann et al., 2012). High levels of soluble Hsp70 proteins were detected in patients with colorectal cancers, suggesting that Hsp70 can be a useful and stage-independent prognostic marker in those patients (Kocsis et al., 2011). Similarly, elevated levels of Hsp70 were detectable in plasma of patients with prostate cancer suggesting that it can be used as a biomarker in conjunction with PSA to identify early stages of the disease (Abe et al., 2004). In another study, high levels of serum Hsp70 were measured in patients with breast cancer suggesting the potential use of serum Hsp70 as a diagnostic marker (Gunaldi et al., 2015).

1.5.5 The development of Hsp70 inhibitors

The importance of Hsp70 in cancer highlights a potential opportunity for cancer therapy (Powers et al., 2010). An effort is now being put into the development of small molecule Hsp70 inhibitors that selectively target the activity of Hsc70/Hsp72 without altering the functions of other chaperones (Powers et al., 2010). To date only few chemical compounds have been generated that are selective against Hsp72 and Hsc70 isoforms (Patury et al., 2009). 15-deoxyspergualin (15-DSG) was the first chemical compound that selectively bound to the Hsc70 isoform (Nadeau et al., 1994). A structurally related compound to DSG was the dihydropyrimidine NSC 630668-R/I that reduced the ATPase activity of Hsc70 in yeast (Fewell et al., 2001). Apoptozole is another inhibitor that binds to human Hsc70 and Hsp72 isoforms and was identified from a cell-based screen searching for agents that induce apoptosis (Williams et al., 2008). However, a more detailed analysis of the selectivity and exact mechanism of action, as well as structural information of inhibitor-bound forms of Hsp70, is needed to understand these agents.

Another small-molecule inhibitor, known as pifithrin-μ (2-phenylehtynesulfonamide), was designed to bind to human Hsp72 and disrupts its interaction with client proteins, including APAF1 (apoptotic protease activating factor-1) and p53 (Leu et al., 2009). Surprisingly, this inhibitor selectively binds Hsp72 versus Hsc70, GRP78 and Hsp90. Cell-based experiments showed that this compound promotes cell death in cancer cells, but not in healthy normal fibroblasts (Leu et al., 2009). However, pifithrin-μ is a very simple molecule and unlikely to be that selective.

A dibenzyl-8-aminoadenosine analog (VER-155008) was developed as an Hsp70 inhbiitor and to date has proven to be the most useful selective Hsp70 tool compound (Williamson et al., 2009). VER-155008 binds to Hsp72 with an IC_{50} of 0.5 μM and Hsc70 with IC_{50} of 2.6 μM (Massey et al., 2010). This compound selectively targets Hsp70 isoforms over Hsp90 proteins, and significantly reduces the expression of clients, such as RAF1 and HER2 proteins, causing growth arrest in the HCT116 cancer cell line (Williamson et al., 2009; Massey et al., 2010). Specifically, VER-155008 acts an ATP-competitive inhibitor by blocking the nucleotide-binding domain, and thus it prevents

the catalytic cycle of substrate binding and release that relies on ATP turnover (Schlecht et al., 2013).

Targeting Hsp70 proteins by development of small-molecule inhibitors raises many challenges. The fact that Hsp70 proteins are highly expressed in several tissues, have housekeeping functions, and represent a large family of isoforms with similar structural properties, makes it difficult to selectively target individual functions of these proteins, for example in mitosis (Powers et al., 2010). Additionally, the flexibility of catalytic site has meant that development of more potent and selective agents that can be tested in particular tumour models has proven very difficult.

1.6 NIMA-related protein kinase family

1.6.1 NIMA

The never-in-mitosis A (NIMA) protein of *Aspergillus nidulans* was first identified through a genetic screen for cell division cycle mutants (Oakley and Morris, 1983). In the screen, two types of cell cycle loss-of-function mutants were identified when incubated at the restrictive temperature: firstly, those that were blocked in mitosis (bim) and secondly, those genes that were never in mitosis (nim) and blocked in G2 phase (Morris, 1975; Oakley and Morris, 1983). When cells were returned to the appropriate temperature, nim cells entered mitosis with weak mitotic spindles and abnormal condensation of chromosomes (Osmani and Ye, 1996). It has since been discovered that overexpression of wild-type NIMA protein led to premature entry into mitosis from any point in the cell cycle (Osmani et al., 1991a). NIMA is a 79 kDa protein kinase and its kinase activity is expressed throughout interphase, but peaks at the G2/M transition and drops upon exit from mitosis (Osmani et al., 1991b). Further experiments in the fungus *Aspergillus* showed that degradation of NIMA is important for mitotic exit, suggesting that it also as a master regulator of mitotic progression along with the Cdc2-cyclin B complex (Pu and Osmani, 1995). During mitosis, NIMA phosphorylates Histone 3 at serine 10 and thus, promoting chromosome condensation (De Souza et al., 2000; Davies et al., 2004).

The fungus *Aspergillus* expresses only one NIMA-related gene or NEK, as do the yeast *Saccharomyces cerevisiae*, where it is known as kin3, and *Schizosaccharomyces pombe*, when it is called fin1 (Fry et al., 2012). The yeast Neks have a range of cellular functions from chromatin condensation, spindle assembly and cytokinesis, and cell cycle progression, but are not essential for viability (De Souza et al., 2000; Grallert et al., 2004). Neks have been identified in many organisms, from protists, such as *Chlamydomonas,* to higher eukaryotes, such as *Drosophila*, *Xenopus*, mice and humans (Fry et al., 2012). The first to be identified in mouse was called Nek1, but since then additional Neks have been revealed in mammals (Letwin et al., 1992; Schultz and Nigg, 1993).

The human genome encodes eleven NEKs, known as Nek1 to Nek11 (Figure 1.8). The structural features of these proteins include an N-terminal catalytic domain that contains motifs typical of serine/threonine kinase and shares approximately 40-45% sequence similarity with the *Aspergillus* NIMA kinase domain (O'Connell et al., 2003). However, Nek10 is completely different by having the kinase domain at the centre, but its amino acid sequence still allocates it to the Nek family. On the other hand, the C-terminal regions of Neks are highly variable in amino acid sequence, length and domain organisation. For example, Nek6 and Nek7 lack a C-terminal domain and consist of only a kinase domain with a short N-terminal extension that may required for substrate recognition (Vaz Meirelles et al., 2010). An oligomerisation motif, usually a coiled-coil, is often found in the C-terminal regions of the Neks, and promotes oligomerisation, autophosphorylation and activation. Nek8 and Nek9 also share a RCC1-like pre-included β-propeller domain in their C-terminal regions. This variability implies different functions, localisation and activity of each Nek protein within the cell, although these remain far from characterised in detail (Table 1.3). However, we can say with confidence that members of the Nek family are implicated in mitotic progression, microtubule regulation, cell cycle checkpoint control, the DNA damage response (DDR) and ciliogenesis (Fry et al., 2012).

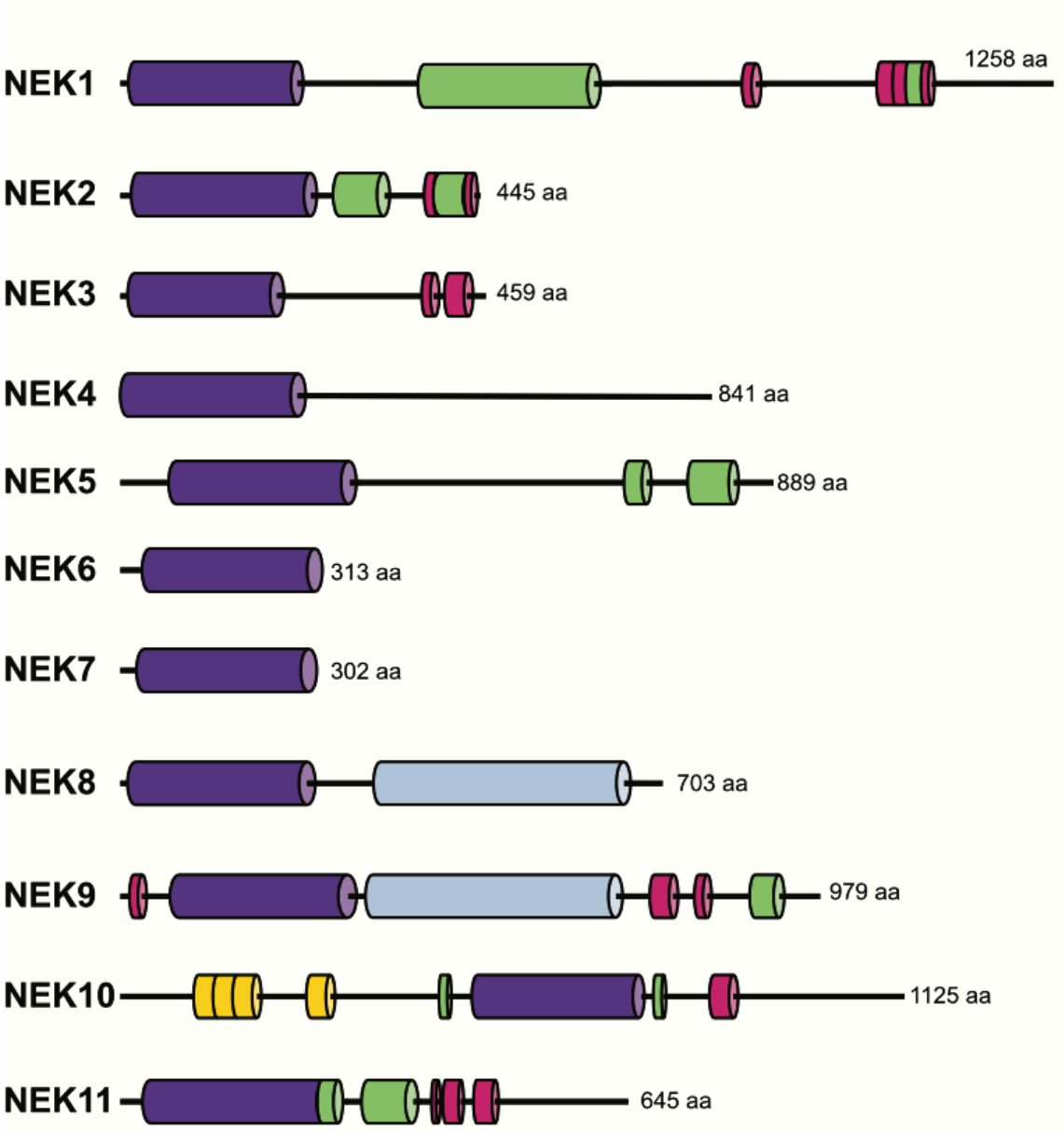

Figure 1.8 The human NIMA-related protein kinase family

A schematic representation of the human NIMA-related kinase (Nek) family. NEKs are organised in different domains as shown above with the kinase domain (purple), coiled-coil domains (green), PEST-like degradation motifs (red), RCC1 (regulator of chromatin condensation 1) domains (light blue) and armadillo repeats (yellow). Amino acids (aa) are indicated. From Fry et al (2012).

NEK	Activity	Localisation	Function
NEK1	Genotoxic insults (IR, UV, crosslinking agents, oxidative injury)	Cytoplasm, centrosomes, cilia, sites of DNA damage	Ciliogenesis and DDR
NEK2	S, G2-M phases	Centrosomes	Centrosome separation
NEK3	Prolactin receptor stimulation	Cytoplasm	Prolactin signalling
NEK4	?	Basal bodies	Ciliogenesis
NEK5	?	?	Centrosome separation
NEK6	Activated by NEK9, mitosis	Mitotic spindle	Spindle assembly
NEK7	Activated by NEK9, mitosis	Weakly to spindle poles	Spindle assembly
NEK8	Serum starvation	Nucleus, centrosomes, cilia	Ciliogenesis, DDR
NEK9	Mitosis (Activated by Cdk1 and Plk1)	Mainly cytoplasmic, nuclear, spindle poles	Spindle assembly
NEK10	UV, G2-M	?	DDR
NEK11	DNA replication inhibitors and genotoxic insults, S to the G2-M phase	Nucleus/Nucleoli, spindle microtubules	DDR

Table 1.3 The activation, localisation and function of human Neks

A summary of the activation, localisation and function of each member of the known Nek kinase family. Unknown function (?). Adapted from Fry et al (2012).

1.6.2 Neks in mitotic regulation

It has been shown that overexpression of NIMA induces premature mitotic entry from any stage of the cell cycle in *Aspergillus* cells, as well as in *Xenopus* oocytes, fission yeast and human cells (Lu and Hunter, 1995). A plethora of experiments has since studied the involvement of the human Neks in mitosis, although no single Nek appears absolutely necessary for mitotic entry. It has been established that four human Neks; Nek2, Nek6, Nek7 and Nek9, are directly involved in mitotic events, including centrosome separation, mitotic spindle assembly and, potentially, nuclear envelope breakdown and chromatin condensation (Fry et al., 2012).

Nek2 is the most well characterised member of the Nek family and is the most closely related by similarity in the catalytic domain to *Aspergillus* NIMA (Schultz et al., 1994). Nek2 is localised to the centrosome and is most highly expressed in S and G2 phases (Fry et al., 1998b). There are at least three isoforms of Nek2, the Nek2A, Nek2B and Nek2C, that are products of differential splicing. Experimental studies showed that overexpression of Nek2A led to premature centrosome separation (Faragher and Fry, 2003), whereas depletion of Nek2A blocks centrosome disjunction without affecting mitotic entry (Fletcher et al., 2005). These experiments suggest that Nek2 has a direct role in centrosome disjunction and formation of mitotic spindle. Functional studies identified two major components of the intercentriolar linker, the C-Nap1 (also known as CEP250) and rootletin as substrates of Nek2. These centrosome linker proteins are phosphorylated by Nek2, leading to disassembly of the intercentriolar linker present in interphase cell and subsequent loss of centrosome cohesion at the G2/M transition (Bahe et al., 2005; Faragher and Fry, 2003; Yang et al., 2006). There is additional evidence suggesting a potential role of Nek2 in the spindle assembly checkpoint with Nek2 interacting with the kinetochore protein, Hec1/Ndc80, and loss of function of Nek2 disrupting Mad2 localisation at the kinetochores (Moniz et al., 2011). Furthermore, Nek2 localises to the midbody of cells in cytokinesis in *Drosophila* cells, and its overexpression disrupts the localisation of actin and anillin proteins during cleavage furrow formation leading to cytokinesis failure (Prigent et al., 2005).

The Nek6, Nek7 and Nek9 kinases also contributed to formation of the mitotic spindle (O'Regan et al., 2007; Sdelci et al., 2011). Antibody microinjection and RNAi depletion studies showed that these three kinases are essential for spindle formation (Roig et al., 2002). The use of inactive or truncated Nek9 mutants also leads to chromosome segregation defects and aberrant spindle formation (Roig et al., 2002; O'Regan and Fry, 2009). Experiments in *Xenopus* egg extracts revealed that depletion of Nek9 inhibited formation of microtubule asters through either the centrosome or chromatin-mediated pathway (Roig et al., 2005). The three kinases act in a cascade with Nek9 to be the upstream activator of Nek6 and Nek7 (Figure 1.8) (Belham et al., 2003). The interaction between Nek9 and Nek6 is strongly detected during mitosis, when Nek9 phosphorylates and activates Nek6 (Belham et al., 2003). At the same time Nek9 also phosphorylates Nek7. Structural studies have shown that Nek9 also activates Nek6 and Nek7 in an allosteric manner by binding and disrupting their auto-inhibitory conformation of these kinases (Richards et al., 2009; Haq et al., 2015).

The Nek6 and Nek7 kinases are very closely related, with more than 85% sequence similarity in the catalytic domain and no C-terminal regulatory domain (Kandli et al., 2000). As indicated above, these two kinases have important roles in mitotic spindle formation, as well as cytokinesis (Yin et al., 2003). Experimental studies showed that overexpression of kinase-inactive Nek6 or Nek7 led to spindle abnormalities, nuclear abnormalities, mitotic arrest and apoptosis (O'Regan and Fry, 2009; Yin et al., 2003). Depletion of Nek6 or Nek7 led to weak mitotic spindles with reduced K-fibres and activation of the spindle assembly checkpoint (O'Regan and Fry, 2009). Like Nek2, Nek6 and Nek7 also localise at the midbody in late mitotic cells with high levels of Nek6 activity during cytokinesis (Kim et al., 2007; O'Regan and Fry, 2009). Additionally, Nek7 and Nek9 kinases localise weakly at centrosomes and contribute to microtubule nucleation and organisation of spindle poles (O'Regan et al., 2007). Nek7 localises at centrosome and is important for recruiting γ-tubulin to spindle poles, as depletion of Nek7 reduces the γ-tubulin levels at the centrosome (Kim et al., 2007). Like Nek7, Nek9 also contributes to nucleation of microtubules by interacting with components of the γ-

TuRC and phosphorylating at recruiting the adaptor protein NEDD1/ γ-TuRC (Roig et al., 2005).

It is believed that one mechanism through which these kinases regulate mitotic spindle assembly in via phosphorylation of microtubule-associated proteins, such as Eg5 (Figure 1.9) (Betran et al., 2011; Rapley et al., 2008). Eg5, a KIF11 kinesin-like protein, is a plus-end directed motor that crosslinks microtubules in an anti-parallel fashion promoting spindle pole separation (Sawin and Mitchison, 1995). Nek6 phosphorylates Eg5 to recruit it to spindle pole, with depletion of Nek6 or Nek9 leading to formation of monopolar spindles (Betran et al., 2011). In a separate set of experiments, the Hsp72 chaperone protein was found to be phosphorylated by Nek6 during mitosis (O'Regan et al., 2015). Nek6 phosphorylates Hsp72 at threonine 66 (T66) allowing Hsp72 to localise to the mitotic spindle with depletion or inhibition of Hsp72 leading to abnormal mitotic spindles in HeLa cells. Further studies revealed that Hsp72 facilitates mitotic spindle assembly through stabilisation and recruitment of the ch-TOG/TACC3 complex that provides K-fibre stability (O'Regan et al., 2015).

1.6.3 Neks in checkpoint control and ciliogenesis

Apart from the mitotic Neks discussed in section 1.6.2, other members of the Nek family have roles in ciliogenesis, the DNA damage response (DDR) and possibly growth-factor regulated signalling pathways (Moniz et al., 2011; Fry et al., 2012). Nek1 is the longest of the Nek family and it has 42% sequence similarity at the N-terminal catalytic domain to *Aspergillus* NIMA, as well as two coiled-coil motifs and PEST-like sequences (Letwin et al., 1992; Fry et al., 2012). Studies have shown that Nek1 is directly implicated in the DNA damage response through a pathway independent of ATM and ATR kinases (Chen et al., 2011). Nek1 kinase is involved in sensing and repair of DNA strand breaks, as well as DNA damage checkpoint control (Pelegrini et al., 2010; Chen et al., 2011). The absence of Nek1 activity causes failure to activate the Chk1 and Chk2 kinases, and thus, no arrest at G1/S or M checkpoints in the presence of DNA damage (Chen et al., 2011). Interestingly,

Nek1 localises at centrosomes during interphase and mitosis, as well as to basal bodies of primary cilia suggesting attractive roles in ciliogenesis (Shalom et al., 2008).

Indeed, overexpression of mutated Nek1 in mouse embryonic fibroblasts led to abnormal cilia formation, while the kinase-inactive Nek1 mutant perturbed centrosome stability (White and Quarmby, 2008; Shalom et al., 2008). Importantly, mutations in the Nek1 kinase have also been identified in patients with ciliopathy-related disorders, such as short-rib polydactyly syndrome Majewski (Thiel et a., 2011).

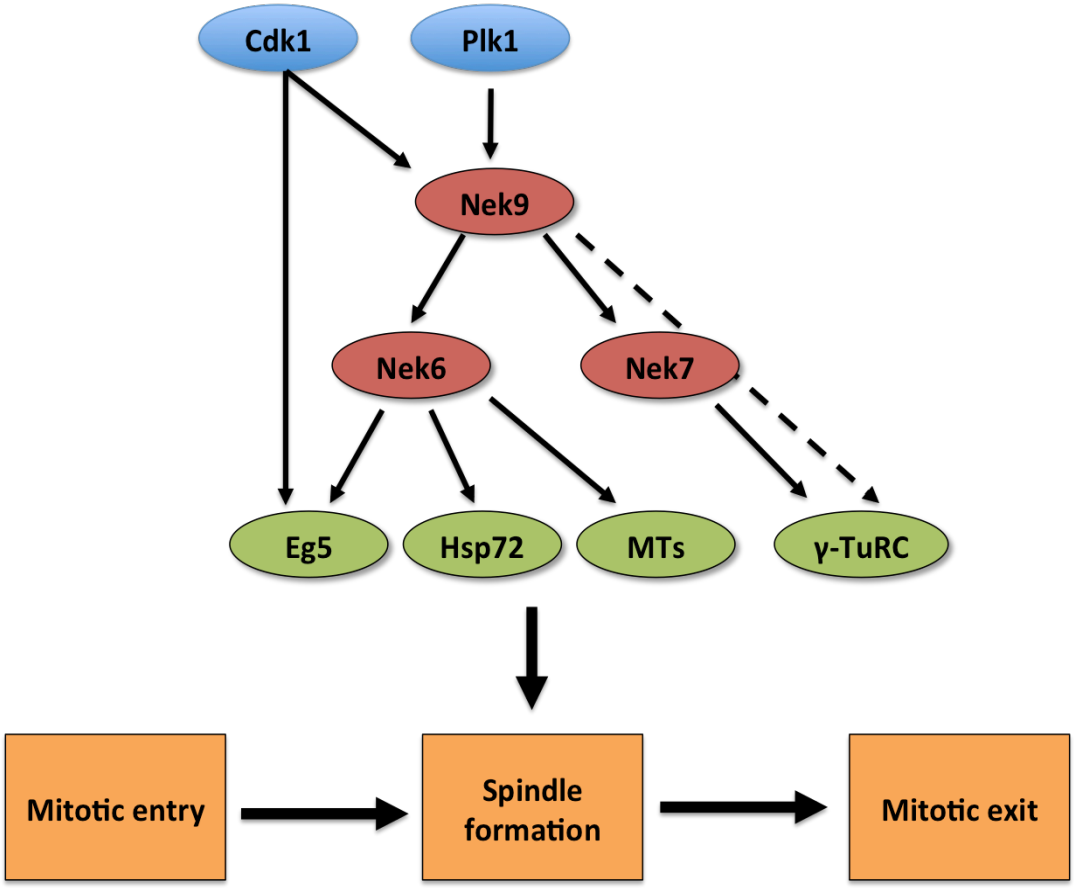

Figure 1.9 The role of Neks in mitotic progression

Upon mitotic entry, CDK1 and PLK1 kinases phosphorylate and activate Nek9. The activated form of Nek9 then phosphorylates and activates Nek6 and Nek7 kinases by allosteric binding. Nek6 kinase in turn phosphorylates microtubule components, Eg5 and Hsp72, whereas Nek7 may phosphorylate components of the γ-TuRC. Nek9 also directly phosphorylates the γ-TuRC adapter protein, NEDD1. All of these proteins contribute to formation of the mitotic spindle. Adapted from Fry et al (2012).

Like Nek1, another member of the Nek family, Nek8, is implicated in both the DDR and ciliogenesis. Nek8 consists of an N-terminal kinase domain and has an RCC1-like domain. Firstly, Nek8 is also implicated in the DNA replication stress response, and is able to interact with the DNA damage checkpoint components, ATR and Chk1 (Choi et al., 2013). However, similar to Nek1, Nek8 localises to primary cilia in kidney epithelial cells. However, Nek8 localisation is lost from primary cilia and increased cilia length was observed in *jck* murine cells (Smith et al., 2006). Nek8 mutations are present in the juvenile cystic kidney (*jck*) mutant mouse strain, and these confer characteristics of polycystic kidney disease (PKD) (Liu et al., 2002). Furthermore, studies showed that Nek8 interacts with polycystin-2 (PC2), a protein that is frequently mutated in autosomal dominant PKD (ADPKD) (Sohara et al., 2008). Apart from PKD, Nek8 mutations are also found in nephronophthisis, a juvenile onset renal ciliopathy disease (Otto et al., 2008).

Another Nek kinase, Nek4, has been suggested to interact with two ciliopathy-associated protein homologs, RPGR interacting protein 1 (RPGRIP1) and RPGRIP1-like protein (RPGRIP1L) to regulate cilium stability (Coene et al., 2011). As for Nek1 and Nek8, ciliogenesis, Nek4 is implicated not only in ciliogenesis but also in the DDR pathway (Ngugen et al., 2012). Loss of Nek4 activity leads to a non-functional DNA damage checkpoint that fails to detect double strand breaks. Nek4 interacts with Ku70, Ku80 and DNA-PKcs forming the DNA-PK complex that enables a response to DNA damage, including both cell cycle arrest and activation of double-strand break repair via non-heterogenous end-joining (Nguyen et al., 2012).

Finally, Nek11 is also implicated in DNA damage response pathways (Sabir et al., 2015; Noguchi et al., 2002). Nek11 consists of an N-terminal catalytic domain that has 33% sequence similarity to *Aspergillus* NIMA, and a C-terminal domain consisting of two coiled-coil motifs and three PEST-like sequences (Noguchi et al., 2002). There are 4 splice variants of Nek11: Nek11 Long (74 kDa), Nek11 Short (54 kDa), Nek11C (56 kDa) and Nek11D (69 kDa) (Noguchi et al., 2002; Sahota et al., 2010; Sabir et al., 2015). Nek11 is highly expressed from S phase to the G2/M transition and its expression rapidly

increases upon DNA damage (Melixetian et al., 2009). However, inhibition of ATM and ATR kinases leads to loss of Nek11 activation without G2/M arrest (Melixetian et al., 2009). The presence of ionizing radiation leads to DNA breaks, which activates ATM/ATR kinases and in turn to Chk1 phosphorylation. The active Chk1 kinase phosphorylates Nek11 and subsequently Nek11 phosphorylates Cdc25A promoting its degradation through binding of the ubiquitin ligase $SCF^{\beta\text{-}TrCP}$. Therefore, this degradation prevents Cdk1/cyclin B activation and mitotic entry (Melixetian et al., 2009; Fry et al., 2012).

Like Nek11, Nek10 has a role in the DNA damage response (Moniz and Stambolic, 2011). Nek10 is implicated in the G2-M DNA damage checkpoint upon UV irradiation (Moniz and Stambolic, 2011). In the presence of UV irradiation, Nek10 forms a trimeric complex with MEK1 and Raf-1. This form activates MEK1, which in turn leads to phosphorylation and activation of ERK1/2 (extracellular signal-related kinase 1/2) and thus G2-M checkpoint activation and cell cycle arrest (Moniz and Stambolic, 2011). Taken together then, the majority of Neks have been implicated either in mitotic progression, the DNA damage response and/or ciliogenesis.

1.7 Aims and objectives

Most vertebrate cells contain two centrosomes that are essential for formation of a functional bipolar spindle. However, it has been frequently observed that the majority of cancer cells not only possess extra centrosomes, but have specific mechanisms, that allow them to cluster them into two poles forming a pseudo-bipolar spindle during mitosis allowing cell survival. However, this behaviour leads to chromosome segregation defects that contribute to chromosomal instability and aneuploidy. The pathways that enable clustering of amplified centrosomes remain poorly understood. Yet, targeting these pathways offers a great promise to selectively kill cells with amplified centrosomes through triggering multipolar spindle formation and mitotic catastrophe (Odgen et al., 2012).

The aims of this project were to (1) determine whether Nek6 and Nek7 kinases and Hsp70 chaperones are implicated in centrosome clustering, (2) to understand the importance of downstream proteins, including ch-TOG, TACC3, dynein and dynactin in MT-kinetochore attachments during centrosome clustering and (3) to explore whether loss of function of Nek6 and Hsp72 proteins has effects in mitotic progression in cancer and non-cancer derived cells.

The experimental objectives of the result chapters are outlined below:

1) To validate centrosome amplification and clustering in adherent and suspension cell lines by using fixed and live cell-imaging methods.

2) Based on the results from objective 1, functional studies will be carried out using siRNA-depletion of Hsp72 or Hsc70 in combination with chemical inhibition and analysed by immunofluorescence microscopy and live cell imaging.

3) In addition, the role of Nek6 and Nek7 in centrosome clustering will be examined using siRNA-depletion and analysed by microscopy. To determine the upstream regulators of Nek6-Hsp72 pathway, chemical inhibitors of Aurora-A and Plk1 will be used to determine the localisation of Hsp72 by immunofluorescence microscopy.

4) To understand how the Nek6-Hsp72 pathway regulates centrosome clustering, functional studies will be carried out using depletion and chemical inhibition of Nek6 and Hsp72 proteins to examine the localisation of dynein/dynactin complex to mitotic spindle and specifically, in MT-kinetochore attachments sites.

5) To optimise immunoprecipitation of dynein I.C. from MDA-MB-231 cells for the purpose of identifying potential interacting partners.

6) To determine the importance of Nek6 and Hsp72 in mitotic progression in cancer and non-cancer derived cells.

Chapter 2

Materials and Methods

2.1 MATERIALS

2.1.1 Reagents

All chemicals were of analytical grade purity or higher and the majority of the chemicals purchased from Sigma (Poole, UK) or Roche (Lewis, UK), or else obtained as stated below. The cell culture solutions were supplied by Gibco Invitrogen (Paisley, UK).

Reagent	Supplier
Precision Plus all blue protein standards	Bio-Rad (Hemel Hempstead, UK)
BCA protein assay reagent	
Hoechst 33258	Calbiochem (Nottingham, UK)
Bovine serum albumin (BSA) fraction V	Fisher Scientific (Loughborough, UK)
EDTA; EGTA; KCL; MgCl2; NaCl;	
Ethanol	
Glycerol	
Methanol	
Tween-20	
ProtoFLOWgel (30% w/v acrylamide)	Flowgen Bioscience (Nottingham, UK)
X-Ray film	Scienftific Lab Supplies (Yorkshire, UK)
Lipofectamine 2000 reagent	Invitrogen/Gibco – Part of Life Sciences (Paisley, UK)
RNase A	
D-MEM with GlutaMAX™-I	
D-MEM:F12 with GlutaMAX™-I	
RPMI with GlutaMAX™-I	
Opti-MEM with GlutaMAX™-I	
Penicillin/streptomycin	
Heat-inactivated Foetal Bovine Serum	
SDS	Melford (Suffolk, UK)
ECL Western blotting reagent	Pierce (Rockford, USA)
Nitrocellulose transfer membrane	GE Healthcare Life Sciences Amersham
Coverslips 22mm/13mm diameter, No 1.5 Glass slides	VWR International (Lutterworth, UK)

2.1.2 Drugs

The following drugs were dissolved in DMSO, unless stated below. The final concentration of each drug was prepared in fresh pre-warmed culture media and mixed well before adding to cells.

Drug	[Stock]	[Final]	Supplier
Aphidicolin	1.6 mg/ml	1.6 µg/ml	Sigma (A0781)
BI-2536 (Plk1 inhibitor)	10 mM	100 nM	MedChem Express (HY-50698)
Griseofulvin	100 mM in DMF	5, 10 or 20 µM	Sigma (G4753)
MLN8054 (Aurora-A inhibitor)	10 mM	0.5 or 1 µM	MedChem Express (HY-10180)
Nocodazole	5 mM	0.5 or 5 µM	Sigma (M1404)
RO-3306 (Cdk1 inhibitor)	10 mM	10 µM	Calbiochem (217699)
VER-155008 (Hsp70 inhibitor)	100 mM	5, 10 or 20 µM	Tocris Bioscience (3803)

2.1.3 Antibodies

2.1.3.1 Primary antibodies

A list of primary antibodies used for Western blotting (WB), indirect immunofluorescence (IF), immunoprecipitation (IP) or immunohistochemistry (IHC). Each antibody is represented with its working dilution and in brackets the final concentration where known. The product code for each antibody is shown in brackets in the supplier column.

Antibody	Dilution	Supplier
Anti- α-tubulin (Mouse monoclonal)	1:2000 (0.3 µg/ml) (IF)	Sigma (T5168)
Anti-α-tubulin (Rabbit monoclonal)	1:2000 (WB); 1:200 (IF)	Abcam (ab15246)
Anti-α-tubulin (Goat polyclonal)	1:100 (1 µg/ml) (IF)	Santa-Cruz Biotechnology (sc-31779)
Anti- γ-tubulin (Mouse monoclonal)	1:500 (0.8 µg/ml) (IF)	Sigma (T6557)
Anti- γ-tubulin (Rabbit monoclonal)	1:2000 (WB)	Sigma (T3559)
Anti- γ-tubulin (Goat polyclonal)	1:250 (0.4 µg/ml) (IF)	Santa-Cruz Biotechnology (sc-7396)
Anti-CEP135 (Rabbit monoclonal)	1:500 (2 µg/ml) (IF)	OriGene (TA311705)
Anti- Centrin-2 (N-17) (Rabbit polyclonal)	1:500 (0.4 µg/ml) (IF)	Santa-Cruz Biotechnology (sc-27793)
Anti-pericentrin (Rabbit monoclonal)	1:500 (IF); 1:4500 (IHC)	Abcam (ab4448)
Anti-ch-TOG (Rabbit polyclonal)	1:5000 (WB)	QED Bioscences (34032)
Anti-TACC3 (H-300) (Rabbit monoclonal)	1:1000 (WB)	Santa-Cruz Biotechnology (sc-22773)
TPX2 (H-300) (Rabbit polyclonal)	1:1000 (WB)	Santa-Cruz Biotechnology (sc-32863)
GAPDH (14C10) (Rabbit monoclonal)	1:1000 (WB)	Cell Signaling (2118)
NEK6 (Rabbit monoclonal)	1:1000 (WB)	Abcam (ab133494)
NEK7 (mouse polyclonal)	1:500 (WB)	Abcam (ab68060)
Anti-Hsp72 (Mouse monoclonal)	1:500 (WB); 1:250 (IF)	Enzo life Sciences (adi-spa-810)
Anti-Hsc70 (Mouse monoclonal)	1:200 (1 µg/ml) (WB)	Santa-Cruz Biotechnology (sc-7298)
Anti-Hsc70 (13D3) (Mouse monoclonal)	1:100 (IF)	Abcam (ab2788)
Anti - Dynein I.C (mouse monoclonal)	1:500 (WB); 1:1000 (IF); 1:100 (IP)	Millipore (MAB1618)
Anti- p150Glued (mouse monoclonal)	1:500 (WB); 1:500 (IF)	BD Transduction (612709)
Anti-Ki-67 (Clone MIB-1) (Mouse)	1:1000 (IHC)	Dako
Anti-CENP-A (mouse monoclonal)	1:500 (2 µg/ml) (IF)	Abcam (ab13939)
Anti-CENP-E (mouse monoclonal)	1:250 (0.8 µg/ml) (IF)	Santa-Cruz Biotechnology(sc-376685)
Anti-CENP-I (Rabbit polyclonal)	1:1000 (IF)	Bethyl Laboratories (ab118796)
Mouse IgGs	2 mg/ml	Sigma

2.1.3.2 Secondary antibodies

Secondary Antibody	Dilution	Supplier
Goat anti-mouse Alexa 488	1:200 (10 µg/ml)	Molecular probes- Life technologies (Paisley. UK)
Goat anti-rabbit Alexa 488	1:200 (10 µg/ml)	
Goat anti-mouse Alexa 594	1:200 (10 µg/ml)	
Goat anti-rabbit Alexa 594	1:200 (10 µg/ml)	
Donkey anti-goat rabbit 647	1:1000	
Donkey anti-mouse 594	1:1000	
Donkey anti-rabbit 488	1:1000	
Goat anti-mouse IgG horseradish peroxidase conjugate	1:5000	Bethyl Laboratories
Goat anti-rabbit horseradish peroxidase conjugate	1:1000	Sigma

2.2 CELL CULTURE

2.2.1 Cell line maintenance

MDA-MB-231, HeLa, NIE-115, HBL-100 and SCC-114 cells were cultured in DMEM (Dulbecco's Modified Eagle Medium) with GlutaMAX^{TM} (Life Technologies, Invitrogen) supplemented with 10% heat-inactivated foetal bovine serum (FBS; Life Technologies, Invitrogen), 100 U/ml penicillin and 100 µg/ml streptomycin (1% Pen/Strep). hTERT-RPE1 cells were cultured in F12 Nutrient Mixture (Hams) DMEM GlutaMAX^{TM} supplemented with 0.348% sodium bicarbonate solution ($NaHCO_3$), 10% v/v FBS and pen/strep (100 U/ml and 100 µg/ml, respectively). Primary B-lymphocytes (PBL), acute lymphoblastic leukaemia (ALL) cells and HBL-100 cells were cultured in RPMI GlutaMAX^{TM} supplemented with 10% v/v FBS, pen/strep (100 U/ml and 100 µg/ml, respectively). In collaboration with Professor Martin Dyer's group in the department of Molecular and Cell Biology and the Leicester Royal Infirmary hospital (Leicester, UK), chronic lymphoblastic leukaemia (CLL) cells from patients were harvested and cultured using a feeder layer of human CD40 ligand (CD154) expressing mouse fibroblast L-cells together with 10 ng/ml rhIL4 (Samuel et al., 2016). For ethical reasons, patient names remained unknown and we labelled samples with numbers.

Cell lines were maintained at 37^{o}C in a humidified 5% CO_2 atmosphere and passaged upon reaching 80-90% confluency. Adherent cells were washed with 1x PBS (phosphate buffer saline; 137 mM NaCl, 8.1 mM Na_2HPO_4, 2.7 mM KCl, 1.4 mM KH_2PO_4, pH 7.4) and detached with 1x PBS containing 0.5 mM EDTA for 10 minutes. Cells were seeded into appropriate dishes containing pre-warmed growth media. Suspension cells were harvested and seeded at the appropriate density into fresh flasks.

Cell lines categorised based on their cell type, tissue/disease, culture method and supplier information. ALL (Acute lymphoblastic leukaemia).

Cell line	Cell type	Tissue/Disease	Culture method	Supplier
MDA-MB-231	Adherent-epithelial	Breast/ adenocarcinoma	DMEM GlutaMAX™	Cell Lines Service
HeLa	Adherent-epithelial	Cervix/adenocarcinoma	DMEM GlutaMAX™	Cell Lines Service
NIE-115 (mouse)	Adherent-neuroblast	Brain/neuroblastoma	DMEM GlutaMAX™	ATCC
SCC-114	Adherent-epithelial	Squamous cell cariconoma	DMEM GlutaMAX™	ATCC
HBL-100	Adherent-epithelial	Breast/healthy mammary gland	DMEM GlutaMAX™	Cell Lines Service
hTERT-RPE1	Adherent-epithelial	Retina, eye/ healthy	F12-DMEM GlutaMAX™	ATCC
14183	Suspension	Peripheral-B lymphocytes/healthy	RPMI GlutaMAX™	Coriell Institute
14295	Suspension	Peripheral-B lymphocytes/Healthy	RPMI GlutaMAX™	Coriell Institute
Hal-01	Suspension	Peripheral-B lymphocytes/ALL	RPMI GlutaMAX™	Leibniz Institute DSMZ
NALM-6	Suspension	Peripheral-B lymphocytes/ALL	RPMI GlutaMAX™	Leibniz Institute DSMZ
MHH-CALL4	Suspension	Peripheral-B lymphocytes/ALL	RPMI GlutaMAX™	Leibniz Institute DSMZ
K231	Suspension	Peripheral-B lymphocytes/ALL	RPMI GlutaMAX™	Leibniz Institute DSMZ
MUTZ5	Suspension	Peripheral-B lymphocytes/ALL	RPMI GlutaMAX™	Leibniz Institute DSMZ
Kasumi-2	Suspension	Peripheral-B lymphocytes/ALL	RPMI GlutaMAX™	Leibniz Institute DSMZ
SEM	Suspension	Peripheral-B lymphocytes/ALL	RPMI GlutaMAX™	Leibniz Institute DSMZ
Z33	Suspension	Peripheral-B lymphocytes/ALL	RPMI GlutaMAX™	Leibniz Institute DSMZ
KOPN8	Suspension	Peripheral-B lymphocytes/ALL	RPMI GlutaMAX™	Leibniz Institute DSMZ
REH	Suspension	Peripheral-B lymphocytes/ALL	RPMI GlutaMAX™	Leibniz Institute DSMZ

2.2.2 Storage of cell lines

Cells lines were washed with 1x PBS, detached using PBS-EDTA and pelleted by centrifugation at 1100 rpm for 5 minutes. The supernatant was removed and the pellet resuspended in 5% v/v DMSO in FBS (MDA-MB-231, SCC-114 NIE-115, PBL and ALL) or 10% v/v DMSO in FBS (HeLa and HBL-100) and transferred to cryotubes (TPP Helena Biosciences). The cryotubes were then incubated in an isopropanol filled cryo 1^{o}C freezing container (Nalgene) and stored at -80^{o}C for at least 16 hours. The cryotubes were then transferred to liquid nitrogen for long-term storage.

To thaw cells, a cryotube was removed from liquid nitrogen and immediately thawed in a 37^{o}C waterbath. Cells were then washed once with the appropriate pre-warmed media, centrifuged (1100 rpm, 5 minutes) at room temperature, resuspended in fresh media and transferred to a culture dish or flask.

2.2.3 Drug treatment of cell lines

Asynchronously growing cells were seeded to give 1 x 10^5 cells/ml either on a 6-well plate or 6 cm dish the day before treatment. The next day, cells were incubated with the appropriate dilutions of each drug shown in table 2.1.2. For aphidicolin or nocodazole treatment, cells were treated for 16 hours, whereas treatment with RO-3306 was performed for 40 hours. Unless otherwise stated, the rest of the drugs were used for 4 hour treatment of cells. Control cells were treated with the same volume of DMSO.

2.2.4 Transient transfections

Asynchronously growing cells were seeded in a 6-well plate 24 hours prior to transfection to reach 70-80% confluency on the day of transfection. Briefly, plasmid DNA and lipofectamine 2000 were mixed at a ratio of 1 µg: 4 µl in Opti-MEM reduced serum medium (Invitrogen), according to the manufacturer's instructions. Transfection mixture was added drop-wise to cell on which the growth media had been replaced with Opti-

MEM media. The plates were incubated for 5 hours after which the media was replaced with pre-warmed growth media and incubated for a further 24 hours before being processed as required.

2.2.5 Centrosome amplification assay

Asynchronously growing cells were plated onto acid-etched glass coverslips at 40% confluency and cultured overnight. The following day, cells were washed once with 1x PBS and placed in fresh media containing 1.6 μg/ml aphidicolin for 16 hours. After treatment, cells were washed once with 1x PBS and released in fresh growth media for 4 hours. Following release, media were replaced with 10 μM RO-3306 and incubated for 40 hours. At the end of the treatment, cells were then fixed and processed for immunofluorescence microscopy.

2.2.6 Microtubule depolymerisation/re-growth assay

Cells were plated onto acid-etched glass coverslips at 40% confluency and cultured overnight. The following day, cells were washed once with 1x PBS and synchronised in M-phase by incubation for 16 hours with 500 ng/ml nocodazole. Cells were then released into a nocodazole-free media and fixed at the required times and analysed by immunofluorescence microscopy.

2.2.7 RNA interference

Cells were seeded in 6-well plates at approximately 30% confluency in Opti-MEM Reduced Serum Medium supplemented with 10% FBS containing no antibiotics and cultured overnight. The following day, cells were washed once with 1x PBS and incubated with 100 nM siRNA oligonucleotides. siRNA duplexes were transfected using Oligofectamine (Invitrogen, UK) according to manufacturer's instructions. Cells were incubated with the siRNA mixture and Opti-MEM media for 5 hours ($37^{o}C$, 5% CO_2). Opti-

MEM with 30% v/v FBS (no antibiotic) was then added to cells and incubated for 72 hours before analysis by immunofluorescence microscopy or Western blotting.

2.2.8 Flow cytometry

To determine cell cycle profiles, cells were harvested, centrifuged at 1100 rpm for 5 minutes at room temperature and pellets re-suspended in 150 µl PBS. Cells were then fixed with 2 ml of ice-cold 70% ethanol in a drop-wise manner, whilst gently vortexing and incubated for 30 minutes at 4^{o}C or kept at -20^{o}C for a week. Briefly, cells were washed twice in 1x PBS, spun at 3000 rpm for 5 minutes at 4^{o}C and re-suspended in 1x PBS containing 100 µg/ml RNase A and 50 µg/ml propidium iodide (PI). Samples were transferred into FACS tubes and incubated overnight at 4^{o}C in the dark and analysed for flow cytometry using a BD FACScanto^{TM} II instrument and analysed using FACSDiva^{TM} 6.0 software (Becton Dickinson). 10,000 events were recorded in each sample to analyse their DNA content.

2.3 MICROSCOPY

2.3.1 Indirect immunofluorescence microscopy

2.3.1.1 Adherent cell line

Cells were plated on acid-etched glass coverslips and treated as appropriate. Cells were washed in 1x PBS, fixed and permeabilized in ice-cold methanol at -20^{o}C for 30 minutes. Coverslips were then washed three times with 1x PBS for 5 minutes each and blocked in 1x PBS supplemented with 1% w/v BSA and 0.2% Triton X-100 for 60 minutes. In the meantime, primary antibodies (Table 2.1.3.1) were diluted in 1x PBS with 3% w/v BSA and spun at 10,000 rpm for 3 minutes to remove any insoluble aggregates. Each coverslip was incubated with 150 µl of primary antibody solution for 2 hours. After incubation, coverslips were washed three times in 1x PBS for 5 minutes each. The secondary antibodies (Table 2.1.3.2) were diluted in 1x PBS supplemented with 1% w/v BSA and spun as before. Coverslips were incubated with the secondary antibody solution

and Hoechst 33528 for 1 hour in the dark at room temperature. After incubation, coverslips were washed again three times in 1x PBS for 5 minutes each and mounted on a glass slide with a drop of mountant solution (80% v/v glycerol, 3% w/v n-propyl-gallate in 1x PBS). Coverslips edges were sealed with clear nail varnish and kept in the dark at 4^{o}C.

A slightly modified staining protocol was used for the Hsp72 and Hsc70 antibodies. Coverslips were washed with 1x PBS and incubated with a pre-extraction buffer (60 mM Pipes, 25 mM Hepes, pH7.4, 10 mM EGTA, 2 mM $MgCl_2$, and 1% Triton X-100) for 30 seconds before fixation with ice-cold methanol. After pre-extraction, the procedure for antibody staining was performed as described above. Fixed cell specimens were analysed and imaged on a Leica TCS SP5 confocal microscope equipped with a Leica DMI 6000B inverted microscope using a 63x oil objective with numerical aperture 1.4. Confocal stills were analysed as maximum intensity projections using LAS-AF software (Leica).

2.3.1.2 Suspension cell line

Suspension cells were grown in the appropriate dilution. When cells reached a density of 1x 10^6 cells/ml, as counted using a haemocytometer, were harvested and spun at 500 rpm for 5 minutes. Cells were washed with 1x PBS and spun again. Cells were re-suspended in 100-150 µl fresh warm media and seeded on a superfrost plus glass slide (Thermo) that coated with a positive charged surface to allow electrostatically attachment of cells. Each glass slide was marked with two circles using a PAP pen (Abcam). Slides were placed in a humidified chamber to prevent the cells from drying out. 100-150 µl of suspension cells were added inside each circle and slides were incubated for 30 minutes at room temperature to allow the cells to adhere. The liquid was tapped off and 50-100 µl of ice-cold methanol applied to each circle. Slides were incubated for 10 minutes at -20^{o}C. Cells were washed three times with 100 µl of PBS. Each circle was then blocked with 100 µl of blocking buffer for 30 minutes at room

temperature. Blocking buffer was prepared in 1x PBS supplemented with 1% BSA and 0.2% Triton X-100. In the meantime, primary antibodies (Table 2.1.3.1) were diluted in 1x PBS supplemented with 3% BSA and spun at 10,000 rpm for 3 minutes. Each circle was incubated with 100 µl of primary antibody solution for 2 hours. After incubation, each circle was washed three times in 1x PBS for 5 minutes each to remove any unbound antibody. The secondary antibodies (Table 2.1.3.2) were diluted in 1x PBS with 1% BSA and spun as before. Each circle was incubated with 100 µl of secondary antibody solution and Hoechst 33528 for 1 hour in the dark at room temperature, washed again three times in 1x PBS for 5 minutes. A drop of mounting solution (80% v/v glycerol, 3% w/v n-propyl-gallate in 1x PBS) was placed onto each circle, a glass coverslip placed on top and sealed with clear nail polish and kept in the dark at 4^{o}C. Fixed cell specimens were analysed by a Leica confocal microscope as described in section 2.3.1.1.

2.3.2 Centrosome number and spindle polarity measurements

For centrosome number counts, cells were analysed by immunofluorescence microscopy using antibodies against centrin-2 or CEP135, centriole proteins, and γ-tubulin or pericentrin, PCM components. Cells were classified as having amplified centrosomes when they had >4 centrioles and >2 PCM dots. Otherwise, cells with 4 (or less) centrioles and 1 or 2 PCM dots were considered as normal. 100 interphase cells were scored and counts repeated three to four times per experiment.

For spindle polarity measurements, we analysed cell populations with either amplified centrosomes that assemble pseudo-bipolar spindles with clustered poles, or those that formed multipolar spindles with un-clustered poles. In these experiments, cells were stained with centrin-2 and α-tubulin to identify centrioles and the spindle microtubule network, respectively. 50 mitotic cells were counted in each sample.

2.3.3 Intensity measurements

Intensity measurements were performed in fixed cell specimens analysed for indirect immunofluorescence microscopy as described above. Images were captured on the same intensity using constant exposure times and gain setting determined to be within the linear range of the camera with a scan zoom factor of 8 or 15 for interphase or mitotic cells, respectively. For analysis of the intensity of Hsp72, pHsp72-T66, dynein I.C. or p150Glued staining, cells were co-stained with the antibody indicated above and α-tubulin. Volocity 6.3 imaging analysis software was used to score staining intensity pixels/volume (μm^3) (PerkinElmer). The fluorescence intensity of the proteins of interest was scored relative to α-tubulin staining. The mitotic spindle as decorated by α-tubulin staining was determined as the region of interest (ROI) for the scoring intensity. 10-15 metaphase cells were captured in each sample. The fluorescent intensity of treated samples was then calculated compared to controls.

2.3.4 Live cell imaging

Live cell imaging was performed on a Leica TCS SP5 LSCM equipped with a Leica DMI 6000B inverted microscope using a 63x oil objective (numerical aperture, 1.4). Cells were cultured on glass-bottomed cultured dishes (MatTek Corporation, MA) and maintained on the stage at 37^{o}C and 5% CO_2 using a microscope stage temperature control system (The Cube and The Box, Life Imaging Services). Cells were detected under brightfield and SiR-tubulin fluorescence dye monitored with 8% of a 633 nm in a HyD4 detector. Scan zoom of 2 was used to select an area of cells for imaging. Z-stacks comprising 20 steps of 0.5 µm sections were acquired every 5 minutes for a minimum of 16 hours. Z-stacks were combined into a single maximum intensity projection per timepoint using Leica LAS AF software.

2.4 IMMUNOHISTOCHEMISTRY

2.4.1 Preparation of cytoblocks

MDA-MB-231 and KOPN8 cells were formalin-fixed and paraffin-embedded to generate cytoblocks and used for analysing centrosome amplification with antibody using immunohistochemistry. Cells were cultured to 80-90% confluency in a 150 cm^2 flask, resuspended and collected by centrifugation (1000 rpm, 5 minutes). Cytoblocks were then produced by the Histology Facility (Core Biotechnology Services (CBS), University of Leicester). Cells were fixed in 10% formal saline for 30 minutes at room temperature before the cytoblock was made using the Shandon Cytoblock Cell Block Preparation System (Thermo Scientific) according to the manufacturer's instructions. Cell buttons were embedded in paraffin wax and stored at room temperature.

2.4.2 Immunohistochemistry staining

After preparing formalin-fixed paraffin-embedded cytoblocks, the Histology Facility (CBS) sectioned and mounted these cytoblocks on Vectabond slides. NovoLink Polymer Detection System (Leica microsystems) was used to perform immunohistochemical analysis of the cytoblocks. According to the manufacturer's instructions, wax was melted by heating slides at 65^{o}C for 10 minutes, before sections were deparaffinised by two incubations in xylene for 3 minutes each, rehydrated by passing through graded alcohols (99%, 99%, 95% v/v IMS) for 1 minute each and finally washed in water for 5 minutes. Slides were then microwaved (750 W; Tecnolec Superwave) in 10 mM sodium citrate buffer for 15 minutes to allow antigen retrieval. Finally, slides were left to cool for 30 minutes at room temperature. Slides were then washed once in dH_2O, incubated with peroxidase block for 5 minutes in a humidified chamber to neutralise endogenous peroxidase and washed twice in TBS for 3 minutes each. Slides were incubated with the protein block for 5 minutes and washed again twice in TBS for 3 minutes each. Primary antibody was diluted in TBS at the appropriate concentration and incubated with cytoblocks overnight at 4^{o}C. Slides were washed twice in TBS for 5 minutes each and incubated with post primary block for 30 minutes. After two frequent washes with TBS

before incubation with Novolink polymer for a further 30 minutes and washes again with TBS, DAB working solution (Dab Chromogen and NovoLink DAB substrate buffer at 1:20, respectively) was freshly prepared and incubated on slides for 5 minutes. Samples were then rinsed in water and then counterstained with Mayer's Heamatoxylin for 30 seconds and washed in running water for 5 minutes. Slides were then dehydrated in graded alcohols, incubated in xylene for 10 minutes and mounted onto coverslips using Dpx mounting medium (Sigma).

2.5 PROTEIN ANALYSIS

2.5.1 Preparation of cell extracts

Cells were washed with 1x PBS and harvested as normal. The cell suspension was spun at 1,200 rpm for 5 minutes. The supernatant was discarded and pellet re-suspended in 250-500 µl of ice-cold **RIPA lysis buffer** (50 mM Tris-HCl (pH 8.0), 150 mM NaCl, 1% w/v SDS, 0.5% v/v NP40 (Igepal), 0.5% w/v sodium deoxycholate, 0.5% Triton, 1x Protease inhibitor cocktail (PIC), 5 mM NAF, 5 mM β-glycerolphosphate, 30 µg/ml RNase, 30 µg/ml DNase I), **NEB lysis buffer** (50 mM HEPES-KOH (pH 7.4), 5 mM $MnCl_2$, 5 mM EGTA, 2 mM EDTA, 100 mM NaCl, 5 mM KCl, 0.1% v/v Nonidet P-40, 5 mM NaF, 5 mM β-glycerolphosphate, 30 µg/ml RNase, 30 µg/ml DNase I, 1x PIC) or **NP-40 lysis buffer** (50 mM Tris-HCl (pH 8.0), 150 mM NaCl, 1% NP-40, 5 mM NaF, 5 mM β-glycerolphosphate, 30 µg/ml RNase, 30 µg/ml DNase I, 1x PIC). Cell extracts were incubated on ice for 30 minutes and lysates passed through a 27G needle for shearing DNA and releasing proteins. Lysates were then centrifuged at 13,000 rpm for 10 minutes at 4^{o}C to remove insoluble material. Supernatants were either analysed directly by SDS-PAGE or for immunoprecipitation or snap frozen and stored at -80^{o}C.

2.5.2 BCA protein assay

Protein concentration of cell lysates was determined using the BCA protein assay. BCA working reagent was prepared according to the manufacturer's instructions. The

following reaction: 800 µl Reagent B with 100 µl Reagent A‘ plus 20 µl of cell lysate was mixed in a cuvette. The assay mixture was then incubated for 15 minutes at room temperature and the absorbance at 650 nm measured. A serial dilution of BSA standards was prepared and assayed in parallel to generate a standard curve from which the protein concentration of the samples could be calculated.

2.5.3 SDS-PAGE

Protein samples were resolved on 10 or 12% polyacrylamide gels by electrophoresis. Gels were cast and resolved using the Mini-PROTEAN 3 polyacrylamide gel electrophoresis (PAGE) system (Bio-Rad). Resolving gel (26.7-40% ProtoFlowgel (30% w/v acrylamide), 126 mM Tris-HCl pH 8.8, 0.1% w/v SDS, 0.13% w/v APS, 0.08% v/v TEMED) was overlaid with stacking gel (13% ProtoFlowgel (39% w/v acrylamide), 126 mM Tris-HCl pH 6.8, 0.1% w/v SDS, 0.15% w/v APS, 0.1% v/v TEMED). Protein samples were mixed with an appropriate volume of 3x leammli buffer (62.5 mM Tris-HCl pH 6.8, 10% v/v glycerol, 2% w/v SDS, 5% v/v β-mercaptoethanol, 0.01% w/v bromophenol blue) and denatured at 95^{o}C for 5 minutes. Precision Plus Protein^{TM} Dual Color Standards (Bio-Rad) were loaded on the same gel. Electrophoresis was performed at 180 V for ~1 hour using SDS-running buffer (25 mM Tris-base, 192 mM glycine, 0.1% w/v SDS).

2.5.4 Coomassie Blue staining for mass spectrometry (MS)

To visualise proteins after SDS-PAGE electrophoresis, resolving gels were submerged in Coomassie Blue staining solution (0.25% w/v Brilliant Blue R, 40% v/v IMS, 10% acetic acid) and then gently agitated for 45 minutes at room temperature. Destain solution (7.5% v/v acetic acid, 25% IMS) was used to wash the gels from the Coomassie Blue solution until protein bands could be distinguished and the background was clear. Proteins to be analysed by mass spectrometry were resolved on a 1.5 mm SDS-PAGE gel. For mass spectrometry analysis, coomassie blue stained gel was submitted to the Protein Nucleic Acid Chemistry Laboratory (PNACL), University of Leicester, and the columns of immunoprecipitated protein and IgG samples were then sectioned and subjected to

digestion by trypsin before being analysed by liquid chromatography-tandem mass spectrometry (LC-MS/MS).

2.5.5 Western blotting

Proteins were transferred from SDS-polyacrylamide gels to nitrocellulose membrane for immunodetection using semi-dry blotting. Transfer was carried out by soaking 0.45 µm pore size nitrocellulose membrane in blotting buffer (25 mM Tris, 192 mM glycine, 10% v/v methanol) along with 6 pieces of Whatman 3 MM chromatography paper. The gel was then placed on the membrane and sandwiched between 3 pieces of blotting paper on either side. This gel sandwich was then transferred in a TE 77 semi-dry transfer unit (Amersham) for 1 hour at 1 mA/cm^2 membrane. Ponceau red stain solution (0.1% w/v Ponceau S, 5% v/v acetic acid) was used to visualize that the protein had transferred successfully. Blots were then blocked in 5% w/v non-fat milk powder in 0.1% v/v Tween-20 in 1x TBS for 1 hour at room temperature on a rocking platform. For Western blotting, the antibodies were diluted in TBS supplemented with 0.1% v/v Tween-20 and 5% non-fat milk powder. The membrane was then incubated with primary antibody at the appropriate dilution in 5% non-fat milk powder/1x TBST overnight at 4^oC. Membranes were washed 3 times in 1x TBST for 10 minutes each and incubated with the horseradish perodixase-conjugated secondary antibody in 5% non-fat milk powder/ TBST for an extra 1 hour at room temperature. Secondary antibodies were diluted in TBS supplemented with 0.1% v/v Tween-20 and 5% non-fat milk powder. Membranes were then washed again 3 times in 1x TBST to remove unbound secondary antibody and developed in enhanced chemiluminescence (ECL) Western blotting detection solution (Pierce) according to the manufacturer's instructions. The proteins were visualised on X-ray film developed using a compact X4 X-ray film processor (Xograph imaging system).

2.5.6 Immunoprecipitation

Whole cell lysates prepared as described in section 2.4.1 were used for immunoprecipitation experiments using dynein I.C. or Hsp72 antibodies bound to

ProteinG-Agarose beads (Sigma). Briefly, 50 µl of proteinG beads were washed three times with 1x PBS and resuspended in 50 µl NP40 lysis buffer. 500 µl of cell lysate was incubated with 20 µl washed bead slurry for 45 minutes rotating at 4^{o}C to pre-clear the lysate of any proteins that non-specifically bind to beads. Lysate-beads sample was then spun for 30 seconds and the supernatant was divided into two fresh tubes, one tube for the protein of interest and one for control mouse IgG. In the meantime, the remaining 30 µl washed beads were incubated with dynein I.C., Hsp72 or control mouse IgG antibodies at the appropriate dilution for 1 hour on ice. Supernatant was then incubated with the antibody-beads mixture overnight at 4^{o}C with rotating agitation. Next day, beads were washed four times with NP40 lysis buffer and boiled in Laemmli buffer for SDS-PAGE analysis.

2.6 MISCELLANEOUS TECHNIQUES

2.6.1 Proximity ligation assay (PLA)

Cells were plated on glass coverslips (13 mm diameter) and treated as required. Cells were washed in 1x PBS, fixed and permeabilized in ice-cold methanol at -20^{o}C for 30 minutes or pre-extracted with a buffer (60 mM Pipes, 25 mM Hepes, pH7.4, 10 mM EGTA, 2 mM $MgCl_2$, and 1% Triton X-100) for 30 seconds before having fixed with ice-cold methanol. Coverslips were then washed three times with 1x PBS for 5 minutes each and blocked in 1x PBS supplemented with 1% w/v BSA and 0.2% Triton X-100 for 60 minutes. In the meantime, primary antibodies (Table 2.1.3.1) were diluted in 1x PBS with 3% w/v BSA and spun at 10,000 rpm for 3 minutes to remove any insoluble aggregates. Each coverslip was incubated with 30 µl of primary antibody solution for 2 hours. Primary antibody solution was placed onto Parafilm and the coverslip inverted onto the antibody solution on the Parafilm. A humid chamber is used for incubation of slides to prevent cells from drying out. After incubation, coverslips were washed three times in 1x PBS for 5 minutes each. The PLA protocol was followed according to manufacture instructions (Duolink In Situ Fluorescence; Sigma). In short, PLA probes were mixed and diluted 1:5 in the blocking buffer (1x PBS supplemented with 1% w/v BSA and 0.2% Triton X-100). The mixture was incubated at room temperature for 20 minutes before

adding to the coverslips. Coverslips were incubated with the probe mixture on the Parafilm in a pre-heated humidity chamber for 1 hour at 37^{o}C. Coverslips were then washed twice in 1x Wash Buffer A for 5 minutes. Ligation-Ligase solution was prepared according to manufacture instructions. Ligase was added to the ligation mixture immediately before adding to the samples. Coverslips were placed in a pre-heated humidity chamber for 30 minutes at 37^{o}C. Cells were washed twice in 1x Wash Buffer A for 2 minutes at room temperature. Amplification-Polymerase solution was prepared and added to the coverslips for 100 minutes at 37^{o}C in a pre-heated humidity chamber. This step had light sensitive reagents and so coverslips have kept in the dark. At the end of the incubation, coverslips were washed twice with 1x Wash Buffer B for 10 minutes each, followed by an extra wash in 0.01x Wash Buffer B for 1 minute. Coverslips were mounted onto slides with a Duolink In Situ Medium with DAPI. The edge of coverslips was sealed with nail polish and slides stored at 4^{o}C in the dark.

2.6.2 Statistical analysis

For data analysis, GraphPad Prism Version 6.0 was used to calculate the mean of three independent experiments, unless otherwise stated. Error bars show standard deviation of the mean (S.D., n=3). One-way ANOVA analysis was used to compare the means of three or more unrelated groups. The one-way ANOVA analysis determined whether any of the means are statistically significant different from each group. One-tailed unpaired Student's t-test was used to compare the means of two unrelated groups and calculate the confidence interval, which must be 95%, for the difference between means to be accurate.

Chapter 3

Measuring centrosome amplification and clustering in adherent and suspension cancer cell lines

3.1 Introduction

The centrosome, a small organelle, is required throughout the cell cycle in most animal cells. Centrosomes duplicate once every cell cycle along with DNA during S phase such that cells contain accurately duplicated DNA and two centrosomes when they enter mitosis (Bornens, 2012; Nigg and Stearns, 2011; Nigg, 2002). Centrosomes are characterised as the major microtubule organizing centres (MTOC) directing nucleation of polymerize microtubules allowing the formation of a bipolar spindle and separation of sister chromatids in mitosis (Conduit et al., 2015; Nigg and Stearns, 2011). Apart from their important roles in mitosis, centrosomes also influence the motility and polarity, as well as forming cilia and flagella (Nigg, 2002; Conduit et al., 2015).

Centrosomes are composed of the centriolar and the pericentriolar domains. The centriolar domain consists of a pair of specific structures called centrioles that are surrounded by an organized matrix of pericentriolar material containing multiple proteins. Centrioles have a barrel-shaped cylinder arrangement and contain many structural proteins (Jakobsen et al., 2011; Woodruff et al., 2014). The pericentriolar domain consists of multiple protein complexes, including γ-tubulin ring complexes (γ-TuRCs), which promote nucleation of microtubules (Mennella et al., 2013; Woodruff et al., 2014). The centrosome cycle describes the series of structural and numerical changes that occurred at the centrosome during the cell cycle. It can be characterized by four major events: centriole disengagement, centriole duplication, centrosome maturation and centrosome disjunction. Each step of the centrosome cycle is tightly controlled by multiple enzymatic proteins including NEK2, PLK-1, PLK-4 and Aurora-A (Nigg and Stearns, 2011; Conduit et al., 2015).

Almost a century ago, researchers observed centrosome abnormalities in many diseases, including cancer. Centrosome defects, either structural or numerical, have been observed in the majority of solid tumours such as brain, ovarian and breast cancer, as well as, in many haematological cancers, including acute and chronic myeloid leukaemia

(Kramer et al., 2005, Gielh et al., 2005; Pihan et al., 1998). A phenotype frequently described in many cancers is centrosome amplification, a feature that often is correlated with poor prognosis and metastasis (Godinho et al., 2014; Nigg, 2006; D'Assoro et al., 2002). A growing body of evidence suggests the existence of a variety of mechanisms that lead to extra copies of centrosomes, including cell-cell fusion, cytokinesis failure, *de novo* centriole assembly, overduplication of centrioles due to prolonged S/G2 phase arrest and loss of function in proteins, such as tumour suppressor and oncogenes, that regulate centrosome cycle (Godinho et al., 2009; Loncarek et al., 2010; Ganem et al., 2007; Brownlee and Rogers, 2013; Fukasawa, 2007). Indeed, it is now clear that the centrosome cycle is controlled by multiple proteins including tumour suppressor genes, such as p53 and RB, and oncogenes, such as Aurora A. In cancer cells, these genes are frequently up- or down-regulated and thus affect the centrosome duplication cycle (Fukasawa, 2007). A hallmark of cancer cells is increased genomic instability and one of its causes is chromosome segregation errors that occur during mitosis as a result of centrosome amplification (Nigg, 2002; Fukasawa, 2007; Janssen and Mederma, 2011; Hanahan and Weinberg, 2011).

It has long been assessed that cells with extra centrosomes undergo formation of multipolar spindles, resulting in mitotic catastrophe and cell death (Nigg, 2002; Godinho and Pellman, 2014; Boveri, 2008). Careful observation has revealed that cancer cells with amplified centrosomes have mechanisms to suppress multipolarity by clustering centrosomes and forming pseudo-bipolar spindles that enable successful mitosis (Ganem et al., 2009; Kwon et al., 2008; Leber et al., 2010). However, this pseudo-bipolar spindle can inappropriately segregate chromosomes by favouring merotelic kinetochore-microtubule attachments, which are extremely dangerous as they poorly detected by the spindle assembly checkpoint (SAC) (Guerrero et al., 2010; Cimini, 2008). As a consequence, this behaviour increases aneuploidy and promotes tumour progression allowing cancer cells to evolve over time (Odgen et al., 2012; Kwon et al., 2008).

The aim of this chapter was to examine centrosome amplification and clustering in adherent and suspension cell lines, as a prelude to investigate mechanisms of centrosome clustering. The initial starting point was therefore to score centrosome numbers in various cancer and diploid cell lines, as well as in haematological cancers such as acute lymphoblastic leukaemia (ALL) and chronic lymphocytic leukaemia (CLL). And whether these cells can cluster their amplified centrosomes to assemble pseudo-bipolar spindles. We used a variety of cell biology techniques, including immunofluorescence microscopy, live cell imaging and immunohistochemistry to visualise and analyse centrosome amplification and clustering.

3.2 Results

3.2.1 Centrosome numbers in adherent cell lines

The first step in studying centrosome clustering mechanisms was to identify *in vitro* model systems with extra centrosomes and the ability to cluster them into a bipolar state in mitosis. It was important to find the appropriate centrosomal markers that would enable scoring of centrioles or PCM. A number of centrosomal proteins are known to localise to each compartment of the centrosome organelle (Jana et al., 2014; Nigg and Stearns, 2011). In our study, we focused in CEP135 and centrin-2 proteins, which are part of the centriole compartment, and γ-tubulin and pericentrin proteins, which localise in the PCM compartment.

To count centrosome numbers, we evaluated a panel of cell lines including MDA-MB-231, NIE-115, SCC-114, HeLa, RPE1 and HBL-100. Asynchronous cells were fixed and processed for immunofluorescence microscopy analysis. Using centrin-2 and γ-tubulin antibodies, we detected centrosomes in interphase cells (Figure 3.1A). Interphase cells were classified as having normal centrosome numbers when they had 4 centrioles and 2 PCM dots, whereas they were scored as having amplified centrosomes if they had >4 centrioles and >2 PCM dots. Based on centrin-2 and γ-tubulin staining, we revealed that 33.5% of interphase cells had amplified centrosomes in MDA-MB-231 cell line (Figure 3.1B). In NIE-115 cell line, 96% of interphase cells were detected with amplified centrosomes. In addition, 35.5% of interphase cells possessed amplified centrosomes in SCC-114 cell line (Figure 3.1B). In contrast, approximately 8% of interphase cells had amplified centrosomes in HeLa cell line (Figure 3.1B). In addition, less than 5% of interphase cells possessed amplified centrosomes in RPE1 and HBL-100 cell lines (Figure 3.1B). Interestingly, the majority of NIE-115 cells harboured excessively amplified centrosomes (>5 centrosomes per cell), whereas most of MDA-MB-231 cells with amplified centrosomes possessed mostly 3-4 centrosomes per cell (Figure 3.1C). Centrosome amplification was also confirmed using antibodies against centrin-2 and α-tubulin, or pericentrin and γ-tubulin in each cell line (Figure 3.2A and 3.2B).

Hence, consistent with published studies by Leber et al and Pannu et al (Leber et al., 2010; Pannu et al., 2014), MDA-MB-231 human breast cancer, NIE-115 mouse neuroblastoma, and SCC-114 squamous cell carcinoma cells exhibited a high frequency of centrosome amplification, whereas HeLa (human cervical cancer), human RPE1 (retinal pigment epithelial cells immortalised with hTERT) and human HBL-100 mammary gland cells have a very low frequency centrosome amplification. Based on these data, we focused on MDA-MB-231 and NIE-115 cells to examine the mechanisms of centrosome clustering in mitosis.

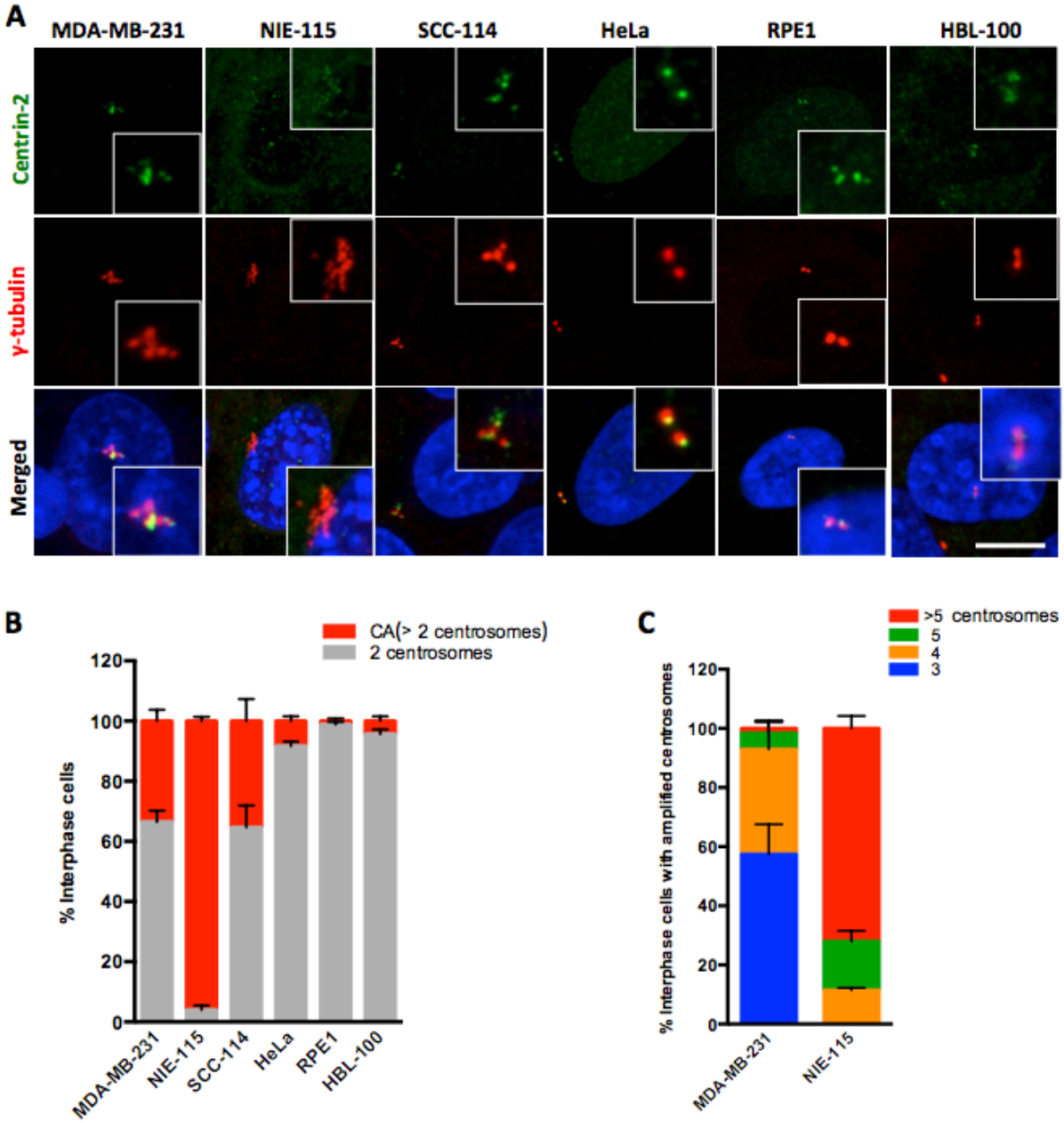

Figure 3.1. Characterization of centrosome numbers in adherent cell lines

A. Asynchronous interphase cells from MDA-MB-231, NIE-115, SCC-114, HeLa, RPE1 and HBL-100 were fixed and stained with centrin-2 (green) and γ-tubulin (red) antibodies. Hoechst 33258 was used for DNA (blue) staining. Centrosomes are indicated with an enlargement of the boxed area. Scale bar, 10 µm. **B.** Histogram represents the mean of interphase cells with 2 centrosomes or centrosome amplification (CA, >2 centrosomes) in each cell line. Data shown are the mean of three independent experiments and SD is indicated. 100 cells were scored per experiment. **C.** Histogram indicates the number of centrosomes as detected by centrin-2 and γ-tubulin staining in MDA-MB 231 and NIE-115 cells. Data represent the mean ± S.D. of three different experiments, where 100 cells were counted per experiment.

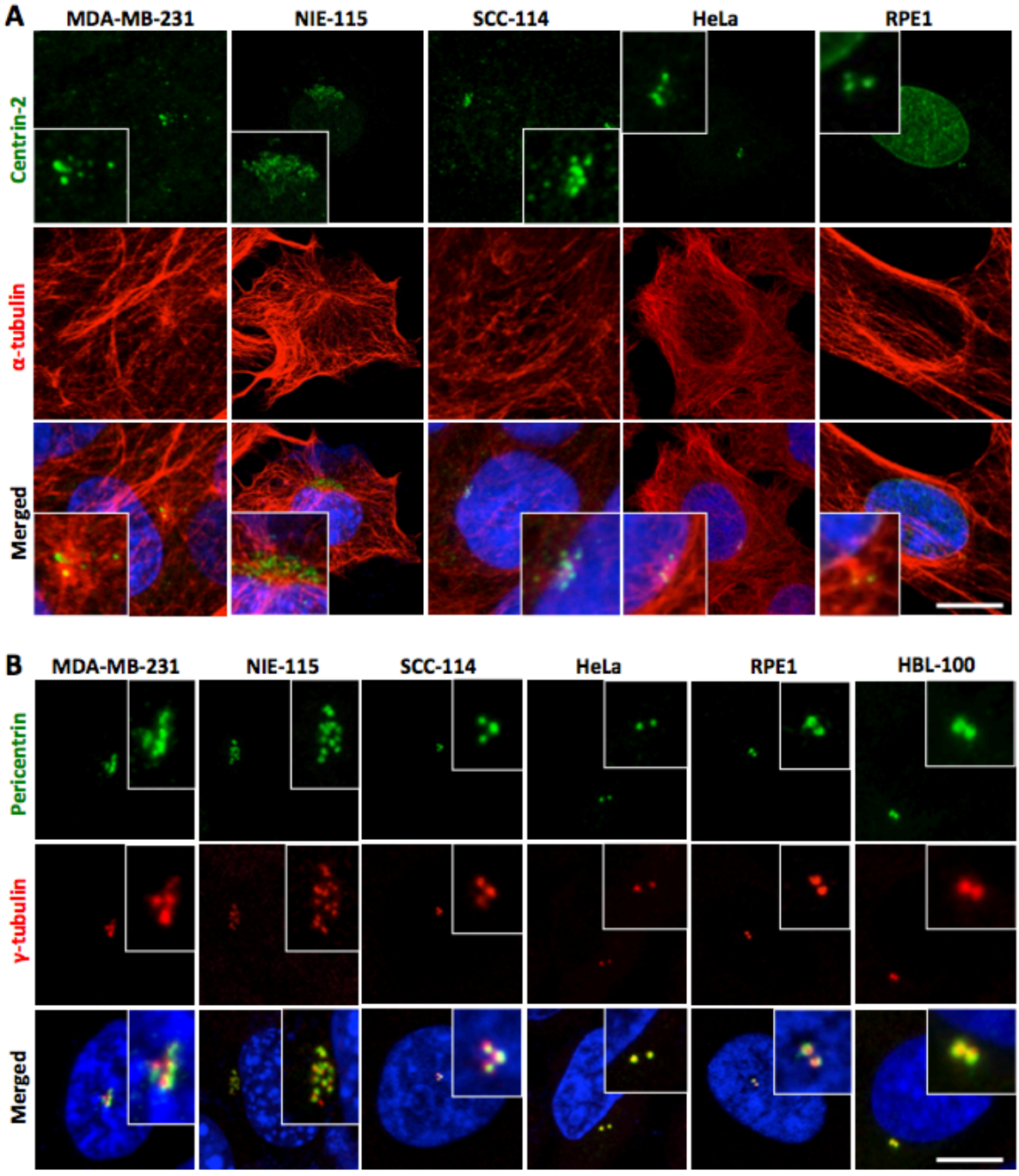

Figure 3.2. Immunofluorescence analysis of centrosome proteins in adherent cell lines

A-B. Asynchronous cells were fixed and stained for immunofluorescence microscopy with centrin-2 or pericentrin (green) and α- or γ-tubulin (red) antibodies. Merged images include DNA (blue) stained with Hoechst 33258. Interphase images were captured in each cell line. Centrosome area is indicated with an enlargement of the boxed area. Scale bar, 10 µm.

3.2.2 Centrosome amplification in acute lymphoblastic leukaemia (ALL) cell lines

In addition to centrosome amplification in solid cancers, a growing body of evidence has revealed centrosome aberrations in haematological malignancies (Kramer et al., 2005; Pihan et al., 1998; Godinho and Pellman, 2014). Numerical and structural centrosome defects have been reported in different types of haematological cancers, including chronic myeloid leukaemia (CML), acute myeloid leukaemia (AML), chronic lymphocytic leukaemia (CLL) and Hodgkin lymphoma (Kramer et al., 2005, Giehl et al., 2005). We therefore wanted to investigate if acute lymphoblastic leukaemia (ALL) cells also possess amplified centrosomes.

To assess centrosome numbers in suspension cells, we first adapted the immunofluorescence microscopy protocol for blood cells (Sampson and Fry, 2016). For the purpose of this study, we used primary B-lymphocytes obtained from peripheral blood of healthy donors and a panel of acute lymphoblastic leukaemia (ALL) cell lines (Chapter 2 Table 2.2.1). Here, centrosome numbers were scored by immunostaining with CEP135, as a centriole marker, and γ-tubulin, as a PCM marker (Figure 3.3A). Centrosome counts were also repeated with pericentrin and α-tubulin antibodies (Figure 3.3B). Less than 5% of healthy primary B-lymphocytes (PBL) had amplified centrosomes, as compared to 10-30% of ALL cells (Figure 3.3C). Four of the ALL cell lines, SEM, Z33, KOPN8 and REH, had a higher frequency of centrosome amplification compared to the other ALL cell lines (Figure 3.3C). Hence, acute lymphoblastic leukaemia (ALL) cells exhibit centrosome amplification. Therefore, ALL cells provide an alternative cell model to investigate centrosome clustering mechanisms.

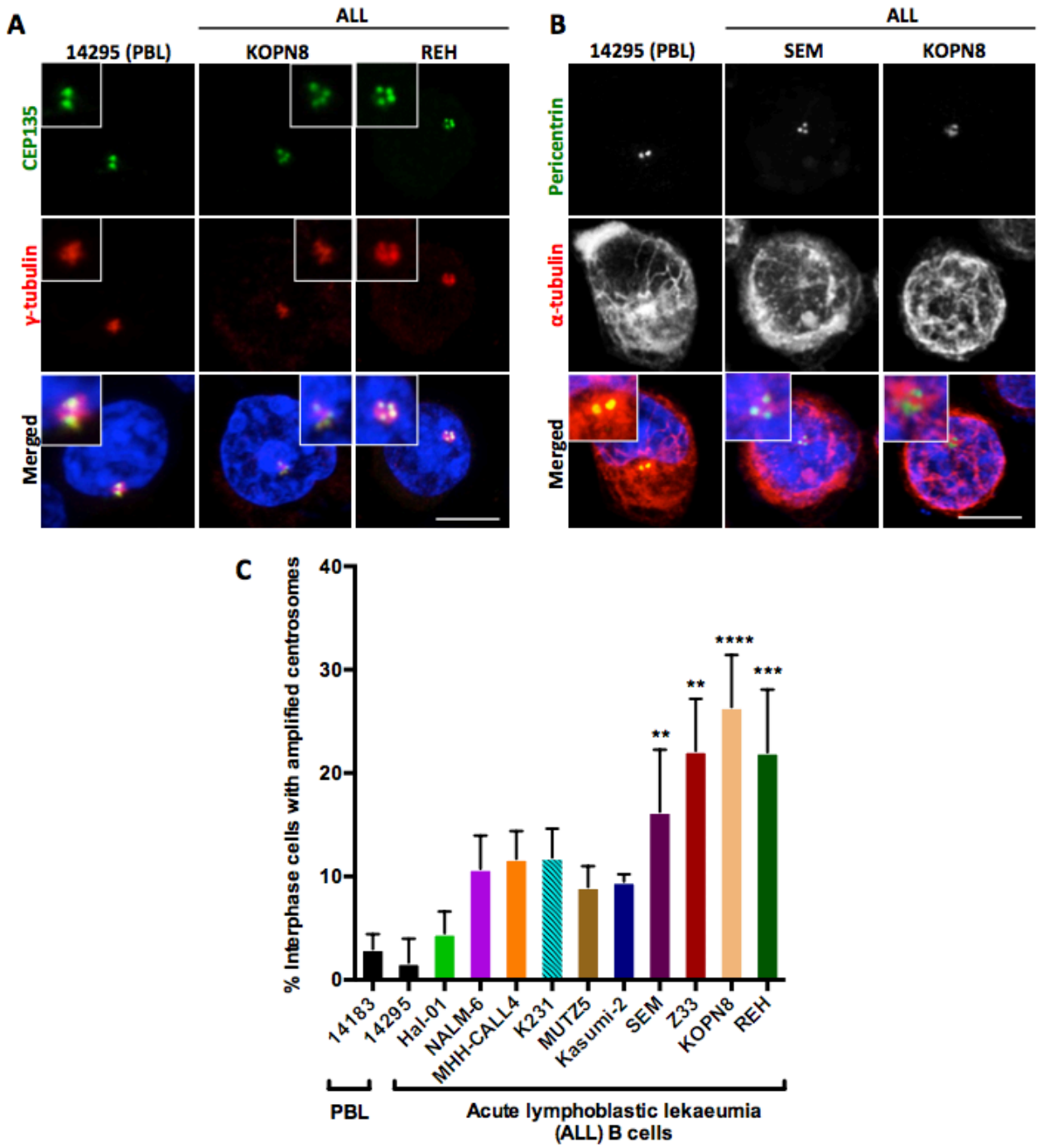

Figure 3.3. Acute lymphoblastic leukaemia (ALL) cells have amplified centrosomes

A-B. Asynchronous peripheral B-lymphocytes (PBL) and ALL cells were fixed and stained for immunofluorescence microscopy with antibodies against CEP135 (green) or pericentrin (green) and γ- or α-tubulin (red). Merged images include DNA (blue) stained with Hoechst 33258. Interphase images were captured in each cell line. Centrosome area is indicated with an enlargement of the boxed area. Scale bar, 2.5 μm. **C.** Histogram represents the percentage of interphase cells with amplified centrosomes scored from each cell line. Data represent the mean (± S.D.) from three different experiments. At least 100 cells were scored from each cell line. ****p<0.0001, ***p<0.001, **p<0.01.

3.2.3 Amplified centrosomes in chronic lymphocytic leukaemia (CLL) patient cells

In the previous section, we found that ALL cells have amplified centrosomes. We therefore wanted to know if centrosome amplification was present in another type of leukaemia, chronic lymphocytic leukaemia (CLL). In this case, we obtained blood samples from CLL patients in collaboration with Professor Martin Dyer in the Department of Molecular and Cell Biology and the Leicester Royal Infirmary. Proliferation was stimulated for 3 and 6 days using a feeder layer of cells, before centrosomes were analysed by immunofluorescence microscopy. Centrosomes were also analysed at day 0 when cells were harvested. CLL cells were stained with CEP135 and γ-tubulin antibodies to score centrosome numbers (Figure 3.4A-B). At day 0, less than 5% of CLL cells had amplified centrosomes. However, approximately 10-35% of CLL cells possessed amplified centrosomes following 3 days of proliferation, while 10-20% of CLL cells had extra centrosomes after 6 days of proliferation (Figure 3.4D).

Hence, patients with chronic lymphocytic leukaemia (CLL) possessed amplified centrosomes. As proliferation was stimulated in CLL cells, centrosome numbers were increased rapidly either at day 3 or 6. However, further experiments are needed to understand how proliferation stimulates centrosome amplification in those cells. Our study is mainly focus on understanding centrosome clustering mechanisms rather than investigating centrosome amplification pathways.

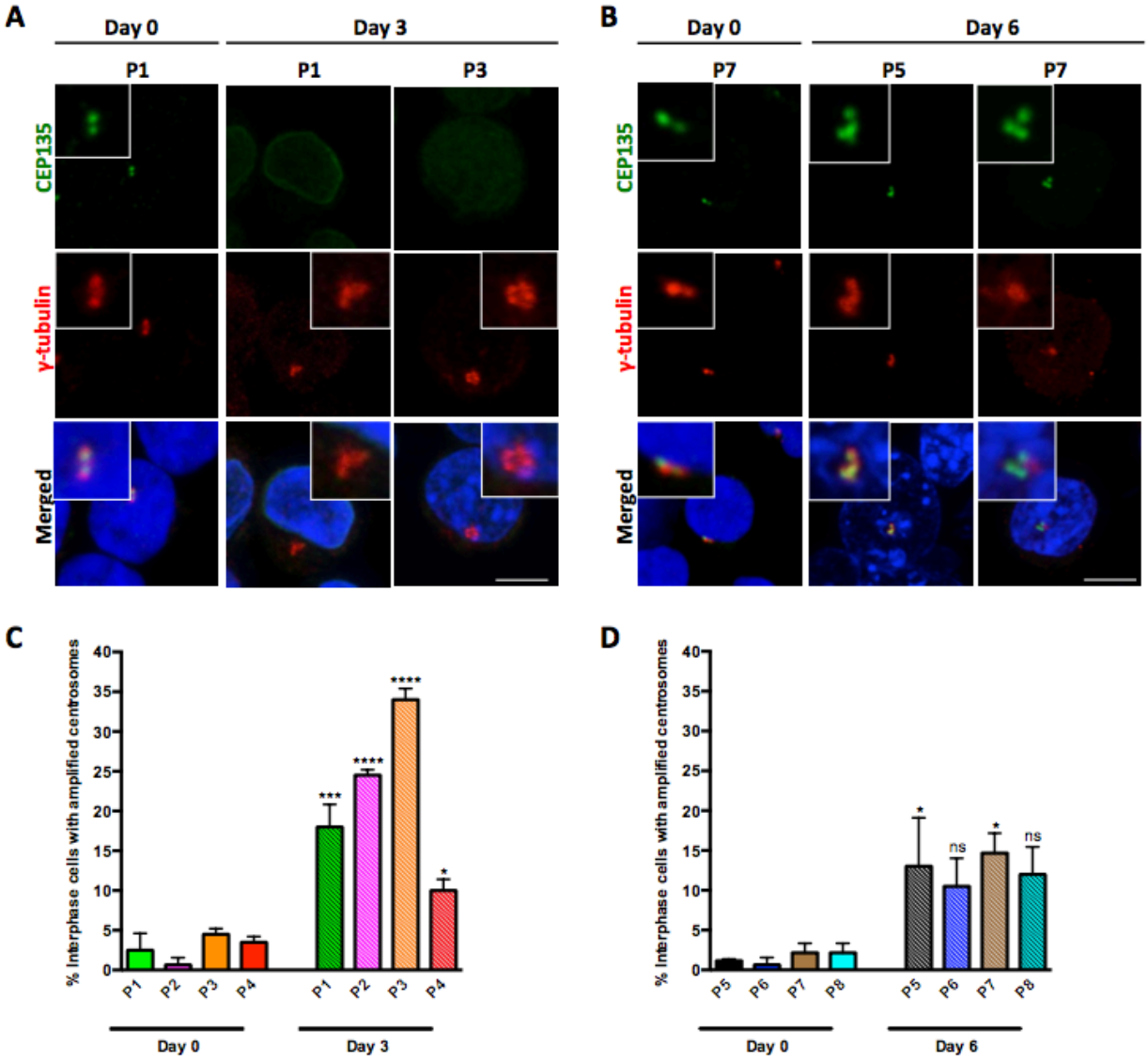

Figure 3.4. Chronic lymphocytic leukaemia (CLL) patient cells have amplified centrosomes

A-B. Asynchronous CLL patient cells were harvested at day 0 and fixed and stained for immunofluorescence microscopy with antibodies against CEP135 (green) and γ-tubulin (red). Merged images include DNA (blue) stained with Hoechst 33258. Cells were stimulated with a feeder layer called CD40 expressing mouse L-cells for 3 or 6 days. Interphase images were captured from each patient sample as indicated. Centrosome area is indicated with an enlargement of the boxed area. Scale bar, 2.5 µm. **C-D.** Histograms represent the percentage of interphase cells with amplified centrosomes scored from each patient based on CEP135 and γ-tubulin staining. Patient samples are indicated with numbers. Data represent the mean (± S.D.) from two different experiments. At least 50 cells were scored from each cell line. ****p<0.0001, ***p<0.001, *p<0.05.

3.2.4 Centrosome clustering in cancer cell lines

To assess centrosome clustering, MDA-MB-231, NIE-115 and SCC-114 cells were stained with antibodies against α-tubulin to detect microtubules and γ-tubulin and centrin-2 to score centrosomes (Figure 3.5A). Scoring only mitotic cells with >2 centrosomes (i.e. >4 centrin-2 dots) showed that 82% MDA-MB-231, 76% NIE-115 and 75% SCC-114 cells formed bipolar spindles with the amplified centrosomes clustered at two poles (Figure 3.5B). The above findings confirmed previous data showing that these three cancer cell lines have the ability to cluster extra centrosomes during mitosis (Leber et al., 2010; Pannu et al., 2014).

To confirm whether or not centrosome clustering occurred in these cell lines, two cancer cell lines, MDA-MB-231 and HeLa, were analysed by microscopy using triple antibody staining. The analysis of interphase cells confirmed that MDA-MB-231 cells had amplified centrosomes, whereas HeLa cells did not show any centrosome amplification (Figure 3.6A). Examining mitotic cells, we observed clustering of extra centrosomes in MDA-MB-231 cells but not in HeLa cells (Figure 3.6B). This is consistent with previous studies that reported centrosome clustering in different types of cancer cells (Pannu et al., 2014; Leber et al., 2010).

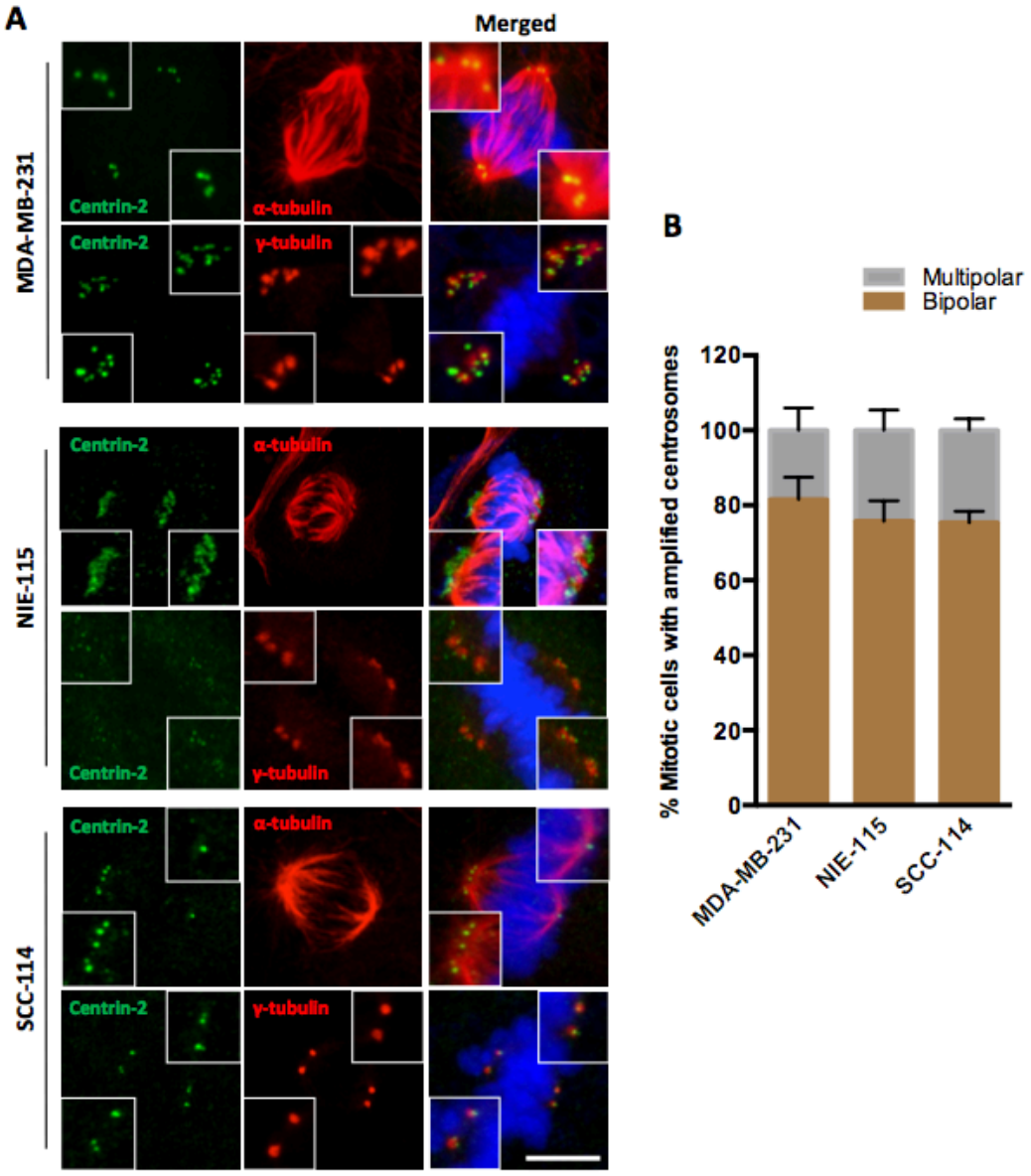

Figure 3.5. Centrosome clustering in MDA-MB-231, NIE-115 and SCC-114 cell lines

A. MDA-MB-231, NIE-115 and SCC-114 cells were fixed and stained with centrin-2 (green) and γ- or α-tubulin (red) antibodies. Merged images include DNA (blue) stained with Hoechst 33258. Images of mitotic cells were captured in each cell line. Magnified views of spindle pole regions with clustered centrosomes are shown. Scale bar, 5 µm. **B.** Histogram represents the percentage of mitotic cells with amplified centrosomes in a bipolar or multipolar stage in each cell line. Data show means ± S.D. of three experiments. Approximately 75 cells were scored per experiment.

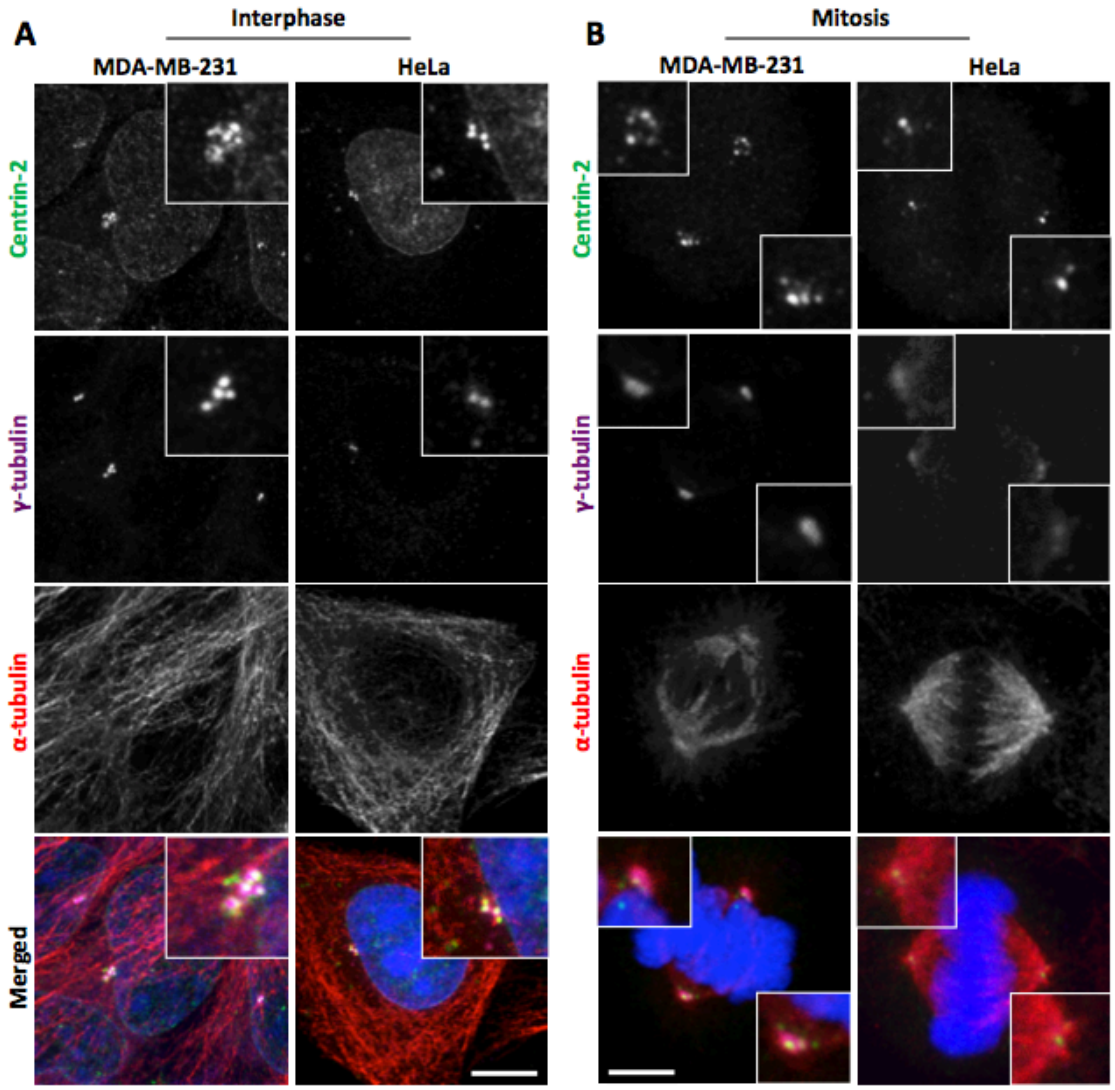

Figure 3.6. Centrosome amplification and clustering in MDA-MB-231 and HeLa cells using triple staining

A. Interphase MDA-MB-231 and HeLa cells were fixed and stained for immunofluorescence microscopy with centrin-2 (green), γ-tubulin (purple) and α-tubulin (red) antibodies. Scale bar, 7.5 µm. Merged panels include DNA (blue) staining with Hoechst. **B.** Cells in mitosis were imaged and stained as described in A. Scale bar, 5 µm.

To analyse how cancer cells achieve centrosome clustering, we took advantage of a far-red fluorescent probe, SiR-tubulin, which can stain microtubules in live cells (Lukinavicius et al., 2014; Sampson and Fry, 2016). We chose to use diploid RPE1 cells with no centrosome amplification and MDA-MB-231 and NIE-115 cancer cells that have a high frequency of amplified centrosomes. In RPE1 cells, live cell imaging with SiR-tubulin, which stained microtubules in interphase and mitosis, revealed formation of a bipolar mitotic spindle by an average of 40 minutes of mitotic entry (Figure 3.7A, C). In NIE-115 cells, SiR-tubulin staining revealed the initial assembly of multiple asters with these subsequently clustering into a bipolar mitotic spindle within an average of 169 minutes after mitotic entry (Figure 3.7B-C). In the majority of MDA-MB-231 cells, time-lapse imaging displayed multiple asters that led to their clustering into a bipolar mitotic spindle within an average of 80 minutes after mitotic entry (Figure 3.7C). Analysis of mitotic duration revealed that NIE-115 cancer cells had longer mitosis by an average of 244 minutes, whereas RPE1 cells remained in mitosis within an average of 102 minutes (Figure 3.7D). In addition, the mitotic duration in MDA-MB-231 cancer cells was an average of 123 minutes (Figure 3.7D).

In conclusion, the majority of NIE-115, MDA-MB-231 and SCC-114 cancer cells with amplified centrosomes have the ability to cluster extra centrosomes at two poles during mitosis. In contrast, HeLa cancer cells do not exhibit high centrosome amplification and clustering was not visible. Time-lapse imaging of cells stained with SiR-tubulin probe showed that NIE-115 and MDA-MB-231 cells can resolve their multiple asters into a bipolar state, whereas RPE1 cells did not show any clustering. In addition, NIE-115 cells had extended mitotic duration, as compared to RPE1 cells. However, the length mitosis in MDA-MB-231 cells was similar to this of RPE1 cells.

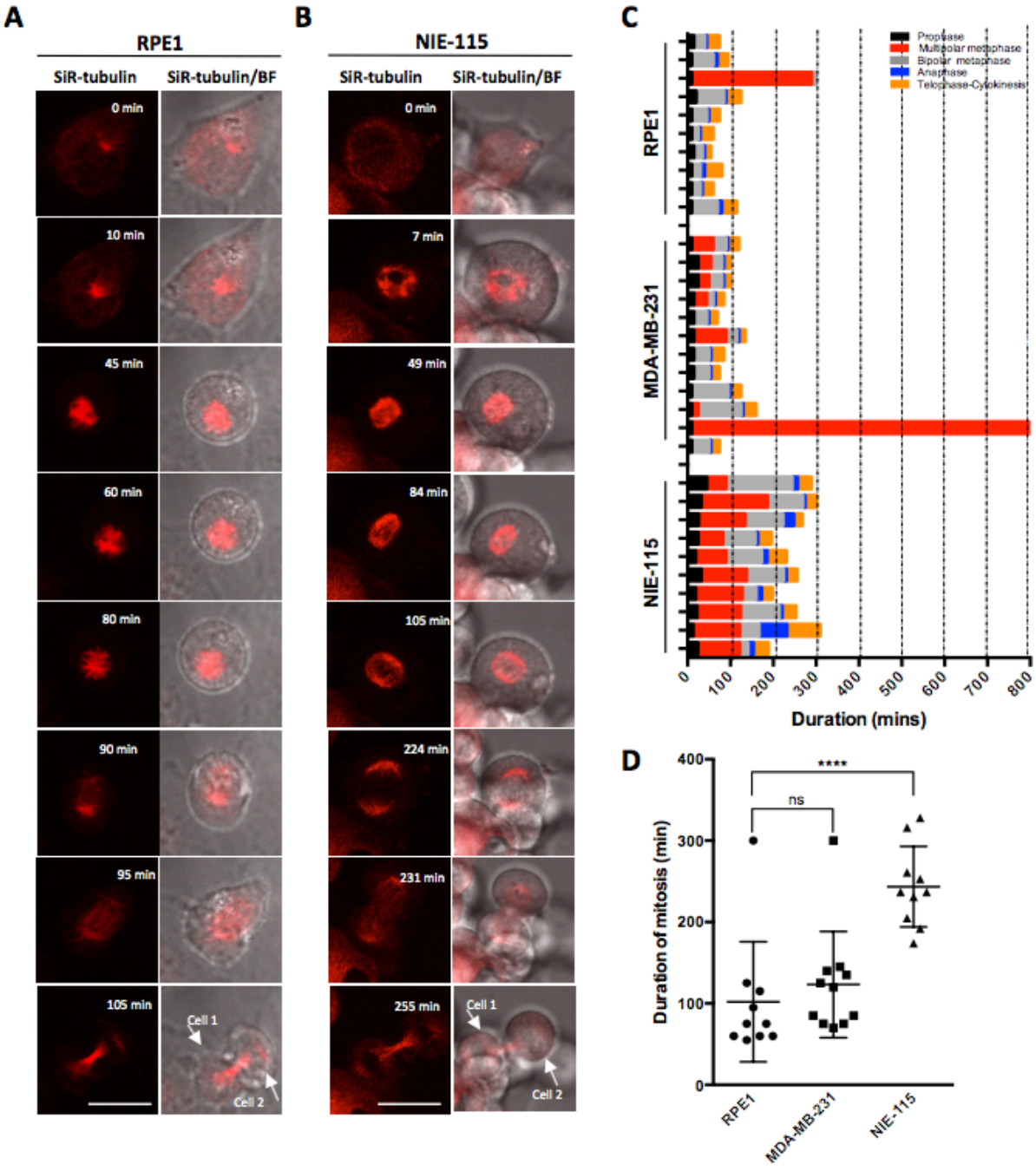

Figure 3.7. Monitoring centrosome clustering and mitotic progression using SiR-tubulin

A-B. Asynchronous RPE1 and NIE-115 cells were plated on glass bottom dishes and incubated with SiR-tubulin fluorescent probe for 7 hours and imaged for 16 hours using a Leica TCS SP5 LSCM. Cells were located under brightfield and the corresponding SiR-tubulin staining detected with 8% power of a 633 nm PMT5 laser. The left image show fluorescent staining and the right image show a merge with brightfield. Images are shown as the maximum intensity projections of the z-stack combined into a single image per timepoint. Time shown as minutes. Scale bar, 10 µm. **C.** Duration of each phase of mitosis was monitored by tracking 10 different cells from each cell line. Durations were represented in minutes. **D.** Dot plot shows the duration of mitosis from each cell line. Each dot represents a single cell. ****p<0.0001.

3.2.5 Detection of centrosomes by immunohistochemistry

Having investigated centrosome amplification and clustering in various adherent and suspension cells, we then determined if we could use immunohistochemistry (IHC) to detect centrosomes in cell samples. To optimise the methodology, we first prepared cytoblocks of MDA-MB-231 and KOPN8 cells by preparing cell pellets that were then formalin-fixed and paraffin-embedded and cut into sections. Antigens from those sections were retrieved by microwaving for 15 minutes in citrate buffer (pH 6.0). Sections were stained with pericentrin, as a PCM marker, or Ki-67, as a proliferation marker, or no primary antibody (NPA) as a control (Figure 3.8A-B). At 1:4500, the pericentrin antibody gave detectable staining of centrosomes in both MDA-MB-231 and KOPN8 cells (Figure 3.8A-B). Ki-67 staining revealed cells that undergo proliferation and used as a positive marker for these experiments to show the efficiency of this technique. Careful examination revealed enriched pericentrin staining in the centrosome area of many cells in both cell lines (Figure 3.9A-B). Considering this particular enriched pericentrin staining, we suggested that these cells could potentially acquire amplified centrosomes (Figure 3.9A-B). In addition, we examined the centrosome positioning in mitotic MDA-MB-231 and KOPN8 cells. Pericentrin staining also detected at centrosomes in mitosis either in bipolar spindles or sometimes tripolar spindles in both MDA-MB-231 and KOPN8 cells (Figure 3.10A-B). Here, we introduced immunohistochemistry, as another technique, for detection of centrosomes in cell samples. We suggested that the enriched pericentrin staining could be correlated with amplified centrosomes, however further analysis is needed to quantify these phenotypes and if possible determine their centrosome content.

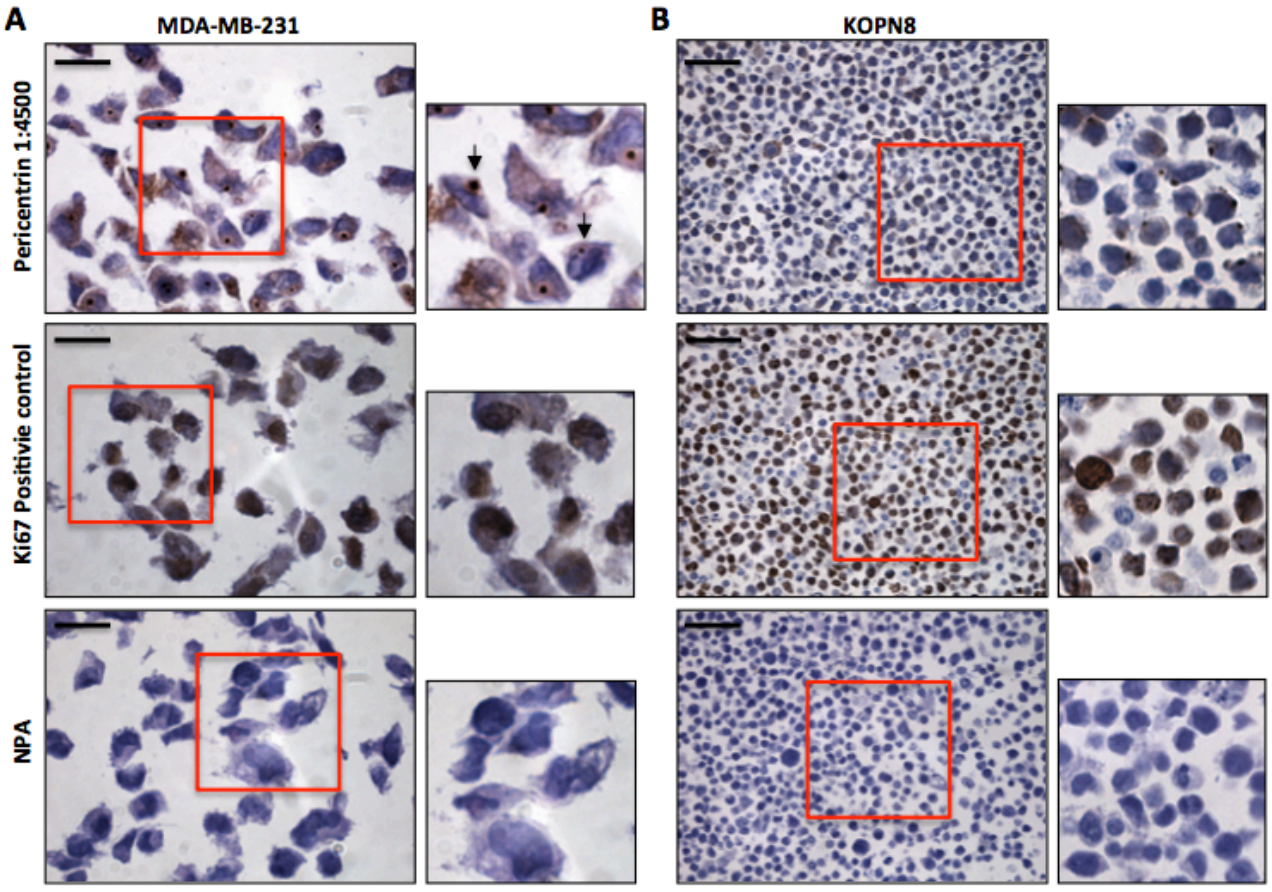

Figure 3.8. Detection of pericentrin in MDA-MB-231 and KOPN8 cells

A. MDA-MB-231 cells were formalin-fixed and paraffin-embedded. Sections were subjected to staining with anti-pericentrin antibody indicated with brown. Ki67 antibody was used as a positive control. NPA indicates no primary antibody. All sections were counterstained with heamatoxylin to detect nuclei (blue). Magnified views of the regions within red boxes are shown. Arrows indicate pericentrin staining in individual cells. Scale bar, 20 µm. **B.** KOPN8 cells were treated in the same way as in A and stained with pericentrin antibody. Scale bar, 50 µm.

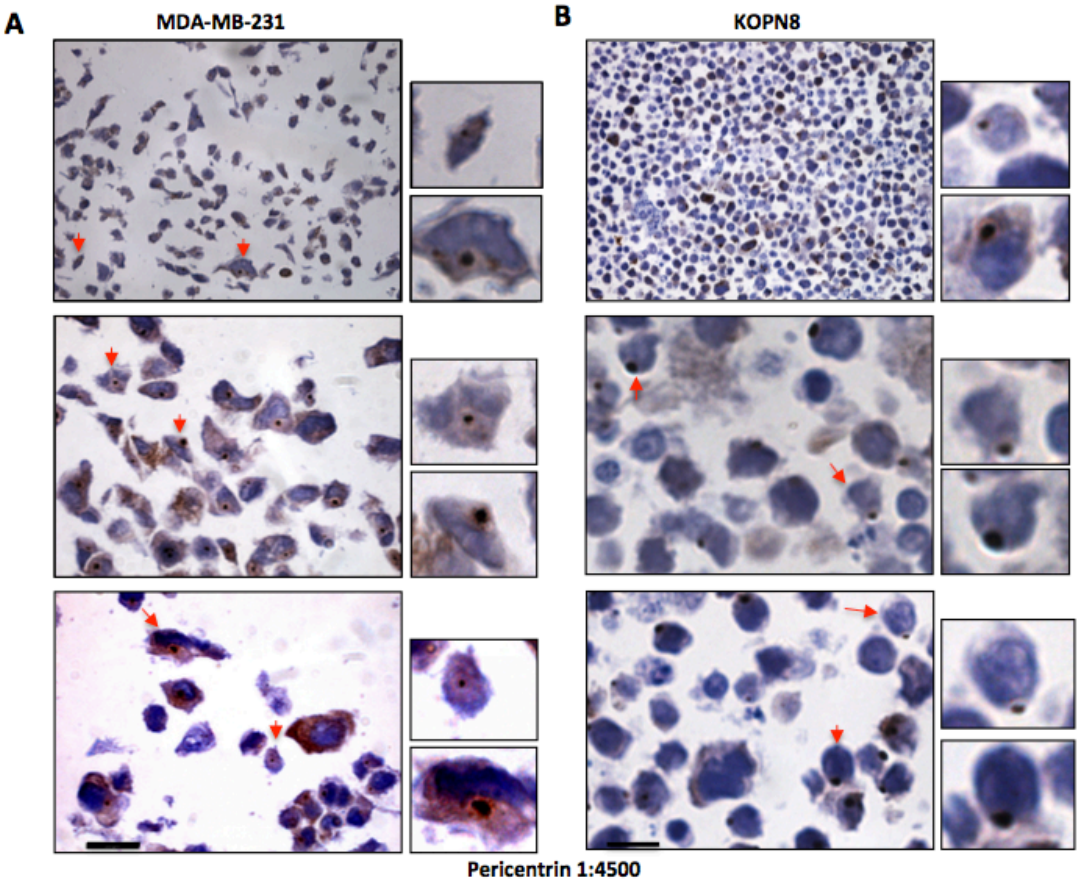

Figure 3.9. Quantification of centrosome amplification using immunohistochemistry

A-B. MDA-MB-231 and KOPN8 cells were formalin-fixed and paraffin-embedded. Sections were subjected to staining with anti-pericentrin antibody indicated with brown. All sections were counterstained with heamatoxylin to detect nuclei (blue). Magnified views of individual cells marked with red arrows are shown. Scale bar, 20 µm.

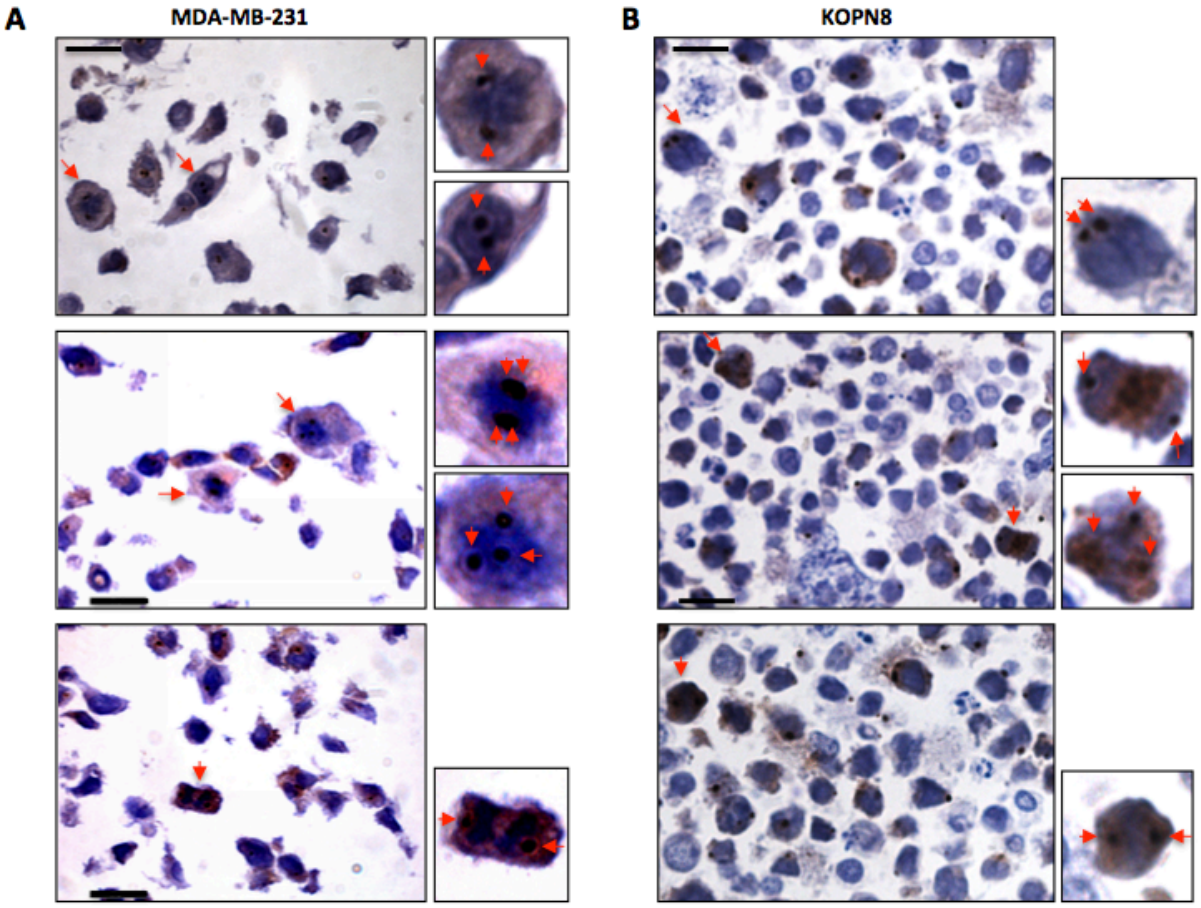

Figure 3.10. Detection of centrosomes in mitotic cells using immunohistochemistry

A-B. MDA-MB-231 and KOPN8 cells were formalin-fixed and paraffin-embedded. Sections were subjected to staining with anti-pericentrin antibody indicated with brown. All sections were counterstained with heamatoxylin to detect nuclei (blue). Magnified views of centrosomes in mitotic cells are marked with red arrows. Scale bar, 20 µm.

3.2.6 Duration of S and G2/M phases is potentially correlated with centrosome amplification in cells

In order to assess if there was a change in cell cycle distribution that correlated with amplified centrosomes, we analysed asynchronous population of cells by propidium iodide based flow cytometry. The cell population in G2/M phase in HeLa and RPE1 cell lines was 15% and 8%, respectively (Figure 3.11A-C). However, MDA-MB-231 and NIE-115 cells had 24% and 35% of cell population in G2/M, respectively (Figure 3.11A-C). In addition, the percentage of cells in S phase in HeLa and RPE1 cell lines was 12% and 4%, respectively. However, we observed that the population of MDA-MB-231 and NIE-115 cells in S phase was 20% and 14%, respectively (Figure 3.11B-C). Asynchronous primary B-lymphocytes (PBL) and acute lymphoblastic leukaemia (ALL) cells were also analysed by flow cytometry (Figure 3.12A). Approximately 13% of 14183 and 14295 cells, PBL controls, were in G2/M (Figure 3.12B-C). In contrast, about 18-22% of SEM, KOPN8 and REH cells were in G2/M phase. In addition, 8-13% of Hal-01, NALM-6 and K231 cells were in G2/M phase (Figure 3.12B-C).

Hence, flow cytometry data showed that NIE-115 and MDA-MB-231 cells had higher population of cells in S and G2/M phases, whereas HeLa and RPE1 cells had lower populations in those phases. In addition, the population of ALL cells including SEM, KOPN8 and REH, in G2/M phase was higher as compared to control PBLs, 14183 and 14295. These observations may suggest a correlation between centrosome amplification and cell cycle phases. It should be noted however that these observations were based in a small group of diploid and cancer cell lines.

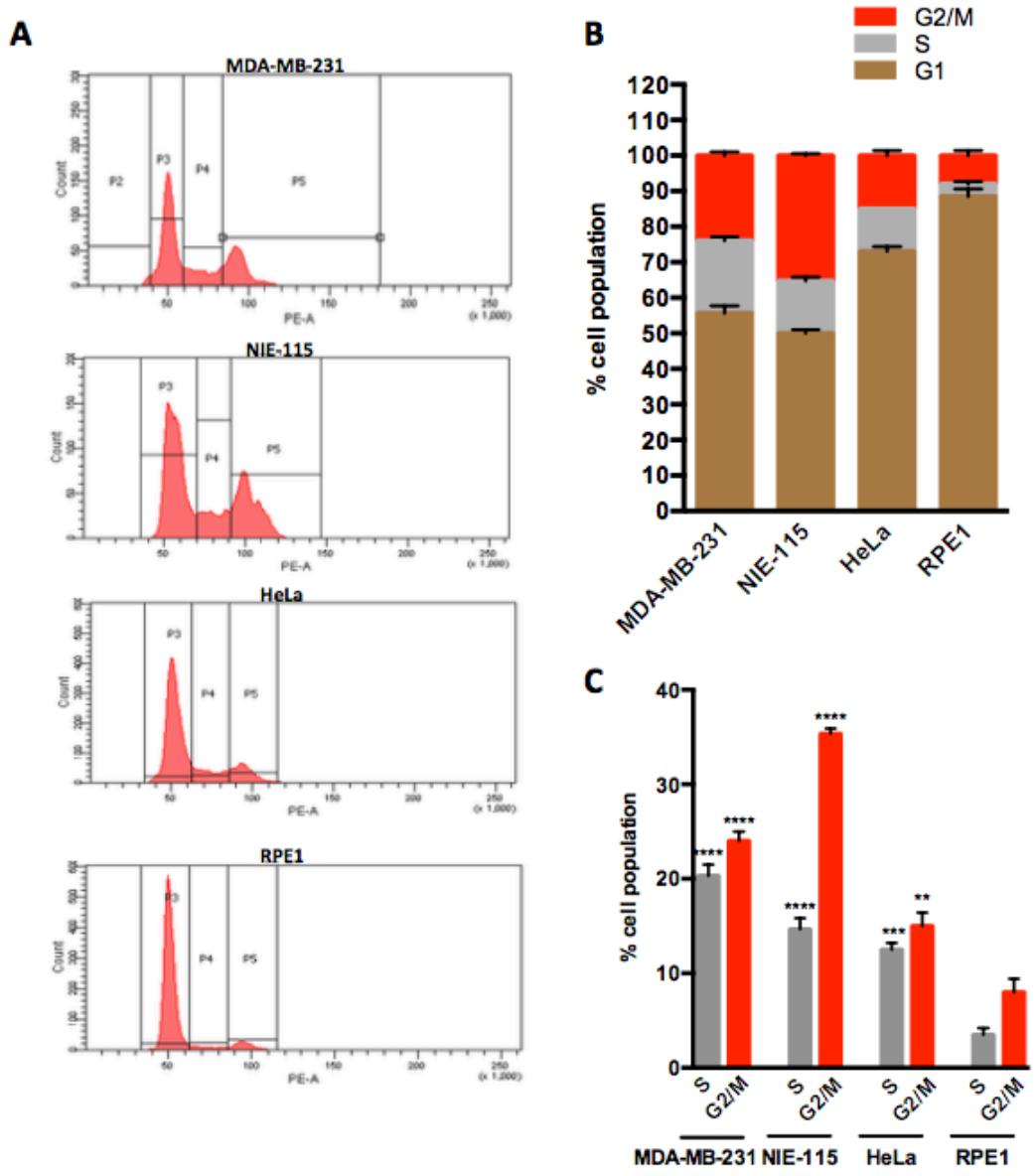

Figure 3.11. Increased population of MDA-MB-231 and NIE-115 in S and G2/M phases

A. Asynchronous MDA-MB-231, NIE-115, HeLa and RPE1 cells were seeded and after 24 hours were harvested and their cell cycle profiles analyzed by flow cytometry. **B.** The percentage of cells in each stage G1, S and G2/M is indicated for each cell line and data represent means (± S.D.) of three independent experiments. **C.** Histogram represents the S and G2/M populations of each cell line. One-way Anova, **** p<0.0001, *** p<0.001, ** p<0.01.

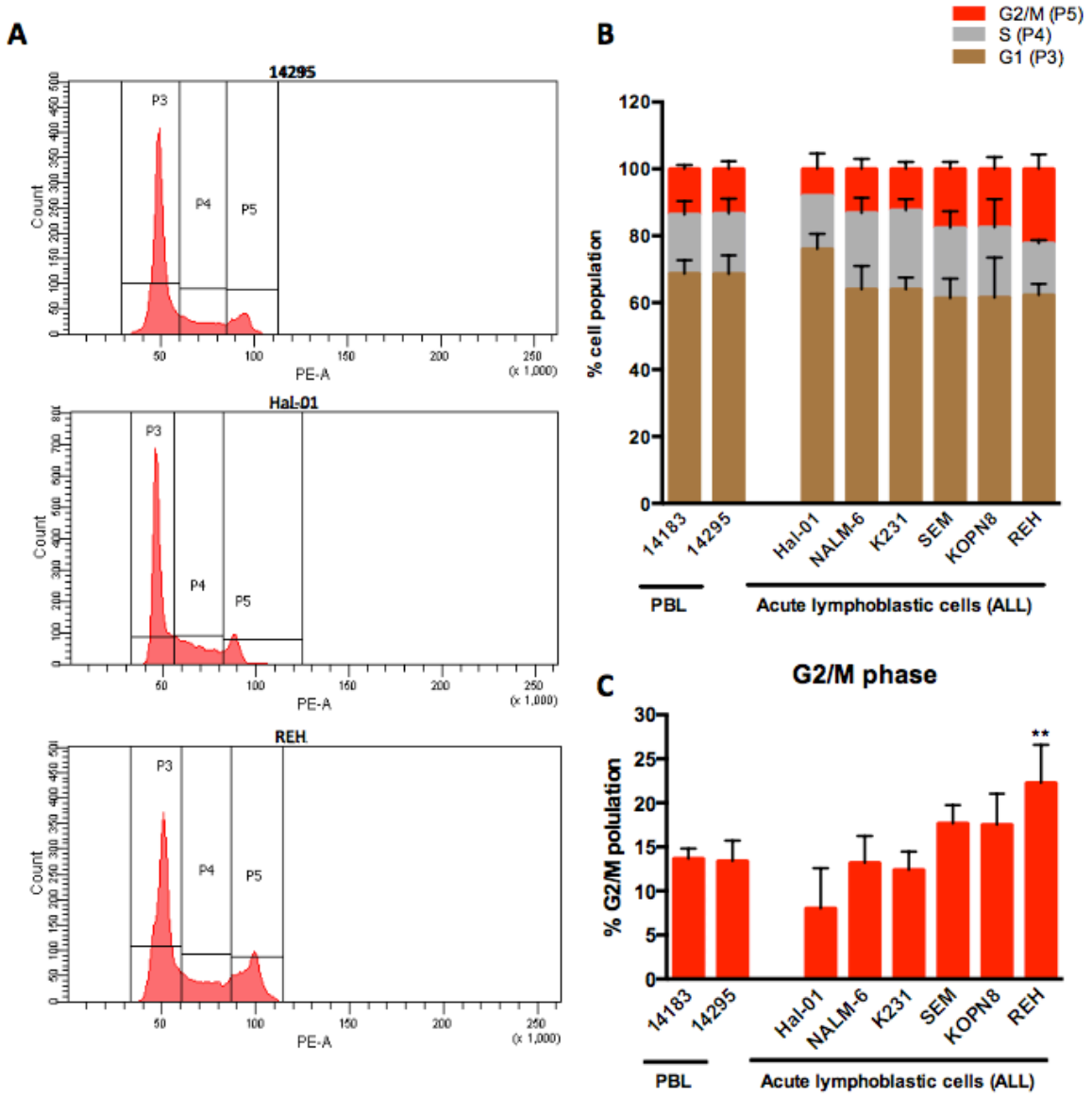

Figure 3.12. Population of ALL and PBL cells in G2/M phase

A. Asynchronous ALL cells were seeded and after 24 hours were harvested and their cell cycle profiles analyzed by flow cytometry. **B.** Histogram represents the percentage of cycling cells at each stage of the cell cycle. Data represent means (± S.D.) of three independent experiments. P3, P4 and P5 gates indicate G1, S and G2/M phase, respectively. **C.** Histogram represents the percentage of G2/M population in each cell line. ** $p<0.01$.

3.2.7 HeLa cells lack the ability to cluster centrosomes

Centrosome duplication is a highly regulated process in a cell that is initiated once in S phase in parallel with DNA replication (Nigg and Stearns, 2011). This coordination of these two processes is precisely controlled by various proteins that ensure the correct number of centrosomes, two, before the cell enters mitosis (Nigg and Raff, 2009; Conduit et al., 2015). However, the presence of extra centrosomes is a common phenotype in many cancers and this is correlated with the fact that various oncogenes and tumour suppressor proteins are involved in centrosome duplication pathways (Geihl et al., 2005; Fukasawa, 2007; Godinho and Pellman, 2014). Interestingly, one of the most common cancer types used for laboratory studies, HeLa cells, do not exhibit high centrosome amplification. We were therefore interested to know whether it has the capacity to cluster extra centrosomes in mitosis. It is possible to induce extra centrosomes in HeLa cells by allowing overduplication during S or G2 arrest (Prosser et al., 2012). We used the protocol for centrosome overduplication in HeLa cell line as described in Prosser et al (Prosser et al., 2012), and illustrated in the schematic figure with the cell cycle profiles after each treatment (Figure 3.13A). Cells were stained with centrin-2 and γ-tubulin antibodies for immunofluorescence imaging (Figure 3.13B). By inducing centrosome overduplication in HeLa cells, we scored 78% of interphase cells with amplified centrosomes, as compared to 8% of control cells (Figure 3.13C). We next examined if HeLa cells with amplified centrosomes, after induced by centrosome overduplication assay, can cluster their extra centrosomes into a bipolar state. Following centrosome overduplication, HeLa and GFP-centrin stable HeLa cell lines were released, from RO-3306 drug, for 2 hours. Staining with centrin-2 and α-tubulin antibodies revealed the frequent presence of tripolar and tetrapolar spindles in both cell lines (Figure 3.13D). Furthermore, more than 80% of mitotic cells displayed multipolar spindles in both cell lines following 2 hours release from RO-3306 (Figure 3.13E). Hence, centrosome overduplication assay induced formation of extra centrosomes in HeLa cells. However, HeLa cells were unable to cluster their amplified centrosomes to assemble bipolar spindles upon RO-3306 washout.

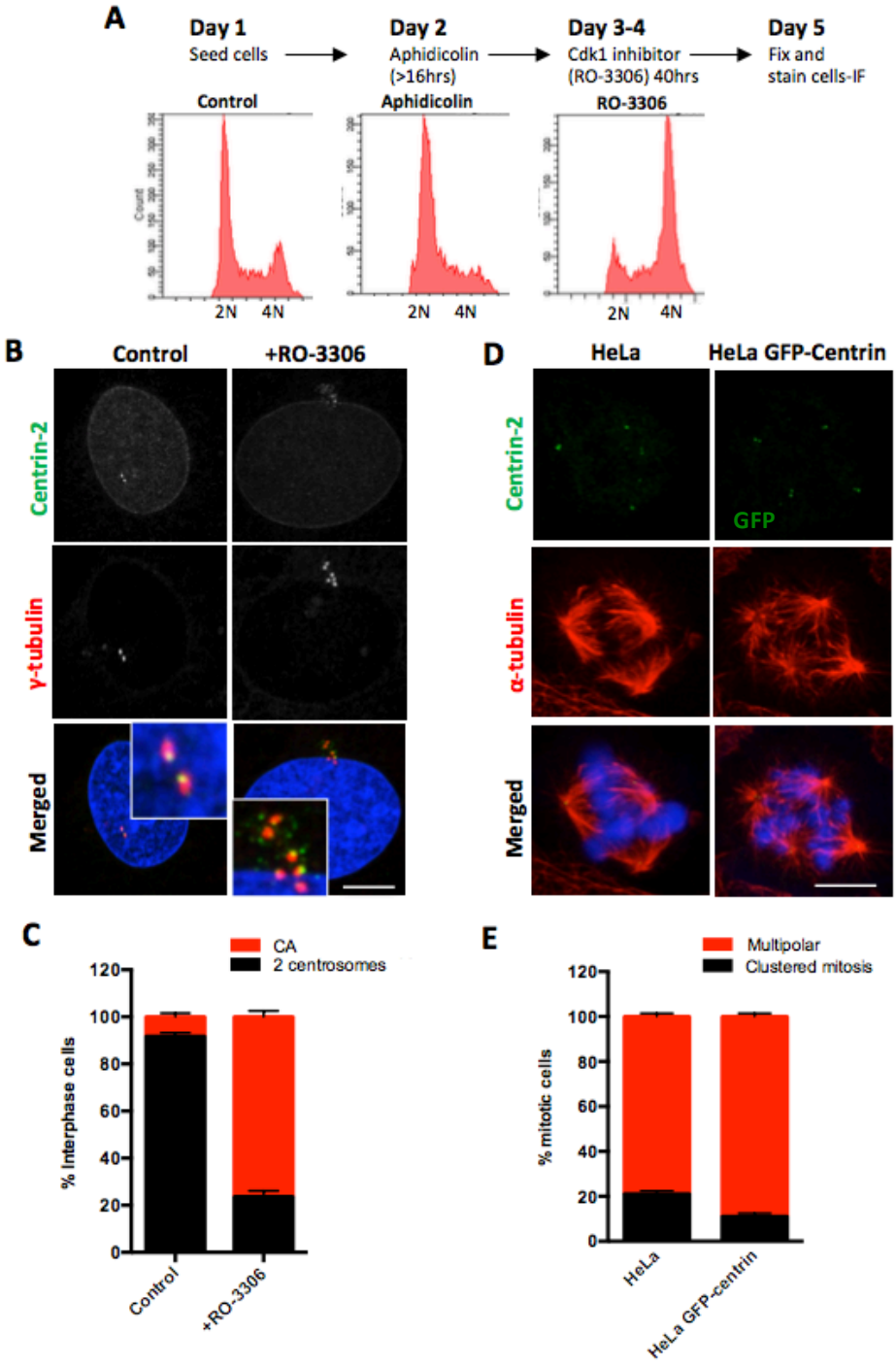

Figure 3.13. Inducing centrosome amplification and lack of centrosome clustering in HeLa

A. Cells were treated with aphidicolin for 16 hours. Following treatment, cells were released into fresh media and then incubated with RO-3306 for 40 hours. Cell cycle profiles of MDA-MB-231 cells are shown under each treatment. **B.** At the end of the treatment, HeLa cells were fixed and stained with centrin-2 (green) and γ-tubulin (red) antibodies. Hoechst 33258 was used for DNA (blue) staining. Centrosomes are indicated with an enlargement of the boxed area. Scale bar, 10 µm. **C.** Quantification of the mean number of γ-tubulin and centrin-2 staining centrosomes in each cell line. Approximately 100 cells were counted per experiment and data are shown as the mean ± S.D. of two independent experiments. **D.** Following centrosome overduplication, cells were then released into a fresh media for 2 hours. At the end of the treatment, cells were fixed and stained with centrin-2 (green) and α-tubulin (red) antibodies. Hoechst 33258 was used for DNA (blue) staining. Scale bar, 5 µm. **E.** Histogram shows the percentage of mitotic cells with amplified centrosomes in a clustered or multipolar mitosis. Approximately 50 cells were counted per experiment and data represent means ± S.D. of two independent experiments.

3.3 Discussion

The centrosome is important for several functions in a cell, including cell shape, motility and formation of the mitotic spindle during cell division (Nigg and Stearns, 2011; Mennella et al., 2014). In recent years, analyses of centrosome regulation identified numerous proteins involved in their biogenesis, duplication and organisation. Since the centrosome is involved in many aspects of cell behaviour and viability, it is not surprisingly that centrosome defects are implicated with a variety of diseases. Indeed, abnormalities in centrosomes have been reported in numerous diseases including cancers, microcephaly and ciliopathies (Pelletier et al., 2012; Betterncourt-Dias et al., 2011).

It was observed almost a century ago that centrosome defects are present in human cancers (Nigg, 2002; Boveri, 2008). A growing body of evidence has identified numerical and structural centrosome abnormalities in a large number of solid tumours and haematological cancers (Kramer et al., 2005; Godinho and Pellman, 2014; Chan, 2011). Centrosome amplification is a key characteristic in many cancers and implicated with aggressiveness of the disease and metastasis (Chan, 2011; Godinho et al., 2014). Diploid cells with amplified centrosomes usually form multipolar spindles that lead to cell death due to mitotic catastrophe. However, although cancer cells with amplified centrosomes have the potential to form multipolar spindles, they solve this issue by clustering the extra centrosomes into two poles, forming a pseudo-bipolar spindle that favours cell survival (Kwon et al., 2008; Leber et al., 2010). However, this also promotes the propagation of chromosome segregation errors that encourage tumour progeny.

Centrosome amplification arises by various mitotic defects including cytokinesis failure, cell-cell fusion and de novo centriole synthesis (Godinho et al., 2009). In addition, loss of function in various proteins such as tumour suppressors and oncogenes, that regulate centrosome duplication cycle, also contribute to centrosome amplification mechanisms (Fukasawa, 2007). Experiments described in this chapter show the analysis of

centrosome numbers in various cell lines and patient samples. Using confocal imaging, we visualised amplified centrosomes in various cancer cell lines including MDA-MB-231, NIE-115 and SCC-114. In contrast, HeLa cancer cells do not exhibit centrosome amplification and clustering was not visible. This suggests that each cancer acquires different mutations and hence, these mutations contribute to initiate and/or enhance centrosome amplification. Apart from solid cancers, many haematological malignancies including acute myeloid leukaemia (AML), non-Hodgkin lymphoma (NHL) and chronic myeloid leukaemia (CML) possess high frequency of amplified centrosomes (Kramer et al., 2005). Our findings revealed that acute lymphoblastic leukaemia (ALL) cell lines and chronic lymphocytic leukaemia (CLL) from patient samples acquire amplified centrosomes. Hence, the use of cell lines mentioned above allow us to investigate how centrosome amplification arise and how centrosome clustering in mitosis allow these cells to survive.

It has been reported by many groups that cells with amplified centrosomes possess mechanisms to either inactivate, reduce or pull together their extra centrosomes to avoid formation of multipolar spindles (Basto et al., 2008; Mikelanze-Dvali et al., 2012; Godinho et al., 2009). Of those cancer cells with amplified centrosomes, the majority can cluster their extra centrosomes into two poles and avoid formation of multipolar spindles. Studies have revealed a number of mechanisms that contribute to centrosome clustering including microtubule attachments to the kinetochores, centrosomes and cell cortex, motor protein activity, microtubule dynamics and spindle assembly checkpoint (SAC) (Kwon et al., 2008; Quintyne et al., 2005; Fielding et al., 2011; Yang et al., 2008; Ganem et al., 2009; Marthiens et al., 2012). Centrosome clustering analysis in cancer cell lines showed that MDA-MB-231, NIE-115 and SCC-114 cells can cluster their amplified centrosomes to form bipolar mitotic spindles and avoid lethal multipolarity. Furthermore, our data from live cell imaging with SiR-tubulin, a far-red fluorescent probe that stains microtubules in live cells, showed clustering of multiple asters into a bipolar state in NIE-115 and MDA-MB-231 cells. This data suggest that cells facilitate centrosome clustering by pulling together their extra centrosomes to form pseudo-bipolar mitotic spindles.

In addition, time-lapse imaging showed that NIE-115 required longer time to resolve their multiple asters into a bipolar state and therefore had extended mitotic duration, whereas RPE1 cells required less time to form mitotic bipolar spindles and complete mitosis. Interestingly, the majority of MDA-MB-231 cells resolved the multiple asters into a mitotic bipolar spindle, but the duration of mitosis was similar to RPE1 cells. We assume that MDA-MB-231 cells had shorter mitotic duration, compared to NIE-115, due to the mixed population of cells with normal and amplified centrosomes (33.5% of centrosome amplification). For the above reasons, we suggested that NIE-115 cells could be more useful to study centrosome clustering by using live cell imaging due to the particularly high frequency of centrosome amplification.

Prosser et al showed that APC/C activity during cell cycle arrest induces centrosome amplification (Prosser et al., 2012). They proposed that a complex of proteins of APC/C and Plk1 have an important role in centriole disengagement and that prolonged G2 arrest induces centriole reduplication (Prosser et al., 2012; Loncarek et al., 2010). By using a combination of aphidicolin, which arrests cells in S phase, and RO-3306, a Cdk1 inhibitor that arrests cells in G2 phase, we successfully induced formation of extra centrioles in HeLa cells. However, these treated HeLa cells were unable to cluster their amplified centrosomes into a mitotic bipolar spindle and the vast majority of cells formed multipolar mitoses. This implies that HeLa cells may lack key proteins that aid centrosome clustering. Our observations were consistent with those from Prosser et al (Prosser et al., 2012). Further analysis is needed to understand why HeLa cells, even with induced centrosome amplification, are unable to cluster their amplified centrosome in mitosis. For the reasons mentioned above, we were unable to use HeLa cells to study centrosome clustering mechanisms, but it could be used as a control in later experiments.

Loncarek et al shown that prolonged G2 arrest can cause reduplication of centrioles by Plk1 function (Loncarek et al., 2010). Plk1 kinase has function in centriole maturation and spindle assembly (Zitouni et al., 2014). We assessed the correlation between cell cycle distribution and centrosome amplification in various cell lines. Interestingly, we observed that MDA-MB-231, NIE-115, KONP8 and REH cell lines, with amplified centrosomes, had prolonged S and G2/M phases in their cell cycle compared to RPE1, HeLa, Hal-01 and NALM-6 cell lines. This implies that cancer cells may require longer period in G2/M phase, firstly to allow maturation of extra centrioles before entering mitosis and secondly, to potentially cluster their amplified centrosomes into mitotic bipolar spindles. However, centriole reduplication mechanisms are poorly understood. Furthermore, this suggests that MDA-MB-231 and NIE-115 cells, which had a high frequency of centrosome amplification, remained longer in S phase to potentially allow centriole duplication. However, HeLa cells, which do not have a high frequency of centrosome amplification, had also higher cell population in S and G2/M phases compared to RPE1. Cell cycle analysis of suspension cells suggested that ALL cell lines such as SEM, KOPN8 and REH cells, which had centrosome amplification, showed high population in G2/M phase. While other ALL cell lines, including Hal-01, NALM-6 and K231 did not show any difference as compared to controls, 14183 and 14295. Furthermore, we should mention that some of those cells with extra centrosomes, such as MDA-MB-231 and NIE-115, may already have duplicated DNA due to cytokinesis failure, therefore once these ploidy cells enter at G1 phase it is diffult to detected at this stage and the flow cytometry analysis categorised them in G2/M phase. We need to emphasize that only couple of cell lines were assessed and therefore, the correlation of centrosome amplification with S and G2/M phases is not yet clear.

Cancers with centrosome amplification are often associated with aggressive disease and metastasis (Chan, 2011; Godinho et al., 2014). Some studies have suggested centrosome amplification as a prognostic biomarker for advanced cancers such as urothelial and prostate cancers (Chan, 2011; Yamamoto et al., 2004). Immunohistochemistry analysis showed enriched pericentrin staining in interphase and the presence of mitotic and multipolar spindles in MDA-MB-231 and KOPN8 cells. Hence, it is mostly like that these

interphase cells with enriched pericentrin staining might have amplified centrosomes compared to those with reduced pericentrin staining. However, further analysis of pericentrin staining is needed to confirm these observations. Immunohistochemistry may help identifying new biomarkers that can be useful for detecting advanced stage and tumour grade in cancer patients. However, some types of cancers or benign breast lesions have no centrosome amplification (Kronenwett et al., 2005; Chan, 2011). This suggests that centrosome amplification is a distinct characteristic in various cancers, but the presence of centrosome amplification alone is not a sufficient characteristic to diagnose malignancy. Hence, a combination of already established factors and centrosome amplification could be used to predict aggressiveness and survival of patients with cancer.

In conclusion, a positive correlation between cell cycle, S and G2/M phases, and centrosome amplification has been observed in cell lines. However, further analysis of multiple cell lines is needed and so the link is far from proven. As centrosome amplification found in aggressive and metastatic tissues, it implies that identifying centrosome biomarkers can be beneficial for prognosis of the disease and using them in combination with other already established markers may be useful for detection of advanced stages in tumours. In addition, the results mentioned above allow us to confirm that MDA-MB-231, NIE-115 and SCC-114 have amplified centrosomes and centrosome clustering during mitosis, as it was previously showed by other studies (Pannu et al., 2014; Kwon et al., 2008; Leber et al., 2010). Interestingly, acute lymphoblastic leukaemia (ALL) and chronic lymphocytic leukaemia (CLL) acquire extra centrosomes, suggesting that indeed haematological malignancies have centrosome defects in numbers. This implies that it would be possible to use those adherent and suspension cell lines to investigate centrosome clustering mechanisms and identify new players in those pathways.

Centrosome amplification in cancer and other diseases is currently under investigation and the molecular pathways involved are not yet fully understood. So whilst this study

will not speculate on whether centrosome amplification arise from de novo centriole synthesis or cytokinesis failure, it will endeavour to elucidate the centrosome clustering mechanisms.

Chapter 4

Hsp70 and Nek6 proteins are required for centrosome clustering in cancer cells

4.1 Introduction

Cancer cells with amplified centrosomes have found ways to survive lethal multipolar mitoses by clustering their extra centrosomes into two poles forming a pseudo-bipolar spindle (Brinkley, 2001; Kwon et al., 2008). Experimental studies have suggested multiple microtubule-associated mechanisms that aid centrosome clustering including microtubule dynamics, motor protein activity, such as HSET and cytoplasmic dynein, and microtubule attachments to the centrosome, cell cortex and chromosomes (Kwon et al., 2008; Quintyne et al., 2005; Leber et al., 2010). Spindle assembly checkpoint (SAC) function is another mechanism essential for effective centrosome clustering, as it allows sufficient time to cluster the extra centrosomes into two poles and delays the metaphase to anaphase transition until complete chromosome congression has been achieved (Basto et al., 2008; Drosopoulos et al., 2014). However, the underlying mechanisms need to be better understood if we are aiming to design methods to inhibit these in cancer cells.

In stressed conditions, cells rely on heat shock proteins (HSPs) to restore proper protein folding and homeostasis (de Billy et al., 2009). Cancer cells are constantly under proteotoxic stress, as well as hypoxia and oxidative stress, and need to deal with their incorrectly folded proteins and abnormal signalling pathways that threaten their survival (Whitesell and Lindquist, 2009). To achieve this, cancer cells rely on the heat shock factor 1 (HSF1) stress response. HSF1 is a stress-inducible transcription factor that regulates the expression of different heat shock proteins (Hsp), including these of the Hsp90 and Hsp70 families (Whitesell and Lindquist, 2009; de Billy et al., 2009). These two major chaperone families play essential roles in cancer cells (Hong et al., 2013; Garrido et al., 2006). Hsp70 is one the most highly conserved HSPs with eight distinct members in human cells with different levels of expression and subcellular localisation (Daugaard et al., 2007). The cytosolic Hsc70 isoform is ubiquitously expressed in all cells, whereas Hsp70-1A and Hsp70-1B, together known as Hsp72, are strongly expressed in response to stressed conditions, including in cancer cells (Powers et al., 2010). Since cancer cells are constantly under stress conditions, they rely on Hsp72 for growth and survival (Garrido et al., 2006; Rohde et al., 2005; Daugaard et al., 2005). Simultaneous

knockdown of Hsc70 and Hsp72 expression by siRNA showed increased cell arrest and death in various cancer cell lines (Powers et al., 2008; Schmitt et al., 2006). Apart from their roles in protein folding and homeostasis, Hsp70 proteins are involved in microtubule dynamics and protect centrosomes of mitotic cells when exposed to heat shock (Liang and MacRae, 1997; Hut et al., 2005; Makhnevych and Houry, 2013). Recently, we showed that Hsp72 is required for mitotic spindle assembly in cancer cells by promoting the stability of K-fibres through recruitment of the ch-TOG-TACC3 complex (O'Regan et al., 2015b). The Nek6 mitotic kinase was found to phosphorylate Hsp72 at threonine 66, an event that was selectively targets Hsp72 to the mitotic spindle (O'Regan et al., 2015b). The novel functions of Hsp72 in mitotic spindle assembly, chromosome congression and microtubule-kinetochore attachments raised the prospect that this stress-induced chaperone protein and its upstream kinase might be interesting regulators of centrosome clustering.

Since chaperone proteins are essential for survival of cancer cells, a large effort is now focused on development of HSP inhibitors. Significant progress has been made in the development of selective Hsp90 targeted drugs (Hong et al., 2013; Mahalingam et al., 2009). In contrast, Hsp70 has proven much less amenable to the development of pre-clinical candidate inhibitors. Nevertheless, a small molecule adenosine-derived inhibitor, known as VER-155008, which targets the ATPase binding domain, has been developed as a selective tool compound that blocks activity of Hsc70 and Hsp72 (Williamson et al., 2009; Massey et al., 2010). To date a number of other chemical inhibitors of Hsp70, including pifthrin-μ, apoptozole and 15-deoxyspergualin (15-DSG), have been described but these tent to be less specific (Nadeau et al., 1994; Powers et al., 2010; Leu et al., 2009; Williams et al., 2008).

Of the mammalian NIMA-related kinase (NEK) family, Nek6, Nek7 and Nek9 have been implicated in mitotic spindle assembly mechanisms (Prosser et al., 2016; Fry et al., 2012). Nek6, Nek7 and Nek9 kinases act in the same pathway with Nek9 to be an upstream activator of Nek6 and Nek7 (O'Regan et al., 2007; Roig et al., 2002; Belham et al., 2003). A cascade of phosphorylation upstream of Nek9 by Aurora-A and Plk1 is required to activate and phosphorylate Nek9 (Bertran et al., 2011; Belham et al, 2003). Despite the

fact that these NEK kinases are implicated in microtubule dynamics during mitosis, none of the NEKs have yet been shown to be involved in centrosome clustering mechanisms. As mentioned earlier the Nek6-Hsp72 pathway stabilizes K-fibres and mitotic spindle, we therefore wanted to know if this pathway is required for clustering of amplified centrosomes.

Since the presence of extra centrosomes and their clustering during mitosis have been observed in a variety of solid and blood cancers, the development of agents that specifically target these pathways could offer a selective approach for cancer therapy. Agents have been described, such as griseofulvin, bromonoscapine, reduced BN (RBN) and the phenanthrene-derived poly (ADP-ribose) polymerase inhibitor (PJ-34), that induce multipolarity in cancer cells (Rebacz et al., 2007; Karna et al., 2011; Inbar-Rozensal et al., 2009; Pannu et al., 2012). Griseofulvin, and its derivatives, was one of the first de-clustering agents (Rebacz et al., 2007; Raab et al., 2012). It was observed that griseofulvin treatment induces multipolarity by generating acentrosomal spindle poles, i.e. poles that are lacking centrosomes (Ogden et al., 2014). However, the mechanism through which griseofulvin induces multipolarity is still unclear.

Together, understanding centrosome clustering pathways and the proteins involved provide important insights on a key survival mechanism of cancer cells. Here, we wished to investigate whether Hsp70 proteins were required for centrosome clustering in cancer cells. Simultaneously, Nek6 acts upstream of Hsp72 for mitotic spindle assembly, we also wanted to investigate whether Nek6 was implicated in centrosome clustering. We wished to analyse whether inhibiting the Nek6-Hsp72 pathway acts in a similar way to griseofulvin in cancer cells. In addition, we explored whether upstream activators of Nek6, the Aurora-A and Plk1, were also implicated in Nek6-Hsp72 pathway in mitotic progression and centrosome clustering in cancer cells.

4.2 Results

4.2.1 Hsp70 inhibition blocks centrosome clustering in cancer cells

As previously described in Chapter 3, MDA-MB-231, NIE-115 and SCC-114 cells, as well as ALL cells have extra centrosomes which can cluster into two poles forming a pseudo-bipolar mitotic spindle. We utilised these cancer cells to investigate the role of Hsp70 proteins in centrosome clustering. We first tested the consequences of increasing doses (5-20 μM) of the Hsp70 inhibitor, VER-155008, on centrosome de-clustering in MDA-MB-231 and NIE-115 cancer cells. Cells were stained for immunofluorescence imaging with antibodies against centrin-2 to visualise centrioles and α-tubulin to detect microtubules. Importantly, we scored only mitotic cells with extra centrosomes, classifying them as having either clustered bipolar or multipolar spindles. In MDA-MB-231 cells, Hsp70 inhibition promoted multipolarity in a dose-dependent manner with 20 μM Hsp70i leading to 37% cells with amplified centrosomes having multipolar spindles (Figure 4.1A-B). In NIE-115 cells, Hsp70 inhibition also favoured multipolar spindles in a dose-dependent manner, with 20 μM Hsp70i leading to 50% cells with amplified centrosomes having a multipolar spindle (Figure 4.1C-D). Hence, we observed that Hsp70 inhibition partially blocked centrosome clustering in both cell lines.

To analyse the role of Hsp70 in centrosome clustering, we used the SiR-tubulin probe to stain microtubules in live cells. SiR-tubulin was added to cells 7 hours prior to imaging and Hsp70i (10 μM) added immediately before imaging. We observed that MDA-MB-231 cells frequently had multiple microtubule organizing centres (MTOCs) at the state of mitosis that eventually clustered into a bipolar state before progression into anaphase and completion of mitosis (Figure 4.2A). However, in the presence of Hsp70 inhibitor, the majority of cells were unable to cluster their MTOCs and retained in this state until the end of the experiment (Figures 4.2A). Analysis of individual cells revealed that there was a small change in the length of prophase in the Hps70i cells compared to controls, although this was not significant.

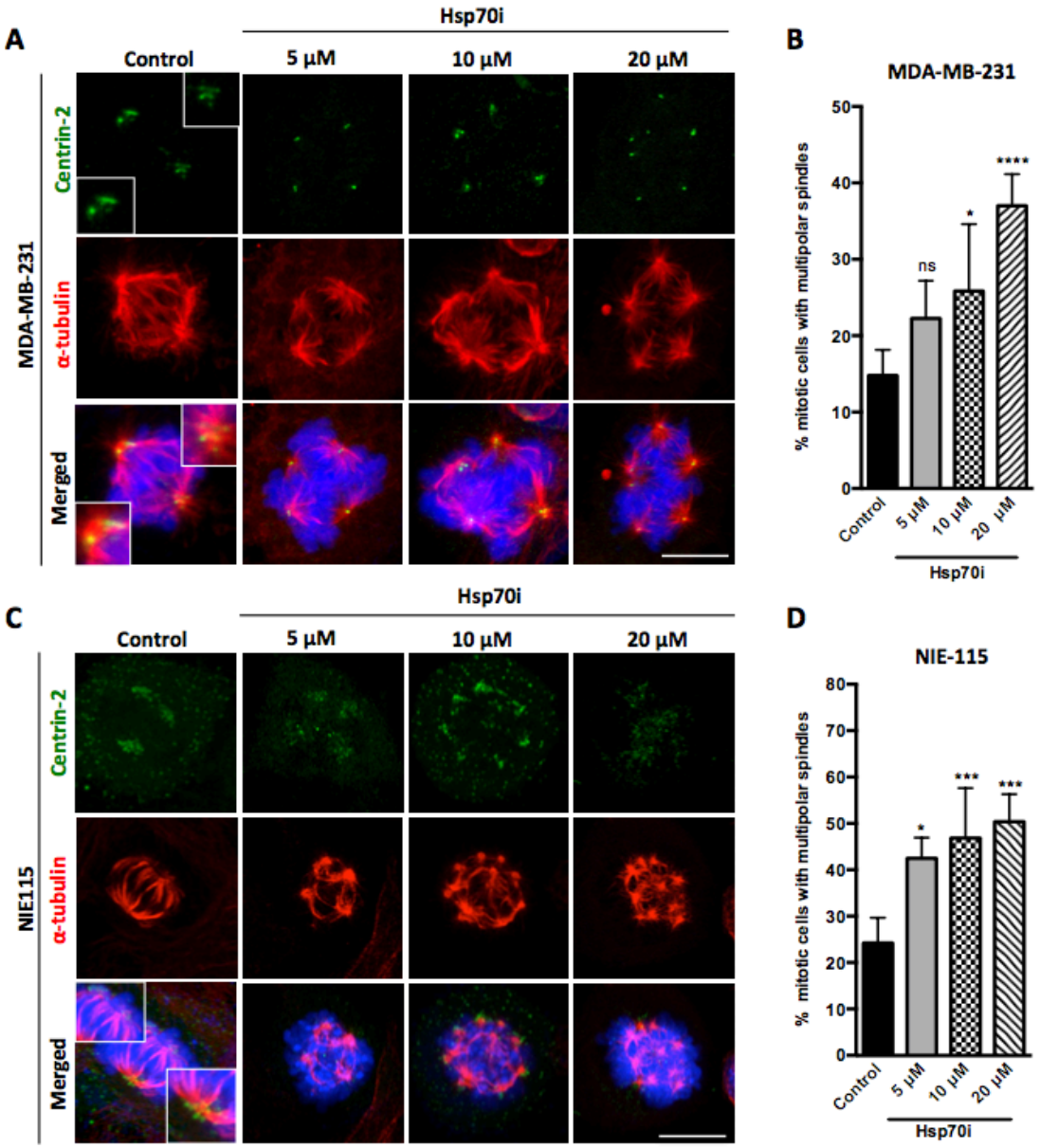

Figure 4.1. Centrosome clustering is blocked by inhibition of Hsp70 in MDA-MB-231 cells

A,C. MDA-MB-231 and NIE-115 cells were treated with 5-20 µM Hsp70 inhibitor, VER-155008, for 4 hours. Cells were fixed and stained for immunofluorescence microscopy with centrin-2 (green) and α-tubulin (red) antibodies. Merged panels include DNA (blue) staining with Hoechst 33258. Scale bar, 5 µm. **B, D.** Histograms represent means of mitotic cells with multipolar spindles for each treatment. Data are the means ± S.D. of four experiments. 50-75 mitotic cells were counted per experiment.

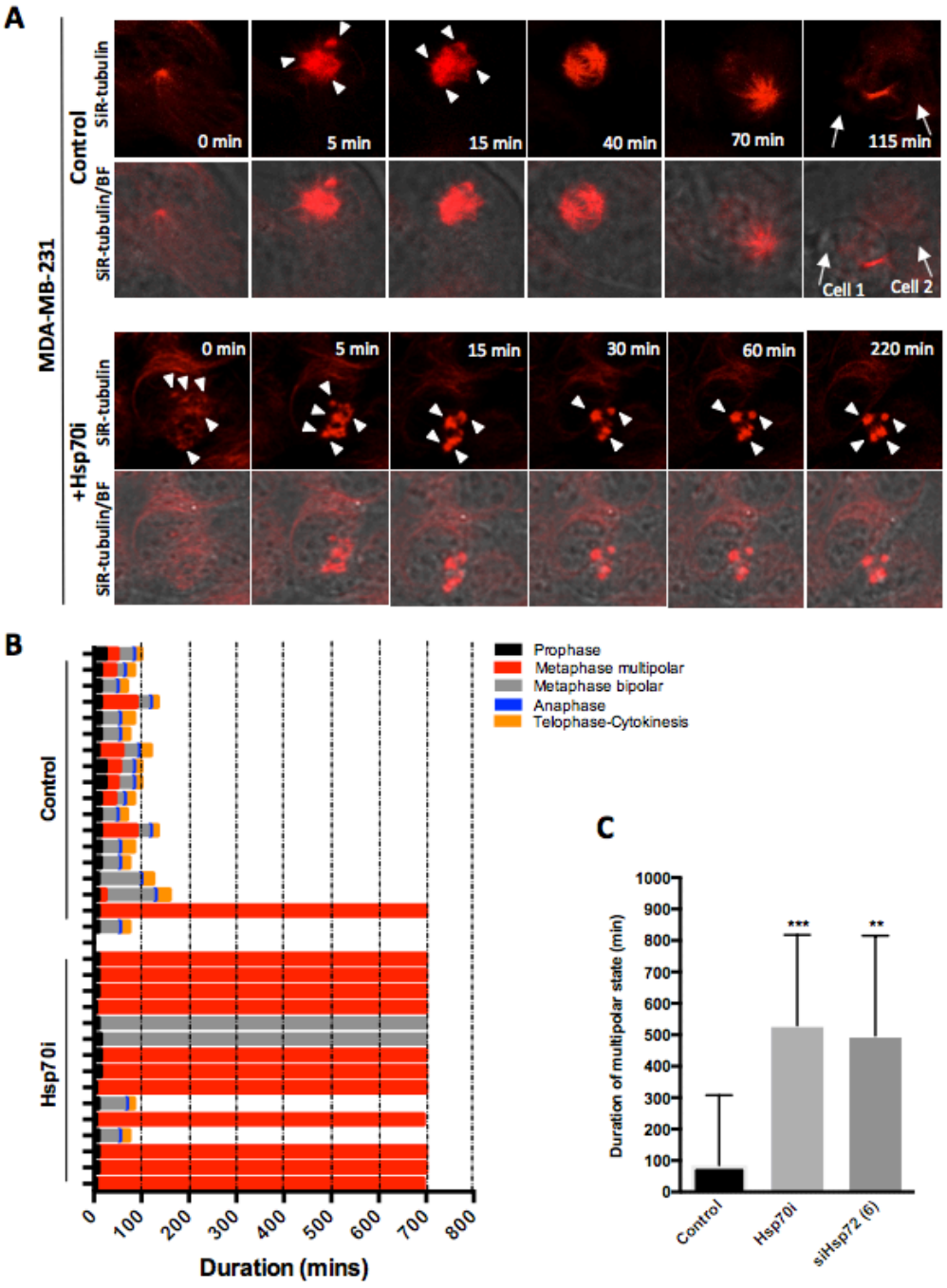

Figure 4.2. Inhibition of Hsp70 blocks centrosome clustering in MDA-MB-231 cells

A. MDA-MB-231 cells were incubated with SiR-tubulin for 7 hours prior to time-lapse imaging in the presence or absence of 10 µM Hsp70i. Still images are shown of SiR-tubulin alone (top rows) and merged with brightfield (BF; bottom rows) at the times indicated. Arrowheads indicate spindle poles; arrows indicate daughter cells following division. Scale bar, 10 µm. **B.** Time-lapse imaging was used to follow MDA-MB-231 cells in the absence or presence of Hsp70i. Each bar is representative of a single cell with the time spent in each stage of mitosis indicated. Imaging was stopped after 700 minutes. **C.** The time spent with a multipolar spindle in control, Hsp70i and siHsp72 (6) treated cells is indicated. Data are the means ± S.D. of two experiments. 10-20 mitotic cells were counted per experiment.

In contrast, we found a large and significant increase in the length of time that Hsp70i treated or Hsp72 depleted cells retained in this multipolar state with mean of 550 minutes, and in many cases until the end of the experiment (Figure 4.2B-C). In the absence of Hps70 inhibitor or depletion of Hsp72, the mean time in a multipolar state was 45 minutes (Figure 4.2C). In neuroblastoma NIE-115 cells incubated with the SiR-tubulin probe, the multipolar spindle state was maintained in the presence of Hsp70i or depletion of Hsp72 for an extended time with a mean of 480 and 560 minutes, respectively, and in many cases remained in this state within the time-frame of the experiment (Figure 4.3A-C). In the absence of Hsp70i, the mean time in a multipolar state was 78 minutes (Figure 4.3C).

To assess the role of Hsp70 proteins in centrosome clustering in ALL cells, we examined spindle multipolarity using antibodies against CEP135 to stain centrioles and α-tubulin to stain microtubules (Figure 4.4A). Importantly, we scored all mitotic cells, rather than only those with amplified centrosomes, classifying them as having either bipolar or multipolar spindles. In the majority of ALL cell lines including SEM, KONP8 and REH, Hsp70 inhibition promoted multipolarity in a dose-dependent manner with 20 μM Hsp70 inhibitor leading to 15-30% cells having multipolar spindles (Figure 4.4B). In other ALL cell lines such as Hal-01, NALM-6 and K231, Hsp70 inhibition showed a small increase in the presence of multipolar mitoses, although this was not significant (Figure 4.4B). In contrast, 14183 and 14295 cells, PBLs used as controls, Hsp70 inhibition (10-20 μM) did not cause a significant increase in formation of multipolar spindles (Figure 4.4A-B). Here, we observed that the frequency of multipolar spindles is strongly correlated with centrosome numbers of each cell line. This suggested that Hsp70 inhibition promoted multipolarity only in cells with amplified centrosomes formed multipolar mitoses upon Hsp70 inhibition.

Having found that Hsp70 inhibition blocks centrosome clustering in MDA-MB-231, NIE-115 and ALL cells, we also examined the effect of Hsp70 inhibition in HeLa cells. As described in Chapter 3, HeLa cells have a very low frequency (8%) of extra centrosomes and centrosome clustering was not visible even when centrosome amplification was

induced by arrest in S/G2 phase. We wanted to observe if multipolarity was induced in HeLa cells upon Hsp70 inhibition.

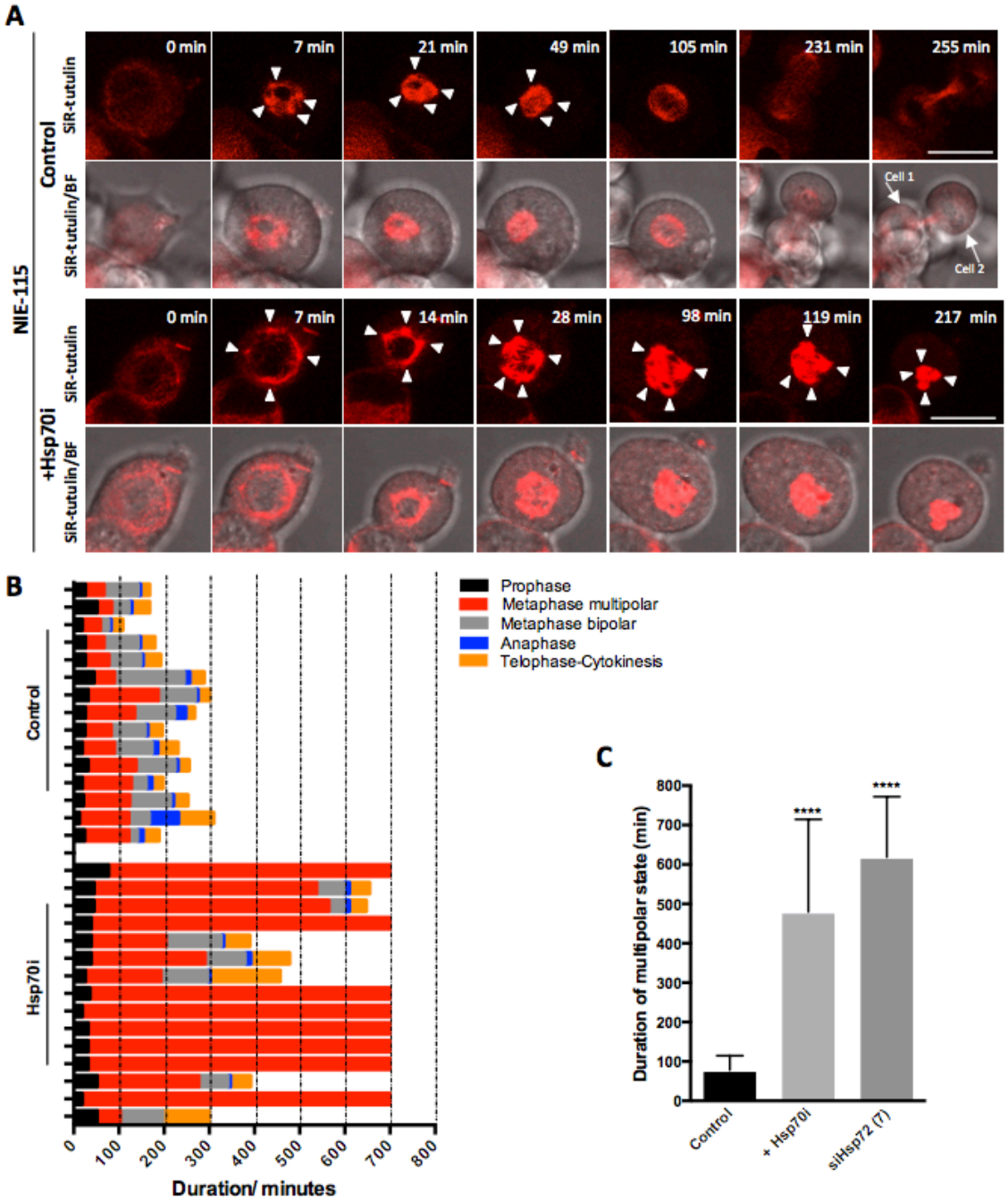

Figure 4.3. Resolution of a multipolar to bipolar state is blocked by Hsp70 inhibition in NIE-115

A. NIE-115 cells were incubated with SiR-tubulin prior to time-lapse imaging in the presence or absence of 10 µM Hsp70 inhibitor. Cells were imaged on a laser scanning confocal microscope for 16 hours after the staining treatment. SiR-tubulin (top rows) and brightfield (BF; bottom rows) stills of control and Hsp70i are shown at the times indicated. Arrowheads indicate spindle poles; arrows indicate daughter cells following division. Scale bar, 10 µm. **B.** Live cell imaging was used to follow NIE-115 cells in the absence or presence of Hsp70 inhibitor. The mitotic duration of cells was measured when MTOC was visible until spindle formation. Time was measured in minutes. Images were captured every 7 minutes. **C.** The time spend with a multipolar spindle in control, Hsp70i and siHsp72 (7) treated cells is indicated; mean ± S.D.; *n*=2; 15 cells.

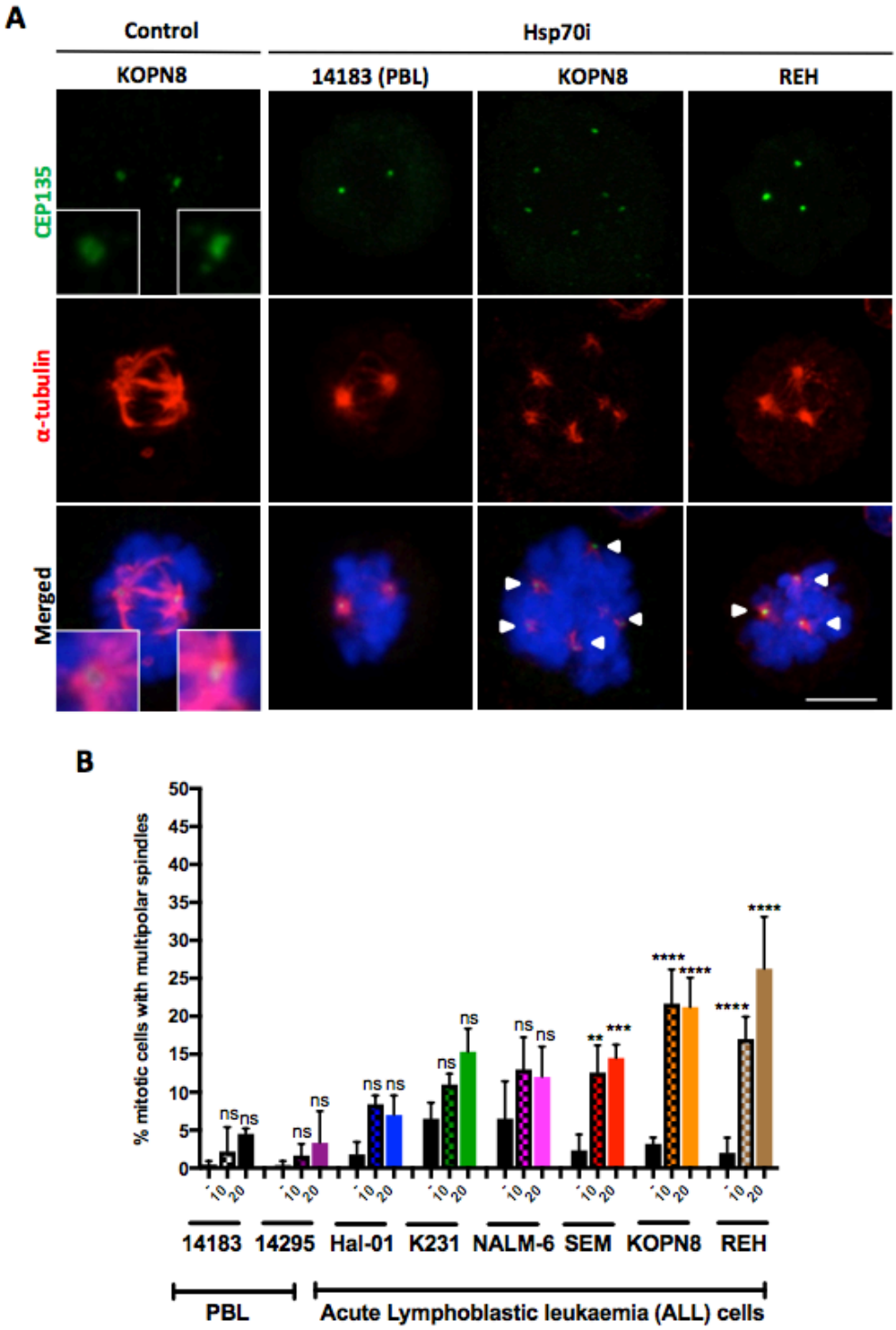

Figure 4.4. Hsp70 inhibition blocks centrosome clustering in ALL cells

A. Cell lines as indicated were either untreated (control) or treated with 10 µM Hps70 inhibitor for 4 hours. Cells were stained with CEP135 (green) and α-tubulin (red) antibodies. Merged panels include DNA (blue) staining with Hoechst 33258. Centrosomes are indicated with an enlargement of the boxed area. Scale bar, 2.5 µm. **B.** Histogram represents the percentage of mitotic cells with multipolar spindles for each treatment (10 or 20 µM). Data represent means ± S.D. of three experiments. 30-50 mitotic cells were counted per experiment. ****p<0.0001, **p<0.01.

Using immunofluorescence staining, we observed that Hsp70 inhibition did not cause a significant increase in formation of multipolar spindles in HeLa cells (Figure 4.5A-B). However, we observed that HeLa cells exhibited misalignment chromosomes upon Hsp70 inhibition consistent with our previous results (O'Regan et al., 2016).

Hence, using immunofluorescence microscopy and live cell imaging, we found that Hsp70 inhibition promoted multipolarity in cancer cells with amplified centrosomes. Furthermore, using a subset of ALL cell lines that harbour amplified centrosomes, we showed that Hsp70 inhibition resulted in increased multipolarity compared to PBLs. Interestingly, loss of Hsp70 activity did not cause formation of multipolar spindles in HeLa cells that do not exhibit centrosome amplification, although we observed high frequency of mitotic cells with misaligned chromosomes committed with a separate role in spindle assembly. Based on these data, we suggest a role for Hsp70 activity in centrosome clustering in cancer cells.

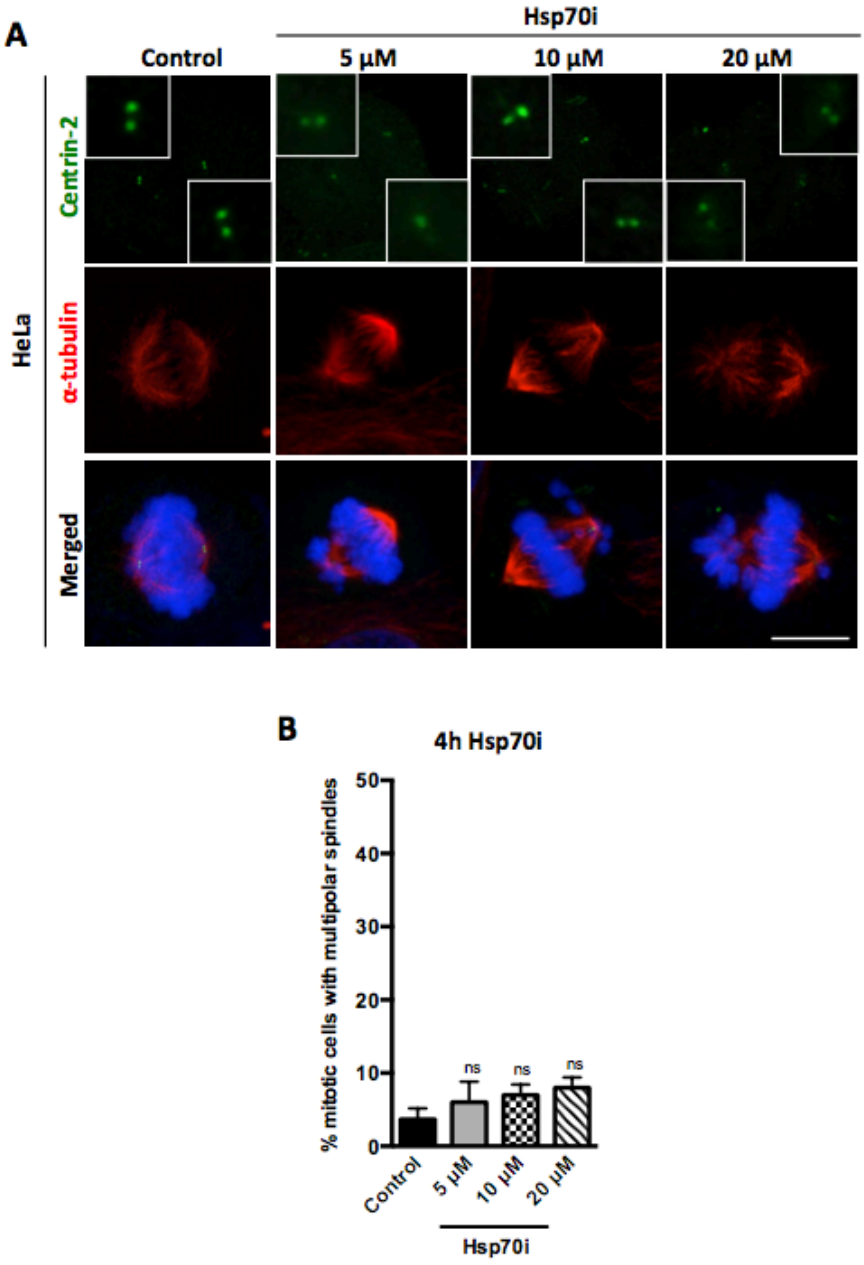

Figure 4.5. Hsp70 inhibition does not induce spindle multipolarity in HeLa cells

A. HeLa cells were treated with 5-20 µM Hsp70 inhibitor for 4 hours. Cells were stained with centrin-2 (green) and α-tubulin (red) antibodies. Merged panels include DNA (blue) staining with Hoechst 33258. Scale bar, 5 µm. **B.** Histogram represents the percentage of mitotic cells with multipolar spindles for each treatment. Data are shown means ± S.D. of three experiments. 50 mitotic cells were counted per experiment.

4.2.2 Depletion of Hsp72 or Hsc70 blocks centrosome clustering

The chemical Hsp70 inhibitor, VER-155008, blocks the catalytic activity in most of the members of the Hsp70 family including Hsp72, Hsc70 and Grp75 (Massey et al., 2010). To investigate which of the Hsp70 isoforms are required for centrosome clustering, we used siRNA interference to deplete the Hsp72 and Hsc70 isoforms from MDA-MB-231 cells. Two independent siRNA oligonucleotides were used to deplete Hsp72, Hsc70 or GAPDH as control for 72 hours (Figure 4.6A-B). Similarly, mouse siRNA oligonucleotides were used to deplete Hsp72 in NIE-115 cells for 72 hours (Figure 4.6C). Using immunofluorescence microscopy to investigate spindle state in cells with amplified centrosomes, we observed that Hsp72 depletion led to 35% of cells with multipolar spindles compared to 14% mock-depleted ones (Figure 4.7A, C). Interestingly, depletion of Hsc70 led to 32% of cells with multipolar spindles (Figure 4.7B,D). Additionally, depletion of Hsp72 in mouse neuroblastoma, NIE-115, cells led to approximately 45% of multipolarity compared to 18% of mock-depletion (Figure 4.7E). These results demonstrate that depletion of either Hsp72 or Hsc70 blocked centrosome clustering in cancer cells with amplified centrosomes.

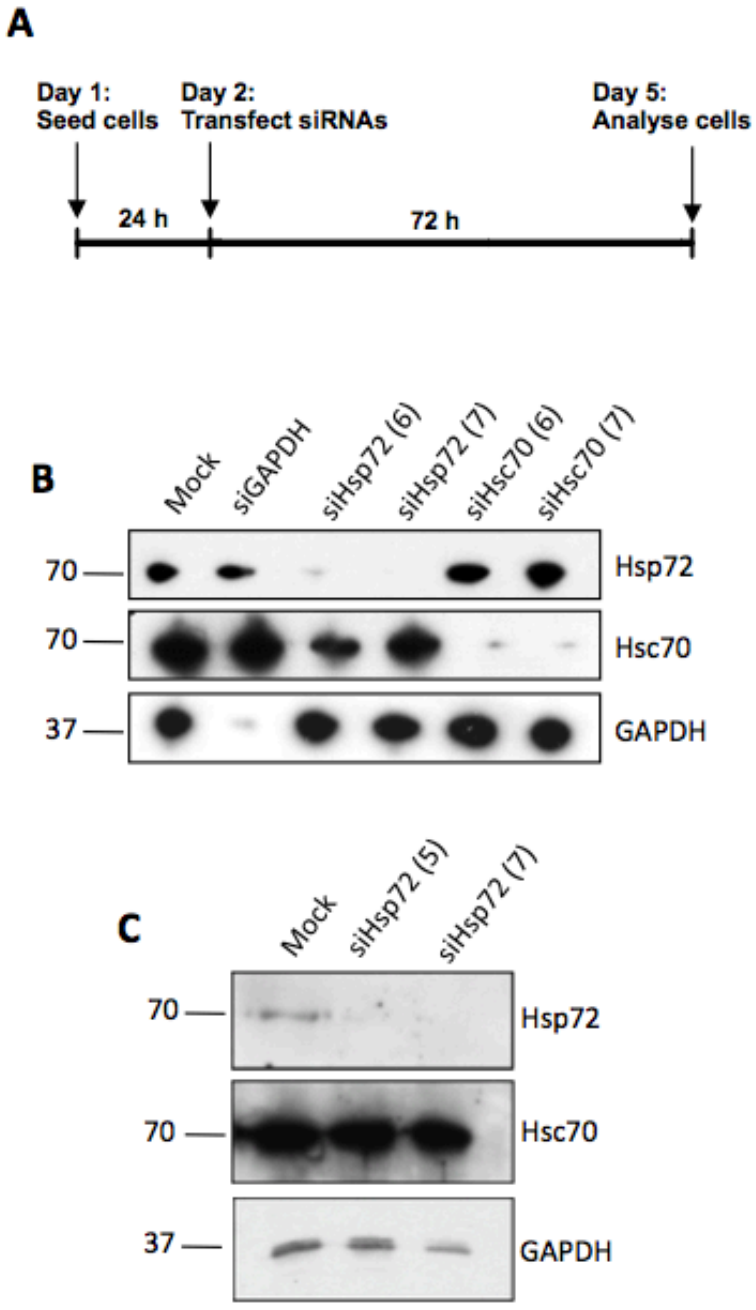

Figure 4.6. siRNA-mediated depletion of Hsp72 and Hsc70 in MDA-MB-231 and NIE-115 cells

A. Protocol for siRNA mediated depletion and analysis of MDA-MB-231 and NIE-115 cells. **B.** MDA-MB-231 cells were mock- or siRNA-transfected with oligonucleotides to deplete Hsp72 (siHsp72-6 or -7) or Hsc70 (siHsc70-6 or -7) or GAPDH for 72 hours. **C.** NIE-115 cells were mock- or siRNA-transfected with mouse oligonucleotides to deplete Hsp72 (siHsp72-5 or -7) for 72 hours. Lysates were analysed by SDS-PAGE and Western blotting for Hsp72, Hsc70 and GAPDH antibodies. Molecular weights are indicated (kDa).

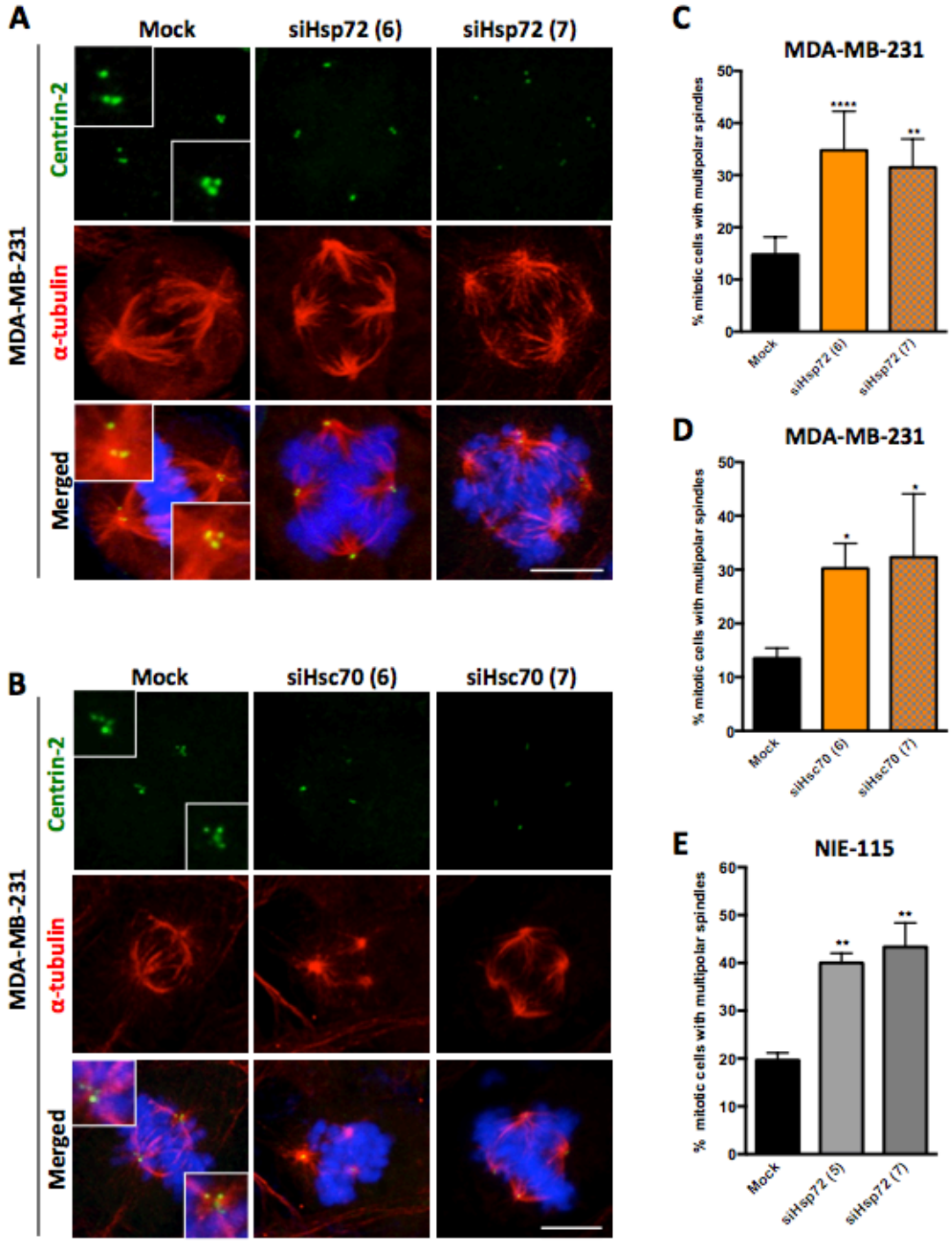

Figure 4.7. Centrosome clustering is blocked by depletion of Hsp72 or Hsc70 in cells with amplified centrosomes

A-B. MDA-MB-231 cells were mock- or siRNA-transfected with oligonucleotides to deplete Hsp72 (siHsp72-6 or 7) or Hsc70 (siHsc70-6 or -7) for 72 hours. Cells were stained with centrin-2 (green) and α-tubulin (red) antibodies. Merged panels include DNA (blue) staining Hoechst 33258. Scale bar, 5 µm. **C-D.** Histograms represent means of mitotic cells with multipolar spindles for each depletion. **E.** NIE-115 cells were mock- or siRNA-transfected with mouse oligonucleotides to deplete Hsp72 (siHsp72-5 or -7). Data shown are means ± S.D. of four experiments. 50 mitotic cells were counted per experiment.

4.2.3 Nek6, but not Nek7, is required for centrosome clustering

To understand the mechanism of how Hsp72 and Hsc70 chaperones were involved in centrosomes clustering, we examined if the NEK family, specifically Nek6 and Nek7, were implicated in centrosome clustering pathways. Members of this family such as NEK6 and NEK7 are important for spindle assembly during mitosis (O'Regan and Fry, 2009). Recently, O'Regan et al have shown that Nek6, but not Nek7, phosphorylates Hsp72 and targets it to mitotic spindle (O'Regan et al., 2015). From this stage, we mainly focused on Hsp72 isoform to investigate further its role in centrosome clustering and its interacting partner Nek6 kinase.

As Hsp72 is required for centrosome clustering, we wanted to determine whether the upstream kinase Nek6 is also involved in centrosome clustering. siRNA interference was utilised to deplete Nek6 and the closely-related Nek7 kinase from MDA-MB-231 cells using two independent siRNA oligonucleotides (Figure 4.8A). Immunofluorescence imaging revealed that depletion of Nek6 led to a substantial increase of multipolarity with 37% of Nek6-depleted mitotic cells with amplified centrosomes having multipolar spindles compared to 14% mock- depleted cells (Figure 4.8B-C). In contrast, Nek7 depletion did not induce multipolarity, with only 15% of mitotic cells with amplified centrosomes having multipolar spindles (Figure 4.8B-C). To confirm the role of Nek6 in centrosome clustering, we used Flag-Nek6 siRNA resistance constructs to rescue centrosome clustering upon Nek6 depletion in MDA-MB-231 cells (Fig. 4.9A). Strikingly, wild-type (WT) but not kinase-inactive (KD) Nek6 rescued centrosome clustering in cells from which Nek6 had been depleted, showing the importance of Nek6 kinase activity in this process (Fig. 4.9B-C).

Based on these results, loss of Nek6, but not Nek7, triggers multipolarity in MDA-MB-231 cells with amplified centrosomes. We therefore propose that Nek6 but not Nek7 kinase is required for centrosome clustering. Our working hypothesis is therefore that cancer cells use the Nek6-Hsp72 pathway to cluster amplified centrosomes in mitosis, however further experiments are needed to understand how this complex works to promote centrosome clustering.

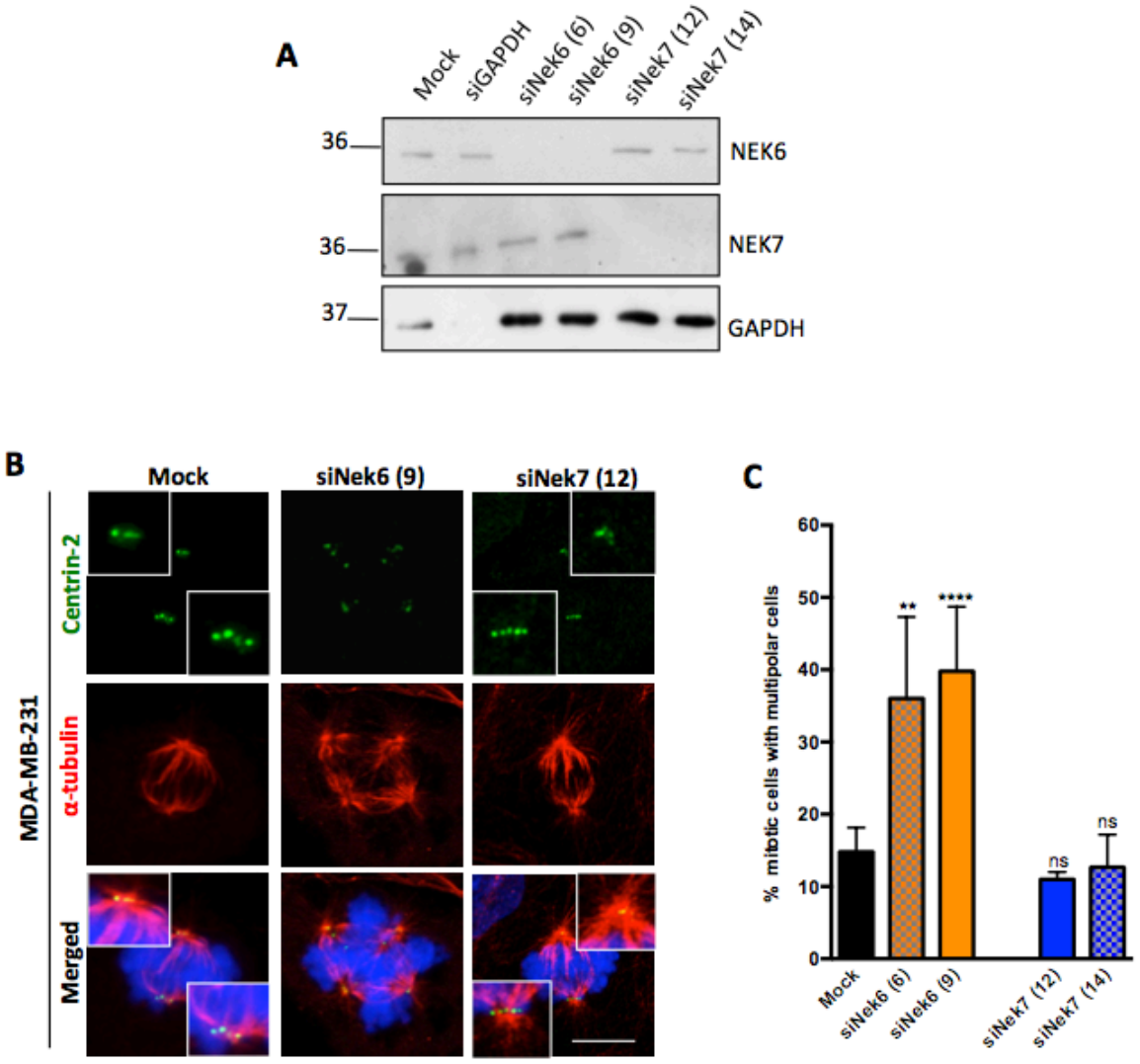

Figure 4.8. Depletion of Nek6 blocks centrosome clustering in MDA-MB-231 cells

A. Cell extracts were prepared from mock-, GAPDH-, Nek6- (siNek6-6 or -9) and Nek7- (siNek7-12 or -14) depleted MDA-MB-231 cells after 72 hours transfection. Western blots showing the expression level of Nek6, Nek7 and GAPDH. **B.** MDA-MB-231 cells were transfected with siRNAs against Nek6 or Nek7 for 72 hours. Cells were stained with centrin-2 (green) and α-tubulin (red) antibodies. Merged panels include DNA (blue) staining with Hoechst 33258. Scale bar, 5 µm. **C.** Histogram represents means of mitotic cells with multipolar spindles in each transfection. Data are the means ± S.D. of four experiments. 50-75 mitotic cells were counted per experiment.

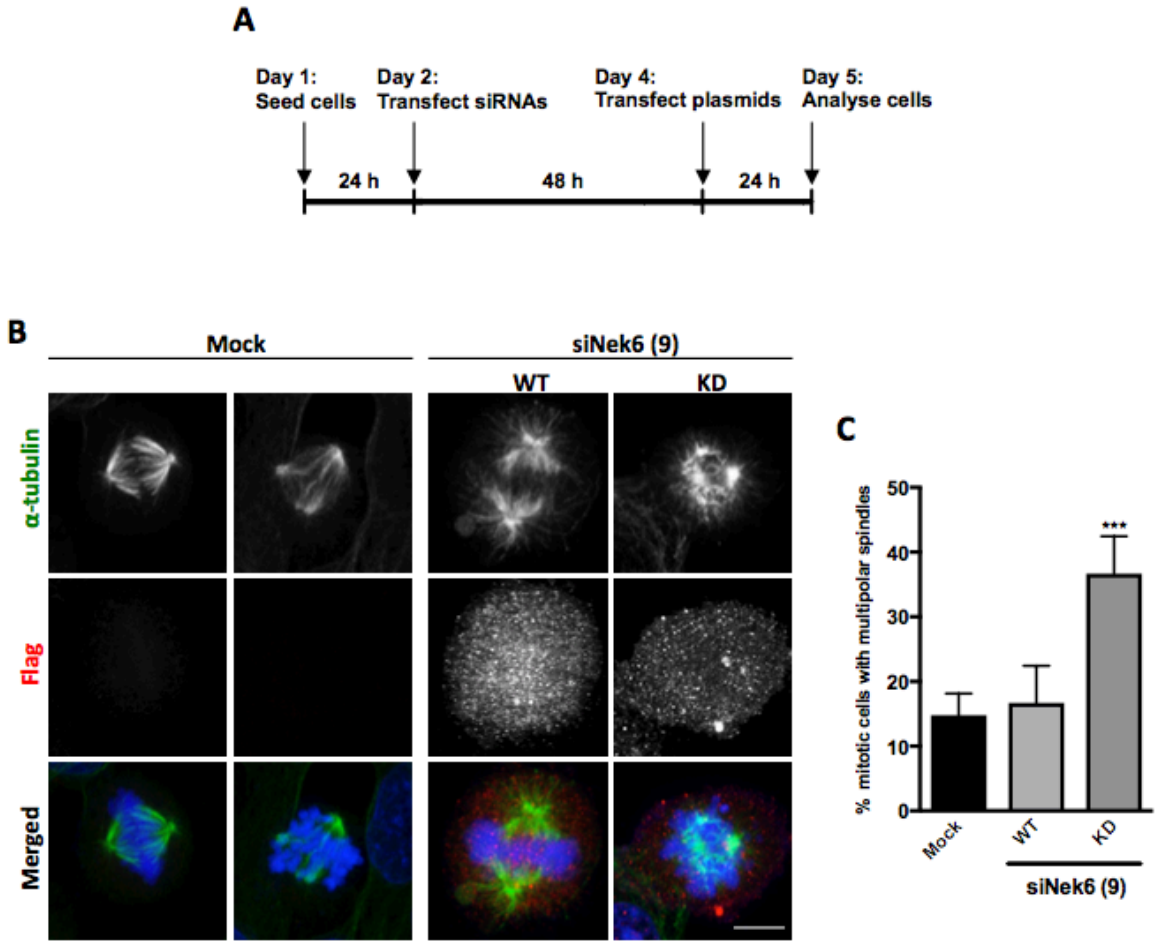

Figure 4.9. WT Nek6 rescues centrosome multipolarity that arise upon Nek6 depletion in MDA-MB-231 cells

A. Protocol for siRNA mediated depletion, plasmid transfection and analysis of MDA-MB-231 cells. **B.** MDA-MB-231 cells were mock- or siRNA-transfected with siRNA oligonucleotides to deplete Nek6 for 48 hours before transfection with Flag-Nek6 constructs as indicated for 24 hours. Cells were stained with α-tubulin (green) and flag (red) antibodies. Merged panels include DNA (blue) staining with Hoechst 33258. Scale bar, 5 µm. **C.** Histogram represents means of mitotic cells with multipolar spindles in each transfection. Data are the means ± S.D. of three experiments. 10-15 mitotic cells were counted per experiment.

4.2.4 Griseofulvin induces formation of acentrosomal spindle poles

Griseofulvin, a well-described centrosome clustering inhibitor, was identified from fungal *Penicillium* extracts and found to induce spindle multipolarity and mitotic arrest in human cancer cell lines (Rebacz et al., 2007). The mechanism of this drug is still not fully understood, however it is known that it binds tubulin and stabilizes microtubules (Raab et al., 2012; Rebacz et al., 2007). We therefore decided to study how griseofulvin treatment compares to the phenotypes that result from blocking the functions of Hsp72 and Nek6.

MDA-MB-231, NIE-115 and HeLa cancer cells were treated with 10 and 20 µM griseofulvin for 4 hours and analysed by immunofluorescence microscopy (Figure 4.10A-B and 4.11A). 10 and 20 µM griseofulvin induced multipolarity 29% and 51% in MDA-MB-231 cells (Figure 4.10C). Griseofulvin treatment promoted multipolarity in a dose-dependent manner with 10 and 20 µM griseofulvin led to 72% and 78% in NIE-115 cells (Figure 4.10D). In addition, 10 and 20 µM griseofulvin induced multipolarity 51% and 75% in HeLa cells (Figure 4.11A-B). Quantification of the number of cells with multipolar spindles after 10 or 20 µM griseofulvin revealed that over 60% of ALL cells showed multipolarity (Figure 4.12A-C). Interestingly, we also observed that griseofulvin treatment led to a substantial increase of multipolarity, 50-60%, in PBLs cells compared to <5% in DMSO-treated cells (Figure 4.12C). Hence, both PBL and ALL cell lines had a high frequency of multipolarity upon griseofulvin treatment.

After establishing the presence of multipolarity upon griseofulvin treatment in MDA-MB-231, NIE-115 and HeLa cells, we carefully examined the multipolar phenotypes in each cell line using the centriole marker, centrin-2. Analysis of centrioles in multipolar mitotic cells revealed that griseofulvin induces formation of ‘‘acentrosomal’’ spindle poles, as defined by poles lacking centrosomes (Figure 4.13A). We observed that in MDA-MB-231 cells 82% of multipolar mitoses had acentrosomal spindles, whereas in NIE-115 cells 35%

of multipolar spindles had acentrosomal poles (Figure 4.13B). Most importantly, 86% HeLa cells with multipolar spindles had acentrosomal poles upon griseofulvin treatment (Figure 4.13B).

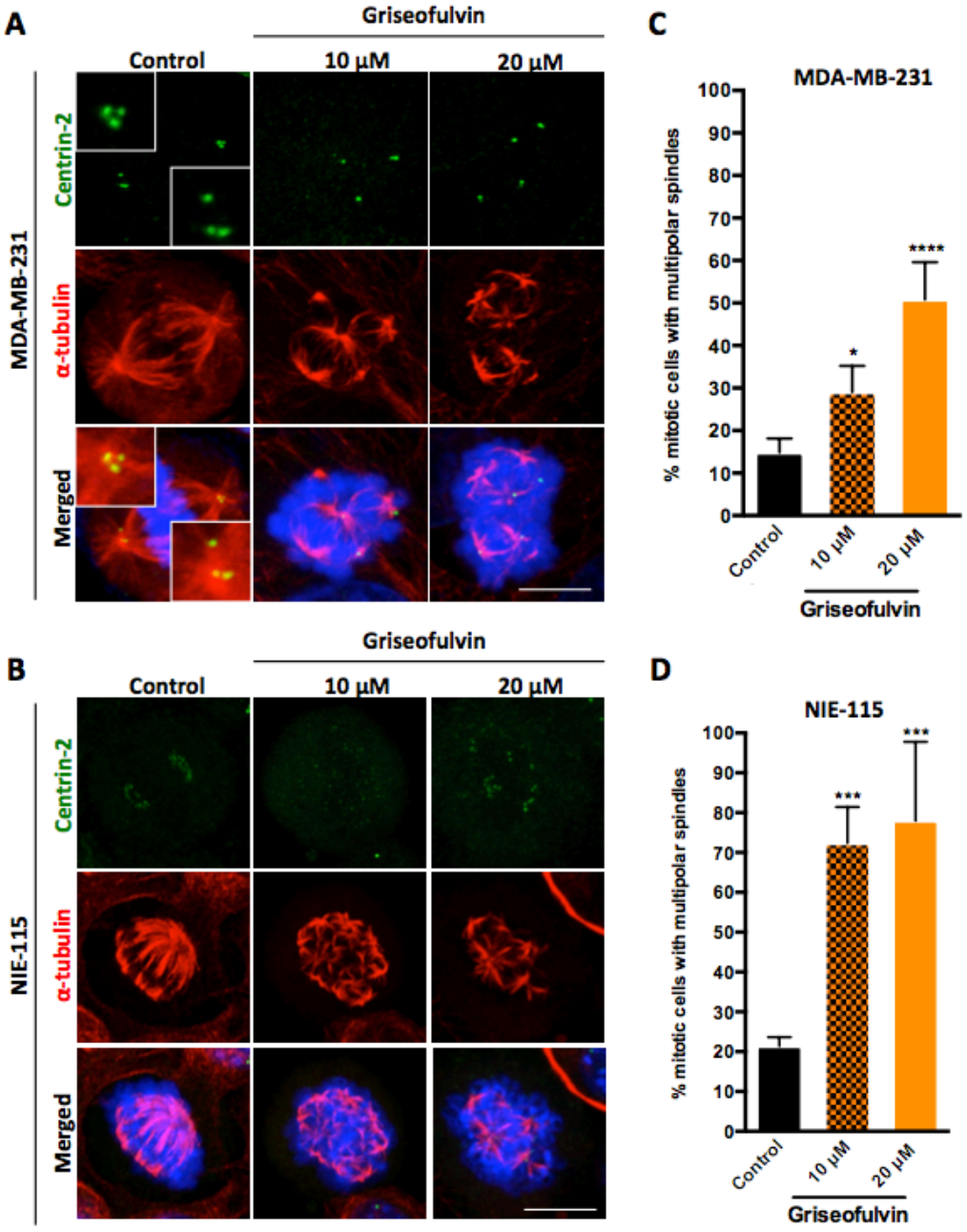

Figure 4.10. Griseofulvin induces multipolarity in mitotic MDA-MB-231 and NIE-115 cells

A-B. MDA-MB-231 and NIE-115 cells were treated with 10 or 20 µM griseofulvin for 4 hours. Cells were stained with centrin-2 (green) and α-tubulin (red) antibodies. Merged panels include DNA (blue) staining with Hoechst 33258. Scale bar, 5 µm. **C-D.** Histograms represent the percentage of mitotic cells with multipolar spindles for each treatment. Data represent means ± S.D. of three experiments. 50 mitotic cells were counted per experiment.

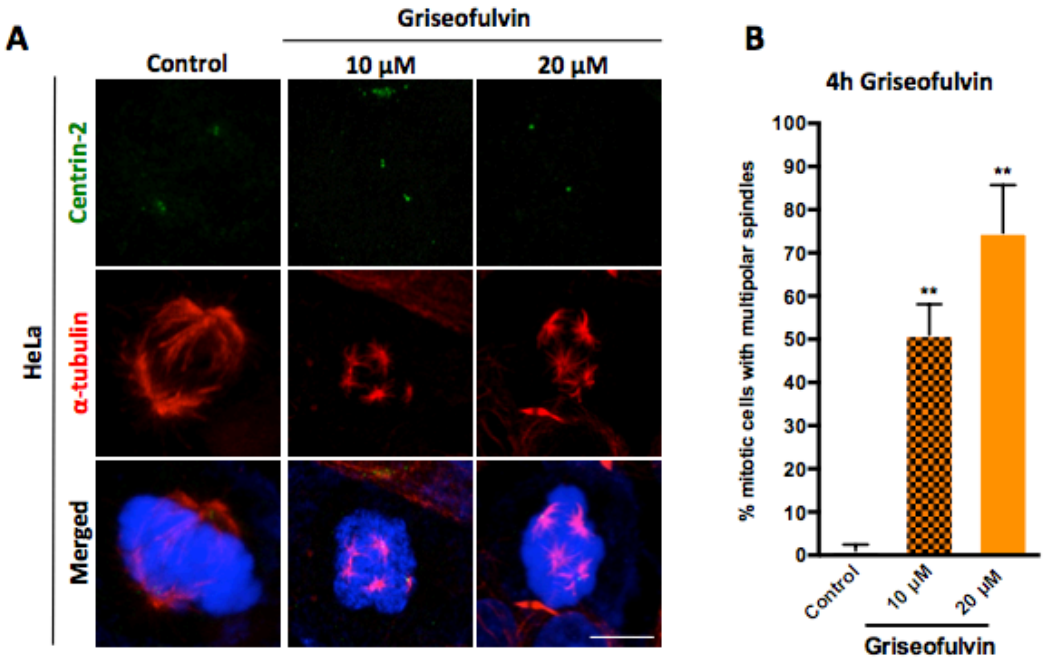

Figure 4.11. Griseofulvin induces multipolarity in mitotic HeLa cells

A. HeLa cells were treated with 10 or 20 µM griseofulvin for 4 hours. Cells were stained with centrin-2 (green) and α-tubulin (red) antibodies. Merged panels include DNA (blue) staining with Hoechst 33258. Scale bar, 5 µm. **B.** Histogram represents the percentage of mitotic cells with multipolar spindles for each treatment. Data represent means ± S.D. of three experiments. 50 mitotic cells were counted per experiment.

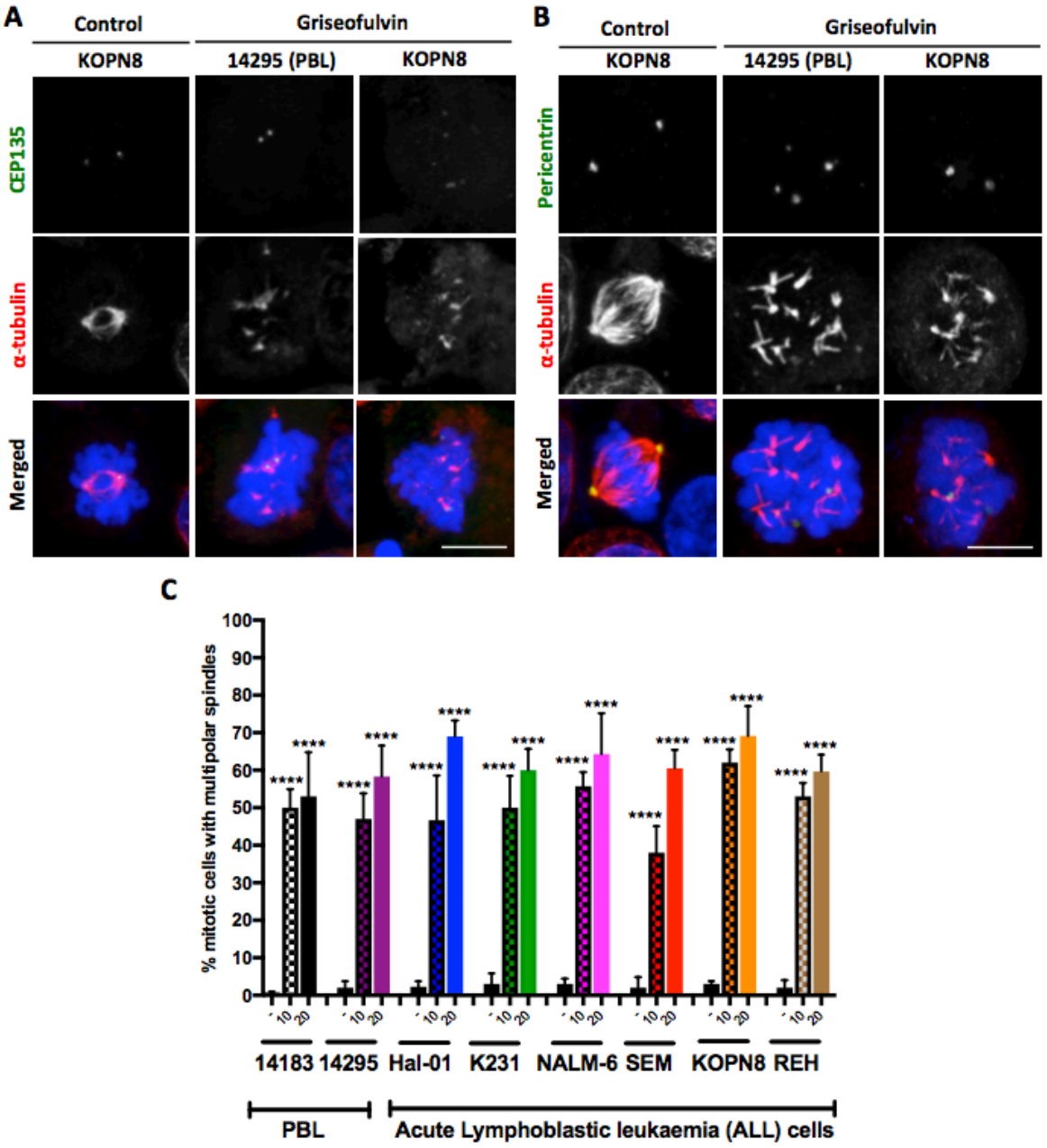

Figure 4.12. Griseofulvin causes multipolarity in mitotic ALL and PBL cells

A-B. Cells as indicated were untreated (control) or treated with 10 µM griseofulvin for 4 hours. Cells were stained with CEP135 or pericentrin (green) and α-tubulin (red) antibodies. Merged panels include DNA (blue) staining with Hoechst 33258. Scale bar, 2.5 µm. **C.** Histogram represents the percentage of mitotic cells with multipolar spindles for each treatment. Data represent means ± S.D. of three experiments. 30-50 mitotic cells were counted per experiment.

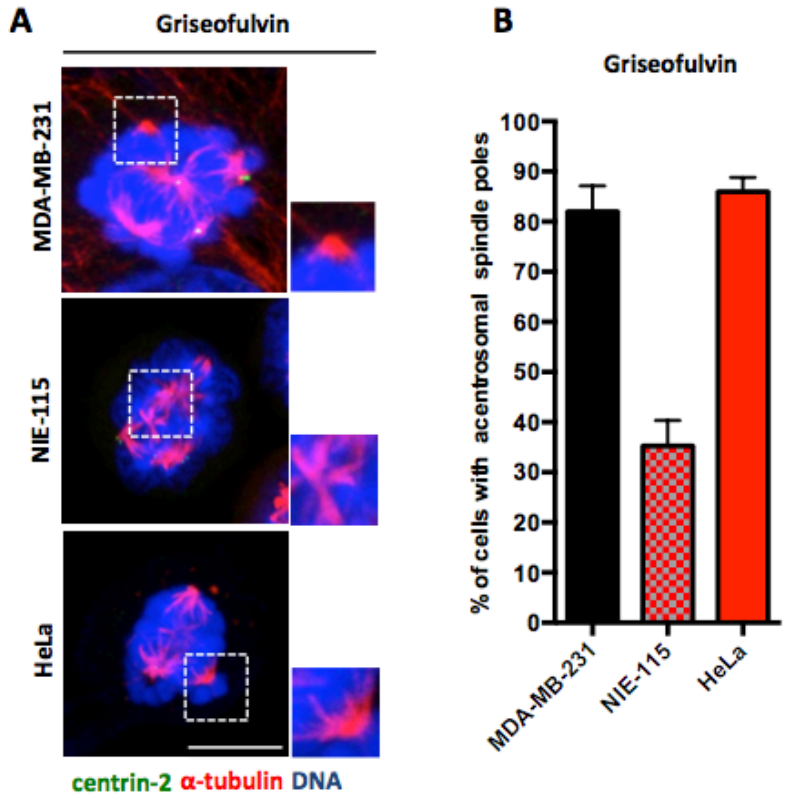

Figure 4.13. Griseofulvin induces acentrosomal spindle poles

A. MDA-MB-231, NIE-115 and HeLa cells were treated with 10 µM griseofulvin for 4 hours. Merged panels include staining of centrin-2 (green), α-tubulin (red) antibodies and DNA (blue) with Hoechst 33258. Acentrosomal spindle poles are indicated with an enlargement of the boxed area. Scale bar, 5 µm. **B.** Histogram represents the percentage of mitotic cells with acentrosomal spindle poles in each cell line. Data represent means ± S.D. of three experiments. 30-50 mitotic cells were counted per experiment.

In conclusion, griseofulvin induces multipolarity in cancer cells at least in part through generation of acentrosomal spindle poles. This was first observed in HeLa cells, which do not possess amplified centrosomes. Furthermore, ALL and healthy PBLs cell lines also formed multipolar mitoses independent of centrosome number.

4.2.5 Loss of Hsp72 or Nek6 function does not promote acentrosomal spindle poles

As described in the previous sections, our data showed that loss of Hsp72 and Nek6 function promotes multipolarity in cancer cells with amplified centrosomes, whereas griseofulvin induces formation of multipolar spindles in all cell lines independent of their centrosome content. Based on our data, we suggested that griseofulvin or Hsp70 inhibition induced multipolarity under different mechanisms, which still remain unclear. To elucidate the origin of multipolar mechanisms, we analysed the phenotypes of multipolar spindles upon each treatment. In sharp contrast to griseofulvin treatment, analysis of multipolar mitoses in MDA-MB-231 cells treated with Hsp70 inhibitor or subject to depletion of Hsp72 or Nek6 showed that the vast majority of the poles in the multipolar spindles contained centrioles (Figure 4.14A-B). Specifically, the percentage of cells with multipolar spindles that had acentrosomal poles were <5% for the Hsp70i and Hsp72 depletion, and <10% for Nek6 depletion (Figure 4.14B).

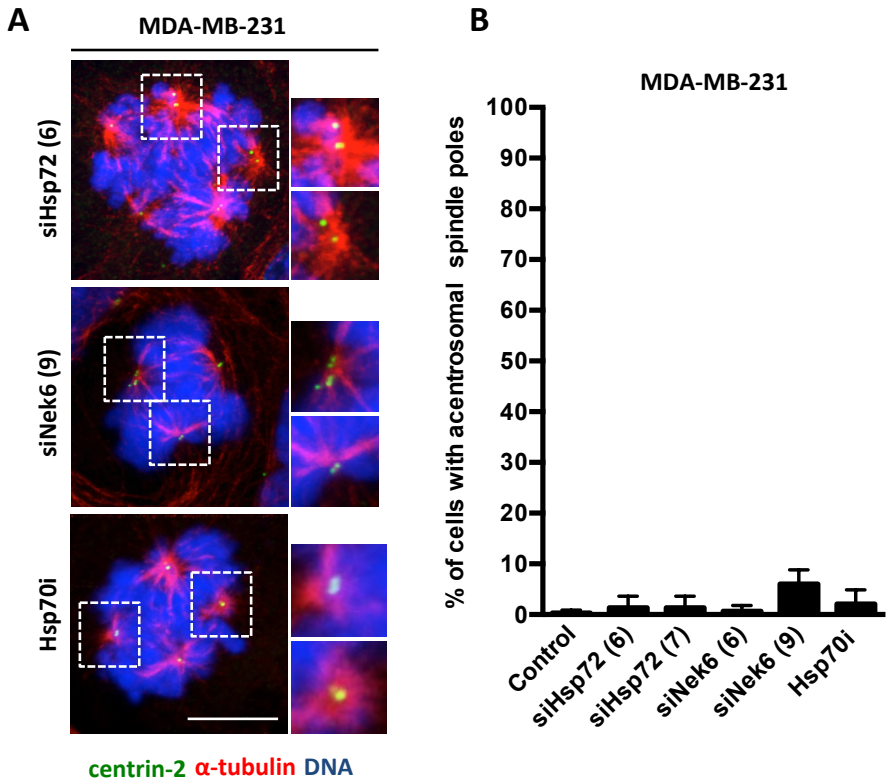

Figure 4.14. Hsp72 or Nek6 depletion does not promote acentrosomal spindle poles

A. MDA-MB-231 were treated with Hsp70i at 10 µM for 4 hours or transfected with siRNA oligonucleotides against Hsp72 (-6, -7) or Nek6 (-6, -9) for 72 hours. Merged panels include staining of centrin-2 (green), α-tubulin (red) antibodies and DNA (blue) with Hoechst 33258. Centrosomal spindle poles (top and bottom boxes) are indicated with an enlargement of the boxed area. Scale bar, 5 µm. **B.** Histogram represents the percentage of mitotic cells with acentrosomal spindle poles followed the treatment indicated. Data represent means ± S.D. of three experiments. 20-30 mitotic cells were counted per experiment.

In order to better understand how loss of Hsp70 or Nek6 activity resulted in formation of multipolar spindles but not acentrosomal poles, we set up a microtubule-regrowth assay using nocodazole, a microtubule-poison drug. Nocodazole reversibly arrests cells in mitosis and upon washout of drug, cells form multiple asters, even in the presence of normal centrosome numbers, that eventually reorganize to a bipolar spindle. To observe how the asters reorganize in the presence of the Hsp70 inhibitor, we treated cells with nocodazole for 16 hours before release in the presence or absence of the Hsp70 inhibitor (Figure 4.15A). Flow cytometry was used to confirm the G2/M arrest of cells treated with nocodazole for 16 hours (Figure 4.15B). MDA-MB-231, NIE-115 and HeLa cells were treated with nocodazole for 16 hours and then released in the presence or absence of the Hsp70 inhibitor. Immunofluorescence imaging was used to analyse MTOC organization at different times after release.

In the MDA-MB-231 cell line, cells released from nocodazole treatment in the absence of Hsp70i had multiple asters at 10 to 30 minutes, but had mostly formed bipolar spindles at 60 minutes (Figure 4.16A-B). However, in the presence of the Hsp70 inhibitor, MDA-MB-231 cells could not resolve their multiple asters into a bipolar state and after 60 minutes, 37% of all mitotic cells remained in a multipolar state compared to 13% of controls cells without Hsp70 inhibition (Figure 4.16A-B). When NIE-115 cells were released into nocodazole-free media in the absence of Hsp70 inhibition, most cells had multiple asters at 10 minutes but clustered them into two asters within 60 minutes (Figure 4.17A-B). However, in Hsp70-treated NIE-115 cells, these multiple asters did not resolve into a bipolar spindle and almost 95% of cells remained in a multipolar state at 60 minutes after nocodazole release (Figure 4.17A-B). In contrast, in HeLa cells, while mitotic cells had multiple asters at 10 minutes following nocodazole washout, the vast majority had resolved to a bipolar spindle in both control and Hsp70-treated cells (Figure 4.18A-B).

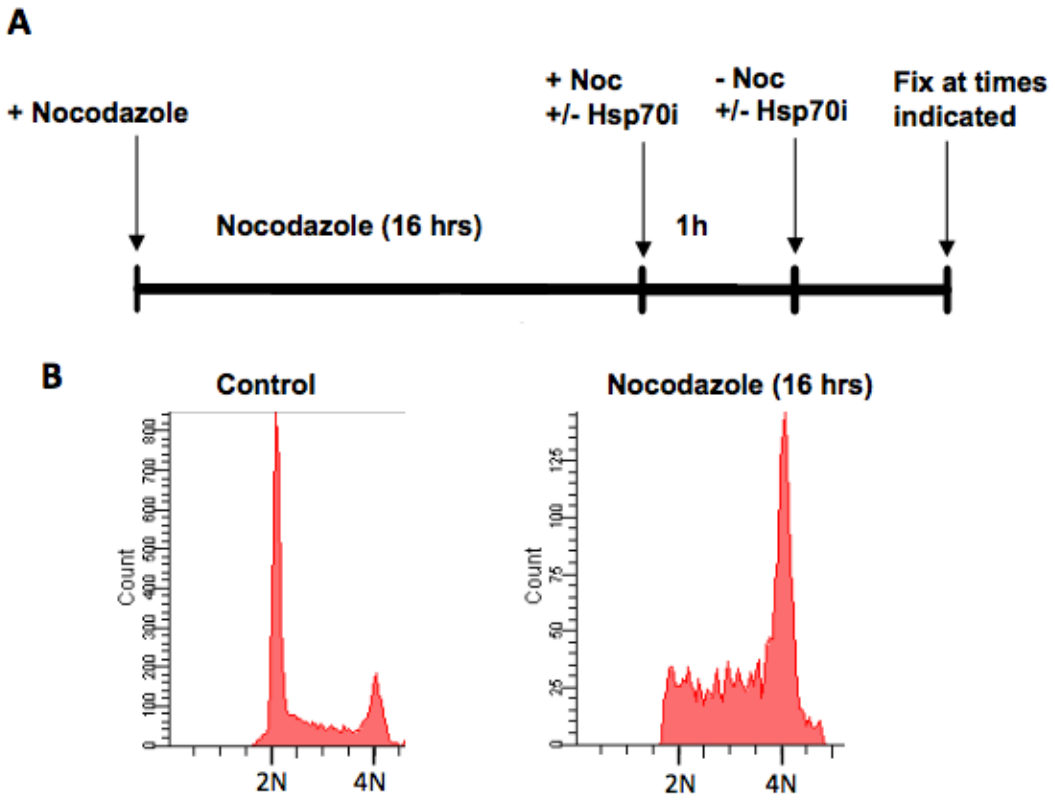

Figure 4.15. Microtubule regrowth assay protocol

A. Schematic protocol used for microtubule (MT)-regrowth assay. In brief, cells were incubated with nocodazole for 16 hours before cells treated with or without 10 µM Hsp70 inhibitor for 1 hour. Cells were then released into a fresh medium in the presence or absence of Hsp70 inhibitor and fixed at the times indicated. **B.** Cells were harvested and analysed by flow cytometry. Cell cycle profiles following control or nocodazole treatment are shown with the population of cells with 2N or 4N DNA indicated.

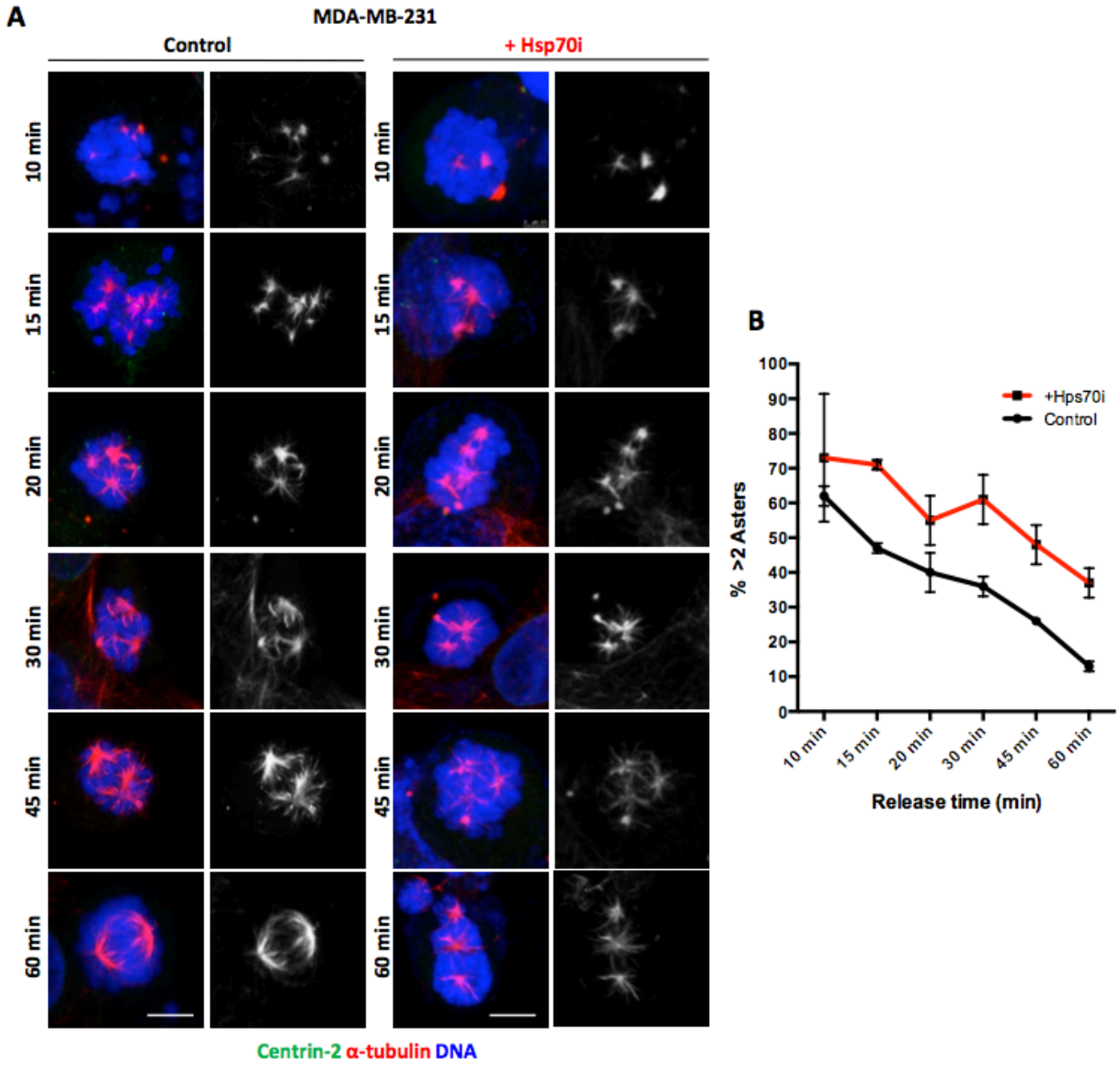

Figure 4.16. Hsp70 inhibition maintains the multiple asters in MDA-MB-231 cells

A. Microtubule regrowth was assessed as described in Figure 4.14A in MDA-MB-231 cells. Cells were stained with centrin-2 (green) and α-tubulin (red) antibodies. Merged panels include DNA (blue). Scale bar, 5 µm. **B.** Histogram represents the percentage of cells with >2 asters at each time point indicated. Data show means ± S.D. of two experiments. 50 mitotic cells were counted per experiment.

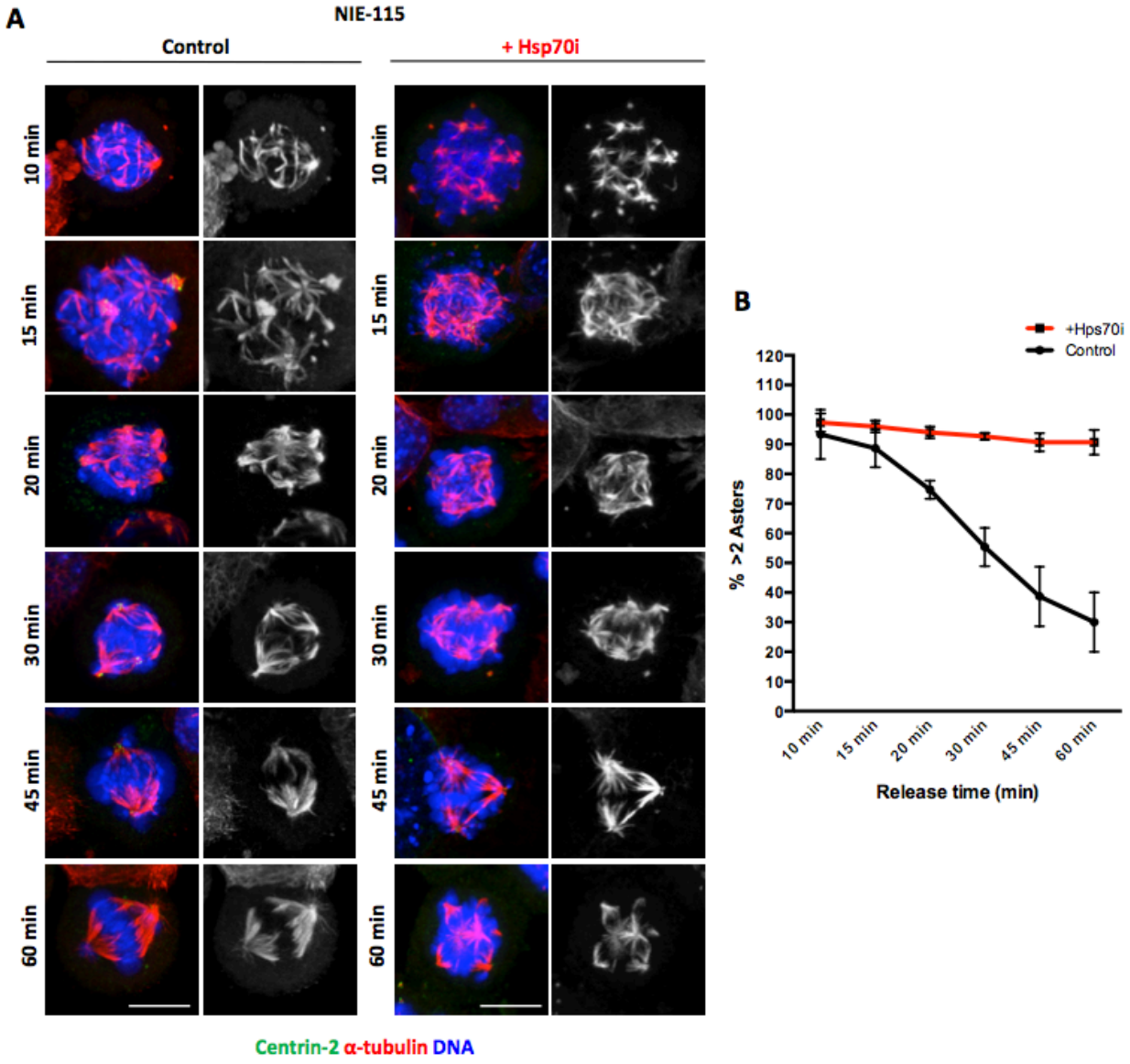

Figure 4.17. Multipolarity is maintained in Hsp70 treated NIE-115 cells

A. Microtubule regrowth was assessed in NIE-115 cells as illustrated in the schematic of figure 4.14A. Cells were stained with centrin-2 (green) and α-tubulin (red) antibodies. Merged panels include DNA (blue). Scale bar, 5 µm. **B.** Histogram represents the percentage of cells with >2 asters at each time point as indicated. Data represent means ± S.D. of three experiments. 50 mitotic cells were counted per experiment.

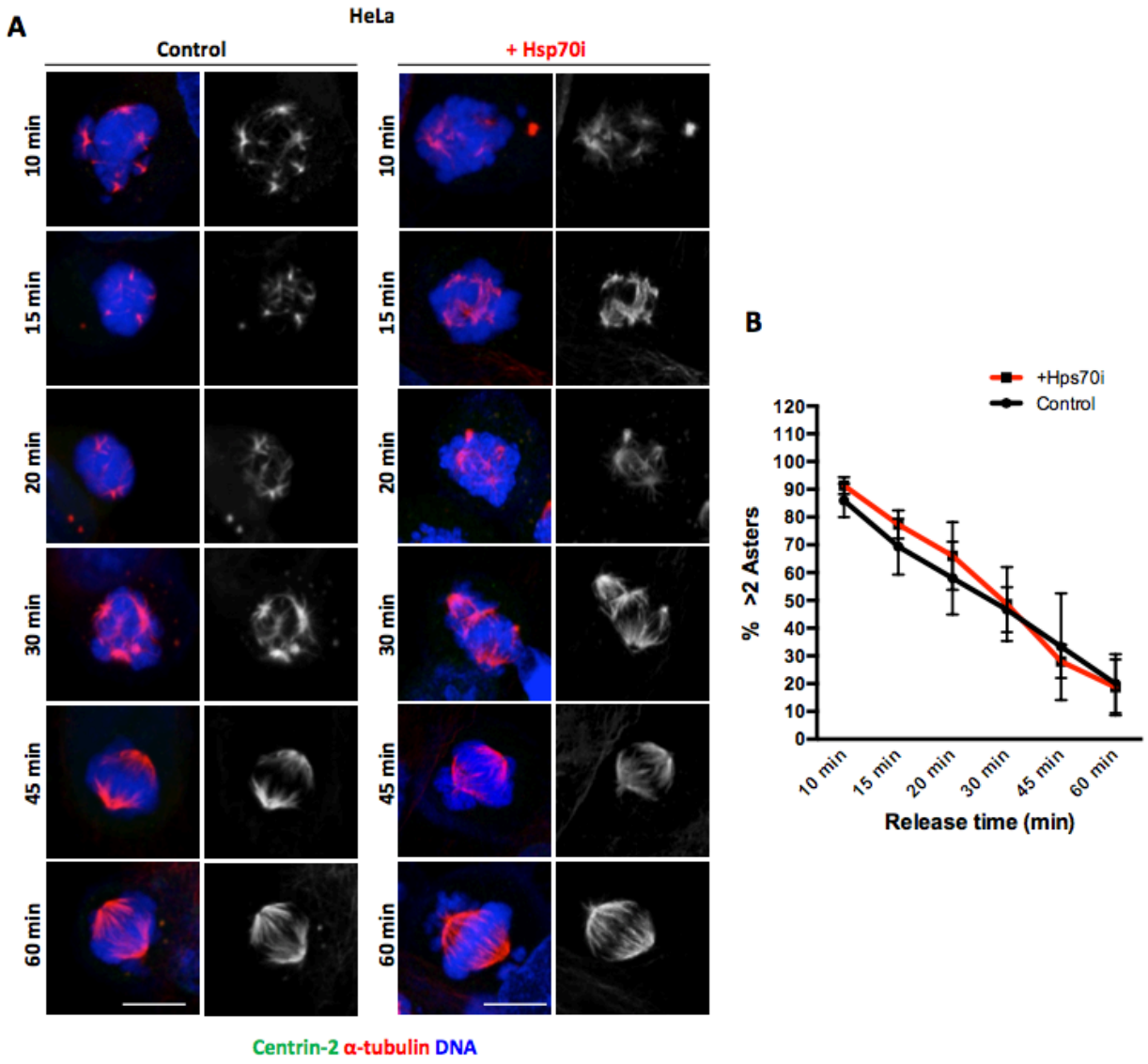

Figure 4.18. Hsp70 inhibition does not maintain the multiple asters in HeLa cells

A. Microtubule regrowth was assessed in HeLa cells, as illustrated in the schematic of figure 4.14A. Cells were stained with centrin-2 (green) and α-tubulin (red) antibodies. Merged panels include DNA (blue) stained with Hoechst 33528. Scale bar, 5 µm. **B.** Histogram represents the percentage of cells with >2 asters at each time point as indicated. Data show means ± S.D. of three experiments. 50 mitotic cells were counted per experiment.

Overall, the data in this section show that griseofulvin treatment induces acentrosomal poles in all cell lines, including those that do not have amplified centrosomes, such as HeLa and PBLs. Conversely, loss of Hsp72 or Nek6 function promoted spindle multipolarity only in cancer cells with amplified centrosomes. The microtubule regrowth assay confirmed that loss of Hsp70 function prevented MTOC clustering in MDA-MB-231 and NIE-115 cells, which possess amplified centrosomes, but not in HeLa cells, which do not exhibit centrosome amplification. This provides evidence that loss of Hsp70 or Nek6 function induces multipolarity in cancer cells with amplified centrosomes through a different mechanism than drugs such as griseofulvin, which cause the generation of spindle poles without centrosomes.

4.2.6 Loss of Nek6, Aurora-A and Plk1 activity reduces Hsp72 and pHsp72-T66 localisation to spindle apparatus

Hsp72 is concentrated at spindle poles in HeLa cells (O'Regan et al., 2015). We next tested whether Nek6 regulates localisation of Hsp72 in MDA-MB-231 cells as previously shown in HeLa cells (O'Regan et al., 2015). Depletion of Nek6, but not Nek7, reduced the localisation of Hsp72 at spindle poles in MDA-MB-231 cells (Figure 4.19A-B), while western blot analysis demonstrated no significant change in Hsp72 expression upon Nek6 or Nek7 depletion (Figure 4.19C). Further evidence that Nek6 regulates Hsp72 localisation came from demonstrating that chemical inhibition of Aurora-A or Plk1 proteins, which both act upstream of Nek6 caused loss of Hsp72 to spindle poles in MDA-MB-231 cells without altering its expression (Figure 4.20A-C). Similarly, loss of Aurora-A or Plk1 activity led to loss of Hsp72 localisation at spindle poles in NIE-115 cells (Figure 4.20D).

In MDA-MB-231 cells that had been detergent-extracted prior to fixation to remove soluble protein, pHsp72-T66 was observed at spindle poles and the midbody (Figure 4.21), consistent with previous observations in other cell types (O'Regan et al., 2015). As predicted, pHsp72-T66 localisation was lost upon Nek6, but not Nek7, depletion in MDA-MB-231 cells (Figure 4.22A). Similar loss of pHsp72-T66 localisation was observed upon loss Aurora-A or Plk1 inhibition in MDA-MB-231 cells (Figure 4.22B). Hence, our results give further evidence for the implication of Aurora-A, Plk1 as upstream activators of Nek6 to target Hsp72 to the spindle apparatus. These results demonstrate a requirement for Aurora-A and Plk1 as upstream activators of the Nek6-Hsp72 pathway.

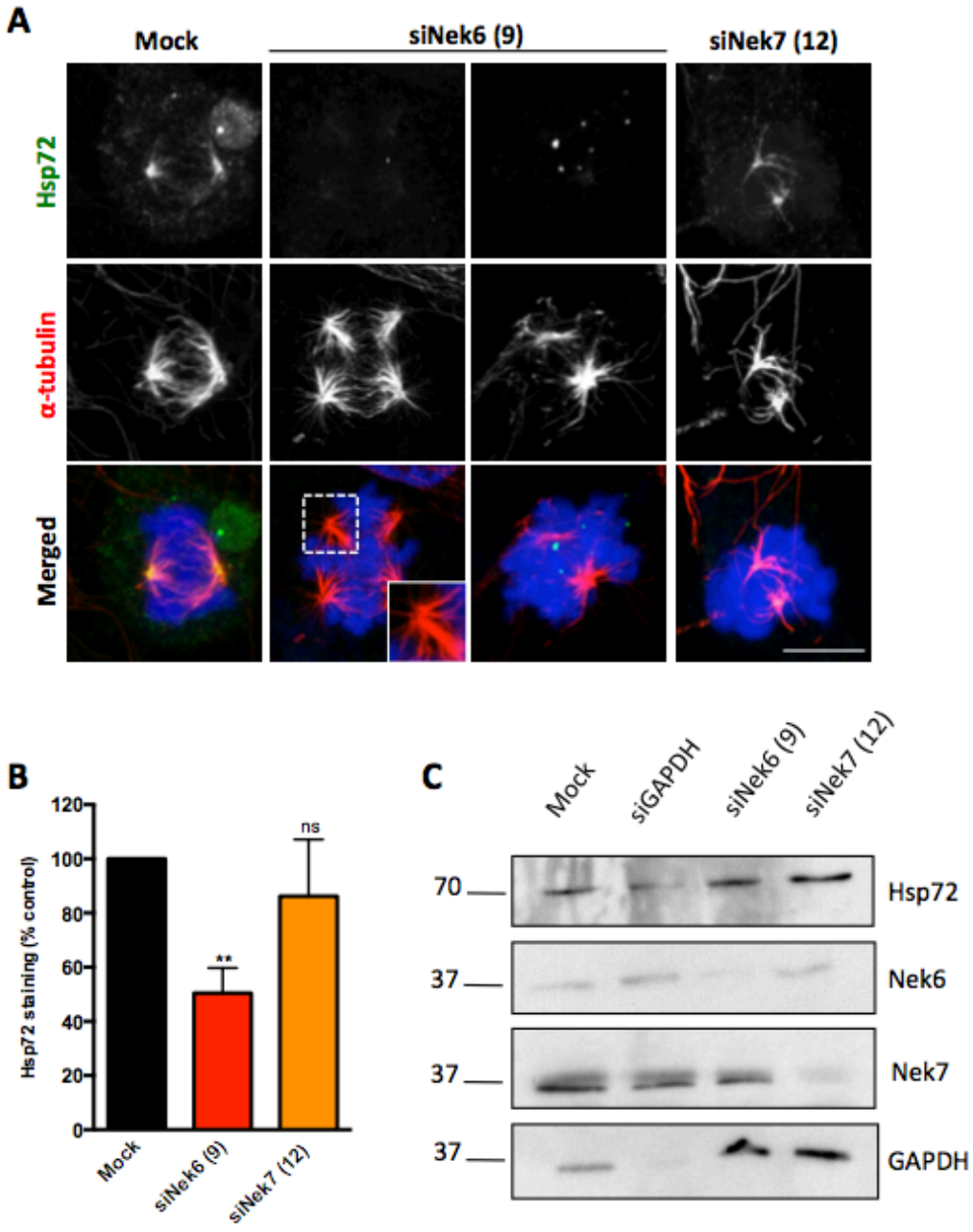

Figure 4.19. Depletion of Nek6 but not Nek7 reduces Hsp72 localisation to mitotic spindle

A. MDA-MB-231 cells were either mock-depleted or transfected with siRNA oligonucleotides to deplete Nek6 or Nek7, as indicated. After 72 hours, cells were pre-extracted with PTMEH buffer for 30 seconds and stained for Hsp72 (green) or α-tubulin (red) antibodies. Merged panels include DNA (blue) staining with Hoechst 33258. Scale bar, 5 μm. **B.** Histogram represents the total Hsp72 intensity of cells in A relatively to mock-depleted cells. Hsp72 intensity was calculated based on α-tubulin intensity. Data show means ± s.d. of three experiments. 10-15 mitotic cells were analysed per experiment. **p<0.01. **C.** MDA-MB-231 cells were mock-depleted or transfected with siRNA oligonucleotides against Nek6, Nek7 or GAPDH. Cells were lysed and analysed by SDS-PAGE and Western blotting with antibodies indicated. Molecular weights are shown (kDa).

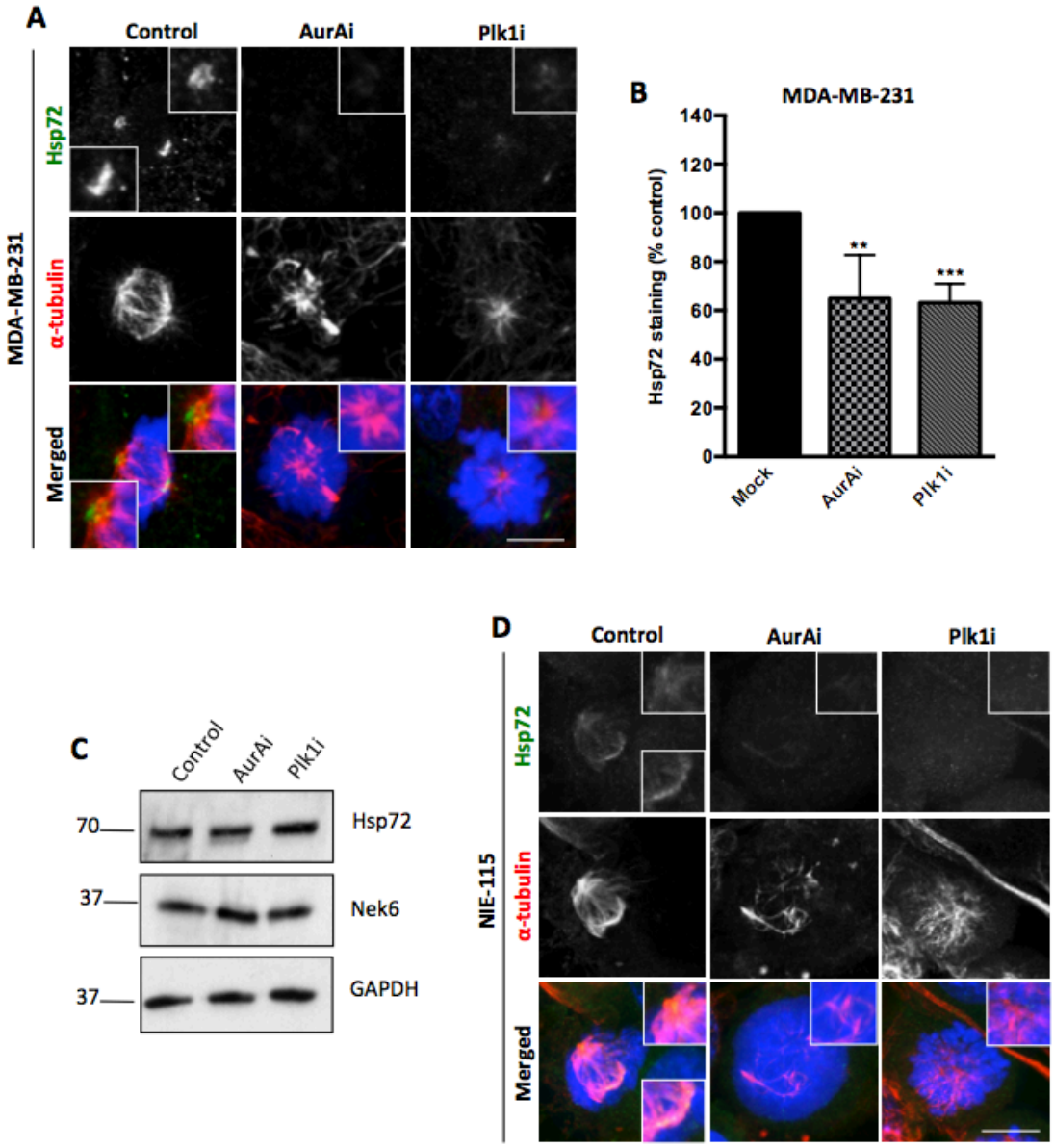

Figure 4.20. Aurora-A or Plk1 inhibition reduces Hsp72 localisation to spindle poles in cancer cells

A. MDA-MB-231 cells were either untreated (control) or treated with either 1 µM Aurora-A or 100 nM PLK1 inhibitors for 4 hours. Cells were pre-extracted for 30 seconds with PTMEH buffer and stained with Hsp72 (green) and α-tubulin (red) antibodies. Merged panels include DNA (blue) staining with Hoechst 33258. Scale bar, 5 µm. **B.** Histogram represents the total Hsp72 intensity of cells in A relatively to control. Hsp72 intensity was calculated based on α-tubulin intensity. Data show means ± S.D. of three experiments. 10-15 mitotic cells were analysed per experiment. **p<0.01, ***P<0.001. **C.** MDA-MB-231 cells were treated with either 1 µM Aurora-A or 100 nM Plk1 inhibitors for 4 hours before cells were lysed and analysed by SDS-PAGE and Western blotting with the antibodies indicated. Molecular weights are shown (kDa). **D.** NIE-115 were treated and stained as A. Scale bar, 5 µm.

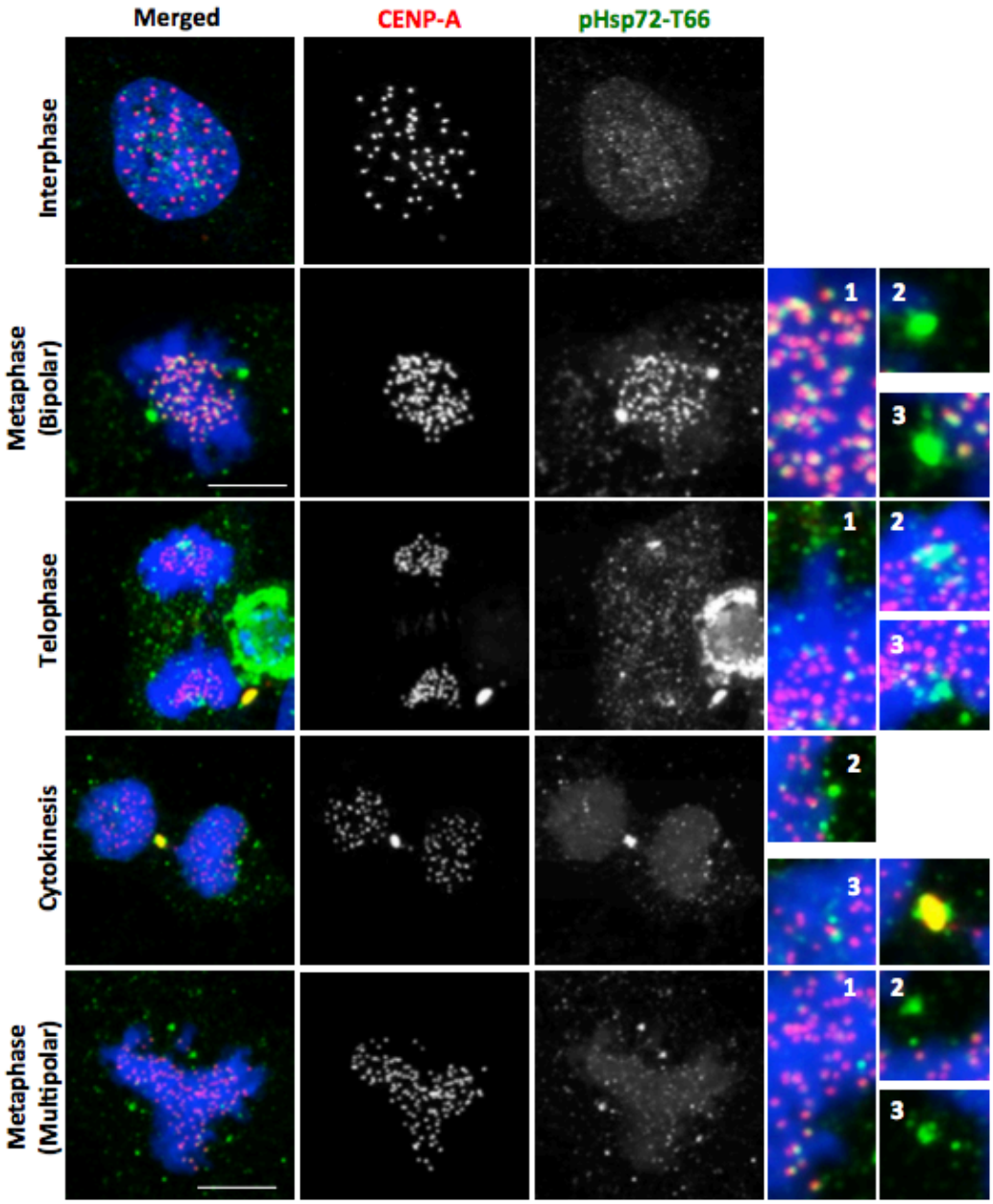

Figure 4.21. pHsp72-T66 localises on spindle poles, kinetochores and the midbody in mitotic MDA-MB-231 cells

MDA-MB-231 cells were pre-extracted for 30 seconds with PTMEH buffer and fixed with methanol before staining with pHsp72-T66 (green) and CENP-A (red) antibodies. Merged panels include DNA (blue) staining with Hoechst 33258. Insets show magnified views of kinetochores (1) and spindle poles (2, 3). Metaphase (Bipolar) image; scale bar, 5 µm, Metaphase (multipolar); Scale bar, 7.5 µm.

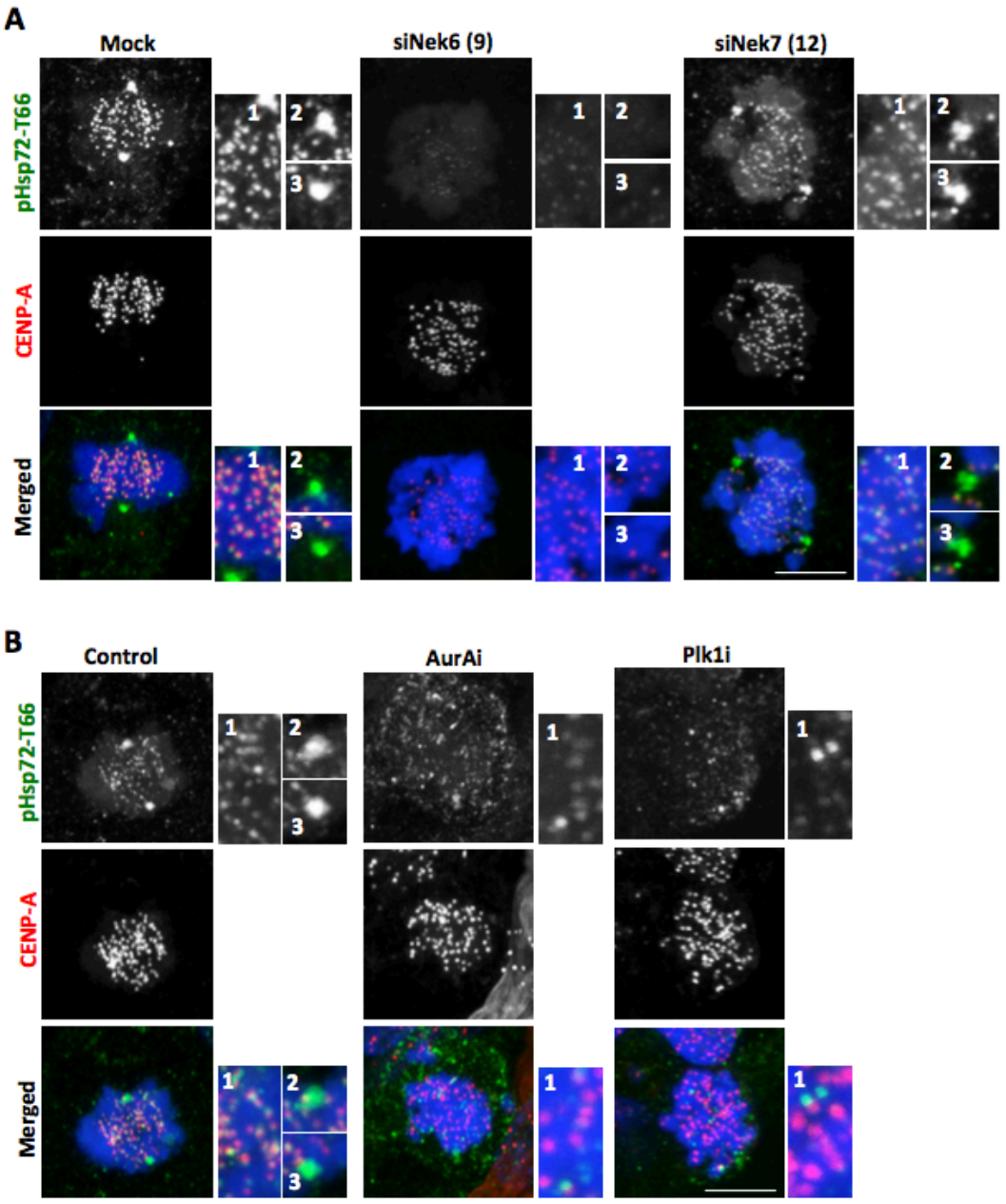

Figure 4.22. Loss of pHsp72-T66 upon depletion of Nek6 or inhibition of Aurora-A and Plk1 in MDA-MB-231 cells

A. MDA-MB-231 cells were either mock-depleted or transfected with siRNA oligonucleotides to deplete Nek6 or Nek7, as indicated. After 72 hours, cells were pre-extracted for 30 sec with PTMEH buffer and fixed with methanol before staining with pHsp72-T66 (green) and CENP-A (red) antibodies. **B.** MDA-MB-231 cells were untreated (control) or treated with either 1 µM Aurora-A or 100nM Plk1 inhibitor for 4 hours. Cells were stained as A. Merged panels include DNA (blue) staining with Hoechst 33258. Insets show magnified views of kinetochores (1) and spindle poles (2, 3). Scale bar, 5 µm.

4.3 Discussion

Over the last decade, significant progress has been made in understanding centrosome clustering mechanisms and identification of proteins involved in these processes. Proteins with specific roles in cell adhesion and polarity, centrosome, cortical and kinetochore-microtubule attachments, the spindle assembly checkpoint (SAC) and microtubule motors i.e. dynein and HSET, all play key roles in centrosome clustering. Hence, a number of these are now consider as attractive targets for development of drugs that block centrosome clustering with the aim that will lead to selective cancer cell death (Kwon et al., 2008; Leber et al., 2010; Gergely and Basto, 2008).

Cancer cells rely on heat shock chaperones, such as Hsp70 proteins, to survive and metastasis (Rodhe et al., 2005; Daugaard et al., 2005). Apart from their function in protecting cells from proteotoxic stress, Hsp70 proteins have found to be important in cell division (Liang and MacRae, 1997; Hut et al., 2005; Makhnevych and Houry, 2013). We showed that Hsp72 is required for mitotic spindle assembly through recruitment of the ch-TOG/TACC3 complex to k-fibres (O'Regan et al., 2015). Centrosome clustering is known to require effective microtubule-kinetochore attachments. Using fixed and live cell imaging, we showed that the Hsp70 chemical inhibitor, VER-115008, blocked centrosome clustering in MDA-MB-231 and NIE-115 cells. Furthermore, depletion of either Hsp72 or Hsc70 promoted multipolarity in MDA-MB-231 cells. Consistent with this, Hsp70 inhibition promoted multipolarity in a set of acute lymphoblastic leukaemia (ALL) cells in a manner that correlated with degree of centrosome amplification. In sharp contrast, we found that Hsp70 inhibition did not induce multipolarity in HeLa and healthy PBL cells that do not have amplified centrosomes. Hence, we conclude that Hsp70 chaperones are required for centrosome clustering in cancer cells with amplified centrosomes.

With respect to the functional role of Hsp70 isoforms in centrosome clustering, we showed that silencing of either Hsp72 or Hsc70 promoted multipolarity in cells with amplified centrosomes. This suggests that both Hsp72 and Hsc70 proteins are required

for centrosome clustering. It was previously shown that the degree of dependence on Hsp70 isoform expression varies between cell lines (Gabai et al., 2005). Generally, Hsc70 isoform is ubiquitously expressed in noncancerous tissues compared to Hsp72 that is expressed in low levels (Daugaard et al., 2007). In contrast, Hsp72 expression levels are significantly increased in several tumours (Garrido et al., 2006). We therefore hypothesize that cancer cells balance the expression levels between Hsp70 isoforms, particularly Hsp72 and Hsc70, to achieve efficient total Hsp70 activity that will respond to proteotoxic stresses and may promote centrosome clustering.

While loss of the Hsp72 and Hsc70 chaperones resulted in increased multipolarity in cells with amplified centrosomes, we found that loss of Nek6, but not Nek7, generated similar results. It is well known that Nek6, as well as Nek7, are important for robust mitotic spindle assembly (O'Regan and Fry, 2009; Roig et al., 2002;). However, there is increasing evidence that Nek6 and Nek7, independed their sequence similarity, are not redundant and have different substitutes (Fry et al., 2012). Moreover, we have shown that Nek6, but not Nek7, interacts with Hsp72 to regulate mitotic spindle assembly through the ch-TOG/TACC3 complex (O'Regan et al., 2015). Interestingly, the ch-TOG/TACC3 complex, which is regulated by integrin-linked kinase (ILK), has been reported to promote centrosome clustering (Fielding et al., 2011). A known binding partner of Hsp70 proteins is clathrin, which targeted with ch-TOG and TACC3 crosslinks microtubules into the k-fibres (Clerico et al., 2015; Hood et al., 2013). It is possible that this phosphorylation of Hsp72 by Nek6 modulates the interaction of clathrin with TACC3 to aid spindle association of the ch-TOG/TACC3/clathrin complex and promote K-fibre stability. However, in a recent study, Gutierrez-Caballero et al suggested that ch-TOG/TACC3 complex permits TACC3 to bind to plus-ends of microtubules independent of clathrin (Gutierrez-Caballero et al., 2015). In addition, depletion of ch-TOG led to a significant fraction of acentrosomal spindle poles (Leber et al., 2010). We therefore assume that the role of Nek6-Hsp72 in centrosome clustering is unlikely to execute purely via ch-TOG protein.

Substantial effort has been invested in recent years to discover agents that block clustering of extra centrosomes and lead to cancer cell death. Griseofulvin, a nontoxic antifungal agent, and its derivatives induce high-grade multipolarity most likely through disrupting microtubules dynamics, although their exact mechanism remains unclear (Raab et al., 2012; Rebacz et al., 2007). Based on our results, griseofulvin induced multipolarity at least in part via generation of acentrosomal spindle poles, i.e. poles without centrosomes. This occurred in both healthy and cancer cell lines, consistent with previous data that suggested that griseofulvin generates multipolar spindles in malignant and non-malignant cell lines (Rathinasamy et al., 2010; Ogden et al., 2014). Similar acentrosomal spindle poles have been seen in response to taxol-based drugs and loss of HSET motor function (Kleylein-Sohn et al., 2012). Therefore, the findings so far suggest that griseofulvin, as well as taxol-based drugs, cause multipolarity due to loss of microtubule dynamics or motors that crosslink microtubules and that this is associated with creation of ectopic, non-centrosomal MTOC. In sharp contrast, loss of Hsp72 and Nek6 function only promoted multipolarity in a manner whereby all spindle poles were associated with centrosomes. Interestingly, microtubule regrowth experiments following nocodazole washout confirmed that in the presence of the Hsp70 inhibitor cells with amplified centrosomes, i.e. NIE-115 and MDA-MB-231, remained in a multipolar state. However, HeLa cells were capable of reorganizing from a multipolar to bipolar state in the presence or absence of the Hsp70 inhibitor. This was supported by time-lapse imaging with the fluorescent tubulin probe that allowed us to directly monitor microtubule organization in live MDA-MB-231 and NIE-115 cells. This revealed the maintenance of the multipolar state in the presence of the Hsp70 inhibition in those cells with amplified centrosomes. Hence, Hsp70 inhibition acts in a more selective way than griseofulvin by targeting only cells with amplified centrosomes.

The Hsp70 inhibitor, VER-155008, has been shown to be selective for members of the Hsp70, as opposed to Hsp90, family (Massey et al., 2009). However, how Hsp70 activity regulated mitosis remains to be fully defined. Besides potentially targeting dynein/dynactin, we previously showed that Hsp70 inhibition blocks the localisation of ch-TOG/TACC3 complex to mitotic spindle, disrupting K-fibres organization and

subsequently chromosome congression during mitosis (O'Regan et al., 2015). Here, we showed that depletion of Nek6, but not Nek7, led to loss of the phosphorylated pHsp72-T66 fraction from spindle poles and kinetochores in cancer cells. As expected, pHsp72-T66 was significantly reduced upon Nek6, but not Nek7 depletion, confirming this to be a Nek6-specific target site (O'Regan et al., 2015). Interestingly, loss of Aurora-A or Plk1 activity led to loss of both Hsp72 and pHsp72-T66 localisation from spindle pole in cancer cell lines. It is well known that Plk1 is activated through phosphorylation by Aurora-A (Macurek et al., 2008). Activated Plk1 then phosphorylates and activates Nek9 kinase, while in turn activates Nek6 (Bertran et al., 2011; Belham et al, 2003). Therefore, our results confirm the requirement of Aurora-A and Plk1 as upstream activators of the Nek6-Hsp72 pathway that contribute to centrosome clustering and mitotic progression through targeting Hsp72 to the mitotic spindle.

A key goal of cancer chemotherapy is the targeting of tumour-specific pathways that will eliminate cancer cells without affecting the healthy ones. Studies have shown that Hsp72 and Nek6 proteins are upregulated in cancers and we have shown here an essential role in centrosome clustering. We therefore suggest that inhibiting Nek6-Hsp72 pathway has therapeutic potential as it could selectively target cells with amplified centrosomes. However, inhibiting this pathway raises many challenges including the question of whether it would interfere with mitotic progression of non-cancerous cells. Targeting Hsp70 for drug development can also be challenging due to its flexible active site, high affinity for nucleotide, complex proteins interactions, high homology between the members of Hsp70 family and pleiotropic contribution to many aspects of the stress response beyond mitosis. On the other hand, targeting Nek6 is more attractive due to its narrow window of activity in mitosis. However, sequence similarity with other members of the Nek family, and particularly Nek7, mean that it could be difficult to develop Nek6-specific inhibitors. That said, there are some ideas of how to make selective Nek6 inhibitors that target allosteric sites required for its activation (Haq et al., 2015). Further work will be necessary to better understand the mechanistic functions of the Nek6-Hsp72 pathway and its downstream targets that are important for both mitotic progression and centrosome clustering.

Taken together, in this chapter we emphasize the importance of Nek6-Hsp72 pathway in mitotic progression of cancer, but not in healthy cells. The fact that cancer cells rely on the Nek6-Hsp72 pathway to facilitate mitosis, as well as centrosome clustering, makes Nek6 and Hsp72 promising targeted proteins for potential development of new drugs.

There is little doubt from our results that the Nek6-Hsp72 pathway is required for the clustering of extra centrosomes in cancer cells, but not for generation of bipolarity in cells with normal centrosome numbers. Furthermore, Hsp70 inhibition in ALL cells caused multipolarity in a manner that correlated with centrosome amplification. However, we haven't explored cell survival in ALL cells upon this treatment as Hsp70 inhibition is likely to have toxic effects independent of centrosome numbers. The generation of Nek6 inhibitors would allow us to explore survival with more confidence that consequences would be exclusively dependent on centrosome numbers. Indeed, future experiments are required to provide a better understanding of the fate of multipolar cells upon each treatment. While we know that loss of Hsp70 or Nek6 acts through a different mechanism to griseofulvin, it remains to be determined how the Nek6-Hsp72 pathway contributes to centrosome clustering. To reveal the molecular mechanism of the Nek6-Hsp72 pathway, as expected, Aurora-A, Plk1 and Nek9 are required for activation of Nek6 and subsequently Hsp72. This suggests a cascade of protein phosphorylation and activation to localise Hsp72 at mitotic spindle apparatus to facilitate centrosome clustering and mitotic spindle stability. In the next chapter, we explore the hypothesis that Nek6 and Hsp72 promote clustering via regrowth of centrosome, cortical and/or kinetochore-microtubule attachments through the minus-end directed microtubule motor dynein.

Chapter 5

The Nek6-Hsp72 pathway regulates localisation of dynein/dynactin complex to the mitotic spindle

5.1 Introduction

Experimental studies have identified at least five distinct mechanisms that regulate centrosome clustering in cancer cells (Leber et al., 2010; Kwon et al., 2008). For example, proteins involved in microtubule dynamics, microtubule attachments to the centrosome, cell cortex and chromosomes, and the spindle assembly checkpoint (SAC) have been found to be essential to cluster amplified centrosomes in mitosis (Leber et al., 2010; Kwon et al., 2008; Basto et al., 2008; Ogden et al., 2012). In this study, we have addressed which of these mechanisms might explain the role of the Nek6-Hsp72 pathway in centrosome clustering.

Importantly, in our previous study on the mechanisms of Nek6 and Hsp72 in mitosis, we suggested that Nek6-Hsp72 pathway acts through the ch-TOG/TACC3 complex to stabilize K-fibres and ensure proper microtubule-kinetochore attachments (O'Regan et al., 2015). Therefore, the ch-TOG/TACC3 complex has important roles in mitotic spindle assembly and microtubule-kinetochore attachments in mitosis. Hence, it is not surprising that these microtubule-associated proteins are likely to be involved in centrosome clustering in cancer cells. These are among several microtubule-associated proteins that have been reported to be involved in centrosome clustering (Fielding et al., 2011). ch-TOG (colonic and hepatic overexpressed gene) and TACC3 (transforming acidic coiled-coil 3) are proteins that interact and bind to the plus-ends of microtubules +TIPs (van der Vaart et al., 2011). The interaction between TACC3 and ch-TOG is evolutionary conserved, having been detected from flies to humans (Thakur et al., 2013). The ch-TOG/TACC3 complex is recruited to the plus-ends of microtubules either by clathrin binding and Aurora-A phosphorylation (Hood et al., 2013), or by the complex itself (Gutierrez-Caballero et al., 2015). ch-TOG was among the genes identified in a screen for centrosome clustering regulators in cancer cells (Leber et al., 2010). Meanwhile, integrin-linked kinase (ILK), which regulates the interaction between the TACC3 and ch-TOG proteins also contribute to centrosome clustering in cancer cells (Fielding et al., 2011).

Another target of the Nek6-Hsp72 pathway that regulates microtubule attachments and kinetochores is the motor protein dynein, which has been showed to regulate centrosome

clustering (Quintyne et al., 2005). In mammalian cells there are two major cytoplasmic dynein complexes, known as cytoplasmic dynein 1 and cytoplasmic dynein 2. Cytoplasmic dynein 2 is mainly required for cilia construction and movement (Mikami et al., 2002). In this study, we have rather focused on cytoplasmic dynein 1, referred to from here on as dynein that is a microtubule-associated protein with major roles in intracellular transport and cell division. Dynein is an ATPase motor protein that moves toward the minus ends of microtubules, carrying cargoes and vesicles. It is a multi-protein complex assembled from two heavy chains and various intermediate, light intermediate and light chains (reviewed in Roberts et al., 2013). Dynein decorates spindle poles and kinetochores in mitotic cells, and centrosomes at S and G2 phase in interphase cells (Quintyne and Schroer, 2002). A major role of dynein is to ensure faithful chromosome segregation by contributing to chromosome congression and separation, as well as silencing of the SAC by moving SAC proteins away from kinetochores (Foley and Kapoor, 2013; Bader and Vaughan, 2010; Yang et al., 2007). Apart from roles in spindle assembly and SAC functions, dynein is also implicated in centrosome positioning through co-interacting forces generated by other motors at the centrosome and cell cortex (Dujardin and Vallee, 2002; Moore et al., 2009). Dynein was among the first proteins suggested to implicate in centrosome clustering (Quintyne et al., 2005). In a recent study, dynein was identified as an important protein for centrosome clustering with a function in mitosis (Leber et al., 2010). Hence, dynein is a multifunctional protein with essential roles in microtubule organization and cell division.

However, dynein requires another adaptor, dynactin, to achieve its cellular functions (King and Schroer, 2000). Dynactin is also a multi-subunit protein complex and essential regulator of dynein that facilitates the movement of dynein and cargo transport along microtubules (Schroer, 2004). Dynactin is assembled from eleven subunits, including dynamitin (p50) and $p150^{Glued}$. Dynactin aids the connection of microtubules to centrosomes and spindle poles (Quintyne and Schroer, 2002). $p150^{Glued}$ is one of the major subunits of dynactin and is important for binding of dynein to microtubule tracks (King and Schroer, 2000). $p150^{Glued}$ localises at both plus and minus ends of microtubules and can act independently of dynein by recruiting other proteins to these sites (Schroer, 2004).

As indicated above, dynein was the first protein suggested to promote centrosome clustering. However, other studies have shown that dynein might not be important for centrosome clustering in *Drosophila* S2 cells or cell lines with experimentally induced centrosome amplification (Nguyen et al, 2008; Goshima et al., 2005). On the other hand, little is known about the importance of dynactin in centrosome clustering. Equally, the role of the dynein/dynactin complex in centrosome clustering is still not clear.

Together, the mechanisms of centrosome clustering in cancer cells remain far from understood. In this chapter, we explored whether the Nek6-Hsp72 pathway targets the ch-TOG/TACC3 complex to regulate centrosome clustering in cancer cells, or whether the dynein/dynactin complex is also regulated by the Nek6-Hsp72 pathway in a manner that might contribute to centrosome clustering in cancer cells.

5.2 Results

5.2.1 Loss of ch-TOG or TACC3 function induces acentrosomal multipolarity in cancer cells

Whilst Nek6 and Hsp70 proteins are important for mitotic spindle assembly in cancer cells, we also showed that these proteins are required for centrosome clustering in cells with amplified centrosomes. To commence our investigation into the mechanism of how the Nek6-Hsp72 pathway regulates centrosome clustering, we first examined the role of ch-TOG/TACC3 complex, as it is known these proteins stabilize the mitotic spindle in cells and they also promote centrosome clustering. We used siRNA interference to deplete ch-TOG and TACC3 proteins from MDA-MB-231 cells (Figure 5.1A). Using immunofluorescence microscopy to identify cells with amplified centrosomes, we observed that ch-TOG depletion led to 57% of cells with multipolar spindles, compared to 14% of mock-depleted ones, while depletion of TACC3 led to 35% of cells with multipolar spindles (Figure 5.1B-C). However, staining using the centriole marker, centrin-2, revealed that both ch-TOG and TACC3 depletions induce formation of acentrosomal spindle poles (Figure 5.1B,D). Quantification confirmed that approximately 65% of those cells with multipolar spindles lacked centrin-2 at spindle poles upon ch-TOG depletion, while 45% of cells with multipolar spindles had acentrosomal spindle poles upon TACC3 depletion (Figure 5.1D).

Similarly, depletion of ch-TOG and TACC3 let to multipolarity in HeLa cells, which do not exhibit centrosome amplification. Specifically, ch-TOG depletion led to approximately 50% of cells with multipolar spindles, whereas TACC3 depletion induced multipolar spindles in 25% of cells (Figure 5.2A-B). Additionally, the percentage of HeLa cells with multipolar spindles that had acentrosomal poles, as defined by centrin-2 staining, was 85% for ch-TOG depletion and 30% for TACC3 depletion (Figure 5.2C). Hence, depletion of ch-TOG and TACC3 induces multipolarity in both MDA-MB-231 and HeLa cells, as previously shown in other studies (Fielding et al., 2011; Leber et al., 2010), but this occurs in large part via generation of acentrosomal spindle poles.

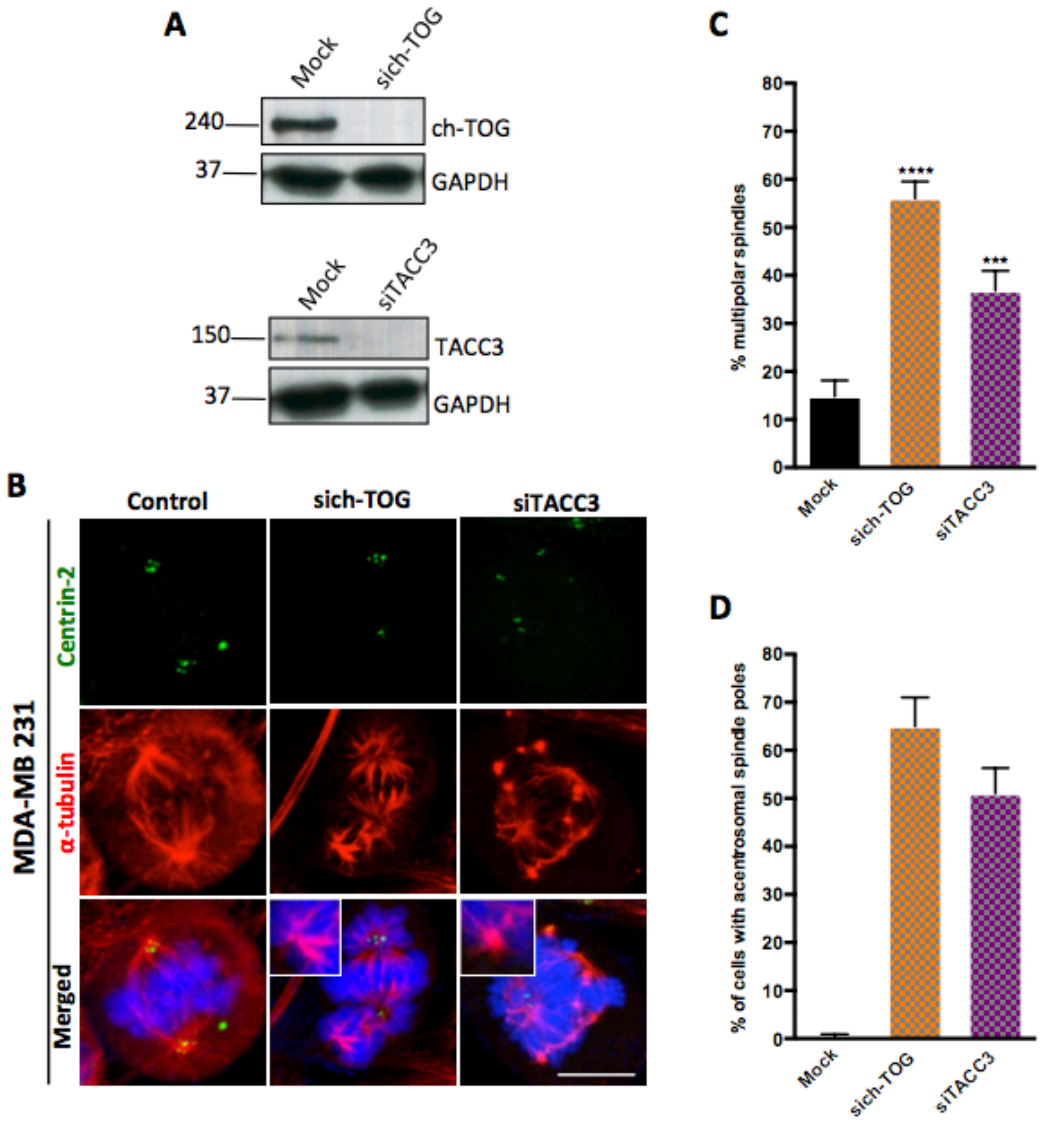

Figure 5.1. Loss of ch-TOG or TACC3 induces multipolarity via acentrosomal spindle poles in MDA-MB-231 cells

A. MDA-MB-231 cells were transfected with siRNA oligonucleotides to deplete ch-TOG or TACC3 as indicated. After 72 hours, cells were lysed and analysed by SDS-PAGE and Western blotting with the antibodies stated. Molecular weights are indicated (kDa). **B.** After 72 hours depletion, cells were fixed and stained for immunofluorescence microscopy with centrin-2 (green) and α-tubulin (red) antibodies. Merged panels include DNA (blue) staining with Hoechst 33258. Scale bar, 5 μm. Insets show magnified views of acentrosomal spindle poles in each treatment. **C, D.** Histograms represent percentage of mitotic cells with multipolar spindles in each depletion. Data show means ± S.D. of three experiments. 50 mitotic cells were counted per experiment.

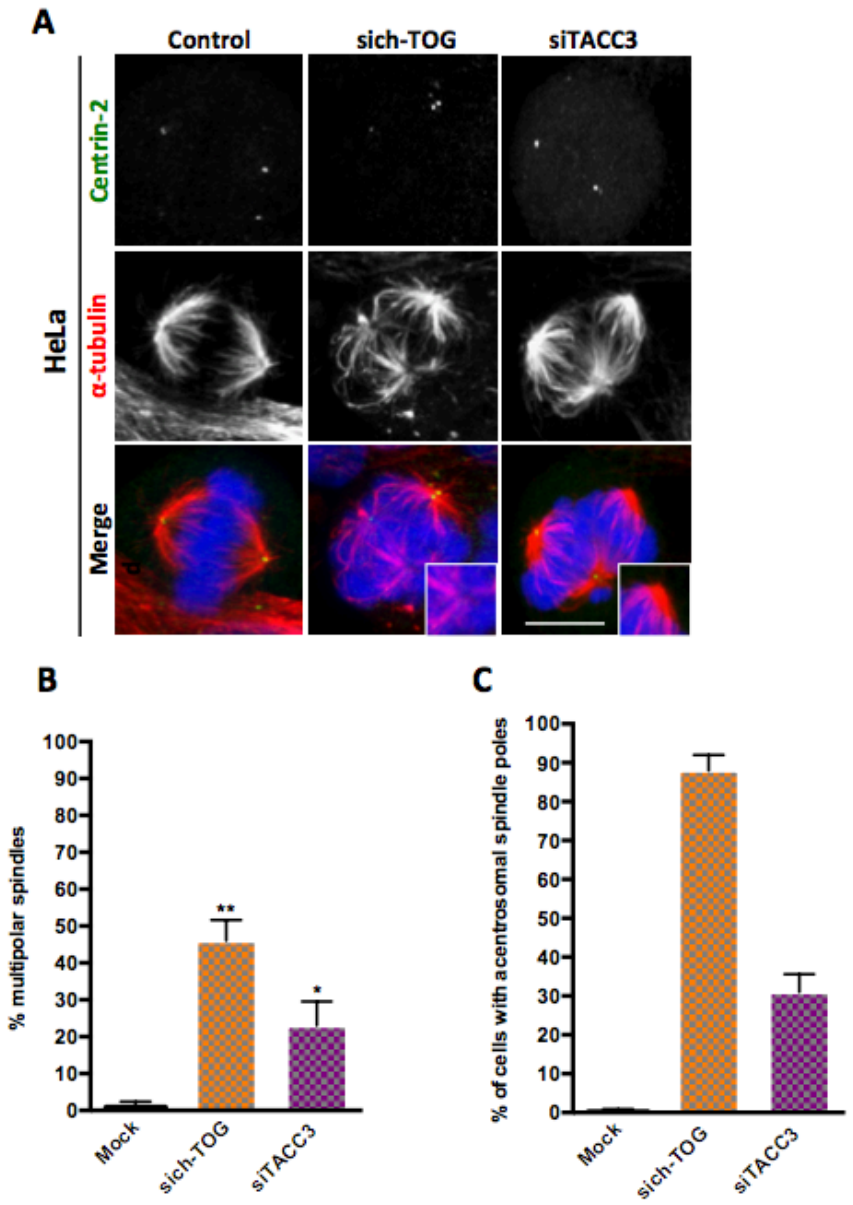

Figure 5.2. Depletion of ch-TOG or TACC3 promotes multipolarity via acentrosomal spindle poles in HeLa cells

A. After 72 hours depletion of ch-TOG or TACC3, HeLa cells were fixed and stained for immunofluorescence microscopy with centrin-2 (green) and α-tubulin (red) antibodies. Merged panels include DNA (blue) staining with Hoechst 33258. Scale bar, 5 µm. Insets show magnified views of acentrosomal spindle poles in each depletion. **B, C.** Histograms represent percentage of mitotic cells with multipolar spindles in each depletion. Data show means ± S.D. of two experiments. 50 mitotic cells were counted per experiment.

5.2.2 Loss of Nek6 or Hsp72 disrupts dynein/p150^{Glued} localisation to the mitotic spindle in cancer cells

In an attempt to understand the mechanism by which Nek6-Hsp72 specifically promotes centrosome clustering, we examined whether the minus-end directed microtubule motor, dynein might be a relevant target. Initially, MDA-MB-231, HeLa and RPE1 cells were stained with anti-dynein intermediate chain (I.C.) and anti-γ-tubulin antibodies. In interphase cells, dynein I.C/p150^{Glued} was diffusely dispersed in the cytoplasm with a discrete localisation at the centrosomes (Figure 5.3A-B). In mitotic cells, dynein I.C/p150^{Glued} localised to the mitotic spindle apparatus with a distinct localisation to what appeared to be kinetochores (Figure 5.3C-D). Interestingly, in mitotic RPE1 cells, dynein staining was significantly less obvious on the spindle apparatus compared to MDA-MB-231 cells, although kinetochore staining remained obvious (Figure 5.3E). Similarly to dynein I.C. staining, careful examination of p150^{Glued} staining on the mitotic spindle apparatus showed approximately a two-fold decrease of p150^{Glued} staining in RPE1 compared to MDA-MB-231 cells (Fig. 5.3F). The dynein/p150^{Glued} intensity on the mitotic spindle in metaphase cells was determined relative to α-tubulin.

MDA-MB-231 cells treated with Hsp70 inhibitor for 4 hours revealed loss of dynein I.C. and p150^{Glued} from the mitotic spindle, specifically at spindle poles and kinetochores (Figure 5.4A-B). In Hsp70i cells, the dynein I.C. intensity found to be approximately 25% less intense as compared to controls, while p150^{Glued} intensity had almost 35% reduction (Figure 5.4.C-D). To investigate this further, MDA-MB-231 cells were incubated with siRNA oligonucleotides against Nek6 or Hsp72 proteins. Depletion of Nek6 or Hsp72 led to a significant decrease of dynein I.C. localisation at spindle poles with quantification revealing almost 30% decrease in dynein I.C. intensity, relative to α-tubulin, for both depletions (Figure 5.5A-C). It was noted that there was no change in dynein I.C. localisation to centrosomes in interphase cells upon Hsp70 inhibition or depletion of Nek6 or Hsp72 (data not shown). Similarly, the blocking of Nek6 or Hsp72 activity disrupted p150^{Glued} from the spindle apparatus, with distinct loss at spindle poles and partially at kinetochores (Figure 5.6A).

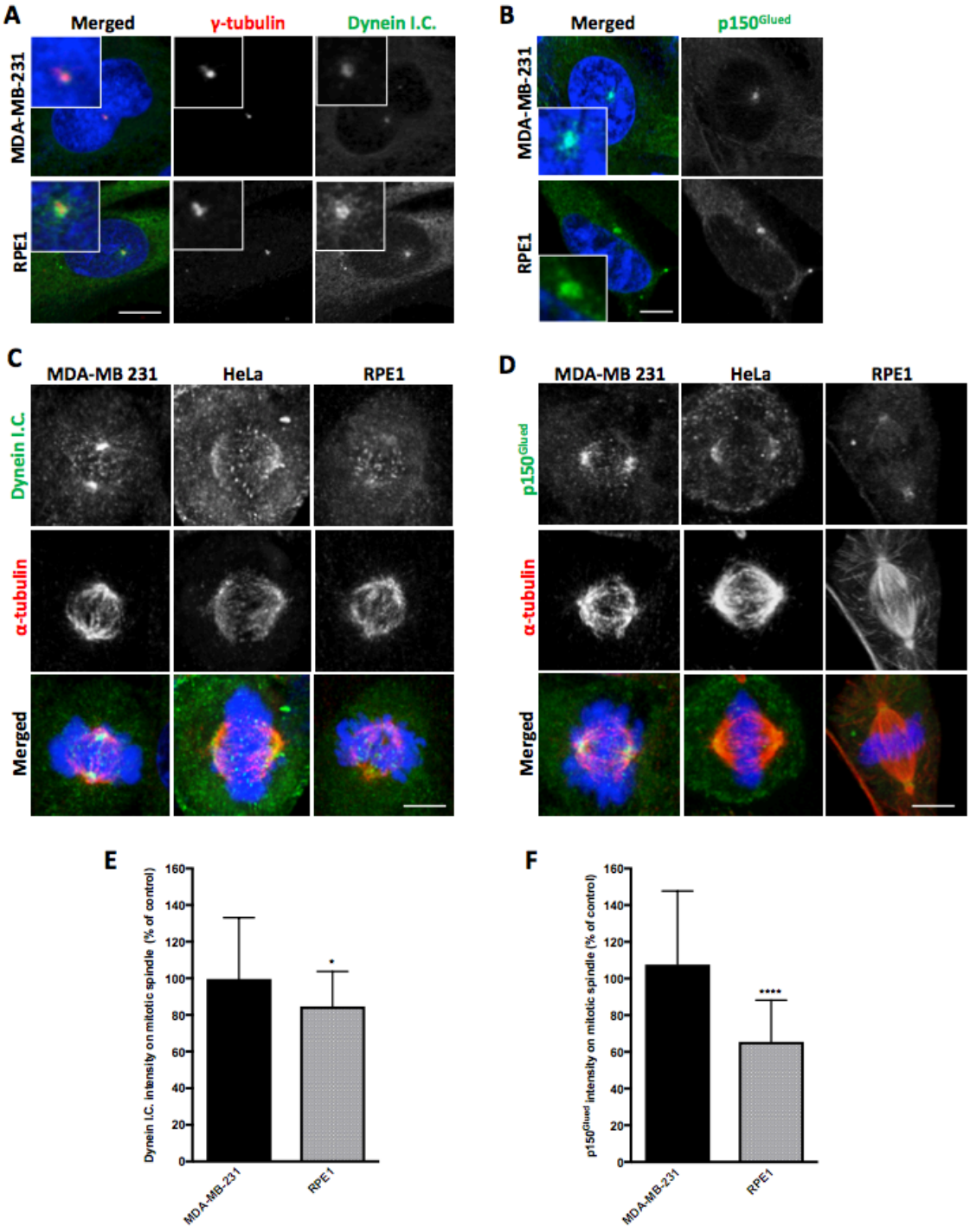

Figure 5.3. Dynein I.C./p150^{Glued} complex localises to centrosomes in interphase cells and mitotic spindle apparatus in mitotic cells

A, B. Cells were stained with dynein I.C. (green) and γ- or α-tubulin (red), or **C,D** with p150^{Glued} (green) and α-tubulin (red) antibodies. Merged panels include DNA (blue) staining with Hoechst 33258. Scale bar; interphase, 10 µm; mitosis, 5 µm. Insets show magnified views of centrosomes. Images are shown of cells in metaphase. **E, F**. Histogram shows the percentage of dynein I.C. intensity on the mitotic spindle, relative to α-tubulin from each cell line. Data show means ± S.D. of three experiments. 10-15 mitotic cells were analysed per experiment.

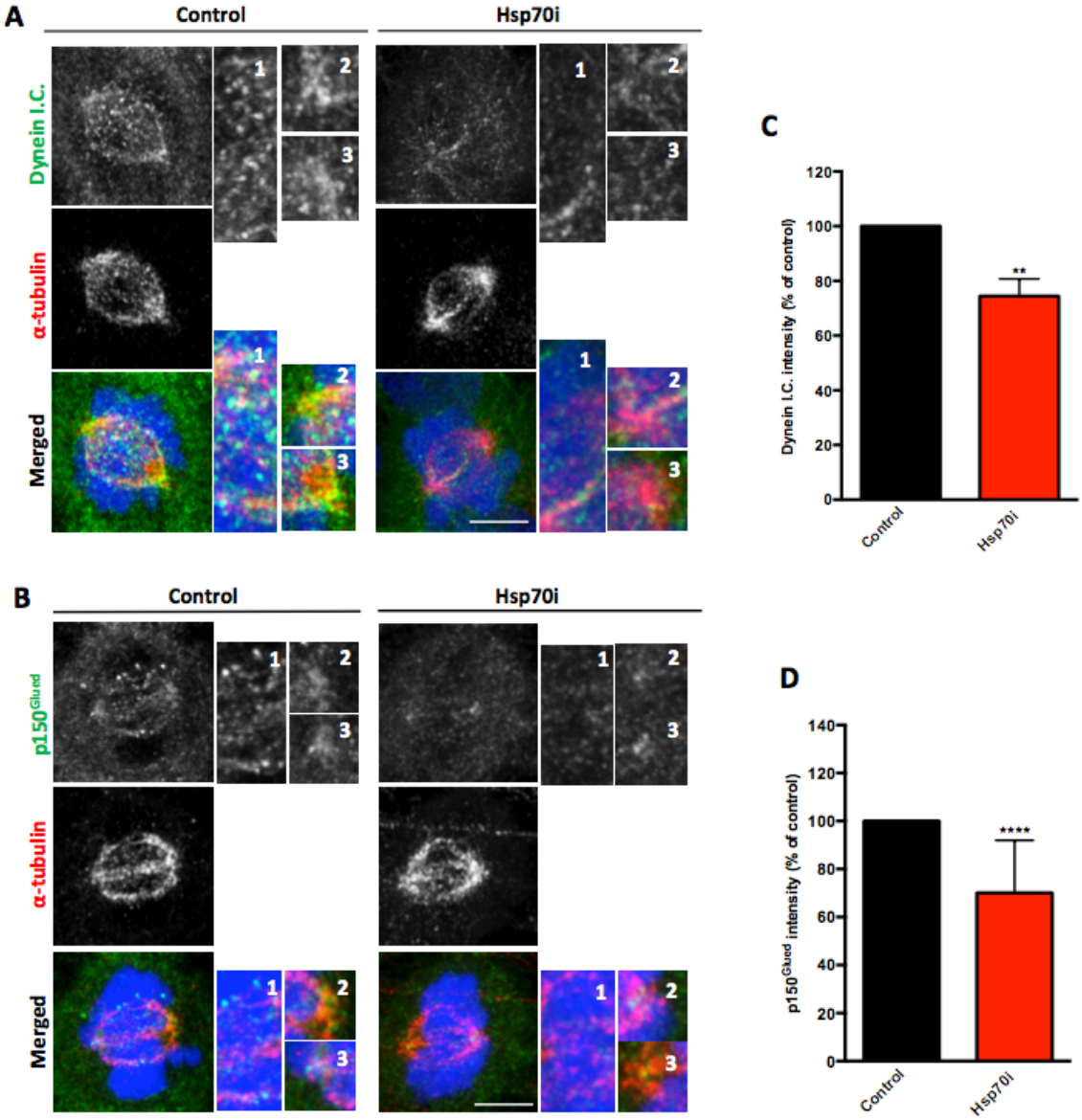

Figure 5.4. Hsp70 inhibition disrupts dynein I.C./p150^{Glued} localisation to the mitotic spindle in MDA-MB-231 cells

A. MDA-MB-231 cells were either untreated (control) or treated with 10 µM Hsp70 inhibitor for 4 hours and stained with dynein I.C. (green) or **B.** p150^{Glued} (green) and α-tubulin (red) antibodies. DNA (blue) was stained with Hoechst 33258. Scale bar, 10 µm. Insets show magnified views of dynein I.C. localisation at kinetochores (1) and spindle poles (2, 3). **C, D.** Histogram shows the percentage of Dynein I.C. and p150^{Glued} intensity on the mitotic spindle relative to α-tubulin from control or Hsp70i treated cells. Data show means ± S.D. of three experiments. 10-15 mitotic cells were analysed per experiment. **p<0.01, ****p<0.0001.

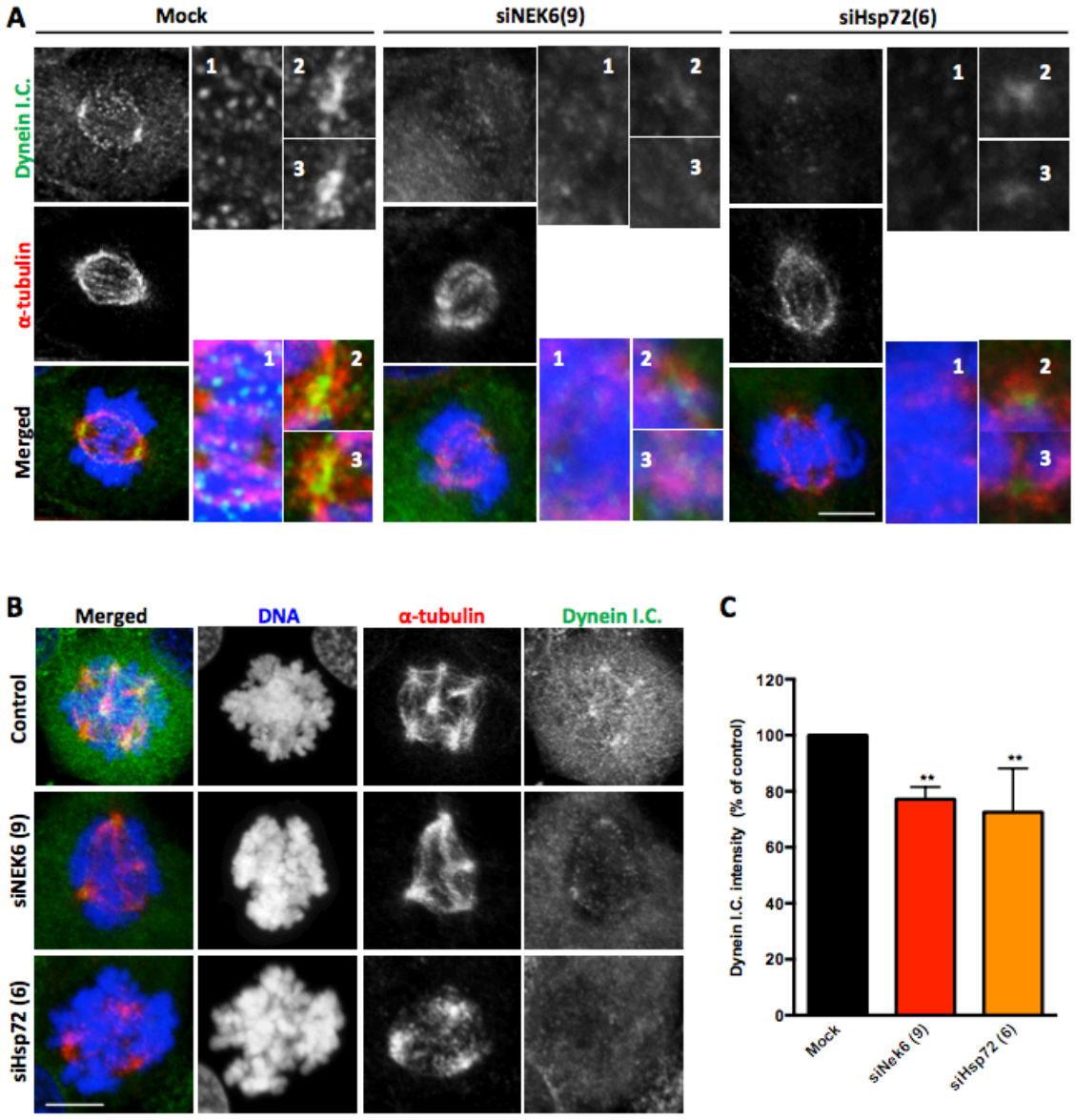

Figure 5.5. Depletion of Nek6 or Hsp72 reduces dynein I.C. at kinetochores and spindle poles in MDA-MB-231 cells

A. MDA-MB-231 cells were either mock-treated or transfected with siRNA oligonucleotides against Nek6 or Hsp72. Cells were stained with dynein I.C. (green), α-tubulin (red) and DNA (blue) with Hoechst 33258. Scale bar, 5 µm. Insets show magnified views of dynein I.C. localisation at kinetochores (1) and spindle poles (2, 3). **B.** Dynein I.C. localisation in multipolar cells from each treatment. **C.** Histogram represents the percentage of total dynein I.C. intensity on whole mitotic spindle relative to α-tubulin from Nek6- or Hsp72-treated cells as correspond to control treated cells. Data show means ± S.D. of three experiments. 10-15 mitotic cells were analysed per experiment. **p<0.01.

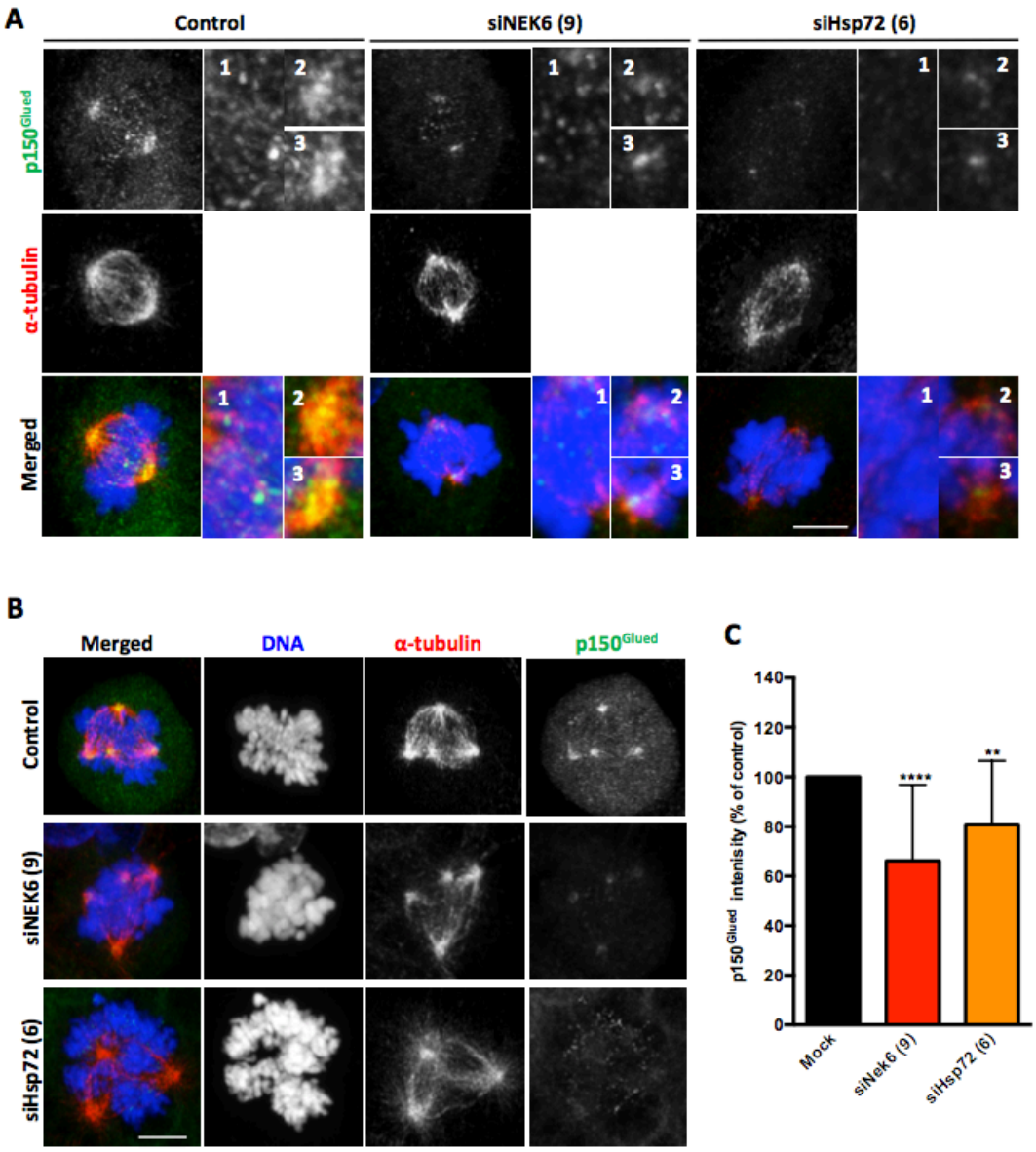

Figure 5.6. Reduction of p150^{Glued} localisation upon depletion of Nek6 or Hsp72 in MDA-MB-231 cells

A, B. MDA-MB-231 cells were mock- or siRNA-transfected with oligonucleotides against Nek6 or Hsp72. After 72 hours, cells were stained with antibodies against p150^{Glued} (green) and α-tubulin (red). Merged panels include DNA (blue) staining with Hoechst 33258. Insets show magnified views at kinetochores (1) and spindle poles (2, 3). Scale bar, 5 µm. **C.** Histogram shows the percentage of total p150^{Glued} intensity of whole mitotic spindle relative to α-tubulin from each treatment. Data show means ± S.D. of three experiments. 10-15 mitotic cells were analysed per experiment.**p<0.01, ****p<0.0001.

Careful examination of multipolar mitoses showed that p150^{Glued} localisation was diminished from spindle poles upon loss of Nek6 or Hsp72 function (Figure 5.6B). Analysis of p150^{Glued} staining in mitotic cells revealed a significant decrease of p150^{Glued} intensity, approximately 35%, in Nek6- or Hsp72-depleted cells compared to mock-treated cells (Figure 5.6C). Hence, this suggests that Nek6 and Hsp72 proteins are important for dynein I.C./p150^{Glued} localisation to the spindle apparatus in mitosis in MDA-MB-231 cells.

In contrast, Hsp70 inhibition did not disrupt dynein I.C. localisation at spindle poles in RPE1 cells (Figure 5.7A-B). Similarly, no significant change of p150^{Glued} had been observed upon Hsp70 inhibition in RPE1 cells (Figure 5.7C-D). In addition, depletion of Nek6 or Hsp72 did not alter either dynein I.C. or p150^{Glued} localisation at the mitotic spindle in RPE1 cells (Figure 5.8A-B). Quantification of either dynein I.C. or p150^{Glued} intensity at spindle poles showed no significant change in both depletions (Figure 5.8C-D). Importantly, neither Hsp70 inhibition nor depletion of Nek6 or Hsp72 altered total dynein or p150^{Glued} expression in MDA-MB-231 or RPE1 cells as tested by Western blot analysis (Figure 5.9A-C).

Together, these data revealed that in interphase cells, dynein I.C. is ubiquitously present in the cytoplasm and enriched at centrosomes, whereas in mitotic cells, dynein is concentrated mostly at spindle poles and partially at kinetochores (Yang et al., 2007; Roberts et al., 2013). However, dynein I.C./p150^{Glued} localisation at spindle poles and kinetochores was significantly reduced upon Hsp70 inhibition or depletion of Nek6 or Hsp72 in MDA-MB-231 cells. In contrast, no change of dynein I.C./p150^{Glued} localisation was observed in response to these treatments in RPE1 cells. Additionally, analysis of dynein expression levels showed no significant change after Hsp70 inhibition or depletion of Nek6 or Hsp72. Hence, this suggests that the Nek6-Hsp72 pathway is important for dynein localisation to the mitotic spindle apparatus in MDA-MB-231 cancer cells.

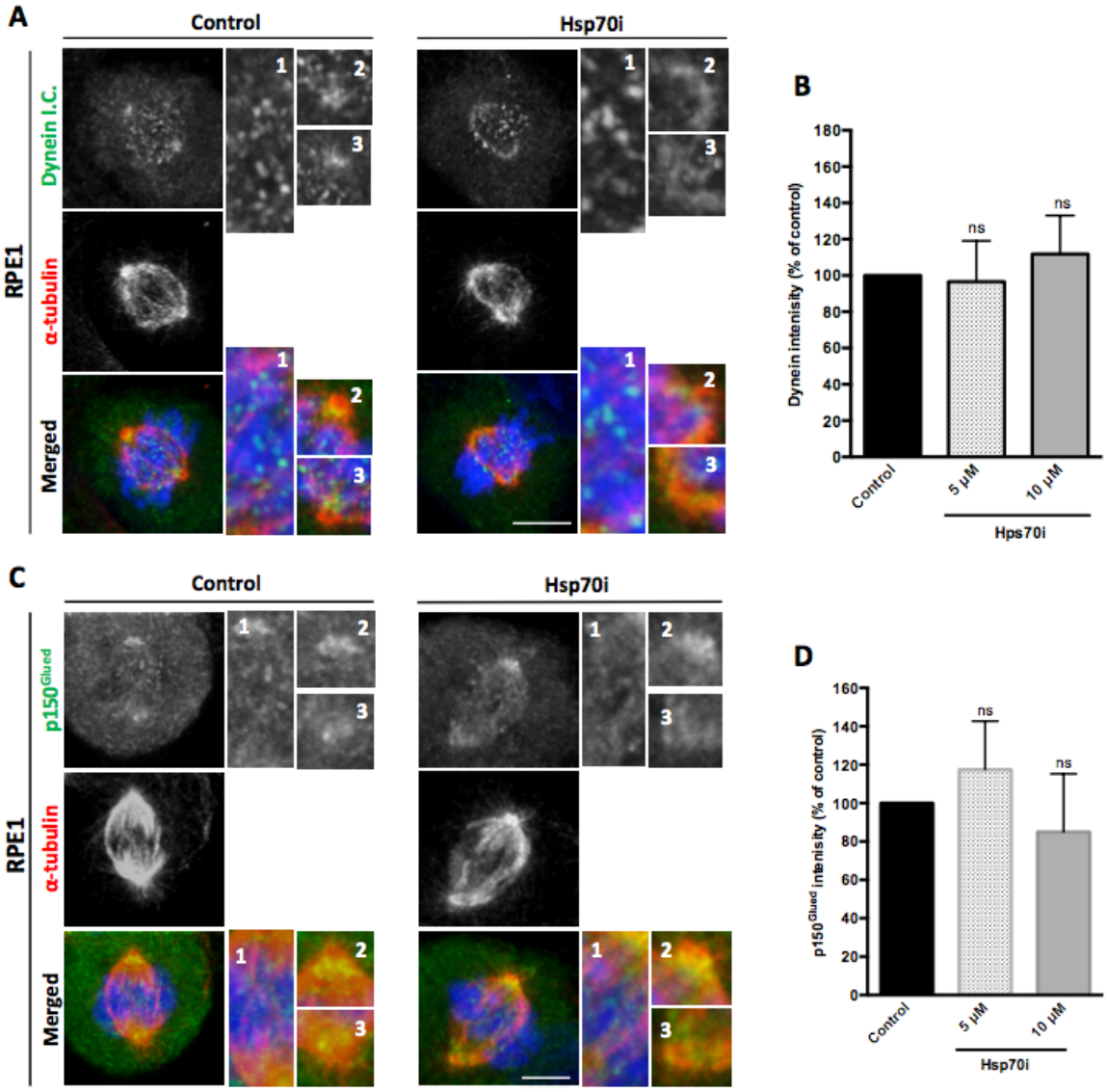

Figure 5.7. Hsp70 inhibition does not alter dynein I.C./p150^{Glued} localisation in RPE1 cells

A. RPE1 cells were treated with Hsp70 inhibitor for 4 hours**.** Cells were stained with antibodies against dynein I.C. (green) or **C.** p150^{Glued} and α-tubulin (red) antibodies. Merged panels include DNA (blue) staining with Hoechst 33258. Scale bar, 5 μm. Insets show magnified views at kinetochores (1) and spindle poles (2, 3). **B, D.** Histogram shows the percentage of dynein I.C. or p150^{Glued} intensity relative to α-tubulin from each treatment. Data show means ± S.D. of three experiments. 10-15 mitotic cells were analysed per experiment.

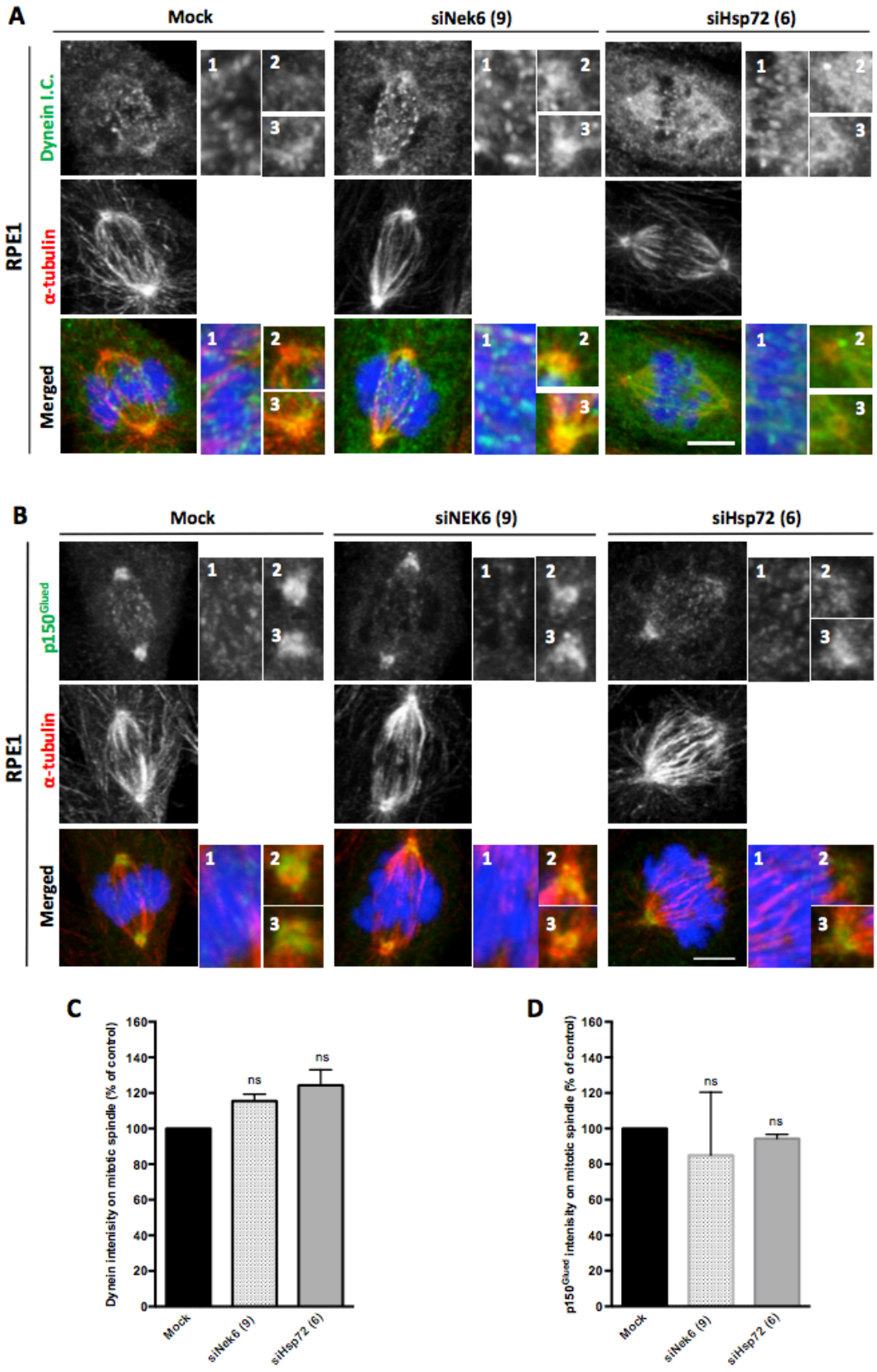

Figure 5.8. Loss of Nek6 or Hsp72 did not affect dynein I.C./p150^{Glued} localisation in RPE1 cells

A. RPE1 cells were mock- or siRNA-transfected with oligonucleotides against Nek6 or Hsp72**.** After 72 hours, cells were stained for dynein I.C. (green) or **B.** p150^{Glued} and α-tubulin (red) antibodies. Merged panels include DNA (blue) staining with Hoechst 33258. Scale bar, 5 µm. Insets show magnified views at kinetochores (1) and spindle poles (2, 3). **C, D.** Histogram shows the percentage of dynein I.C. or p150^{Glued} intensity relative to α-tubulin from each treatment. Data show means ± S.D. of three experiments. 10-15 mitotic cells were analysed per experiment.

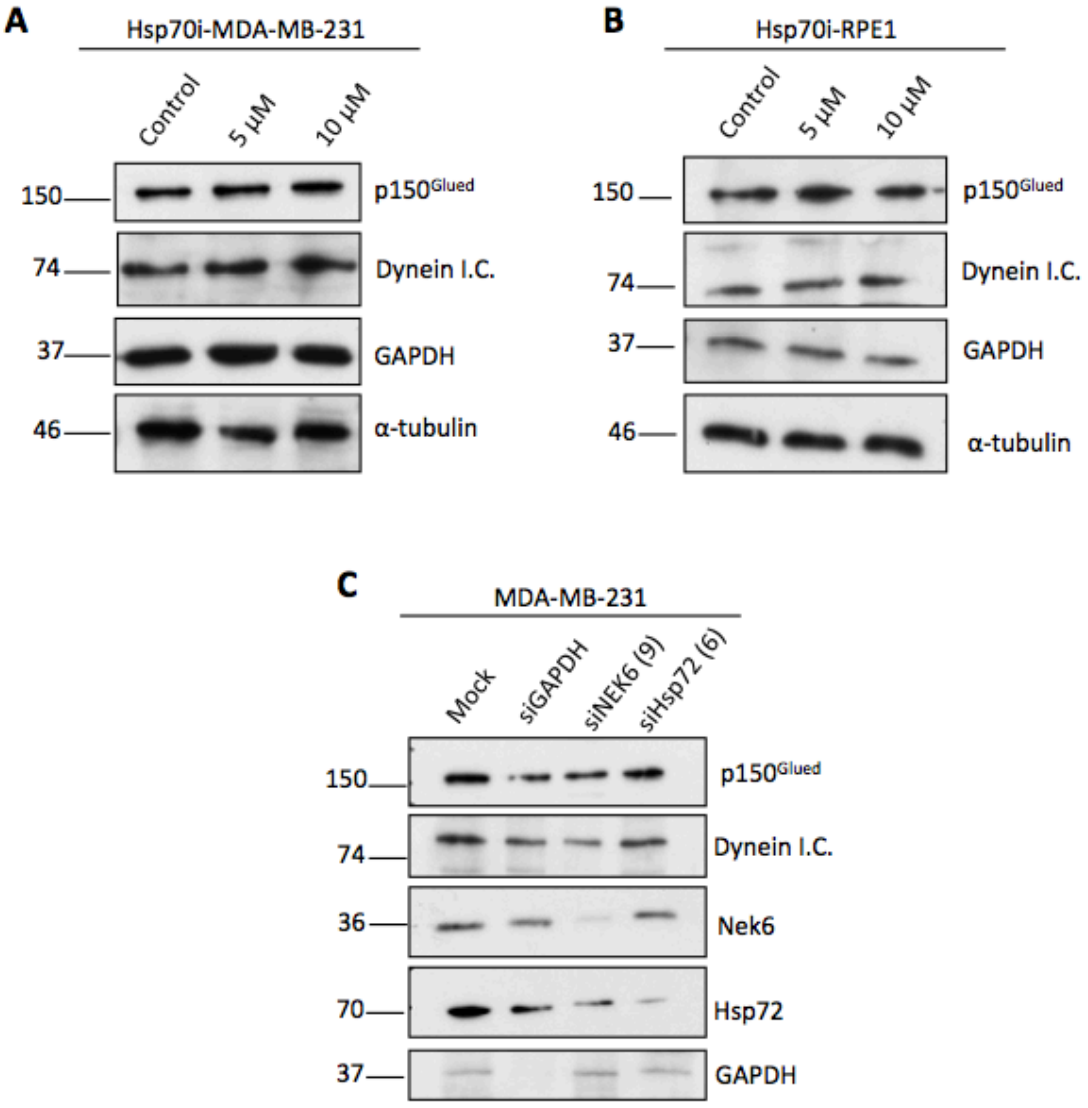

Figure 5.9. Dynein I.C. expression does not change upon loss of Hsp70 or Nek6 function in MDA-MB-231 or RPE1 cells

MDA-MB-231 and RPE1 cells were treated with 5 or 10 μM Hsp70 inhibitor for 4 hours (**A, B)** or were transfected with siRNA oligonucleotides against Nek6, Hsp72 or GAPDH for 72 hours (**C**). Cells were lysed and analysed by SDS-PAGE and Western blotting with antibodies indicated. Molecular weights are indicated (kDa).

5.2.3 Dynein/p150^{Glued} and pHsp72-T66 localisation at kinetochores is lost upon Nek6 and Hsp72 depletion

Dynein localises at kinetochores in prometaphase and aids faithful segregation of chromosomes during mitosis (Foley and Kapoor, 2013; Roberts et al., 2013). In the previous section, we showed that depletion of Hsp72 or Nek6 led to loss of dynein I.C. from the spindle apparatus and potentially from kinetochores. To determine directly whether Nek6-Hsp72 regulates dynein/p150^{Glued} localisation to kinetochores, we examined the localisation of dynein I.C./ p150^{Glued} and a centromere kinetochore marker, CENP-I. Staining revealed a clear co-localisation of dynein I.C. and CENP-I at kinetochores in control MDA-MB-231 cells. However, upon Hsp70 inhibition dynein was lost from kinetochores in the interpolar area (1) (Figure 5.10A). Similarly, Hsp70 inhibition reduced p150^{Glued} from kinetochores compared to control (Figure 5.10B). We therefore conclude that Hsp70 inhibition leads to reduced localisation of dynein I.C./p150^{Glued} at kinetochores.

We have previously showed that Nek6 phosphorylates Hsp72 at Thr-66 and targets it to the mitotic spindle, specifically at kinetochores and spindle poles (O'Regan et al., 2015). Using phosphospecific antibodies designed against Hsp72-T66, we therefore investigated the localisation of pHsp72-T66 at kinetochores and spindle poles in MDA-MB-231 cells. These antibodies confirmed that pHsp72-T66 is concentrated at spindle poles and kinetochores in MDA-MB-231 cells as previously shown in HeLa cells (O'Regan et al., 2015). It also co-localised with dynein I.C. at kinetochores in untreated metaphase cells (Figure 5.11A). However, staining of both dynein I.C. and pHsp72-T66 was lost upon Hsp70 inhibition (Figure 5.11A). Similarly, both p150^{Glued} and pHsp72-T66 were detected at kinetochores in untreated MDA-MB-231 cells (Figure 5.11B). In the presence of Hsp70 inhibitor, both p150^{Glued} and pHsp72-T66 were reduced from kinetochores (Figure 5.11B).

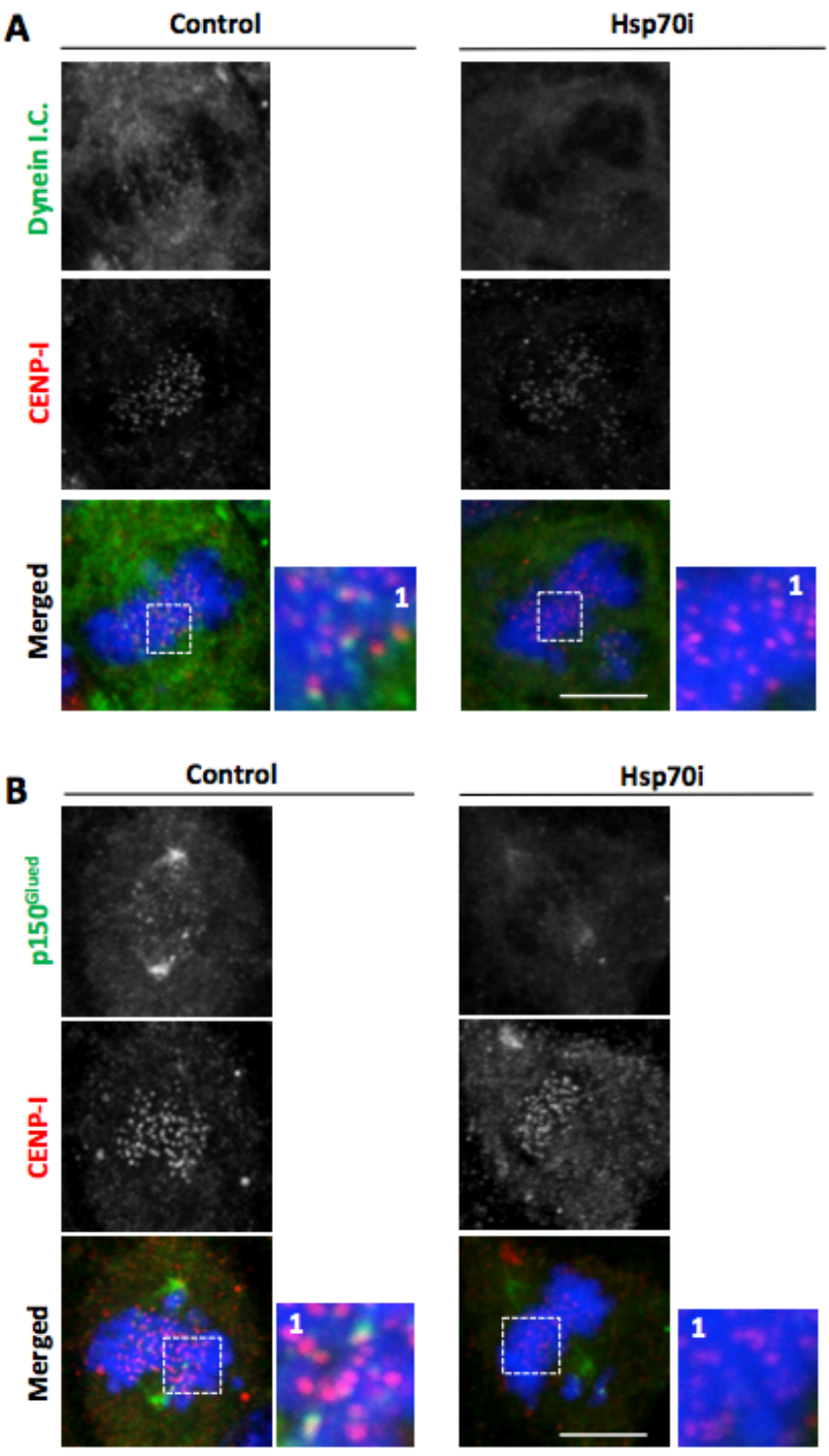

Figure 5.10. Loss of dynein I.C./p150^{Glued} from kinetochores upon Hsp70 inhibition

MDA-MB-231 cells were untreated (control) or treated with 10 µM Hsp70 inhibitor for 4 hours. Cells were stained with antibodies against dynein I.C. (green) (**A**) or p150^{Glued} (green) (**B**) and CENP-I (red). Merged panels include DNA (blue) staining with Hoechst 33258. Insets show magnified views at kinetochores (1). Scale bar, 5 µm.

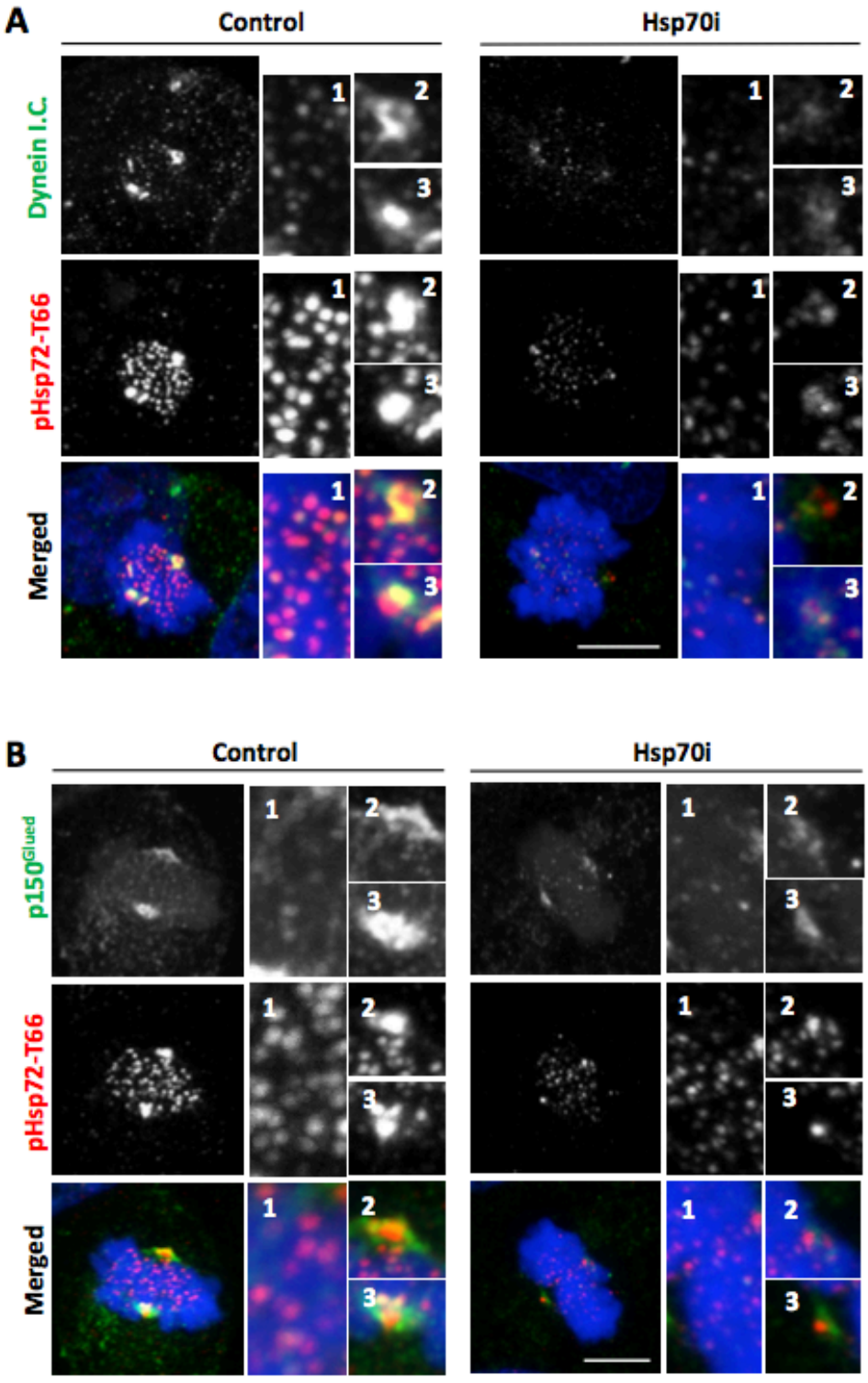

Figure 5.11. Reduced pHsp72-T66 at kinetochores and centrosomes upon Hsp70 inhibition

MDA-MB-231 cells were either untreated (control) or treated with 10 µM Hsp70 inhibitor for 4 hours. Cells were pre-extracted for 30 sec with PTMEH buffer and then fixed with methanol before staining with antibodies against dynein I.C. (green) (**A**) or p150^{Glued} (green) (**B**) and pHsp72-T66 (red). Merged panels include DNA (blue) staining with Hoechst 33258. Insets show magnified views of kinetochores (1) and spindle poles (2, 3). Scale bar, 5 µm.

Furthermore, depletion of either Nek6 or Hsp72 also blocked dynein I.C and pHsp72-T66 localisation at kinetochores in MDA-MB-231 cells (Figure 5.12). In a similar manner, $p150^{Glued}$ and pHsp72-T66 localisation was significantly reduced at kinetochores upon depletion of either Nek6 or Hsp72 (Figure 5.13A). Close examination of multipolar mitoses showed loss of $p150^{Glued}$ and pHsp72-T66 localisation in Nek6- and Hsp72-depleted cells compared to mock-treated ones (Figure 5.13B). Hence, blocking Nek6 or Hsp72 activity led to significant loss of not only dynein/$p150^{Glued}$, but also pHsp72-T66 at kinetochores in MDA-MB-231 cells.

To detect potential interaction of dynein I.C./$p150^{Glued}$ and pHsp72-T66 at kinetochores, this localisation was examined using a proximity ligation assay (PLA) in MDA-MB-231 cells. This assay generates a fluorescent signal only when the two secondary antibodies are within 40 nm. Importantly, dynein, as well as $p150^{Glued}$, and pHsp72-T66 proteins gave clear PLA signals at presumably kinetochores in metaphase cells (Figure 5.14A-B). In contrast, depletion of Nek6 clearly reduced the number of PLA signals of dynein or $p150^{Glued}$ and pHsp72-T66 in metaphase cells (Figure 5.14C-D). Specifically, the majority of mock-treated cells had a mean of 15 PLA signals of dynein-pHsp72-T66 compared to 7 in Nek6-depleted cells (Figure 5.14E), while the $p150^{Glued}$/pHsp72-T66 staining had 17 PLA signal in mock-treated compared to 6 PLA signals per cell in Nek6-depleted cells (Figure 5.14F). Hence, this is the first evidence, apart from immunofluorescence analysis, of interaction at kinetochores of dynein/$p150^{Glued}$ and pHsp72-T66 proteins.

Taken together, we suggest that loss of Nek6 and Hsp72 activity disrupts dynein/$p150^{Glued}$ at kinetochores. As observed, it also leads to loss of pHsp72-T66 at kinetochores. These data also reveal association of dynein/$p150^{Glued}$ with phosphorylated Hsp72 at kinetochores in metaphase MDA-MB-231 cells. Thus, we propose that Nek6 and Hsp72 proteins aid dynein/dynactin localisation to the compartments of mitotic spindle apparatus and hence, may be allow centrosome clustering in cancer cells.

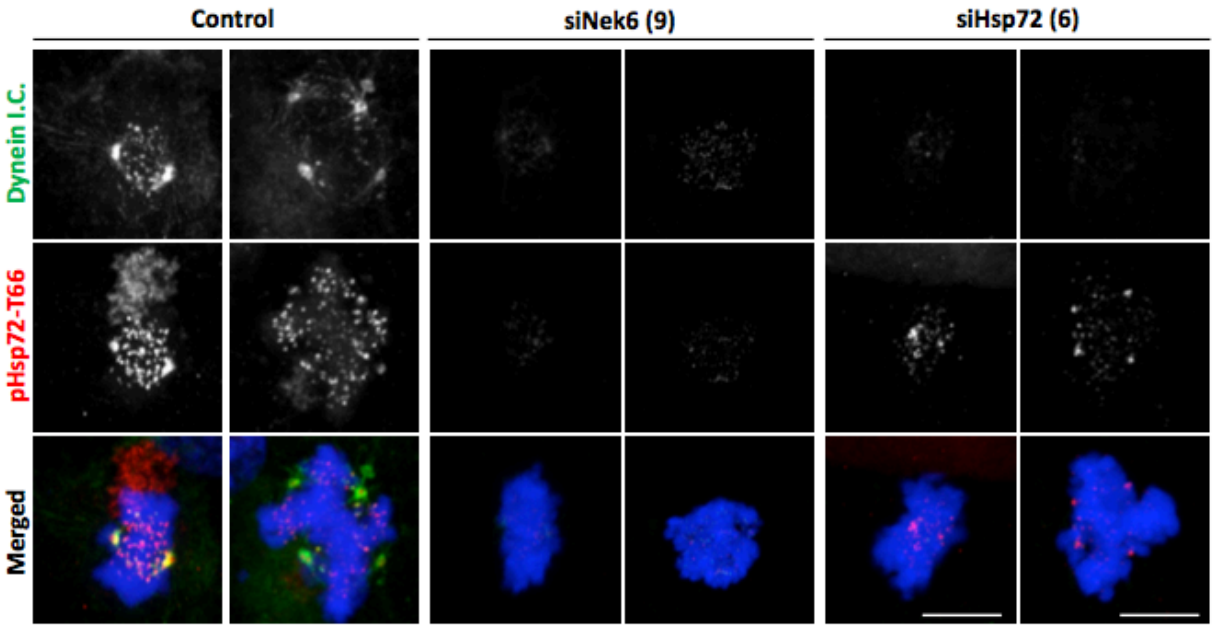

Figure 5.12. Depletion of Nek6 or Hsp72 disrupts pHsp72-T66 at kinetochores in MDA-MB-231 cells

MDA-MB-231 cells were transfected with siRNA oligonucleotides against Nek6 or Hsp72. After 72 hours, cells were pre-extracted for 30 sec with PTMEH buffer and then fixed with methanol before staining with antibodies against dynein I.C. (green) and pHsp72-T66 (red). Merged panels include DNA (blue) staining with Hoechst 33258. Scale bar of multipolar; 7.5 µm, bipolar; 5 µm.

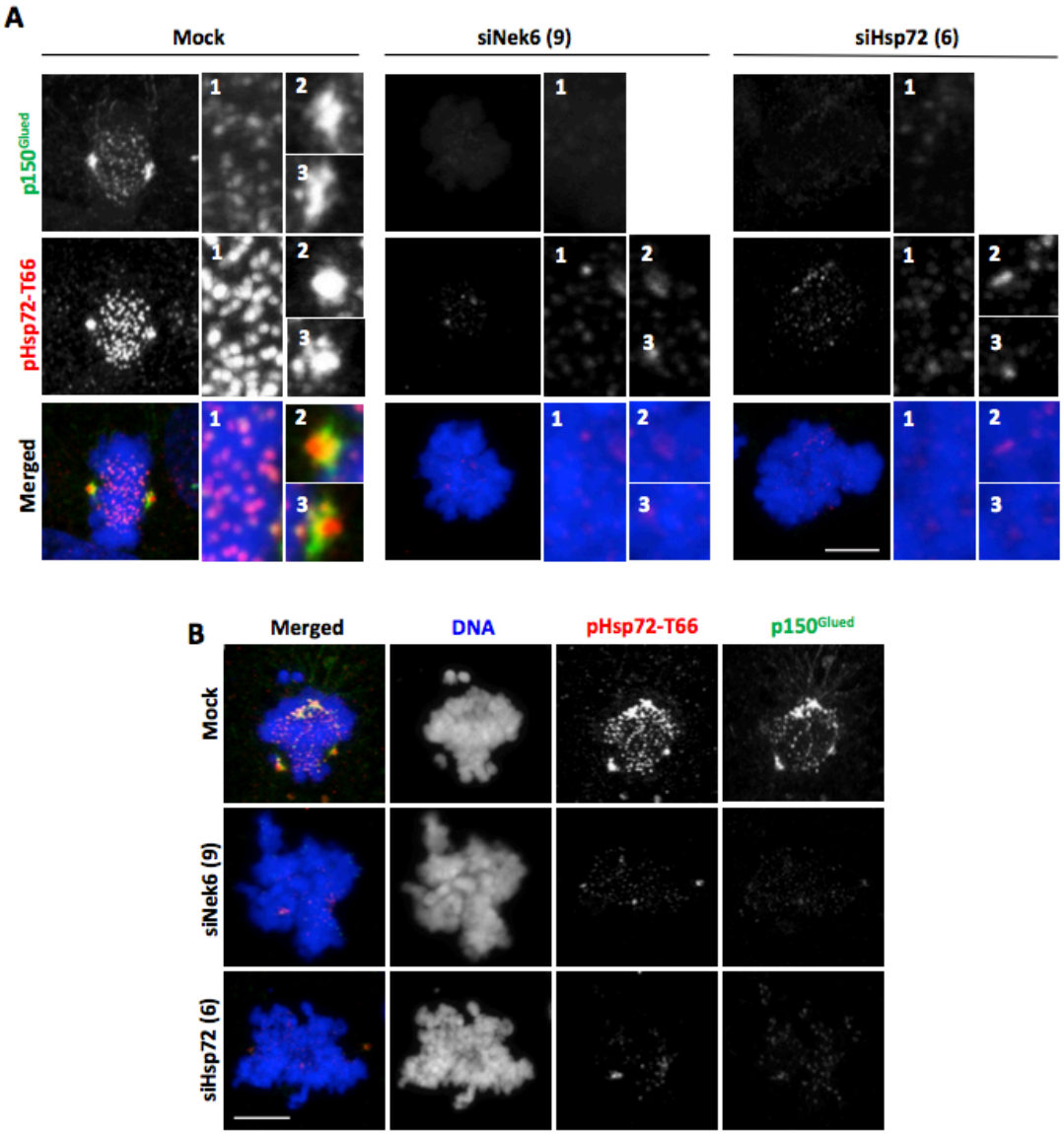

Figure 5.13. Loss of Nek6 or Hsp72 activity disrupts pHsp72-T66 from kinetochores in MDA-MB-231 cells

A,B. MDA-MB-231 cells were transfected with siRNA oligonucleotides against Nek6 or Hsp72. After 72 hours, cells were pre-extracted for 30 sec with PTMEH buffer and then fixed with methanol before staining with antibodies against p150Glued (green) and pHsp72-T66 (red). Merged panels include DNA (blue) staining with Hoechst 33258. Insets show magnified views of kinetochores (1) and spindle poles (2, 3). Scale bar of bipolar; 5 µm, multipolar; 7.5 µm.

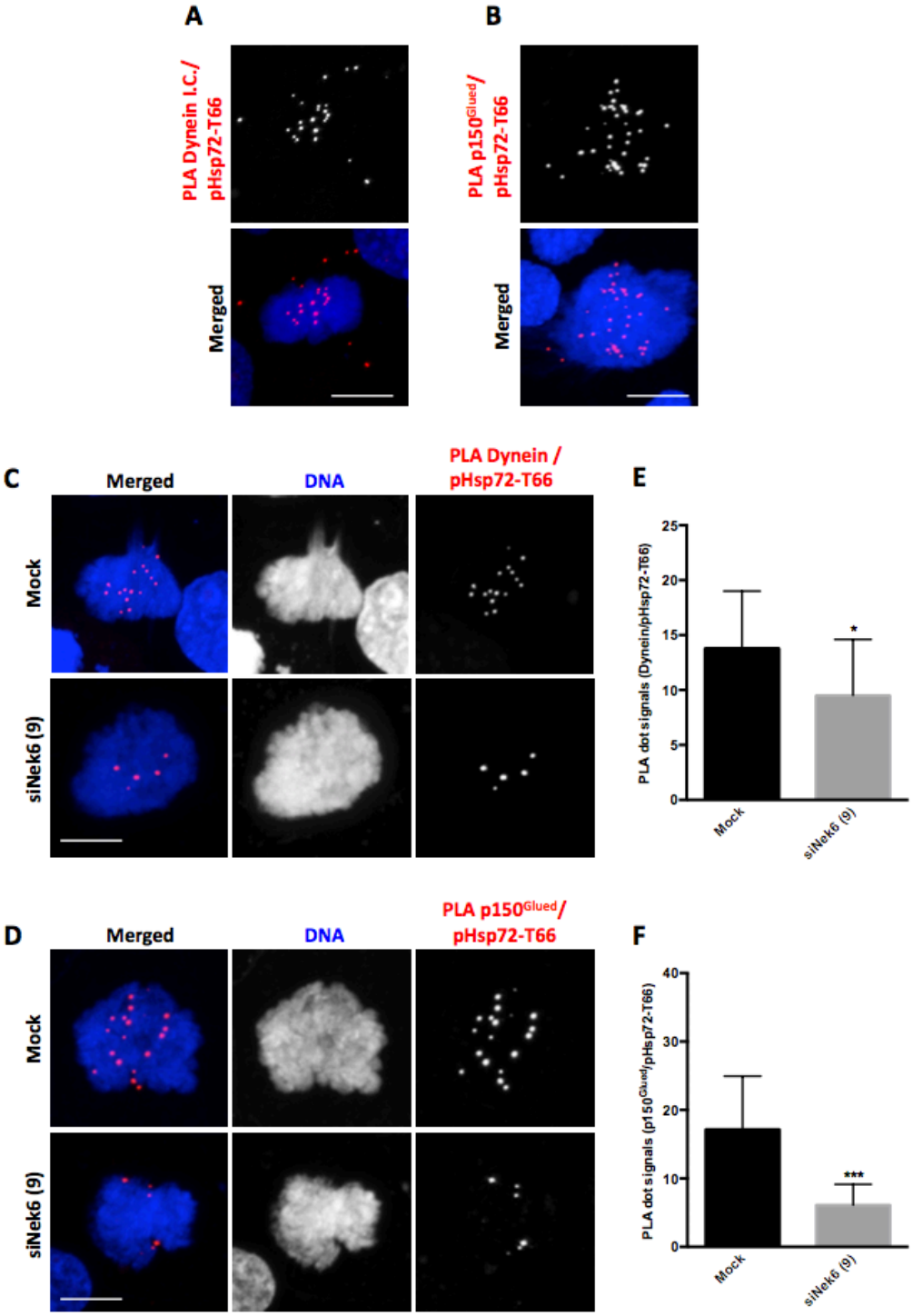

Figure 5.14. Interaction of dynein/p150^{Glued} and pHsp72-T66 at kinetochores detected by PLA assay

MDA-MB-231 cells were pre-extracted for 30 sec with PTMEH buffer and then fixed with methanol before stained for dynein I.C. (green) (**A**) or p150^{Glued} (green) (**B**) and pHsp72-T66 (red) antibodies. Merged panels include DNA (blue). MDA-MB-231 cells were mock- or siRNA-transfected with oligonucleotides against Nek6 or Hsp72. After 72 hours, cells were pre-extracted for 30 sec with PTMEH buffer and then fixed with methanol before staining with antibodies against dynein I.C. (**C**) or p150^{Glued} **(D)** and pHsp72-T66 for PLA assay. Merged panels include DNA (blue) staining. PLA signals were detected in 561nm wavelength. Scale bar, 5 µm. **E, F.** Histogram shows the number of PLA dynein or p150^{Glued} pHsp72-T66 signals for each treatment. Data represent means ± S.D. of two experiments. 20 mitotic cells were counted per experiment.

5.2.4 Hsp70 inhibition disrupts microtubule-kinetochore attachments during mitosis

To gain further insight into how the Nek6-Hsp72 pathway might regulate the dynein/dynactin complex, we examined whether loss of this pathway also disrupts other kinetochore proteins or proteins with roles in microtubule-kinetochore attachments. To investigate the role of Hsp72 and pHsp72-T66 in spindle tension and microtubule-kinetochore attachments, MDA-MB-231 cells were treated with Hsp70 inhibitor for 4 hours and stained for immunofluorescence analysis with pHsp72-T66 and total Hsp72 antibodies. In the presence of Hsp70 inhibitor, pHsp72-T66 localisation was disrupted from the kinetochores and spindle poles, whereas total Hsp72 localisation did not change in MDA-MB-231 cells (Figure 5.15A). A closer examination of pHsp72-T66 at kinetochores, using a CENP-A as a kinetochore marker, showed a significant reduction in the intensity, approximately 50% that was relative to CENP-A intensity, upon Hsp70 inhibition in MDA-MB-231 cells (Figure 5.15B-C).

We next examined the intensity of other kinetochore components including CENP-A, CENP-I and CENP-E. Interestingly, Hsp70 inhibition did not disrupt the localisation or intensity of these kinetochore proteins (Figure. 5.16A-C). However, it should be noted that even though CENP-E intensity at kinetochores did not alter, there was an obvious loss of CENP-E staining at spindle poles upon Hsp70 inhibition (Figure 5.17A). Similarly, co-staining of pHsp72-T66 and CENP-E showed loss from spindle poles in the presence of Hsp70 inhibition (Figure 5.17B). In addition to loss of CENP-E localisation, we also observed a high frequency of misalignment chromosomes in Hsp70i treated cells, similar to those phenotypes seen with dynein I.C. and p150Glued experiments. In addition to immunofluorescence staining, we further examined the association of CENP-E and α-tubulin using PLA. MDA-MB-231 cells were treated with Hsp70 inhibitor for 4 hours following staining with CENP-E and α-tubulin antibodies and subsequently, PLA staining. PLA of CENP-E and α-tubulin gave positive signals at kinetochores of control cells with a mean of 13 PLA signal dots per cell compared to a reduced number of 6 PLA signals in Hsp70i cells (Figure 5.17C-D).

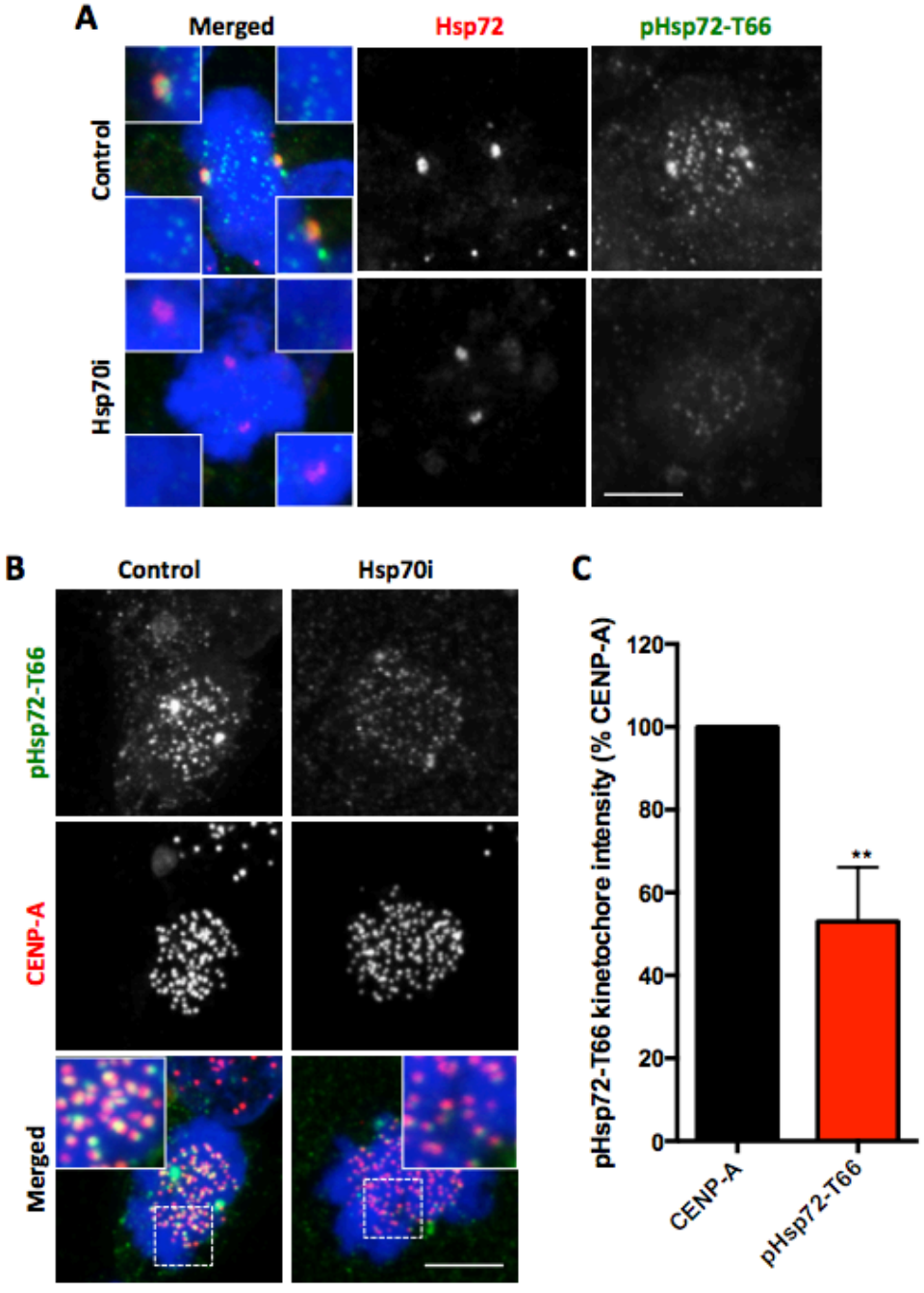

Figure 5.15. Hsp70 inhibition reduces pHsp72-T66 at kinetochores in MDA-MB-231 cells

MDA-MB-231 cells were treated with 10 µM Hsp70 inhibitor for 4 hours. Cells were pre-extracted for 30 sec with PTMEH buffer and then fixed with methanol before staining with antibodies against pHsp72-T66 (green) and Hsp72 (red) (**A**) or pHsp72-T66 (green) and CENP-A (red) (**B**). Merged panels include DNA (blue) staining with Hoechst 33258. Merged panels include DNA (blue) staining with Hoechst 33258. Insets show magnified views of kinetochore area. Scale bar, 5 µm. **C.** Histogram shows the percentage of pHsp72-T66 at kinetochores relative to CENP-A upon Hsp70 inhibition. Data represent means ± S.D. of four experiments. 10-15 mitotic cells were counted per experiment. **p<0.01

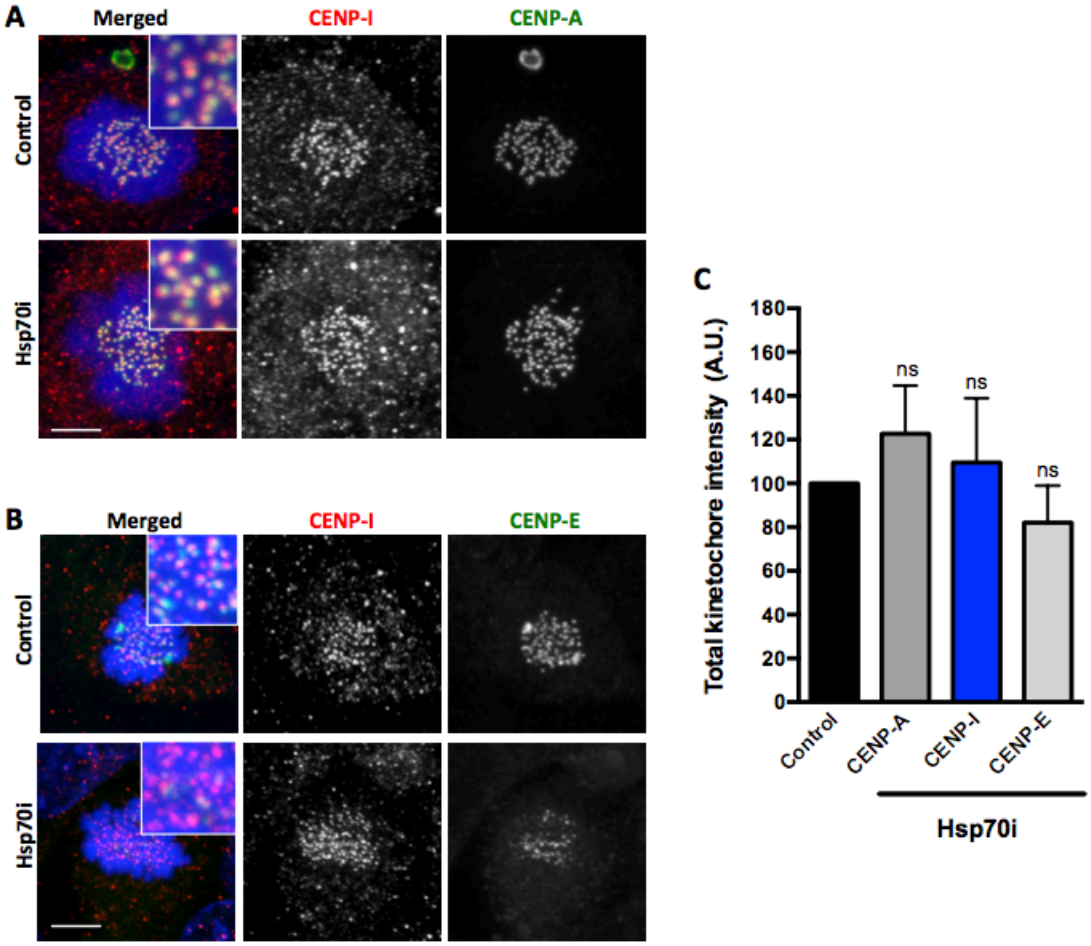

Figure 5.16. Hsp70 inhibition does not alter the intensity of CENP-A, CENP-I and CENP-E at kinetochores

MDA-MB-231 cells were treated with 10 µM Hsp70 inhibitor for 4 hours. Cells were fixed with methanol before staining with antibodies against CENP-A (green) (**A**) or CENP-E (**B**) and CENP-I (red). Merged panels include DNA (blue) staining with Hoechst 33258. Insets show magnified views of kinetochore area. Scale bar, 5 µm. **C.** Histogram shows the total kinetochore intensity of each kinetochore protein upon Hsp70 inhibition. Data represent means ± S.D. of four experiments. 10-15 mitotic cells were counted per experiment.

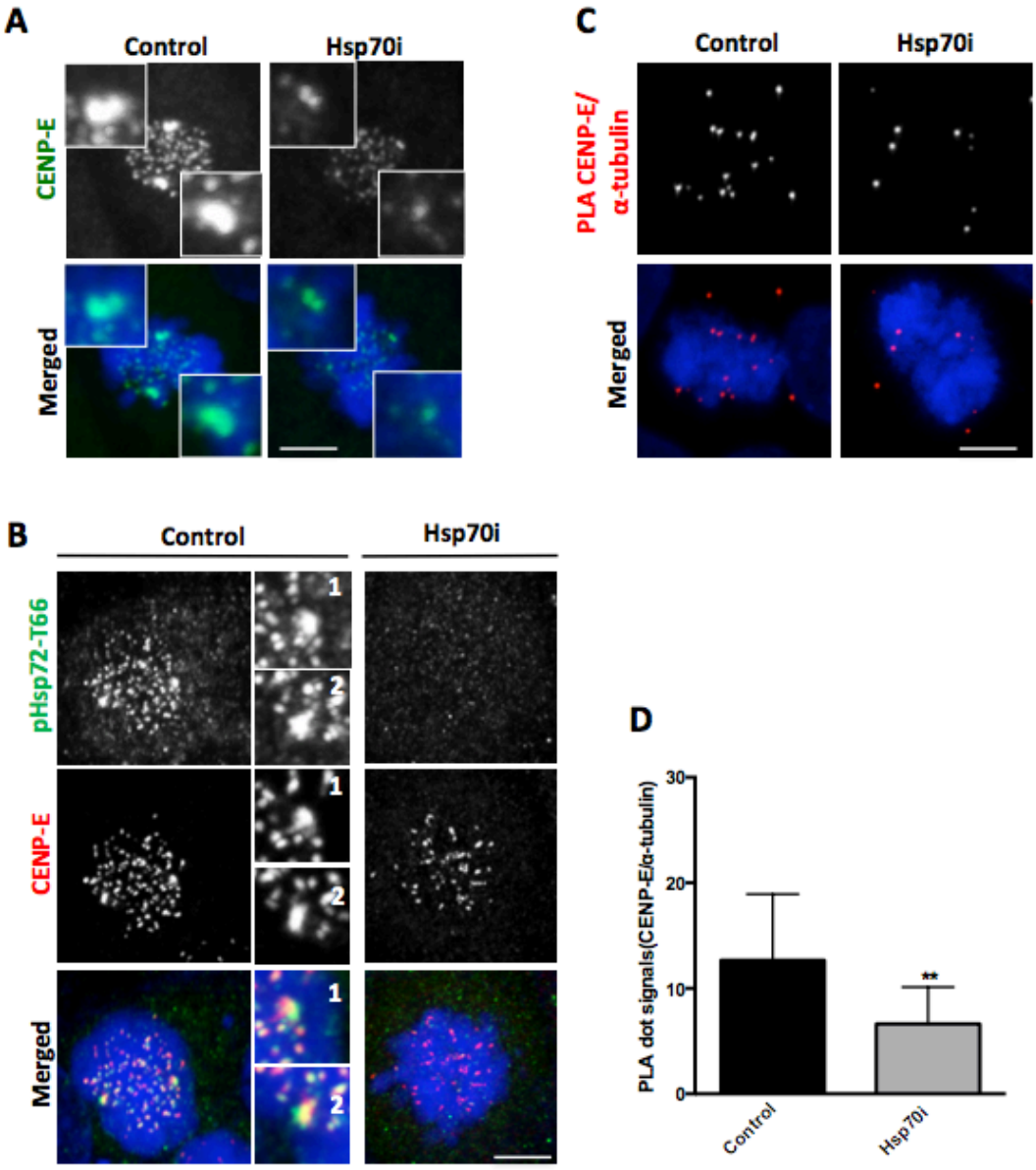

Figure 5.17. Loss of association of CENP-E at spindle poles upon Hsp70 inhibition

MDA-MB-231 cells were treated with 10 µM Hsp70 inhibitor for 4 hours. Cells were fixed with methanol before staining with antibodies against CENP-E (green) (**A**) or pHsp72-T66 (green) and CENP-E (red) antibodies (**B**). Merged panels include DNA (blue) staining with Hoechst 33258. Insets show magnified views of spindle poles (1, 2). Scale bar, 5 µm. **C.** Cells were stained with the same antibodies as B for PLA assay. **D.** Histogram shows the number of PLA CENP-E/α-tubulin signals for each treatment. Data represent means ± S.D. of two experiments. 10-15 mitotic cells were counted per experiment. **p<0.01.

However, further analysis is necessary to validate this loss of CENP-E from the spindle poles. In addition to the kinetochore markers, we have also tested the presence of BubR1, a SAC protein, in the presence or absence of Hsp70 inhibitor. To induce mitotic arrest, we arrested MDA-MB-231 cells with nocodazole for 16 hours, where Hsp70 inhibitor was added at the last 4 hours before the end of the treatment (Figure 5.18A). BubR1 staining at kinetochores remained unaltered in both control and Hsp70-treated cells (Figure 5.18B-C).

Taken together, Hsp70 inhibition led to significant loss of pHsp72-T66, but not Hsp72 as shown in Chapter 4, at kinetochores and spindle poles. However, Hsp70 inhibition did not alter the localisation of CENP-A, CENP-I and CENP-E kinetochore proteins. Additionally, BubR1 was active in the presence and absence of Hsp70 inhibitor. Interestingly, we noted that CENP-E localisation was reduced at the spindle poles upon Hsp70 inhibition.

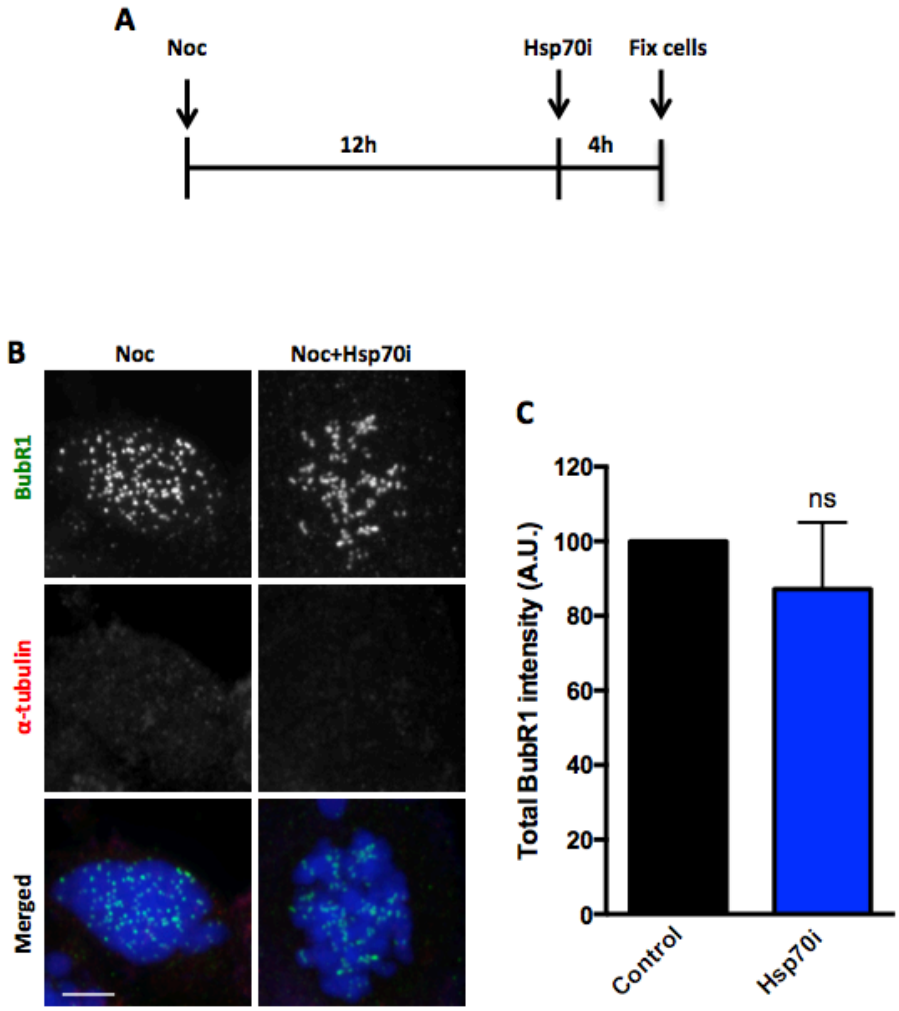

Figure 5.18. Hsp70 inhibition does not disrupt BubR1 in MDA-MB-231 cells

A. Protocol for mitotic arrest using nocodazole and analysis of MDA-MB-231 cells. **B.** MDA-MB-231 cells were treated as A with 10 µM Hsp70 inhibitor for 4 hours. Cells were fixed with methanol before staining with antibodies against BubR1 (green) and α-tubulin (red). Merged panels include DNA (blue) staining with Hoechst 33258. Scale bar, 5 µm. **C.** Histogram shows the total BubR1 intensity at kinetochores after each treatment. Data represent means ± S.D. of three experiments. 10-15 mitotic cells were counted per experiment.

5.2.5 Hsp72 identified as a novel dynein binding partner using MS analysis

To explore whether Hsp72 might physically interact with the dynein/dynactin complex, we first examined their association using immunoprecipitation. MDA-MB-231 cells were arrested in mitosis with nocodazole for 16 hours followed by treatment with or without Hsp70 inhibitor for 1 hour. Cells were then released in a nocodazole-free media but still in the presence or absence of Hsp70 inhibitor for 1 hour. Using the dynein I.C. antibodies, we first optimised immunoprecipitation conditions and next, examined binding of total Hsp72 by western blotting the dynein immunoprecipitated lysates with Hsp72 antibodies. In MDA-MB-231 cells, a weak band of 70 kDa, presumably Hsp72, was detected in the absence, but not presence, of the Hsp70 inhibitor (Figure 5.19A). In RPE1 cells, dynein I.C. was also successfully immunoprecipitated from mitotic cells prepared as described above. Interestingly though, there was no association with Hsp72 in the presence or absence of the Hsp70 inhibitor (Figure 5.19B). However, it should be noted that Hsp72 protein expression is much lower in RPE1 cells. Hence, we suggested that Hsp72 physically interacts with dynein in cancer cells, however, this interaction was not seen in healthy cells.

As we wanted to identify other binding partners that may associate with dynein in mitosis in an Hsp70-dependent manner, MDA-MB-231 cells were arrested in mitosis and treated with or without Hsp70 inhibitor as described above. Lysates were subjected to immunoprecipitation with dynein I.C. antibodies or rabbit IgGs as control. Complex protein mixtures in immunoprecipitate dynein samples were then analysed by liquid chromatography-tandem mass spectrometry (LC-MS/MS). Briefly, trypsin digested sample mixtures were separated by liquid chromatography (HPLC), before individual peptides were then ionised and sorted by mass-to-charge ratio (m/z). Fragments of each m/z ratio were then subjected an extra round of MS to determine the peptide sequence of each protein for identification purposes.

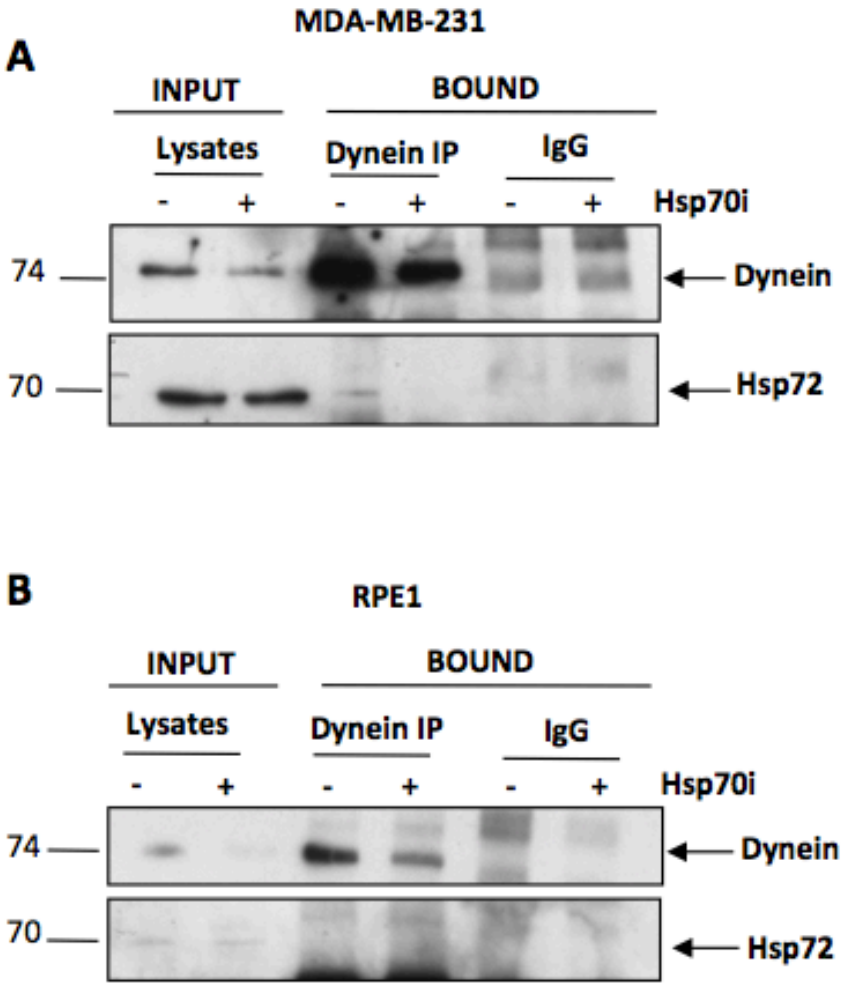

Figure 5.19. Dynein I.C. coprecipitates with Hsp72 in mitotic MDA-MB-231 cells, but not in RPE1 cells

A, B. Cells were treated with 0.5 µM nocodazole for 16 hours and then treated with (+) or untreated (-) Hsp70 inhibitor for 1 hour before the end of the treatment. Cells were released into fresh media without nocodazole but still with or without Hsp70i as before for 1 hour and harvested by mitotic shake-off. Cells were lysed and lysates subjected to immunoprecipitation with dynein I.C. antibody. Input (Lysates) and bound samples were separated by SDS-PAGE and analysed by Western blotting with antibodies indicated. Molecular weights are indicated in kDa.

A list of proteins was generated using Mascot protein identification software (Matrix Science) and the human UniProt database, and then analysed using Scaffold4 proteomics software. A number of parameters were set to minimise the number of false-positive results. Firstly, proteins for which less than 3 different peptides were identified were removed along with proteins with a statistical confidence level less than 95% based on sequence analysis. Secondly, common protein contaminants, such as keratins, were removed (Mellacheruvu et al., 2013). Thirdly, proteins were discarded when also identified in the IgG control sample. This led to a list of 37 potential interacting partners of dynein I.C. in mitotic MDA-MB-231 cells. Proteins identified were then grouped according to their functions (Table 5.1 and 5.2).

First, it was reassuring to see other co-proteins of the multi-subunit dynein in the dynein I.C. immunoprecipitate, including heavy, intermediate and light chains (DYNC1H1, DYNC1I2, DYNC1LI1, DYNC1LI2, DYNLL1 and DYNLT1) (Table 5.1). These were identified in approximately equal amount in the presence or absence of Hsp70 inhibitor, suggesting that assembly of the dynein motor is not depending on Hsp70 activity in mitosis. It should be noted that dynactin complex including $p150^{Glued}$ subunit was not detected in presence or absence of Hsp70 inhibitor. One of the interesting hits that emerged from the proteomic analysis was Hsp72. Hsp72 was identified both with and without the inhibitor arguing that Hsp70 activity is not required for dynein interaction (Table 5.1). Another isoform of Hsp70 family, the HSPA2, was also identified. In line with the co-immunoprecipitation results, we suggested that dynein I.C. potentially interacts with Hsp72 in mitotic MDA-MB-231 cells. However, it is not clear yet whether this interaction is lost upon Hsp70 inhibition, as we previously showed by western blot analysis of co-immunoprecipitates with Hsp72, and will require further validation.

Importantly, members of the Hsp90 chaperone family, including Hsp90-alpha (HSP90AA1) and Hsp90-beta (HSP90AB1) were identified equally in the two samples (Table 5.1). Proteomic analysis revealed another family of motor proteins, myosin, to potentially interact with dynein I.C. Specifically, members of the myosin family including myosin-9 (MYH9), myosin-10 (MYH10), myosin light polypeptide 6 (MYL6) and myosin

regulatory light chain 12A (MYL12A) were identified in dynein immunoprecipitates. Importantly, these myosins were not detected in the presence of Hsp70 inhibitor suggesting that these associations with dynein were regulated by Hsp70 activity. Proteins from the actin family, including ACTN1 and ACTC1, and tubulin family, such as TUBB and TUBB4B, that are associated with microtubule cytoskeleton and filaments were also identified as potential interacting partners with dynein (Table 5.1).

Moreover, a number of proteins with cellular functions, such as transcription regulation, filament organization, adaptor proteins, ubiquitination, DNA helicases and enzymes have also been identified in the presence or absence of Hsp70 inhibitor in dynein IP samples (Table 5.2). It should be noted that filamin-A (FLNA) and cofilin-1 (CFL1), which are implicated with actin cytoskeleton and filament organization, were also identified in dynein immunoprecipitates in the presence or absence of Hsp70 inhibitor (Table 5.2). Furthermore, members of 14-3-3 adaptor protein family were also identified in presence and absence of Hsp70 inhibitor, in which 14-3-3 protein beta/alpha and 14-3-3 protein epsilon were only detected in the presence of Hsp70 inhibitor (Table 5.2). Based on the LC-MS/MS analysis, we identified 37 proteins as potential interacting partners of dynein I.C. From this analysis, candidate proteins were grouped based on their family and function, as illustrated in Figure 5.20.

Protein (gene)	Molecular Weight (kDa)	-Hsp70i Dynein IP (Peptides)	+Hsp70i Dynein IP (Peptides)
Dynein family			
Cytoplasmic dynein 1 heavy chain (DYNC1H1)	532	174	175
Cytoplasmic dynein 1 Intermediate chain 2 (DYNC1I2)	71	31	27
Cytoplasmic dynein 1 Light intermediate chain 1 (DYNC1LI1)	57	14	13
Cytoplasmic dynein 1 light intermediate chain 2 (DYNC1LI2)	54	6	6
Dynein light chain 1, cytoplasmic (DYNLL1)	10	1	1
Dynein light chain Tctex-type 1 (DYNLT1)	12	3	2
Hsp70 family			
Heat shock related 70 kDa protein 2 (HSPA2)	71	1	1
Heat shock 70 kDa protein 1B (HSPA1B)	70	4	5
Hsp90 family			
Heat shock protein HSP 90-alpha (HSP90AA1)	85	6	6
Heat shock protein HSP 90-beta (HSP90AB1)	83	5	4
Myosin family			
Myosin-9 (MYH9)	227	42	25
Myosin-10 (MYH10)	229	1	-
Myosin light polypeptide 6 (MYL6)	27	4	-
Myosin regulatory light chain 12A (MYL12A)	20	4	-
Actin family			
Alpha-actinin-1 (ACTN1)	103	7	2
Actin, alpha cardiac muscle 1 (ACTC1)	42	16	15
Tubulin family			
Tubulin beta chain (TUBB)	50	3	1
Tubulin beta-4B chain (TUBB4B)	50	2	2

Table 5.1. Cytoskeletal and chaperone proteins identified in mitotic dynein I.C. immunoprecipitates by LC-MS/MS analysis

Listed are 20 proteins out of 55 identified in the mass spectrometry analysis of dynein I.C. immunoprecipitate samples from MDA-MB-231 cells. Table shows the gene name in brackets and predicted molecular weight. Proteins with 3 peptides hit and 95% statistical confidence level are indicated. The exclusive unique peptide count of each protein in -/+ Hsp70i samples is indicated. Proteins are categorized according to their families. The number of peptides of each protein is also indicated. All the proteins were not detected in control IgG sample.

Protein (gene)	Molecular Weight (kDa)	-Hsp70i Dynein IP (Peptides)	+Hsp70i Dynein IP (Peptides)
14-3-3 family			
14-3-3 protein beta/alpha (YWHAB)	28	-	1
14-3-3 protein epsilon (YWHAE)	29	-	1
14-3-3 protein zeta/delta (YWHAZ)	28	1	-
14-3-3 protein theta (YWHAQ)	28	4	5
Miscellaneous			
Cofilin-1 (CFL1)	23	4	3
Filamin-A (FLNA)	246	11	-
X-ray repair cross-complementing protein 6 (XRCC6) Ku70	64	5	8
X-ray repair cross-complementing protein 5 (XRCC5) ku80		3	4
Heterogeneous nuclear ribonucleoprotein A0 (HNRNPA0)	31	6	4
Heterogneneous nuclear ribonucleoprotein K (HNRNPK)	51	7	3
Interferon-induced GTP-binding protein Mx1 (MX1)	76	21	15
Nucleolin (NCL)	77	3	-
Nucleophosmin (NPM1)	33	5	-
60 kDa heat shock protein, mitochondrial (HSPD1) Hsp60	61	4	5
Scaffold attachment factor B1 (SAFB)	103	-	3
Elongation factor 2 (EEF2)	95	6	3
GTP- binding nuclear protein RAN (RAN)	26	2	-
Pyruvate kinase PKM (PKM)	58	19	15
Polymerase I and transcript release factor (PTRF)	43	7	8

Table 5.2. Miscellaneous proteins identified in mitotic dynein I.C. immunoprecipitates by LC-MS/MS analysis

Listed are 22 proteins out of 55 identified in the mass spectrometry analysis of dynein I.C. immunoprecipitate samples from MDA-MB-231 cells. Table shows the gene name in brackets and predicted molecular weight. Proteins with 3 peptides hit and 95% statistical confidence level are indicated. The exclusive unique peptide count of each protein in the presence or absence of Hsp70 inhibitor samples is indicated. The number of peptides of each protein is also indicated. All the proteins were not detected in control IgG sample.

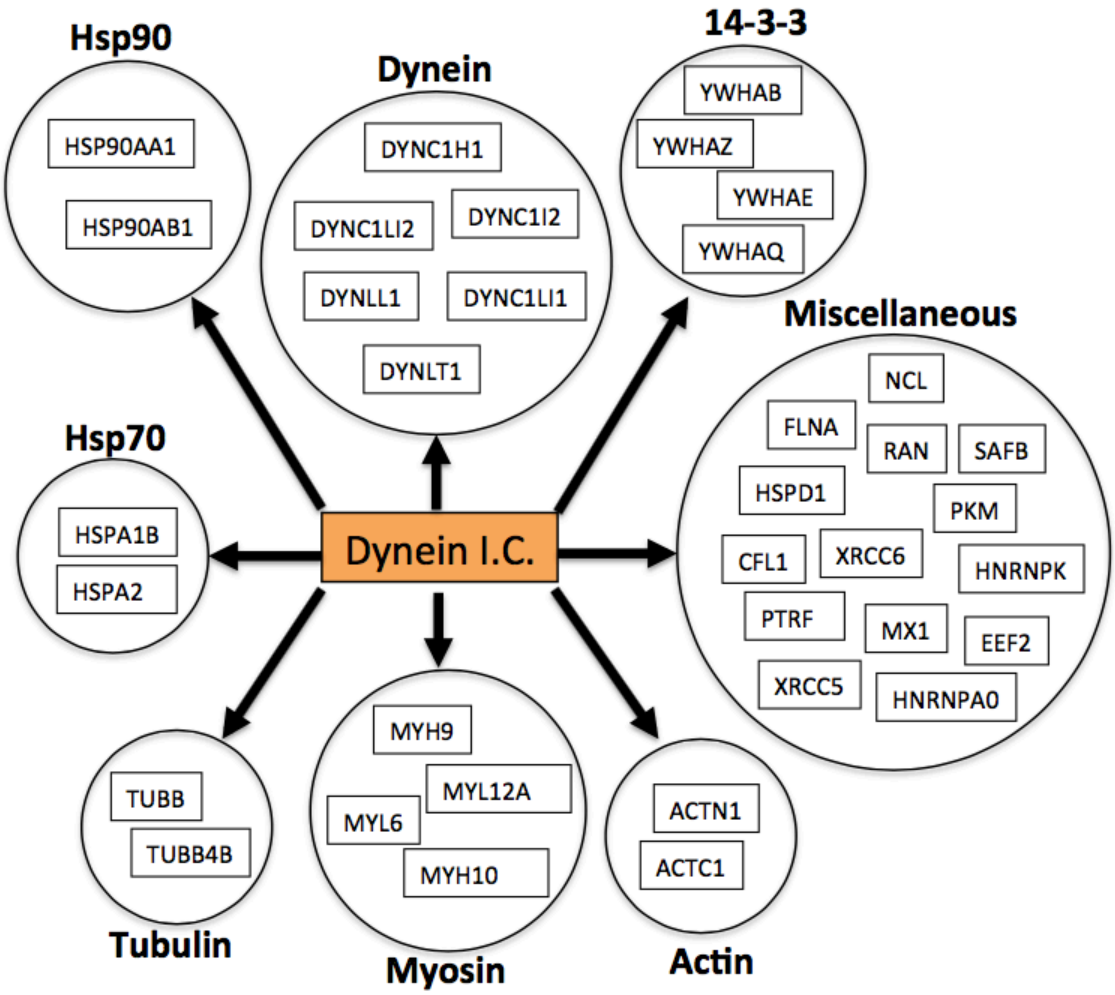

Figure 5.20. Overview of candidate interacting partners of dynein in mitotic MDA-MB-231 cells

In this diagram, 42 out of 55 candidate interacting proteins of dynein I.C. were identified by LC-MS/MS analysis. Proteins were grouped into families including dynein, Hsp90, Hsp70, tubulin, myosin, actin and 14-3-3. The remaining miscellaneous proteins were placed in a separate circle as indicated.

5.3 Discussion

Over the last decade, at least five distinct centrosome clustering mechanisms have been described in cancer cells (Kwon et al., 2008; Leber et al., 2010; Godinho et al., 2009). These mechanisms allow division and survival of cancer cells with amplified centrosomes. Several proteins with functions in mitosis have been implicated in those mechanisms. In this chapter, we attempted to understand how microtubule-based motor proteins associate with Nek6-Hsp72 to aid centrosome clustering in cancer cells.

5.3.1 Nek6-Hsp72 pathway is unlikely to achieve centrosome clustering via the ch-TOG/TACC3 complex

Among the best-known plus-end microtubule-binding proteins are the ch-TOG/XMAP215 protein and its interacting partner TACC3 (Thakur et al., 2013; van der Vaart et al., 2011). The ch-TOG/TACC3 complex stabilises the minus and plus ends of microtubules. The complex is localised to microtubules either directly or indirectly via clathrin binding and Aurora-A phosphorylation (Hood et al., 2013; Gutierrez-Caballero et al., 2015). A genome-wide RNAi screen identified ch-TOG as required for centrosome clustering in cancer cells (Leber et al., 2010). Interestingly, integrin-linked kinase (ILK) promotes centrosome clustering through the ch-TOG/TACC3 complex, although how it is not clear (Fielding et al., 2011). We previously showed that the Nek6-Hsp72 pathway target the ch-TOG/TACC3 complex to the spindle to stabilize K-fibres during mitosis (O'Regan et al., 2015). In this study, as we identified a novel function of Nek6-Hsp72 pathway in centrosome clustering, we examined whether this might also be controlled via its regulator of the ch-TOG/TACC3 complex. Consistent with previous data, we found that loss of ch-TOG and TACC3 activity induced high-grade multipolarity in MDA-MB-231 cells with amplified centrosomes. However, it also induced multipolarity in HeLa cells with no centrosome amplification, while careful examination revealed acentrosomal spindle poles in the majority of multipolar mitoses upon ch-TOG or TACC3 depletion in both cell lines. Our results were consistent with previous studies that also reported a high frequency of acentrosomal poles upon depletion of these proteins (Fielding et al., 2011; Leber et al., 2010). Importantly,

though, our results showed that Nek6 and Hsp72 depletion led to multipolarity without formation of acentrosomal poles. Hence, we propose that the Nek6-Hsp72 pathway is unlikely to promote centrosome clustering purely through regulation of ch-TOG and TACC3.

5.3.2 Nek6-Hsp72 pathway regulates localisation of the dynein/dynactin complex

Dynein, a microtubule-based motor, was one of the first proteins found to regulate centrosome clustering (Quintyne et al., 2005). Subsequent experiments suggest that loss of dynein promotes multipolarity without forming acentrosomal spindle poles in cells with amplified centrosomes (Leber et al., 2010). This is similar to the multipolar mitoses we observed upon loss of the Nek6-Hsp72 pathway. Here, we showed that depletion of Nek6 or Hsp72 led to significant loss of dynein I.C. at spindle poles in mitotic MDA-MB-231 cells, but not in RPE1 cells. This supports previous findings that depletion of dynein subunits led to loss of spindle pole focusing and weak spindle microtubule organization (Raaijamakers et al., 2013). As, dynein I.C. expression levels did not change upon Hsp70 inhibition, it is unlikely that Hsp70 simply act to prevent its turn over. Interestingly, RPE1 cells had lower levels of dynein I.C. at the mitotic spindle apparatus than MDA-MB-231 cells and these levels were unchanged by Hsp70 inhibition. We propose that aneuploidy cancer cells with amplified centrosomes may recruit more dynein to the mitotic apparatus to facilitate spindle organisation and chromosomes alignment. Interestingly, loss of dynein was reported not to inhibit centrosome clustering in human keratinocytes and fibroblasts cells with induced centrosome amplification or in *Drosophila* S2 cells (Ngugen et al., 2008; Goshima et al., 2005). These observations suggest that dynein may not be required for centrosome clustering in all cell lines, suggesting the different dependencies on clustering mechanisms between cell types. Moreover, the molecular mechanism for how dynein contributes to centrosome clustering remains elusive.

For trafficking purposes, dynein generally requires an adaptor protein, the dynactin, to facilitate its interactions with cargoes. Indeed, the dynein/dynactin complex is required for

chromosome capture and movement in mitosis (Raaijmakers et al., 2013). In our study, we used antibodies against the $p150^{Glued}$ to assess dynactin localisation. Similar to the dynein, dynactin was significantly increased on the spindle in MDA-MB-231 cells compared to RPE1 cells. This suggests that dependence on the dynein/dynactin complex for mitotic progression may vary between healthy and cancer cells. Also similar to dynein, dynactin localisation was significantly reduced at the mitotic spindle upon Hsp70 inhibition or depletion of Hsp72 and Nek6 activity in MDA-MB-231 cells, whereas it was not altered in RPE1 cells. Likewise, no change was observed in $p150^{Glued}$ expression levels upon Nek6 or Hsp72 depletion in either MDA-MB-231 or RPE1 cell lines.

Kinetochores are the connection points between chromosomes and the plus-ends of spindle microtubules that create tension to allow chromosome movement and bipolar attachment (Cheeseman and Desai, 2008). Kinetochores also have an important role in the spindle assembly checkpoint (SAC) that prevents errors in chromosome segregation and aneuploidy (Shah and Cleveland, 2000). Dynein, and dynactin, concentrate at kinetochores during prometaphase and subsequently translocate along microtubules to spindle poles when the SAC is inactivated (Hoffman et al., 2001; Wojcik et al., 2001). Dynein/Dynactin is believed to transport various proteins, including the SAC component Mad2 and BuBR1, to facilitate proper microtubules-kinetochore attachments (Wojcik et al., 2001; Liang et al., 2007). Our results showed the presence of BubR1 indicating that the SAC was active in the presence and absence of Hsp70 inhibitor, even with the loss of dynein/dynactin complex from the mitotic spindle. In our previous study, we observed the presence of active SAC upon Hsp70 inhibition that leads to metaphase arrest in cancer cells (O'Regan et al., 2015). Furthermore, previous studies from our laboratory showed that the mitotic kinase Nek6 regulates Hsp72 by phosphorylating at T66 and therefore this controls the localisation of Hsp72 to the spindle apparatus, particularly at kinetochores and spindle poles (O'Regan et al., 2015). Here, we show that the phosphorylated Hsp72 (pHsp72-T66) co-localised with dynein/dynactin at spindle poles and kinetochores. Moreover, PLA assays revealed tight association of dynein/dynactin and pHsp72-T66 at kinetochores. Hence, this suggests that the phosphorylated version of Hsp72, which is targeted to spindle poles and kinetochores

by Nek6, associates with the dynein/dynactin complex to ensure proper microtubule-kinetochore attachments.

A large number of other proteins localise at kinetochores to aid the correct attachment of chromosomes to microtubules during mitosis (Cheeseman and Desai, 2008). This includes the CENP-E, CENP-A and CENP-I proteins. CENP-E is a microtubule-dependent plus-end directed motor of the kinesin-7 subfamily that localises at outer part of the kinetochore and is essential for microtubule attachment of chromosomes during mitosis (Gudimnchuk et al., 2013). On the other hand, CENP-A and CENP-I are core proteins in the inner part of the kinetochore. Our results showed that loss of Hsp70 activity did not alter the localisation of either CENP-E or CENP-A and CENP-I at kinetochores. Apart from the localisation of CENP-E at kinetochores, we also noted that it localises at spindle poles, and in the presence of Hsp70 inhibitor, CENP-E was reduced at those sites. Interestingly, both CENP-E and pHsp72-T66 co-localise at kinetochores and spindle poles, but in the presence of Hsp70 inhibition both proteins were reduced from the spindle poles. We therefore suggest that possibly the Hsp70 might play a role in the movement of CENP-E/pHsp72-T66 from the spindle poles to kinetochores. However, further experiments are needed to validate these observations.

Taken together, we suggest that the Nek6-Hsp72 pathway regulates localisation of dynein/dynactin complex and potentially other proteins such as CENP-E to mitotic spindle apparatus to regulate centrosome clustering in cancer cells. It should be noted that dynein and dynactin are composed of multiple subunits and each subunit may have individual functions. For example, depletion of $p150^{Glued}$ had no effect on spindle pole focusing suggesting that in some cases dynein is acting independently of dynactin (Raaijmakers et al., 2013). Hence, the study here relied on localisation of single subunit of dynein and dynactin and further studies should investigate how blocking the Nek6-Hsp72 pathway affects other dynein and dynactin subunits.

5.3.3 Dynein interacts with multiple partners that may contribute to centrosome clustering

Identification of Hsp72 partners related to centrosome clustering is challenging, as chaperones have multiple functions and targets. On the other hand, analysis of proteins whose interaction with dynein depend on Hsp70 activity might be a better way to identify relevant interactions. We therefore performed immunoprecipitation and mass spectrometry (MS) analysis to identify mitotic binding partners of dynein I.C. and to gain further insight into pathways and processes in which it may be involved.

Based on the LC-MS/MS analysis, we identified 37 unique proteins involved in a number of cellular processes, including multiple proteins involved in cytoskeleton organization. Importantly, the proteomic study identified a number of other dynein subunits that interact with dynein I.C., including the cytoplasmic dynein 1 heavy chain (DYNC1H1), cytoplasmic dynein 1 light intermediate chain 1 and 2 (DYNC1LI1 and DYNC1LI2) and some dynein light chains such as dynein light 1 (DYNLL1) and Tctex-type 1 (DYNLT1). Each of these subunits contributes to the proper function of dynein, and may of those subunits have a function in mitosis. For example, the dynein intermediate chain 1 and 2 play key role at the kinetochore sites by interacting with dynactin and Nde/L1 proteins. Furthermore, dynein light chain 1 (DYNLL1) is required for spindle orientation during mitosis and localisation of dynein to the cell cortex through the CHICA protein (Duncsh et al., 2012). Hence, the dynein subunits identified in our screen are important for the function of dynein in mitosis, and it confirms the success of our approach in identifying intact dynein complexes.

Surprisingly, we did not identify any of the dynactin subunits in the mass spectrometry analysis. We therefore suggest that even though dynactin is important for dynein functions in mitosis, it might act independently of dynein functions or have interactions with other dynein subunits rather than dynein I.C. in mitosis. We also suggest that dynein I.C. might potentially form protein complexes in mitotically arrested cells, which differ from those formed by dynactin. In line with this hypothesis, it has been suggested that dynactin is

important for recruitment of dynein to kinetochores, but is not essential to dynein function in organizing the mitotic spindle (Raaijmakers et al., 2013). Furthermore, dynactin can act independently of dynein in some aspects of mitotic spindle organization and is not required for spindle formation (Raaijmakers et al., 2013). However, it is still far from clear what the exact role of dynactin is with respect to the dynein complex in mitotic processes.

One of the most reassuring hits from the mass spectrometry analysis was Hsp72 (HSPA1A). Immunoprecipitation experiments followed by Western blot had suggested interaction of dynein with Hsp72 in mitotic MDA-MB-231 cells. This interaction between Hsp72 and dynein was therefore confirmed by mass spectrometry analysis. Interestingly, in the Western blot analysis, the interaction appeared to be lost upon Hsp70 inhibition suggesting the interaction was dependent on Hsp72 activity. However, there was no loss of interaction upon Hsp70 inhibition by mass spectrometry analysis. It will be important to test in more detail whether the dynein-Hsp72 interaction is lost upon Hsp70 inhibition. It will also be very interesting to investigate which domains of Hsp72 and which subunits of dynein might be necessary to facilitate this interaction between Hsp72 and dynein, and importantly to know whether this interaction is direct.

As well as Hsp70, members of the Hsp90 family were identified in the dynein immunoprecipitates. Mass spectrometry analysis identified the heat shock protein Hsp90-alpha (HSP90AA1) and -beta (HSP90AB1). Like Hsp70, Hsp90 is a chaperone family that is expressed under the control of HSF1, in response to stress conditions such as hypoxia, high temperatures and oxidative damage (Young et al., 2004). In mitosis, Hsp90 is required for kinetochore assembly with loss of Hsp90 leading to chromosome misalignment and aneuploidy (Niikura et al., 2006). Hsp90 is clearly implicated in centrosome and spindle pole functions, along with dynein, it contributes to centrosome duplication (Prosser et al., 2009). Dynein was also contributed to in this centrosome overduplication pathway along with Hsp90 (Prosser et al., 2009). However, it is unclear how Hsp90 and dynein might communicate during mitosis and whether they cooperate in centrosome clustering mechanisms.

Another group of proteins identified as interacting partners of dynein I.C. were the tubulin and actin families. From the tubulin family, tubulin beta-chain (TUBB) and tubulin beta-4B chain (TUBB4B) were identified as interacting partners of dynein I.C. Both proteins are components of microtubules consistent with the role of dynein in transporting cargoes, on the mitotic spindle (Roberts et al., 2013). Furthermore, two actin binding proteins, alpha-actinin-1 (ACTN1) and actin cardiac muscle 1 (ACTC1) were identified. Alpha-actinin-1 is a cytoplasmic actin-binding protein that localises to actin filaments and adhesion sites in non-muscle cells. It has several functions including bundling of actin filaments, connecting the actin cytoskeleton to the plasma membrane and acting as a platform for trafficking of various proteins, although none of these are known to be important for mitosis (Sjoblom et al., 2008).

In addition to actin, we identified a number of other actin regulators, including cofilin-1 and filamin-A. Cofilin-1 is an important regulator of remodelling actin filaments promoting cell migration (Wang et al., 2007). Up- or down-regulation of cofilin activity is implicated in various cancers including breast, prostate and ovarian cancers (Wang et al., 2007; Martoglio et al., 2000; Davila et al., 2003; Yoshioka et al., 2003). Interestingly, increased levels of phosphorylated colifin-1 were detected in MDA-MB-231 cells (Yoshioka et al., 2003). Filamin-A was among the prominent hits of our mass spectrometry analysis. Filamin-A is another actin filament cross-linking protein implicated in cell adhesion and migration (Nakamura et al., 2011), with filamin mutations common in human breast and colon cancers (Sjoblom et al., 2006). Taken together, cofilin-1 and filamin-A proteins regulate cytoskeletal organization to control both cell migration and cell division. However, further experiments are required to understand the relevance and importance of these interactions with dynein in mitosis.

Perhaps of most interesting was the identification of members of the non-muscle myosin family in the dynein immunoprecipitates. These were the most abundant non-dynein partners identified and exhibited clear Hsp70 activity dependence. Myosin is another group of cytoskeletal motor proteins that move along the actin filaments powered by ATP

(Peckham, 2016). A typical structure of myosin consists of heavy chains (1 or 2) and light chains. Based on their sequence similarity, myosins are classified into 12 sub-families (Peckham, 2016). In our screen, we identified MYL6 and MYL12A, which are regulatory light chains implicated in cytokinesis and cell migration, as well as two members of the non-muscle myosin class 2 (NM2) family, MYH9 (NM2A) and MYH10 (NM2B). The NM2 family is important for cell polarity, migration, adhesion and cytokinesis (Peckham, 2016; Newell-Litwa et al., 2015), with mutations implicated in various neuronal and cardiovascular diseases (Newell-Litwa et al., 2015). Moreover, increased expression levels of NM2A (MYH9) have been found in bladder, gastric and non-small cell lung cancers, whereas other studies suggest that NM2A can act as a tumour suppressor (Peckham, 2016). In terms of mitosis, NM2 family regulates cytokinesis through concentrating within the cytokinetic ring (Ou et al., 2010). However, in cancer cells, the absence of BRCA2 alters the localisation of NM2 proteins potentially contributing to aneuploidy and chromosomal instability through cytokinesis failure (Takaoka et al., 2014). In addition to cell division functions, NM2 proteins are important for cell migration. Specifically, NM2A (MYH9) localises at protrusions at the front of cells promoting adhesion, whereas NM2B (MYH10) localises at the rear part of cells and regulates detachment from substrate allowing the cell to move in a forward direction (Newell-Litwa et al., 2015). However, abnormal NM2 functions can accelerate cell detachment stimulating tumour invasion (Vasiliev et al., 2004). In addition, NM2 proteins contribute to formation of blood vessels in cancer, known as angiogenesis (Newell-Litwa et al., 2015). Interestingly, Myo10 is implicated in centrosome clustering by applying forces to astral microtubules, aiding position of centrosomes (Kwon et al., 2008). This suggest that myosin proteins might play an important role along with dynein functions to apply forces, allowing centrosome positioning and clustering. Hence, the NM2 family is implicated in multiple aspects of cancer progression from regulation of cell migration and metastasis to angiogenesis and cell division. Whether they also play a role in centrosome clustering is an exciting and novel possibility.

Our proteomic analysis revealed interaction of dynein with a number of pre-mRNA binding proteins, DNA repair proteins and serine/threonine adaptor proteins. Among those

proteins identified were the heterogeneous nuclear ribonucleoprotein K (HNRNPK) and heterogeneous nuclear ribonucleoprotein A0 (HNRNPA0). These proteins bind to pre-mRNA poly (C) sequences and regulate transcription of mRNAs. Among the functions of dynein is to carry cargoes including mRNA-containing ribonucleoprotein complexes (Wilkie and Davis, 2001). HNRNPK is overexpressed in several human cancers and is involved in cancer progression (Barboro et al., 2014). Furthermore, HNRNPK acts as transcription factor and induces expression of oncogenes and other proteins involved in cell extracellular matrix, cell motility and angiogenesis (Gao et al., 2013). In addition to the mRNA processing factors, Ku70 (XRCC6) and Ku80 (XRCC5) DNA repair proteins were identified as potential interacting partners of dynein I.C. Ku70 interacts with Ku80 and together act in DNA non-homologous end joining (NMEJ) repair system (Downs and Jackson, 2004). Given that dynein is important for transporting cargoes such as transcription factors and apoptotic proteins, it is interesting to investigate how Ku70 and Ku80 interact with dynein to regulate apoptosis and transcription.

Members of the 14-3-3 proteins were also identified in the dynein I.C. immunoprecipitates. The 14-3-3 family is composed of seven members and are phospho-serine/phospho-threonine binding proteins (Morrison, 2009). In our analysis, we identified four members, including 14-3-3 beta/alpha, epsilon, zeta/delta and theta that interact with dynein. From a mitotic perspective, the 14-3-3 proteins have multiple roles, including regulating cytokinesis (Saurin et al., 2008; Fujiwara et al., 2005). However, as so many proteins are phosphorylated in mitosis, including many of the other proteins unfolded here, it will be difficult to determine the specific relevance of this interaction.

Our approach allowed us to compare differences in peptides detected in samples with and without Hsp70 inhibitor. The majority of proteins were detected with similar numbers of peptides in both samples. However, some of them were found in mainly higher abundance in the absence of the inhibitor. Interestingly, myosin-10 (NM2B or MYH10), myosin light polypeptide 6 (MYL6) and myosin regulatory light chain 12A (MYL12A) were exclusively identified in the sample without Hsp70 inhibitor. Additionally, myosin-9 (NM2A or MYH9)

had far fewer peptides in presence of Hsp70 inhibitor. Furthermore, filamin-A was only identified in the absence of the inhibitor, as the 14-3-3 zeta/delta protein. However, this mass spectrometry approach is semi-quantitable and Western blot, IP and GST pull down will be required to confirm whether interactions of proteins with dynein are lost upon Hsp70 inhibition.

In conclusion, using a combination of immunoprecipitation and mass spectrometry, we have identified a number of potential mitotic binding partners of dynein I.C. This includes a number of interesting proteins including Hsp72, tubulin, actin, myosins and other cytoskeletal regulators. There is clear evidence that cytoskeletal proteins, including myosins, filamin-A, cofilin-1 and actin can contribute to centrosome clustering by controlling microtubule attachments to the cell cortex, as well as regulating cell shape and cell adhesion (Kwon et al., 2008; Leber et al., 2010). It will be interesting to investigate further how Hsp72 might affect the interaction of these proteins with dynein and whether this contributes to their role in centrosome clustering. In particular, further examination of the interaction between dynein and non-muscle myosins and how this regulates mitotic progression and potentially centrosome clustering will be interesting given the dependence of this interaction on Hsp70 activity.

Chapter 6

Nek6 and Hsp72 are not required for mitotic progression in non-cancer derived cells

6.1 Introduction

Multiple protein complexes are involved in the mechanism of microtubule-kinetochore capture, including microtubule motors, such as dynein and CENP-E proteins (Cheeseman and Desai, 2008). However, errors can occur in chromosome segregation, including improper microtubule-kinetochore attachments that interfere with accurate chromosome segregation (McBride et al., 2015). Cells monitor and correct these problems by activating components of the spindle assembly checkpoint (SAC) to ensure proper bipolar microtubule-kinetochore attachments are made before cells pass the metaphase-anaphase transition (Ganem and Pellman, 2012).

The majority of cancer cells exhibit defects in mitosis characterized by extended mitotic duration and abnormal chromosome segregation. Together, this leads to aneuploidy accelerating tumorigenesis (Ganem and Pellman, 2012). A hallmark of cancer is the chromosome instability that results from abnormal mitosis. This leads to deregulation of many genes involved in essential processes, such as cell cycle control, DNA replication and repair, and proliferation and apoptosis (Janssen and Medema, 2011; McBride et al., 2015). Mutations or altered expression of SAC proteins or proteins involved in microtubule-kinetochore attachments are key drivers of chromosomal instability (CIN), which contributes to tumour growth (Ganem and Pellman, 2012). A key mechanism that leads to CIN is the generation of abnormal spindles due to the presence of extra centrosomes in a cancer cell. Centrosome amplification is strongly associated with CIN and cancer progression (Gergely and Basto, 2008). Therefore, a good strategy to kill cancer cells is to specifically target cells with amplified centrosomes. The aim is to severely disrupt mitosis either by promoting multipolar spindle formation or causing cells to arrest in mitosis. This should eventually lead to mitotic catastrophe and cell death.

Multiple proteins are essential for mitotic progression of cancer cells, including the Nek6 kinase and its substrate Hsp72 (O'Regan et al., 2015). Recently, we demonstrated that

Hsp72 is a mitotic substrate of Nek6 that contributes to formation of a robust mitotic spindle through promoting assembly of the ch-TOG/TACC3 complex in the k-fibres (O'Regan et al., 2015). Nek6 kinase is upregulated in many cancers including breast, liver, esophageal and colon (Kasap et al., 2012; Nassirpour et al., 2010). Similarly, the stress-inducible Hsp72 protein is also upregulated in cancer cell growth and often correlates with metastasis and poor prognosis (Rohde et al., 2005; Patury et al., 2009). Hence, both Nek6 and Hsp72 are overexpressed in many cancers.

Importantly, their role in mitotic progression in normal, non-cancer derived cells and centrosome clustering is not clear. Hence, in this chapter, we examined whether the Nek6-Hsp72 pathway is necessary for mitotic progression not only in cancer cells, but also in non-cancer cells.

6.2 Results

6.2.1 Loss of Nek6 or Hsp72 activity leads to misaligned chromosomes in cancer, but not in non-cancer derived cells

In the previous chapters, we have shown that loss of Nek6-Hsp72 causes high-grade multipolarity in cancer cells with amplified centrosomes. Apart from the presence of multipolar spindles, we also observed the presence of misaligned chromosomes upon Nek6 or Hsp72 depletion in cancer cells. To assess the importance of the Nek6-Hsp72 pathway activity in chromosome congression in non-cancer derived cells, we first compared the effect of Hsp70 inhibition in cancer and non-cancer derived cell lines. The cancer-derived cell lines, MDA-MB-231 and HeLa cells, were treated with Hsp70 inhibitor for 4 hours and then stained with antibodies against CENP-A, a kinetochore protein, and α-tubulin. Hsp70 inhibition blocked chromosome alignment on the metaphase plate in both MDA-MB-231 and HeLa cell lines (Figure 6.1A). In sharp contrast, Hsp70 inhibition did not affect chromosome congression in the non-cancer derived, RPE1 and HBL-100 cell lines (Figure 6.1B). In the MDA-MB-231 cell line, 5 and 10 μM Hsp70 inhibitor induced errors in chromosome alignment in 47% and 57% cells, as compared to 8% in controls (Figure 6.1C). In HeLa cells, 5 and 10 μM Hsp70i induced chromosome misalignment approximately 57% to cells, compared to 8% in controls (Figure 6.1C). Conversely, in RPE1 and HBL-100 cell lines, Hsp70 inhibition did not induce errors in chromosome alignment (Figure 6.1C). Hence, Hsp70 inhibition induced errors in chromosome alignment in metaphase in MDA-MB-231 and HeLa cell lines, but not in RPE1 and HBL-100 cell lines.

We next examined the effects of Hsp72 or Nek6 depletion on chromosome congression in those cell lines. Immunofluorescence imaging revealed that depletion of either Nek6 or Hsp72 led to a substantial increase of mitotic cells with misaligned chromosomes in both MDA-MB-231 and HeLa cell lines, but not in RPE1 and HBL-100 cell lines (Figure 6.2A-B). In the MDA-MB-231 cell line, Hsp72 or Nek6 depletion led to 48% and 38% of mitotic cells with misaligned chromosomes importantly, compared to 5% in mock-depleted controls (Figure 6.2C). Similarly, in HeLa cells,

Hsp72 or Nek6 depletion promoted chromosome misalignment in approximately 27% cells compared to 8% of controls (Figure 6.2C). In contrast, Hsp72 or Nek6 depletion did not cause any significant increase in misaligned chromosomes in the non-cancer derived cells lines, RPE1 and HBL-100 (Figure 6.2C). Hence, both Hsp70 inhibition and depletion of Hsp72 or Nek6 suggest that the Nek6-Hsp72 pathway is essential for chromosome congression in cancer but not non-cancer derived cells.

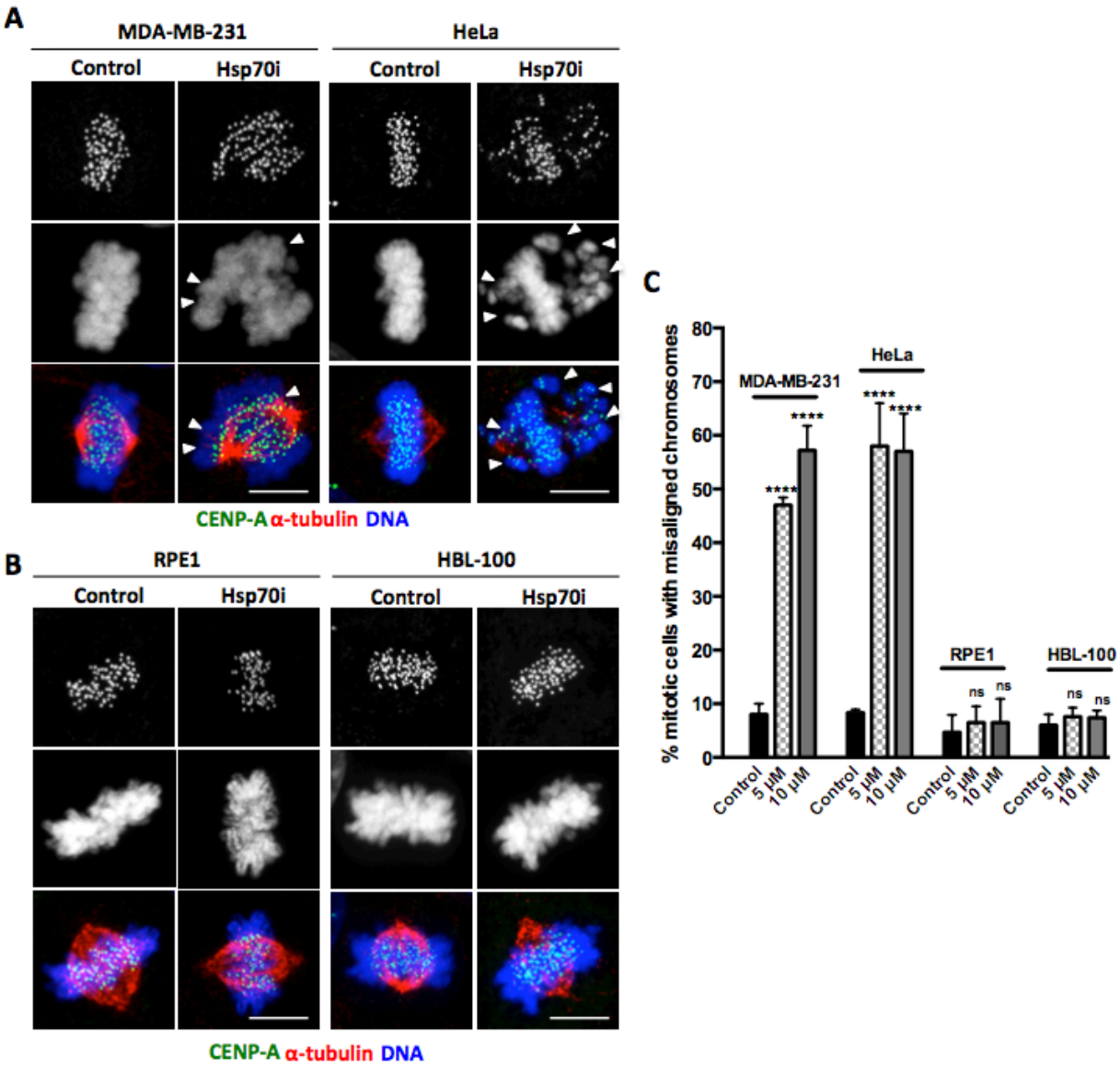

Figure 6.1. Hsp70 inhibition leads to chromosome misalignment only in cancer cells

A, B. Cells as indicated were treated with DMSO (control) or 10 μM Hsp70 inhibitor for 4 hours. Cells were stained with CENP-A (green) and α-tubulin (red) antibodies. Merged panels include DNA (blue) staining with Hoechst 33258. White arrowheads indicate misaligned chromosomes. Scale bar, 5 μm. **C.** Histogram represents the percentage of mitotic cells with chromosome misalignment in each cell line treated with Hsp70i at the dose indicated. Data show means ± S.D. of three experiments. 50 mitotic cells were counted per experiment.

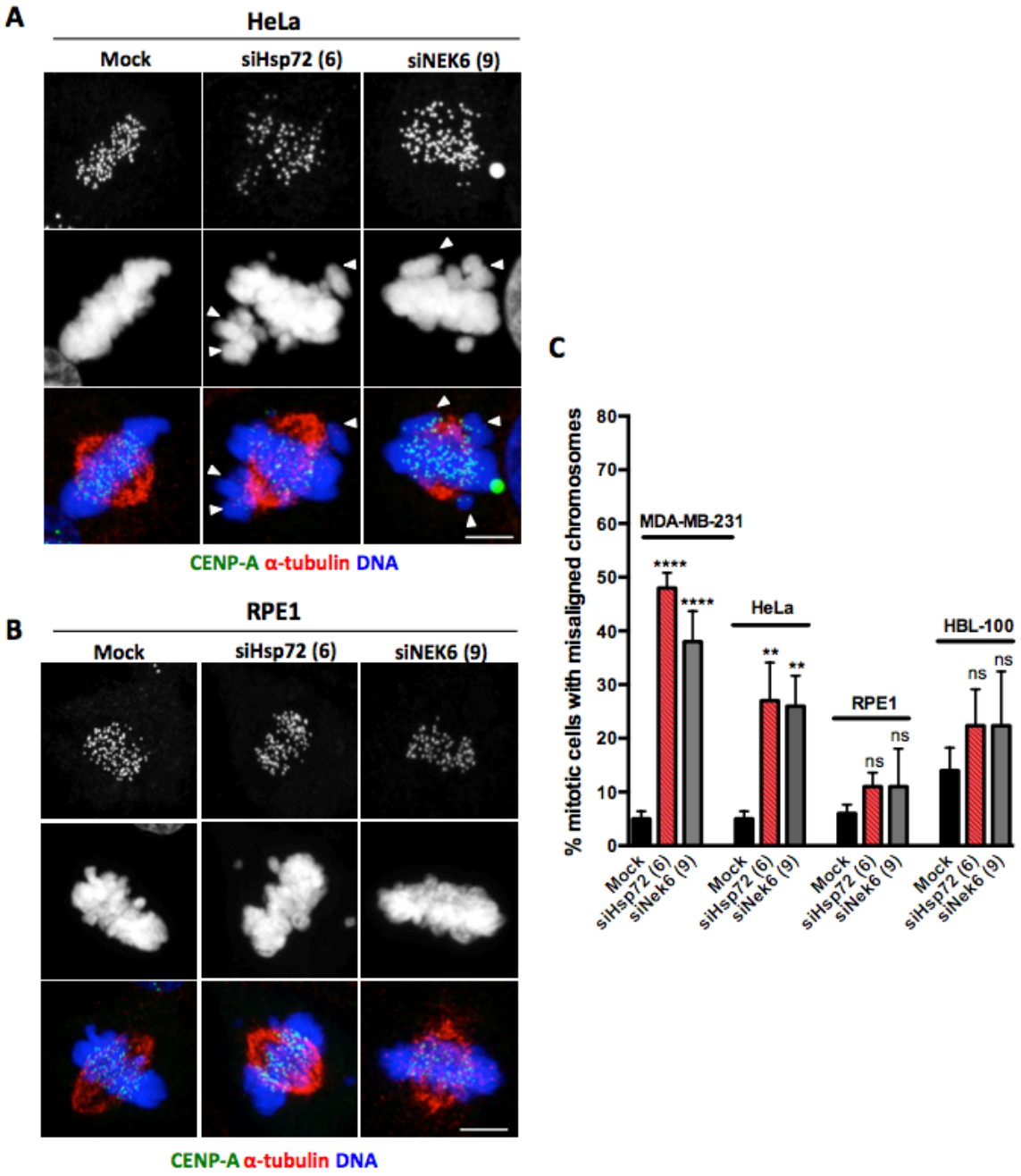

Figure 6.2. Loss of Hsp72 or Nek6 leads to chromosome misalignment only in cancer cells

A, B. HeLa and RPE1 cells were mock-transfected or transfected with the siRNAs indicated to deplete Hsp72 or Nek6 for 72 hours. Cells were stained with CENP-A (green) and α-tubulin (red) antibodies. Merged panels include DNA (blue) staining with Hoechst 33258. White arrowheads indicate misalignment chromosomes. Scale bar, 5 µm. **C.** Histogram represents the percentage of mitotic cells with misaligned chromosomes in each cell line. Data show means ± S.D. of three experiments. 50 mitotic cells were counted per experiment.

6.2.2 Loss of Hsp70 activity induces mitotic arrest in cancer, but not in healthy cells

In addition to studying chromosome congression, we also examined mitotic progression in cancer and non-cancer derived cell lines after Hsp70 inhibition. Using phospho-histone H3 (pHH3) antibodies, we observed a significant percentage of MDA-MB-231 and HeLa cells arrested in mitosis, but not RPE1 or HBL-100 cells (Figure 6.3A-B). In the MDA-MB-231 cell line, Hsp70 inhibition at 5 and 10 μM led to 14% and 12%, respectively, of mitotic cells compared to 8% of controls (Figure 6.3A-B). Similarly, 5 and 10 μM of Hsp70 inhibitor induced mitotic arrest of approximately 12% HeLa cells compared to 6% in controls (Figure 6.3A-B). In sharp contrast, Hsp70 inhibition did not block mitotic progression in RPE1 and HBL-100 cells (Figure 6.3A-B). Furthermore, time-lapse imaging of RPE1 cells incubated with the SiR-tubulin probe revealed no significant change in mitotic duration (mean approximately 93 minutes) upon treatment with either Hsp70 inhibition or Hsp72 depletion (Figure 6.4A-C). Hence, our data indicate that Hsp72 is required for mitotic progression in cancer but not in non-cancer derived cells.

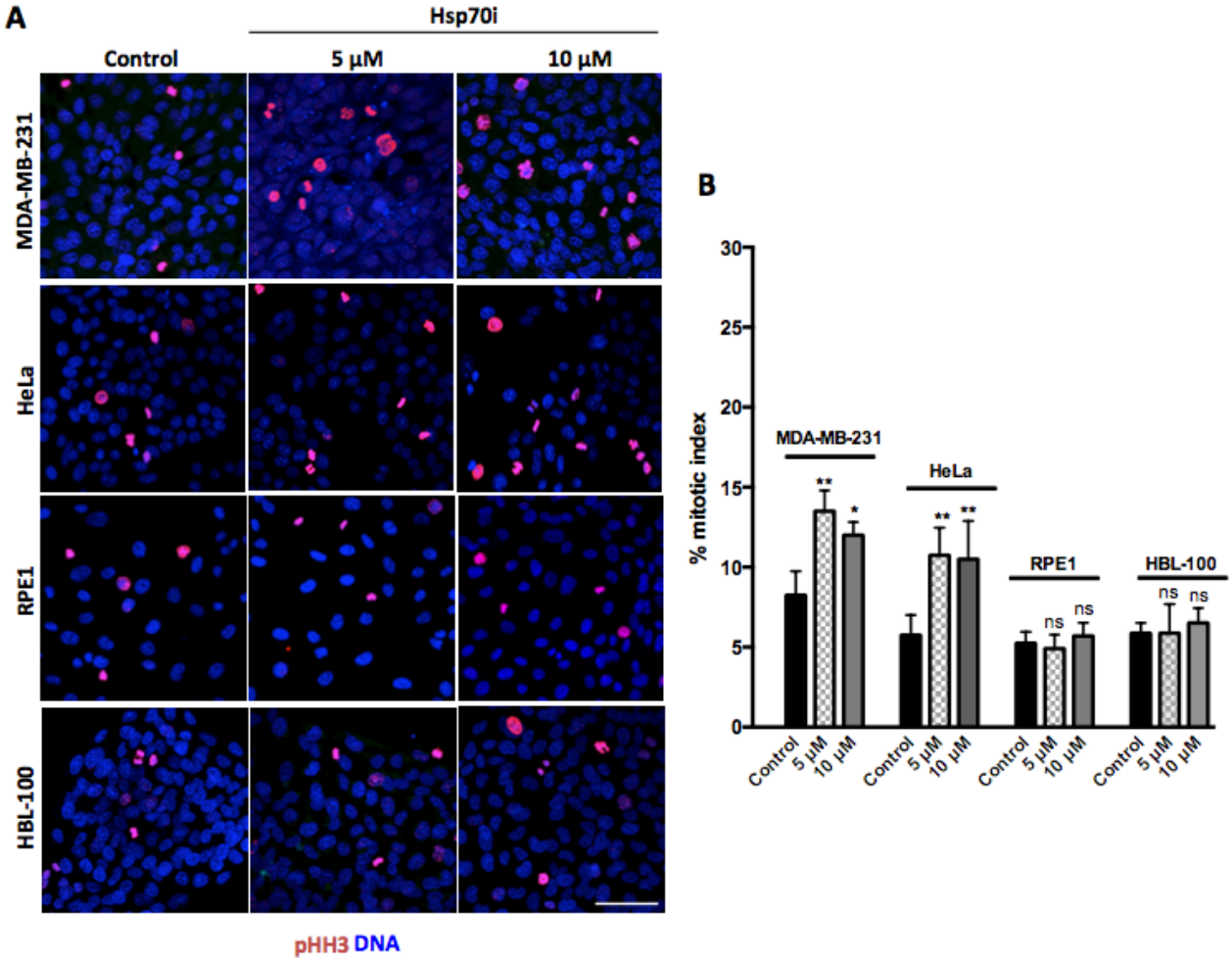

Figure 6.3. Hsp70 inhibition induces mitotic arrest in cancer but not in non-cancer derived cells

A. MDA-MB-231, HeLa, RPE1 and HBL-100 cells were treated with 5 or 10 µM Hsp70i for 4 hours. Cells were fixed and stained with phospho-histone H3 (pHH3, red) and DNA (blue). Scale bar, 50 µm. **B.** The histogram shows the mitotic index upon Hsp70i treatment at the dose indicated based on imaging as shown in A. Data represent means ± S.D.; n=4, >400 cells.

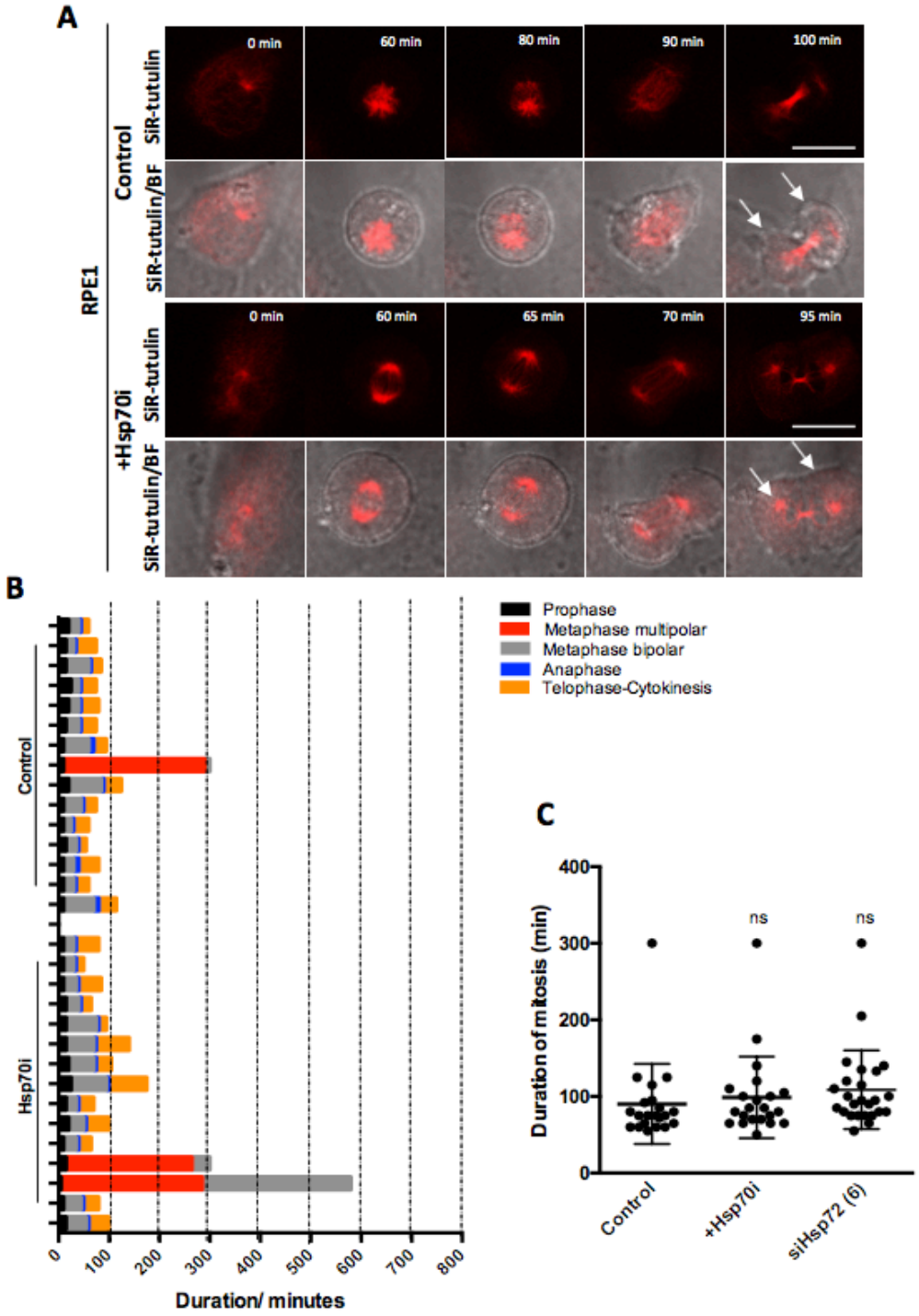

Figure 6.4. RPE1 cells complete mitosis at the same rate in the presence or absence of Hsp72

A. RPE1 cells were incubated with SiR-tubulin for 7 hours prior to time-lapse imaging in the presence or absence of Hsp70 inhibitor. Still images are shown of SiR-tubulin alone (top rows) and merged with brightfield (BF; bottom rows) at the times indicated. Arrows indicate daughter cells following division. Scale bar, 20 µm. **B.** Time-lapse imaging was used to follow cells in mitosis in the absence or presence of Hsp70i. Each bar is representative of a single cell with the time spent in each stage of mitosis indicated. **C.** Dot plot shows the time spent in mitosis in control, Hsp70i treated cells or cells depleted of Hsp72. Data are the means ± S.D. of two experiments. At least 15 mitotic cells were counted per experiment.

6.2.3 Hsp72 is expressed at low levels in non-cancer derived cell lines

Members of the Hsp70 family are differentially expressed in cancer and non-cancer derived cell lines (Rodhe et al., 2005). Using immunofluorescence microscopy, we examined the localisation of the two major Hsp70 isoforms, Hsp72 and Hsc70 proteins, in the cancer MDA-MB-231 and non-cancer derived RPE1 cell lines. Asynchronous cells were fixed and stained with antibodies against Hsp72 or Hsc70 and α-tubulin. Examination of Hsp72 in MDA-MB-231 cells revealed strong localisation at spindle poles in mitotic cells and the midbody in cytokinesis, but no distinct localisation in interphase MDA-MB-231 cells (Figure 6.5). On the other hand, Hsc70 antibodies weakly decorated the spindle poles throughout mitosis, and the centrosomes in interphase of MDA-MB-231 cells (Figure 6.6). Interestingly, in RPE1 cells, Hsp72 was not detected at spindle poles at any stage of mitosis and did not detect specific structures in interphase (Figure 6.7), whereas Hsc70 weakly localised the interphase centrosome, mitotic spindle poles and the midbody in cytokinesis (Figure 6.8). Our data suggest a strong localisation of Hsp72 at spindle poles in cancer-derived MDA-MB-231 cells, but not non-cancer derived RPE1 cells, whereas Hsc70 weakly localised to spindle poles and interphase centrosomes in both cell lines.

In line with these observations, western blotting analysis revealed that the non-cancer derived RPE1 and HBL-100 cell lines exhibited lower expression levels of Hsp72 compared to the cancer cell lines, MDA-MB-231 and HeLa (Figure 6.9A-B). On the other hand, the expression levels of Hsc70 were similar in both cancer and non-cancer derived cell lines. The expression of Nek6 kinase was similar in all cell lines. In addition, we examined the expression pattern of these proteins in acute lymphoblastic leukaemia (ALL) and peripheral-B lymphocytes (PBL) cell lines. The majority of ALL cell lines had high Hsp72 expression, whereas PBL cell lines expressed less Hsp72 (Figure 6.10A-B). Hsc70 was expressed at a similar level in all cells. Similarly, both ALL and PBL cell lines exhibited similar expression levels of Nek6

kinase (Figure 6.10A-B). Hence, the stress-inducible Hsp72 isoform was expressed in the majority of cancer but not non-cancer derived cell lines, whereas Hsc70 and Nek6 expression levels were expressed at similar levels across all cell lines.

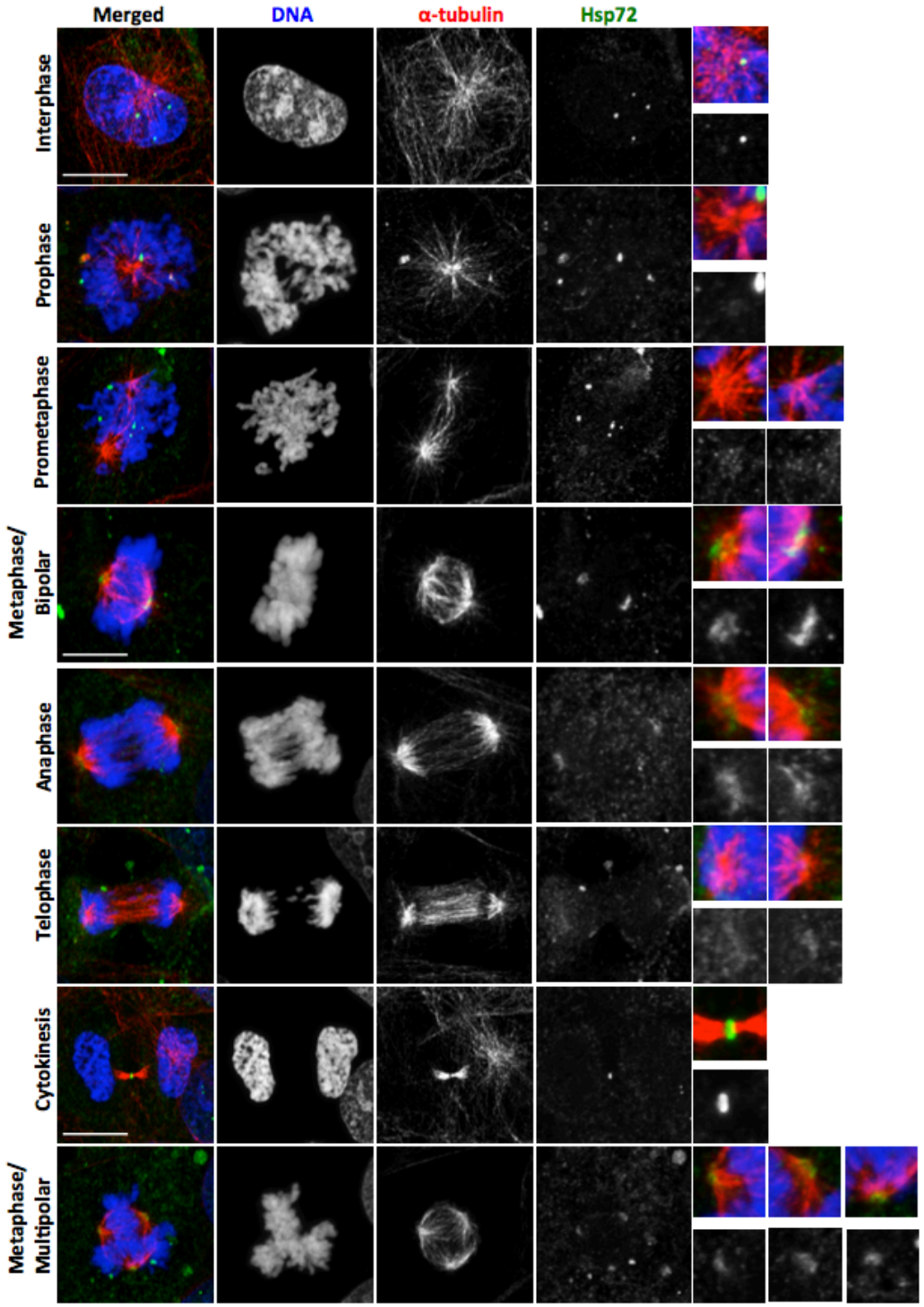

Figure 6.5. Hsp72 localises at metaphase spindle poles and the midbody in MDA-MB-231 cells

MDA-MB-231 cells were pre-extracted for 30 sec with PTMEH buffer and fixed with methanol before staining. Cells were stained with antibodies against Hsp72 (green) and α-tubulin (red). Merged panels include DNA (blue) staining with Hoechst 33258. Metaphase, scale bar, 5 µm. Interphase, cytokinesis, scale bar, 10 µm.

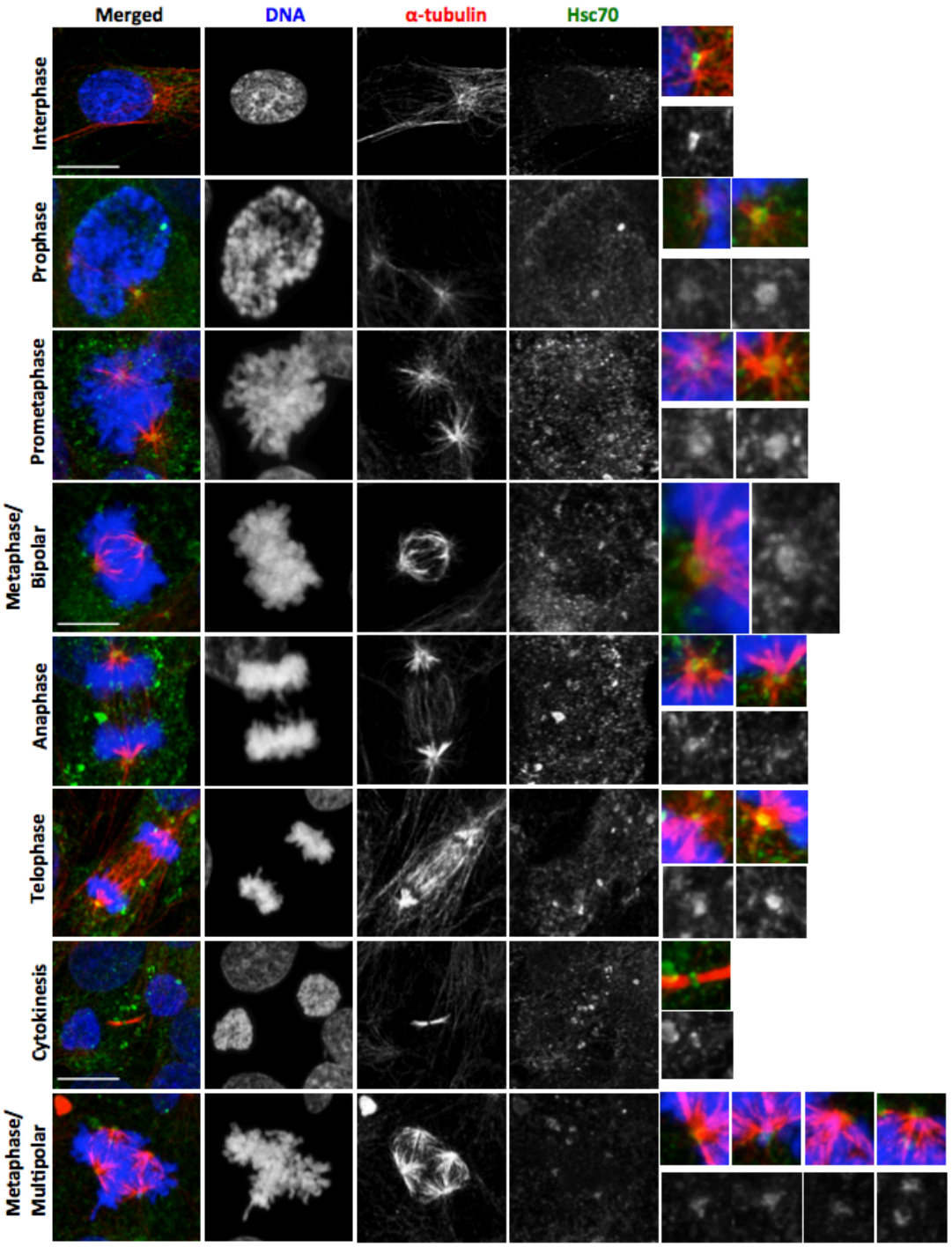

Figure 6.6. Hsc70 localises at spindle poles and the midbody in MDA-MB-231 cells

MDA-MB-231 cells were pre-extracted for 30 sec with PTMEH buffer and then fixed with methanol before staining. Cells were stained with antibodies against Hsc70 (green) and α-tubulin (red). Merged panels include DNA (blue) staining with Hoechst 33258. Metaphase, scale bar, 5 µm. Interphase, cytokinesis, scale bar, 10 µm.

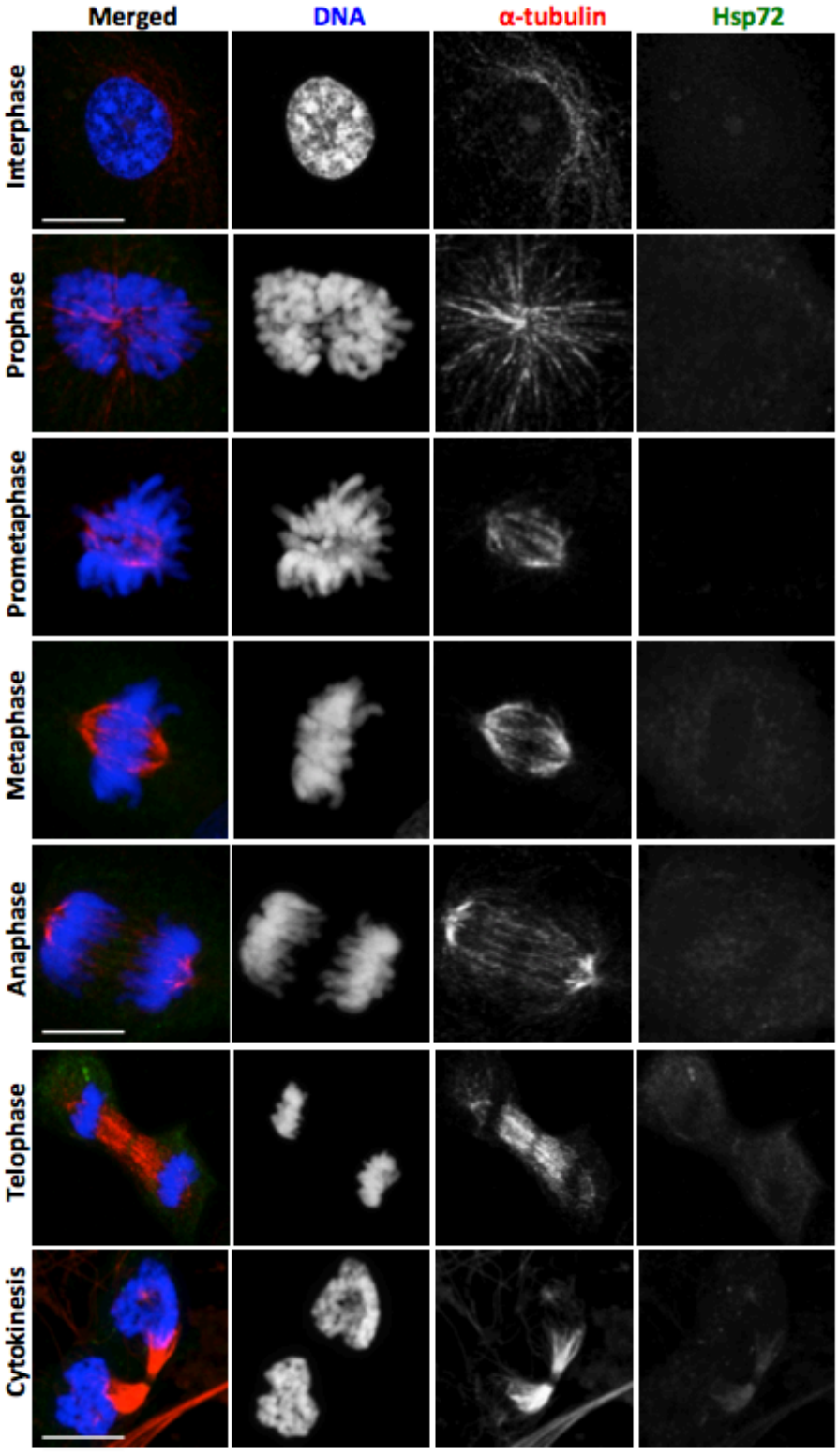

Figure 6.7. Hsp72 localisation is not detected in RPE1 cells

Asynchronous RPE1 cells were pre-extracted for 30 sec with PTMEH buffer, fixed with methanol and stained with Hsp72 (green) and α-tubulin (red) antibodies. Merged panels include DNA (blue) staining with Hoechst 33258. Interphase, cytokinesis, scale bar, 10 µm. Anaphase, scale bar, 5 µm

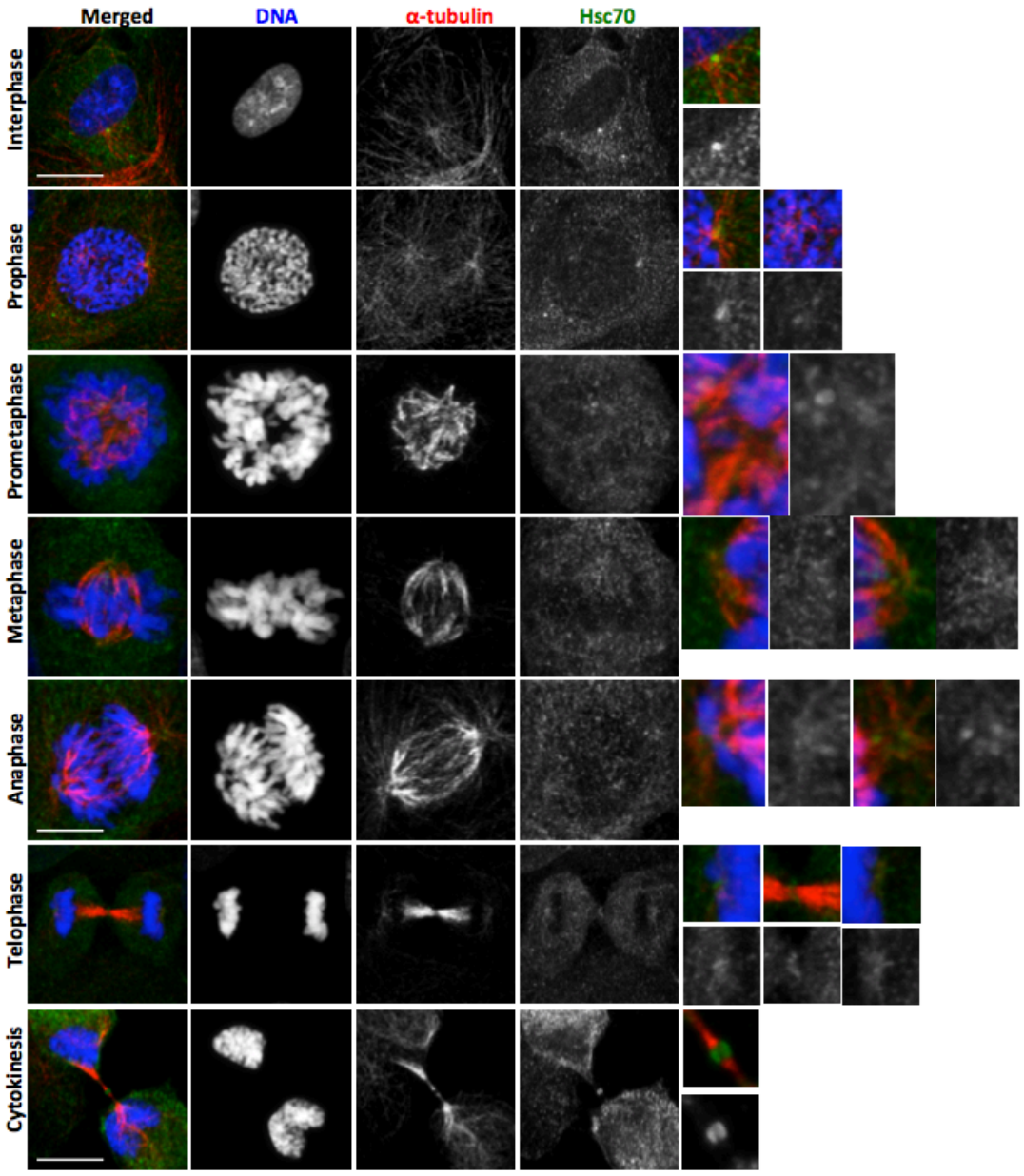

Figure 6.8. Localisation of Hsc70 to spindle poles and the midbody in RPE1 cells

Asynchronous RPE1 cells were pre-extracted for 30 sec with PTMEH buffer, fixed and stained with Hsc70 (green) and α-tubulin (red) antibodies. Merged panels include DNA (blue) staining with Hoechst 33258. Interphase, cytokinesis images; scale bar, 10 µm. Anaphase, scale bar, 5 µm.

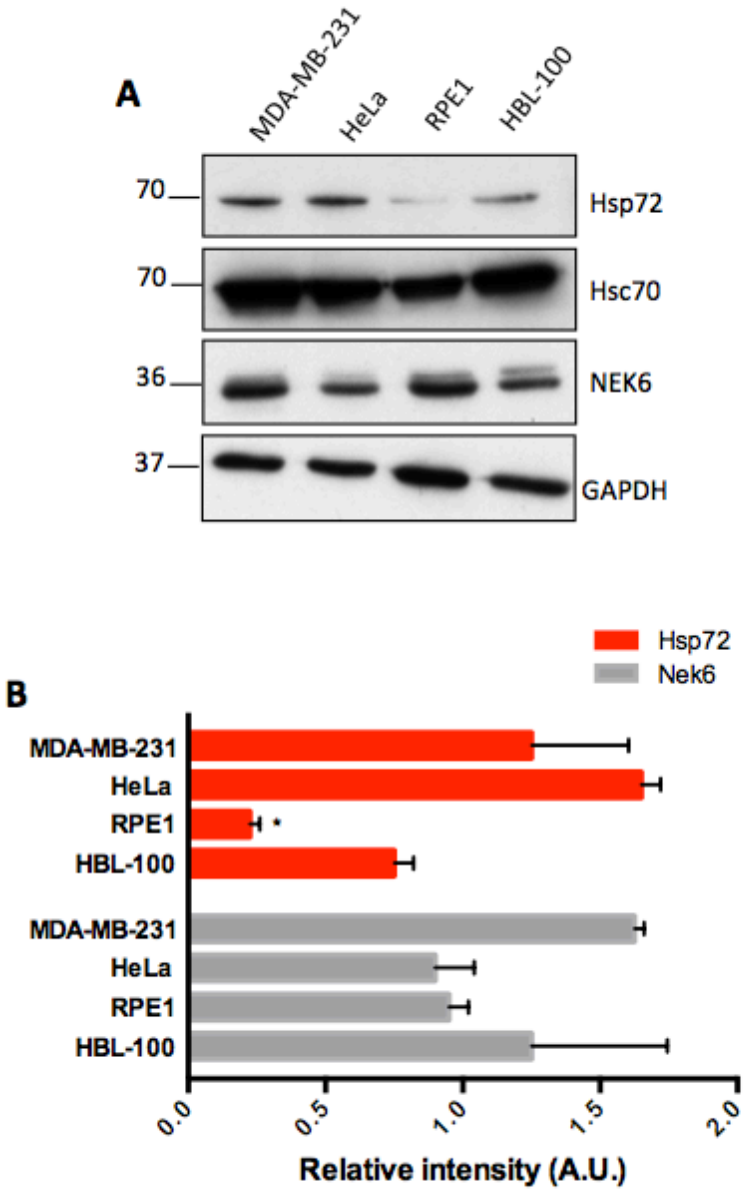

Figure 6.9. Reduced expression of Hsp72 in RPE1 and HBL-100 cells

A. Asynchronous cells, as indicated, were lysed and analysed by SDS-PAGE and Western blotting for Hsp72, Hsc70, Nek6 and GAPDH. **B.** The protein expression of Hsp72 and Nek6 was determined relative to GAPDH for each cell line from A. Experiment repeated twice. *$p<0.05$.

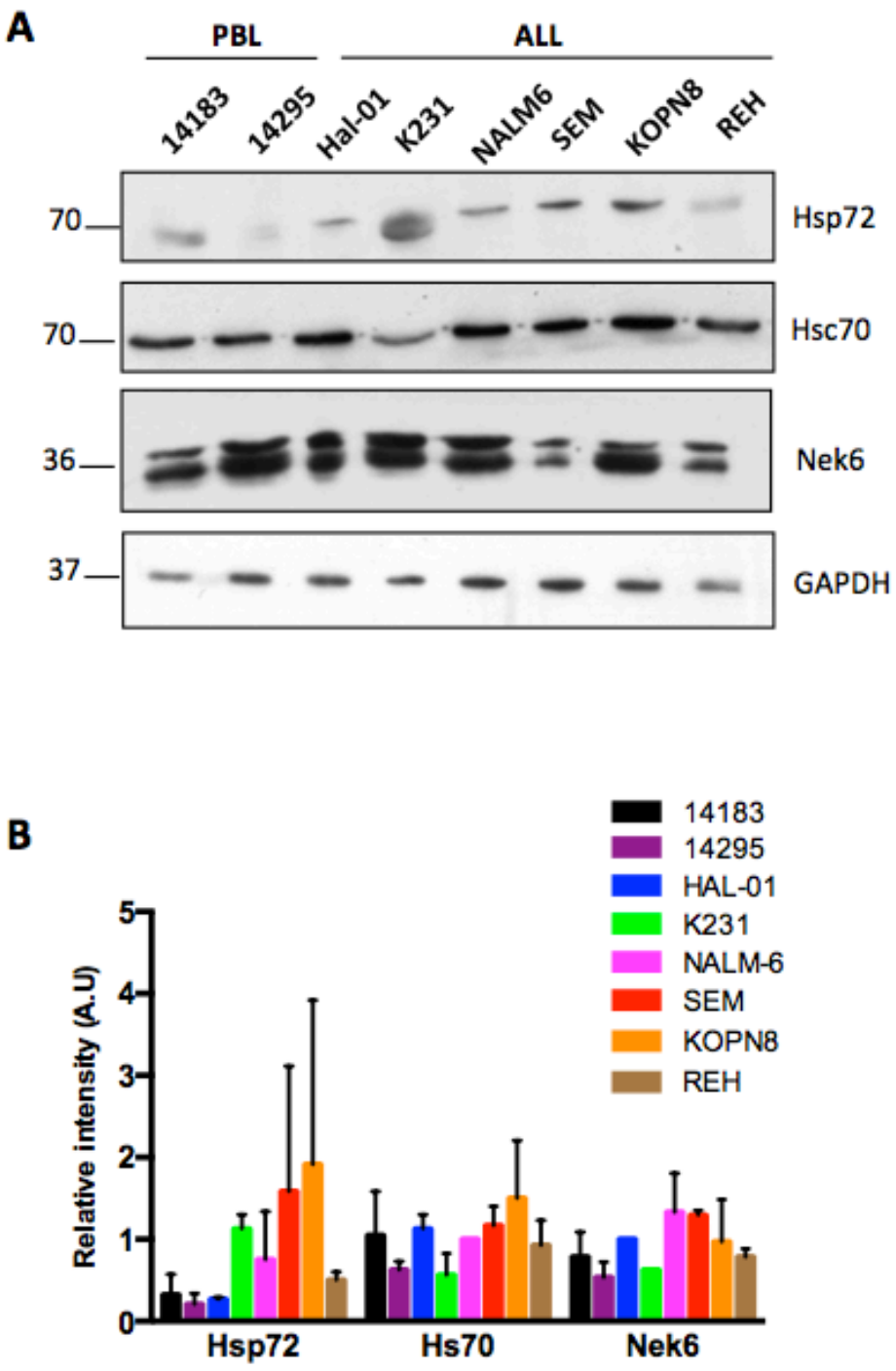

Figure 6.10. Reduced expression of Hsp72 in PBL versus ALL cells

A. Peripheral B-lymphocytes (PBL) and acute lymphoblastic leukemia (ALL) cells were lysed and analysed by SDS-PAGE and Western blotting with the antibodies indicated. Molecular weights are shown in kDa. **B.** Histogram shows the relative intensity (A.U.) of bands in each cell with the antibodies indicated and measured using ImageJ. Data from two independent experiments.

6.2.4 Hsp70 inhibition does not alter Hsp72 localisation to mitotic spindle in cancer cells

Hsp70 inhibitor, VER-155008, has been shown to be highly selective against Hsp70 family rather the Hsp90. Specifically, VER-155008 targets Hsp72 with IC_{50} 0.5 μM and Hsc70 with IC_{50} 2.6 μM (Massey et al., 2010). In Chapter 5, we showed that the Hsp70 inhibitor disrupts the localisation of pHsp72-T66 from spindle poles and at kinetochores in MDA-MB-231 cells. We therefore wished to examine how the Hsp70 inhibitor affects the localisation and expression of the specific Hsp72 and Hsc70 isoforms in cancer MDA-MB-231 cells. In the presence of the Hsp70 inhibitor, there were no detectable change of Hsp72 localisation at spindle poles and the midbody in MDA-MB-231 cells (Figure 6.11). Similarly, the localisation of Hsc70 at spindle poles did not alter upon Hsp70 inhibition in MDA-MB-231 cells (Figure 6.12). Western blotting revealed no change in the total expression of either Hsp72 or Hsc70 upon Hsp70 inhibition in either MDA-MB-231 or RPE1 cells (Figure 6.13A-B). Hence, our results suggest that Hsp70 inhibition does not affect the localisation or expression of total Hsp72 or Hsc70.

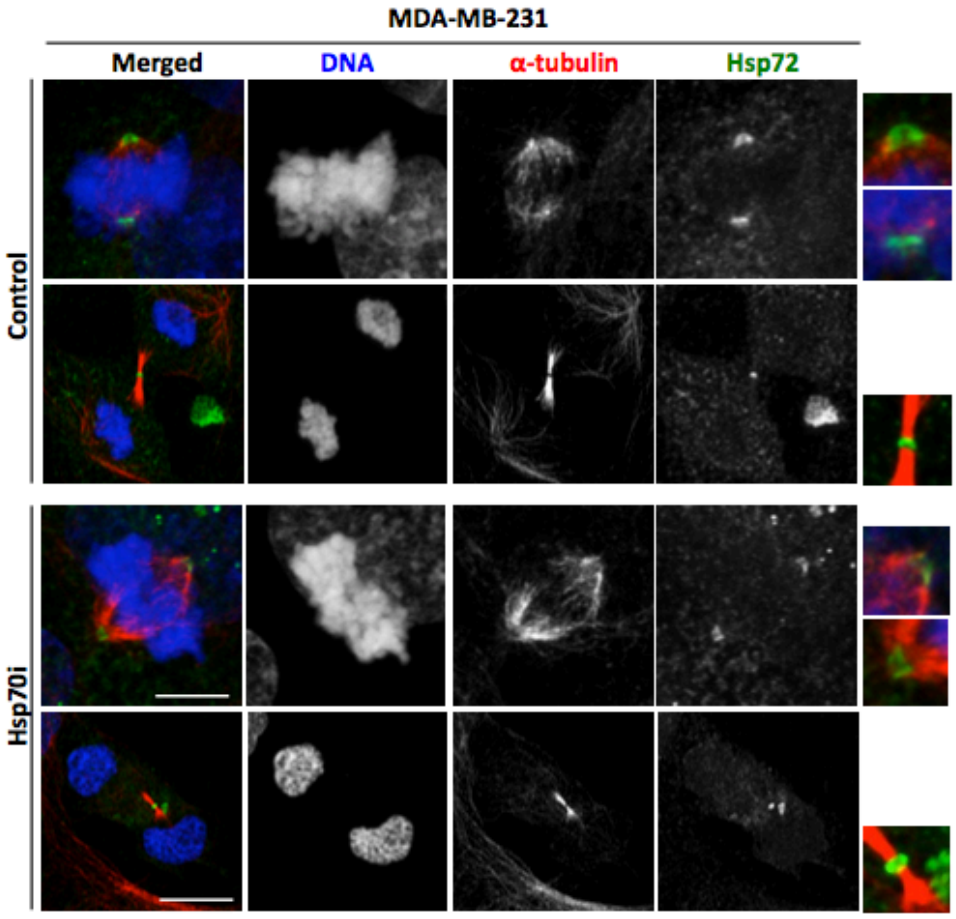

Figure 6.11. Hsp70 inhibition does not alter Hsp72 localisation in MDA-MB-231 cells

MDA-MB 231 cells were untreated (control) or treated with 10 µM Hsp70 inhibitor for 4 hours. After treatment, cells were pre-extracted with PTMEH buffer fixed and stained with Hsp72 (green) and α-tubulin (red) antibodies. Merged panels include DNA (blue) staining with Hoechst 33258. Metaphase images, scale bar, 5 µm. Cytokinesis images, scale bar, 7.5 µm.

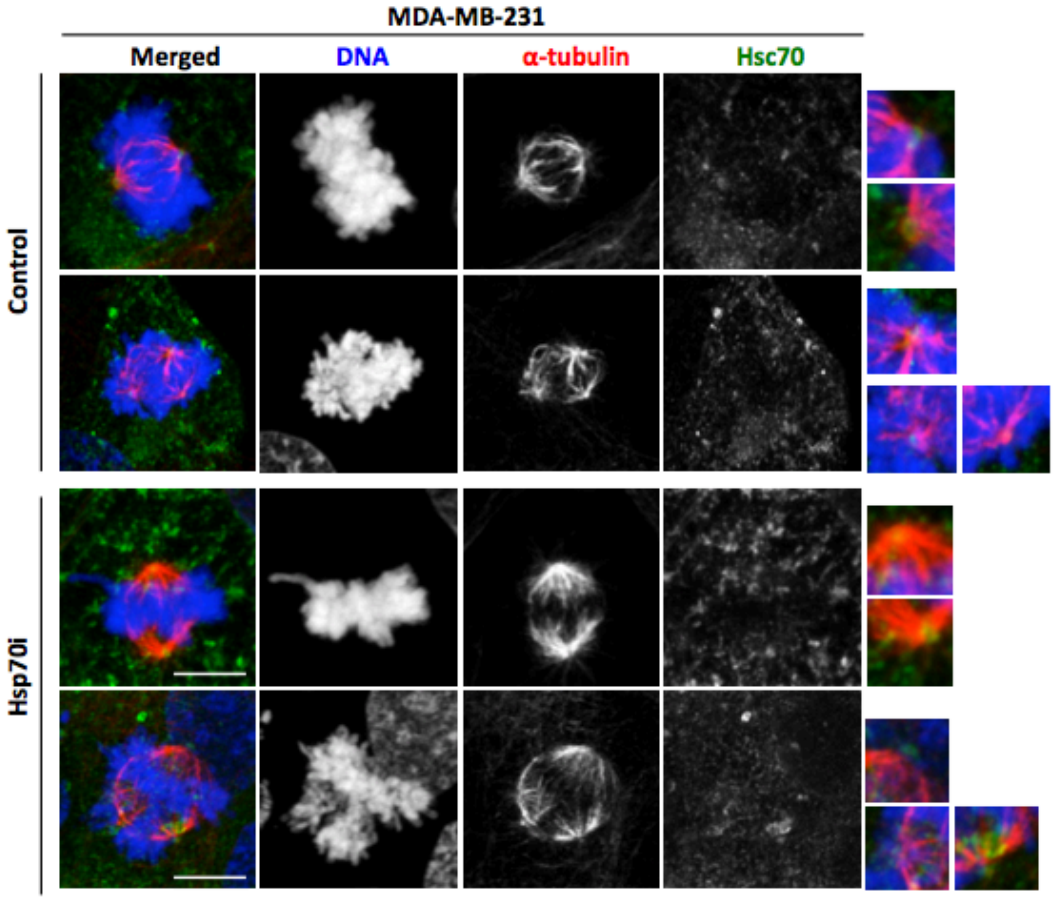

Figure 6.12. Hsp70 inhibition does not alter Hsc70 localisation in MDA-MB-231 cells

MDA-MB-231 were untreated (control) or treated with Hsp70 inhibitor, 5 or 10 µM, for 4 hours. After treatment, cells were pre-extracted with PTMEH buffer fixed and stained with Hsc70 (green) and α-tubulin (red) antibodies. Merged panels include DNA (blue) staining with Hoechst. Metaphase images, scale bar, 5 µm. Multipolar images, scale bar, 7.5 µm.

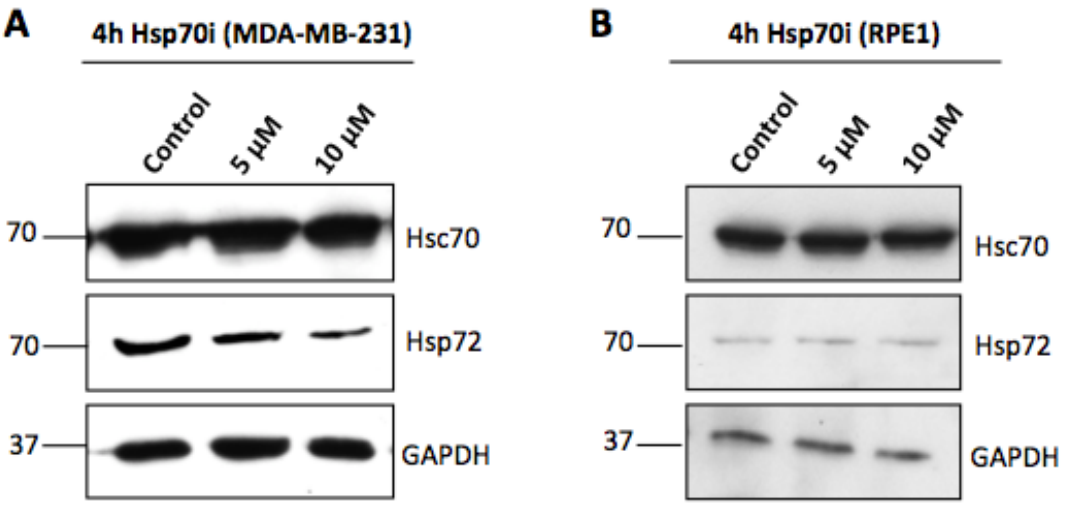

Figure 6.13. Hsp70 inhibition does not change Hsp72 or Hsc70 expression in MDA-MB-231 or RPE1 cell lines

A, B. Asynchronous cells were untreated (control) or treated with 5 or 10 µM Hsp70 inhibitor for 4 hours, lysed and analysed by SDS-PAGE and Western blotting for Hsc70, Hsp72 and GAPDH. Molecular weights are indicated in kDa.

6.3 Discussion

Chromosomal instability (CIN) is one of the main characteristics of a cancer cell. This arises from abnormal segregation of chromosomes during mitosis, one cause of which is the presence of extra centrosomes (McBride et al., 2015). Cancer cells have mechanisms that prevent formation of lethal multipolar spindles in the presence of amplified centrosomes and overcome the errors that occur in chromosome capture during mitosis, thus allowing their survival (Janssen and Medema, 2011). In the previous chapters, we identified a role for the Nek6-Hsp72 pathway in centrosome clustering possibly via regulation of the dynein/dynactin complex in cancer cells. In this chapter, we specifically asked whether the Nek6-Hsp72 pathway was required for mitotic progression in healthy cells.

Excitingly, we found that loss of Nek6 or Hsp72 activity induces errors in chromosome segregation in cancer cells, but not in healthy cell lines. Additionally, Hsp70 inhibition led to a substantial increase of mitotic index in cancer, but not in healthy cell lines. Using time-lapse imaging, we confirmed that Hsp70 inhibition does not affect the mitotic progression or chromosome segregation in non-cancer derived RPE1 cells. In our lab, we recently showed the importance of Nek6-Hsp72 pathway in mitotic progression via ch-TOG/TACC3 complex in cancer cells (O'Regan et al., 2015). In line with our results, previous findings suggest the specific importance of Nek6 kinase in cancer, but not in normal, fibroblast cells (Nassirpour et al., 2010). Furthermore, silencing of Hsc70 and Hsp72 proteins inhibited cell proliferation and activated apoptosis in cancer cell lines, while this dual silencing did not affect proliferation in healthy cell lines (Powers et al., 2008). We therefore suggest that cancer cells depend heavily on the Nek6-Hsp72 pathway for mitotic progression, whereas healthy cells have a much reduced requirement for this pathway.

It is known that Nek6 and Hsp72 proteins are overexpressed in cancers compared to healthy tissue (Powers et al., 2010; Nassirpour et al., 2010). Here, we showed that

the stress-inducible Hsp72 is highly expressed in the majority of cancer lines tested, including acute lymphoblastic leukaemia (ALL) cell lines. Similarly, studies have shown that Hsp72 is frequently overexpressed in various high-grade malignant tumours including osteosarcoma, breast and leukaemia (Garrido et al., 2006; Ray et al., 2004; Santarosa et al., 1997). On the other hand, western blot analysis showed that Hsc70 and Nek6 proteins were expressed at similar levels in both healthy and cancer cell lines. These findings are consistent with the notion that Hsc70 acts as a housekeeping protein and is ubiquitously expressed in most tissues, whereas Hsp72 is expressed at low levels in non-stressed conditions (Daugaard et al., 2010). In line with the previous results showed in this project, we suggest that the increased levels of Hsp72 in cancer versus healthy cells and the essential role of the Nek6-Hsp72 pathway in mitotic progression and centrosome clustering provide strong justification for these to be considered for targeted therapies.

Interestingly, Hsp70 inhibition did not alter the localisation of either the total Hsp72 or Hsc70 in cancer cells. Previous studies have shown that the Hsp70 inhibitor, known as VER-155008, is highly selective against Hsp70 isoforms, specifically Hsp72 and Hsc70, but not for Hsp90 chaperones (Massey et al., 2009). Surprisingly, we previously observed that Hsp70 inhibition disrupts localisation of pHsp72-T66, but not the total Hsp72 or Hsc70 proteins. It is known that Hsp70 inhibition reduces the expression of CRAF and ERBB2 proteins (Powers et al., 2008), however there is no information for down-regulation of other proteins. In this chapter, we explored another specific aspect of the Nek6-Hsp72 pathway, which is found to be important for mitotic progression of cancer cells, but not in non-cancer derived cells. This provides a potential patient-benefit in targeting the Nek6-Hsp72 pathway as both proteins are overexpressed in cancer, but not in healthy cells.

Chapter 7

Discussion

7.1 Discussion

The majority of solid and haematological malignancies possess abnormal numbers of centrosomes, usually being more than two (Nigg, 2002; Kramer et al., 2005; Godinho and Pellman, 2014). Often these cancers with amplified centrosomes also exhibit aneuploidy and chromosomal instability (Ganem et al., 2009; Godinho and Pellman, 2014). Centrosome amplification is also associated with poor prognosis and frequently detected in high-grade metastatic cancers (Denu et al., 2016). It is likely that the genetic heterogeneity seen in tumours may also result in part from the increased chromosomal instability that is induced by centrosome amplification (McBride et al., 2015).

The presence of amplified centrosomes leads to formation of multipolar spindles that would be expected to promote cell death. However, cancer cells overcome this and survive by clustering their extra centrosomes in two poles forming a pseudo-bipolar spindle (Gergely and Basto, 2008; Marthiens et al., 2012). Microtubule-based processes contribute heavily to centrosome clustering with motor protein activity, microtubule attachments to the centrosome, chromosomes and cell cortex, and microtubule dynamics are involved (Kwon et al., 2008; Leber et al., 2010; Marthiens et al., 2012). In addition to these processes, the spindle assembly checkpoint (SAC) aids centrosome clustering by delaying anaphase onset until chromosome congression is complete, providing extra time for centrosome clustering (Odgen et al., 2012; Leber et al., 2010). In this study, we have confirmed that the MDA-MB-231 and NIE-115 cell lines, which possess amplified centrosomes, can cluster their extra centrosomes during mitosis. Interestingly, the majority of acute lymphoblastic leukaemia (ALL) cell lines and patient samples with chronic lymphoblastic leukaemia (CLL) also exhibit centrosome amplification, although the range of amplification varied between patients. Immunofluorescence microscopy analysis and time-lapse imaging techniques were used to identify a novel molecular pathway for centrosome clustering in these cancer cells.

7.2 Identification of Nek6-Hsp72 as a novel pathway for centrosome clustering

Recent work in our lab had identified a new role for the Nek6 kinase in regulating mitotic progression (O'Regan et al., 2015). Interestingly, Hsp72 was found to be a strong interacting partner and substrate of Nek6 with both proteins necessary for mitotic spindle formation in cancer cells. Further analysis revealed that the Nek6-Hsp72 pathway regulates mitotic spindle formation through the microtubule-associated ch-TOG/TACC3 complex (O'Regan et al., 2015). Having established an essential role for the Nek6-Hsp72 pathway in mitotic progression, we analysed whether these proteins might also regulate centrosome clustering in cancer cells. In this study, siRNA interference and a range of pharmacological inhibitors were used to demonstrate that these proteins were indeed required for clustering of amplified centrosomes in cancer cells. Moreover, we demonstrated that loss of the Nek6-Hsp72 pathway promoted formation of multipolar spindles in acute lymphoblastic leukaemia (ALL) cell lines with amplified centrosomes. The key to this study was the observation that loss of function of either Nek6 or Hsp72 promoted formation of multipolar spindles in various cancer cells with amplified centrosomes. Hence, we suggest that Nek6-Hsp72 pathway is required not only for mitotic progression, but also for clustering of amplified centrosomes during mitosis in cancer cells.

Upstream of Nek6-Hsp72, there are a number of other known mitotic kinases, including Aurora-A and Plk1, that stimulate Nek6 activation (Belham et al., 2003; Macurek et al., 2008). Inhibition of Aurora-A and Plk1 kinases disrupted Hsp72 and pHsp72-T66 localisation at spindle poles without affecting total Hsp72 expression. This supports and extents our understanding of this novel pathway in centrosome clustering. Importantly, in this cascade of phosphorylation, Aurora-A and Plk1 regulate Nek9, which then in turn activates Nek6 (Belham et al., 2003). It will therefore be important to confirm that loss of the Nek9 kinase has a similar effect as Aurora-A or Plk1 inhibition in terms of both Hsp72 localisation and centrosome clustering. Interestingly, we showed that loss of Nek7 does not affect the localisation

of Hsp72 or centrosome clustering, confirming previous results that Nek6, but not Nek7, mediates Hsp72 phosphorylation (O'Regan et al., 2015). It should be noted that several components of this pathway including Aurora-A, Nek6 and Hsp72 are frequently overexpressed in many cancers (Nassirpour et al., 2010; Garrido et al., 2006), making this pathway amenable to potential therapeutic approaches. Hence, based on our results we present a novel and actionable pathway of Nek6-Hsp72 and upstream activators for promoting centrosome clustering in cancer cells.

7.3 How does the Nek6-Hsp72 pathway promote centrosome clustering?

In order to understand the mechanism used by Nek6-Hsp72 pathway to promote centrosome clustering, we compared the phenotypes generated upon inhibition of this pathway with those generated by a well-known declustering agent, griseofulvin. We observed that inhibition of Hsp70, or depletion of Hsp72 or Nek6, promoted multipolarity with spindle poles that always containing centrioles, whereas griseofulvin induced formation of multipolar spindles that had some poles without centrioles, so called "acentrosomal" poles. This suggests a distinct mechanism of action. Further evidence for this come from experiments that showed the multiple acentrosomal spindle poles that formed upon nocodazole treatment of HeLa cells, which have normal centrosome numbers, clustered efficiently in the presence of the Hsp70 inhibitor upon washout of nocodazole. Hence, these results suggest that inhibition of the Nek6-Hsp72 pathway promotes multipolarity in a different way to griseofulvin in cells with amplified centrosomes.

A number of small molecules have been described as centrosome declustering agents, including griseofulvin, noscapinoids and PARP inhibitors (Rebacz et al., 2007; Karna et al., 2011; Castiel et al., 2011). These agents are thought to work by interfering with microtubule dynamics causing depolymerisation, stabilisation or bundling of microtubules through blocking centrosome clustering and leading to multipolar

mitoses and mitotic catastrophe (Odgen et al., 2012). However, this process, like treatment of cells with taxol, also generates acentrosomal poles. Indeed, griseofulvin has been reported to induce acentrosomal multipolar spindles in various cancer cells (Drosopoulos et al., 2014; Rebacz et al., 2007). The fact that we never saw acentrosomal poles upon loss of Nek6 or Hsp72 activity, suggests that the Nek6-Hsp72 pathway acts through some other mechanism to promote multipolarity in cancer cells with amplified centrosomes.

The role of the Nek6-Hsp72 pathway in assembly and recruitment of the ch-TOG/TACC3 complex suggests that it may be necessary for microtubule to kinetochore attachments and that this could be the mechanism through which it regulates centrosome clustering (O'Regan et al., 2015). A previous study had reported a role for the integrin-linked kinase (ILK) through regulation of the ch-TOG/TACC3 complex (Fielding et al., 2011). However, both we and others found that loss of ch-TOG causes acentrosomal phenotypes (Leber et al., 2010), a phenotype completely different to the one from loss of Hsp72 or Nek6. Hence, our results suggest that the Nek6-Hsp72 pathway is unlikely to promote centrosome clustering purely via regulation of the ch-TOG/TACC3 complex.

Another interesting downstream target of Nek6 is the kinesin motor protein Eg5. Eg5 is a plus-end-directed motor that drives spindle poles apart by crosslinking microtubules in an anti-parallel fashion (Sawin and Mitchison, 1995). Nek6 phosphorylates Eg5 and thus regulates centrosome separation and formation of a bipolar spindle. Consistent with that loss of Nek6 or Nek9 function was shown to result in formation of monopolar spindles, potentially due to the absence of phosphorylation by Eg5 (Bertran et al., 2011; Rapley et al., 2008). Based on these results, it will be interesting to know whether Nek6 alone or the Nek6-Hsp72 pathway potentially promote centrosome clustering via the Eg5 kinesin. This could be directly targeted with Eg5 inhibitors, such as STLC, to determine whether Eg5

plays a role in centrosome clustering and by testing whether Eg5 is also regulated by Hsp72.

7.4 Is dynein/dynactin a target of the Nek6-Hsp72 pathway in centrosome clustering?

Dynein was one of the first proteins found to be required for centrosome clustering in cancer cells (Quintyne et al., 2005). Loss of dynein promoted formation of multipolar spindles only in cells with amplified centrosomes, first indicating an important role for microtubule and microtubule-associated motor proteins (Quintyne et al., 2005). In a subsequent siRNA screen, dynein was again found to be one of they key proteins that regulate centrosome clustering in cancer cells (Leber et al., 2010). However, the molecular mechanism through which dynein promotes centrosome clustering is still unclear. Dynein depletion promotes multipolarity with centrioles in each spindle pole rather than generate of acentrosomal pole, a phenotype similar to that observed upon Nek6 and Hsp72 depletion. This raises the possibility that dynein is a potential target of the Nek6-Hsp72 pathway. Specifically, depletion of Nek6 or Hsp72, or inhibition of Hsp70, led to a reduction in dynein intermediate chain and the dynactin, $p150^{Glued}$ subunit, at spindle poles and kinetochores. We assume these proteins reflect the localisation of the dynein/dynactin holoenzymes, although this needs to be confirmed.

In mitosis, the dynein/dynactin complex is heavily concentrated at spindle poles and kinetochores. This contributes to chromosome congression to the metaphase plate (Yang et al., 2007). Once all chromosomes are properly attached to the microtubules, dynein/dynactin complex inactivates the SAC by removing Mad2 and BubR1 from kinetochores along microtubule towards the spindle poles (Wojcik et al., 2001; Liang et al., 2007). We have shown that phosphorylation by Nek6 is required to localise Hsp72 to the mitotic spindle and that phosphorylated Hsp72 is concentrated at kinetochores and spindle poles. Here, we show that pHsp72-T66 co-

localised with dynein/dynactin at spindle poles and kinetochores. This tight association between pHsp72-T66 and dynein/dynactin at these sites was confirmed by a proximity ligation assay. From a mechanistic perspective, these data suggest that pHsp72-T66 and dynein/dynactin complex could cooperate at kinetochores to ensure proper microtubule-kinetochore attachments. Strikingly, we found that the Nek6-Hsp72 pathway regulates the localisation of dynein, and its partner dynactin, at the mitotic spindle apparatus in cancer cells.

The kinetochore has two important roles during chromosome segregation: first in mediating attachment of chromosomes to the plus ends of spindle microtubules and second activating the SAC in the presence of unattached kinetochores (Foley and Kapoor, 2013). Studies have revealed three distinct layers at kinetochores: the inner kinetochore that attaches to the centromeric chromatin, and the outer kinetochore and fibrous corona where microtubules attach. Many proteins are concentrated within these three regions, many with the aid of microtubule motors (Cheeseman and Desai, 2008). CENP-E, a plus-end directed microtubule motor, and dynein/dynactin, a minus-end directed microtubule motor, both localise to the fibrous corona of the kinetochore, whereas CENP-A and CENP-I are core proteins of the inner kinetochore (Cheeseman and Desai, 2008). Loss of Hsp70 activity did not alter the localisation of CENP-A or CENP-I indicating no effect on inner kinetochore structure. However, we observed partial loss of CENP-E from kinetochores upon Hsp70 inhibition. Additionally, some CENP-E staining was normally detected at spindle poles, but this staining was reduced upon Hsp70 inhibition. Based on these data, we assume that pHsp72-T66 mainly interacts with components of the fibrous corona at kinetochores, but not with inner kinetochore proteins such as CENP-A and CENP-I. Furthermore, we speculate that phosphorylated Hsp72 might be bound at kinetochores by the CENP-E motor, as well as contributing to targeting of CENP-E to spindle pole by dynein. However, further analysis will be necessary to test this hypothesis using interacting studies to identify the direct binding partners of phosphorylated Hsp72 in mitosis.

Taken together, the results of this study have led us to propose a model in which Nek6 and Hsp72 sit at the heart of a pathway with a cascade of upstream components, including Aurora-A, Plk-1 and Nek9, that activate Nek6, and its a number of potential downstream targets, including the dynein/dynactin complex and potentially CENP-E, whose localise to the mitotic spindle apparatus is regulated by Hsp72 (Figure 7.1). This model explains how Nek6 and Hsp72 may contribute to the capture of chromosomes by microtubules during mitosis allowing clustering of amplified centrosomes and formation of a pseudo-bipolar spindle. Dynein is also important in prometaphase for lateral attachment and rapid poleward motion of chromosomes prior to bi-orientation at metaphase and hence, loss of dynein activity leads to misalignment chromosomes (Yang et al., 2007). This is consistent with the misaligned chromosomes observed upon loss of the Nek6-Hsp72 pathway.

Additionally, we used a combination of immunoprecipitation and mass spectrometry to identify mitotic binding partners of dynein, using antibodies against dynein I.C. Reassuringly, in our analysis, we identified the Hsp72 chaperone, as well as the co-chaperone Hsp90. Whether Hsp90 is also required for centrosome clustering is an interesting question to answer. In addition, we isolated a number of cytoskeletal proteins, including tubulin, myosin, actin and various cytoskeletal regulators. This association with tubulin is also reassuring the fact that this is a microtubule-directed motor. A particularly interesting hit was the non-muscle myosin 2 (NM2) family. Moreover MYH9 as this interaction seemed to be most obviously blocked by the Hsp70 inhibitor. The NM2 proteins are important motors involved in regulating cortical actin distribution during cytokinesis and cell migration (Peckham, 2016). The evidence of an interaction between dynein and non-muscle myosins provides another very attractive explanation for their potential roles in centrosome clustering via cortical attachment. Future experiments will be required to test how dynein and NM2 proteins interact and whether this contributes to centrosome clustering given the dependence of this interaction on Hsp70 activity. Interestingly, Myo10 identified as a key motor protein, along with HSET, for centrosome clustering in cancer cells with extra centrosomes (Kwon et al., 2008). Therefore, we speculate that may be

dynein and myosin proteins cooperate at astral microtubules to apply forces and allow centrosome positioning and clustering. Therefore, cortical attachments have a significant role in centrosome clustering mechanisms.

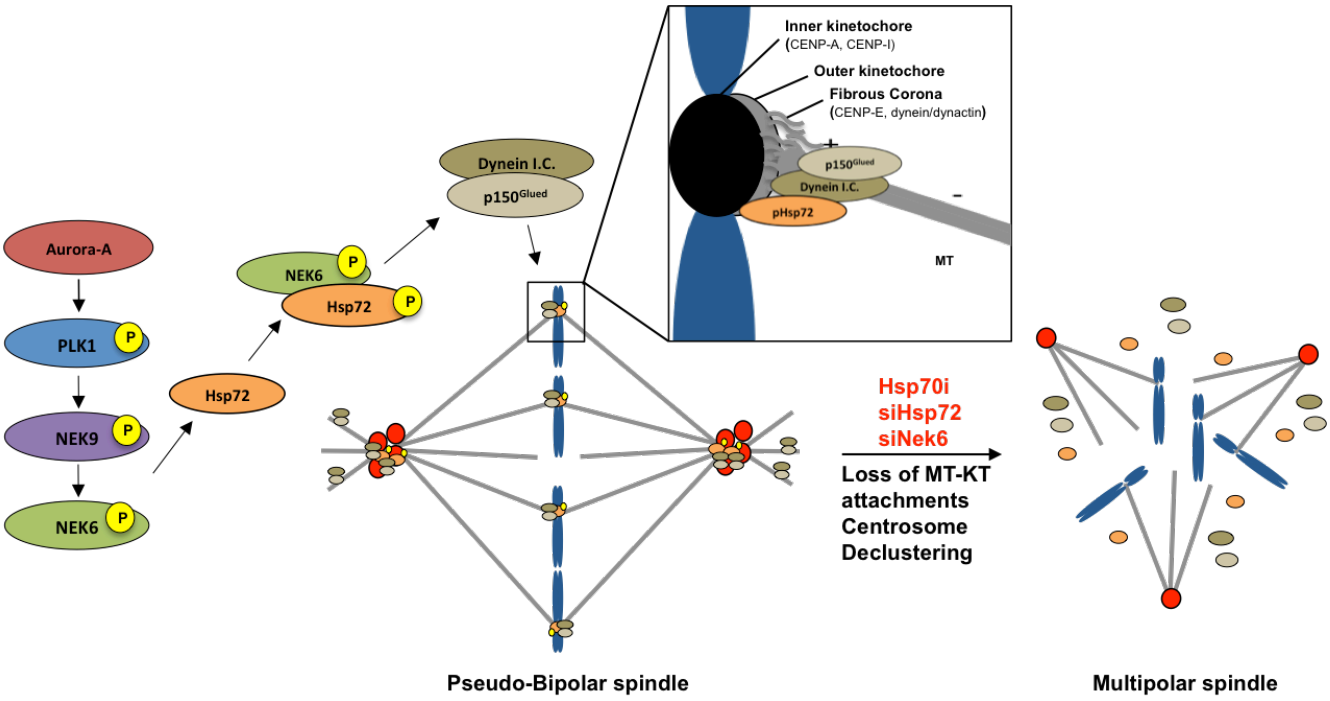

Figure 7.1. A model for the role of Nek6-Hsp72 activity in centrosome clustering

In this model, a cascade of upstream kinases including Aurora-A, Plk-1 and Nek9 activates the Nek6-Hsp72 pathway. Nek6 targets Hsp72 protein to kinetochores and spindle poles, and at the same time Hsp72 recruits the dynein/dynactin complex. A zoomed boxed illustrates the three kinetochore domains, emphasizing the localization of dynein, $p150^{Glued}$ and pHsp72. This interaction favours clustering of centrosomes (red dots) and formation of pseudo-bipolar spindle (centre). Hsp70 inhibition or depletion of Hsp72 or Nek6 results in centrosome declustering and multipolarity (right) with displacement of the dynein/dynactin complex and Hsp72 from the mitotic spindle.

7.5 The Nek6-Hsp72 pathway is required for mitotic progression in cancer but not normal cells

Nek6 and Hsp72 proteins are frequently upregulated in many cancers (Nassirpour et al., 2010; Powers et al., 2010). Hsp72 is a stress-inducible member of the Hsp70 family and is upregulated through the HSF1 transcription factor in response to the proteotoxic stress present in mitotic cancer cells (Hartl et al., 2011). The mechanism between Nek6 upregulation is less clear. Here, we confirmed that Nek6 and Hsp72 activity are essential for chromosome congression and mitotic progression in HeLa and MDA-MB-231 cancer cells. Importantly though, the non-cancer RPE1 and HBL-100 cells exhibited no detectable changes in mitotic progression or chromosome segregation upon loss of the Nek6-Hsp72 pathway. This implies that normal cells have either a reduced or no requirement for the Nek6-Hsp72 for mitotic progression. Indeed, these cell types express very low levels of Hsp72 and Nek6.

An interesting observation is that dynein was more strongly detected on the mitotic spindle apparatus of cancer cells than normal cells. Dynein was also highly expressed in oral cancer cell lines versus normal oral keratinocytes (Quintyne et al., 2005). We hypothesise that healthy cells with normal chromosome and centrosome numbers may require less Hsp72, and subsequently dynein/dynactin, to facilitate spindle organisation during mitosis. It will be interesting to test whether dynein expression correlated with centrosome amplification. Taken together with the potential role of dynein in centrosome clustering, we believe that our results support a direct participation between the Nek6-Hsp72 pathway and dynein complex during mitotic spindle formation and centrosome clustering.

7.6 Future perspectives: targeting of Nek6 for cancer therapy

A major challenge is to identify mechanisms that play an essential role in centrosome clustering but which can be safely inhibited in normal cells. Multipolar spindle can result from perturbation of many different spindle associated proteins, but there are few examples so far of proteins that show selective effects in cancer cells with amplified centrosomes and that are amenable to inhibition with a drug-like molecule. One example is the HSET/KIFC1, a minus end-directed microtubule motor of the kinasin-14 family (Wu et al., 2013). Multipolar spindle formation is induced upon treatment of cancer cells possessing amplified centrosomes with distinct HSET inhibitors (Watts et al., 2013).

The work presented within this thesis identifies the Nek6-Hsp72 pathway as a novel actionable pathway that regulates centrosome clustering in cancer cells. This provides further evidence for its importance in mitotic progression in cancer cells. This pathway involves activation and phosphorylation of Nek6 kinase by upstream proteins, including Aurora-A, Plk1 and Nek9, followed by downstream phosphorylation of Hsp72 and subsequently targeting of dynein/dynactin complex to spindle poles and kinetochores. We proposed that this is regulated to generate spindle tension to allow centrosome clustering in cancer cells. Clearly more work is needed though to determine the mechanisms through which phosphorylated Hsp72 regulates dynein/dynactin in cancer cells.

As cancer cells are constantly under stress, the elevated levels of Hsp72 make this an attractive target in cancer treatment. However, the development of Hsp70 drugs could be challenging for many reasons, not least that it would be difficult to inhibit Hsp72 without inhibiting the other members of the Hsp70 family that have housekeeping functions in protein homeostasis. Drugs against upstream proteins that are more specific to mitosis, such as Nek6, might therefore provide benefit to those cancers with

high Hsp72 expression. From a practical perspective, there are limitations in directly targeting Hsp72. First, Hsp70 family has multiple members with a highly similar structural active site making it difficult to develop a catalytic inhibitor that does not also target other family members. Therefore, measuring cell survival in response to Hsp70 inhibition may not reveal a direct correlation with centrosome number. Second, Hsp70 has a high nucleotide affinity, making it a challenging target for drug development (Powers et al., 2010). On the other hand, Nek6 kinase could be a more attractive target than Hsp72. Significant progress on structural analyses of Nek7 has shown the potential for generating selective inhibitors that target not only the catalytic site but also the allosteric sites required for activation (Haq et al., 2015). The similarity between Nek6 and Nek7 suggests that this could also be tried with Nek6.

Interestingly, pharmacological inhibition of Hsp70 in ALL cell lines promoted significant loss of centrosome clustering with a frequency of multipolar spindles that closely reflected the extent of centrosome amplification. ALL cells represent a good model for a disease that has traditionally been treated with anti-mitotic chemotherapies. However, we haven't explored cell survival after Hsp70 inhibition due to the likely effect on other Hsp70 proteins. Another Hsp70 inhibitor, pifithrin-μ, was demonstrated to exhibit antileukemic effects promoting cell cycle arrest and apoptosis in acute myeloid leukaemia (AML) and acute lymphoblastic leukaemia (ALL) (Kaiser et al., 2011). However, whether these effects were related to a mitotic role of pifithrin-μ was not clear. Since the majority of ALL cells have extra centrosomes, centrosome number could potentially be a valuable and relative easy to measure biomarker in haematological malignancies, including also chronic myeloid leukaemia (CML) and diffuse large B-cell lymphoma (DLBCL) (Kramer et al., 2005). Future work may also identify genetic signatures that identify cells that are particularly sensitive to centrosome de-clustering strategies.

It is surprising how cancer cells with amplified centrosomes are able to cluster them in a bipolar fashion and complete mitosis. However, it is not surprising that it is proteins with functions in microtubule organisation that have roles in centrosome clustering. This study was focused on how the Nek6-Hsp72 pathway favours centrosome clustering and revealed a potential mechanism through the dynein/dynactin complex. Centrosome clustering avoids the lethality of multipolar mitoses while also contributing to chromosomal instability and tumour evolution. There is clearly exciting clinical promise to therapies that prevent centrosome clustering, and that could lead to new targeted agents that are selective for cancer cells with amplified centrosomes.

Chapter 8

Bibliography

8. Bibliography

Abe, M., Manola, J. B., Oh, W. K., Parslow, D. L., George, D. J., Austin, C. L. and Kantoff, P. W. (2004). Plasma levels of heat shock protein 70 in patients with prostate cancer: a potential biomarker for prostate cancer. *Clin Prostate Cancer,* 3(1), pp. 49-53.

Acquaviva, C. and Pines, J. (2006). The anaphase-promoting complex/cyclosome: APC/C. *J Cell Sci,* 119(Pt 12), pp. 2401-4.

Akhmanova, A. and Steinmetz, M. O. (2008). Tracking the ends: a dynamic protein network controls the fate of microtubule tips. *Nat Rev Mol Cell Biol,* 9(4), pp. 309-22.

Akhmanova, A. and Steinmetz, M. O. (2015). Control of microtubule organization and dynamics: two ends in the limelight. *Nat Rev Mol Cell Biol,* 16(12), pp. 711-26.

Alves-Cruzeiro, J. M., Nogales-Cadenas, R. and Pascual-Montano, A. D. (2014). CentrosomeDB: a new generation of the centrosomal proteins database for Human and Drosophila melanogaster. *Nucleic Acids Res,* 42(Database issue), pp. D430-6.

Arquint, C., Gabryjonczyk, A. M. and Nigg, E. A. (2014). Centrosomes as signalling centres. *Philos Trans R Soc Lond B Biol Sci,* 369(1650).

Arquint C, Sonnen KF, Stierhof YD, Nigg EA. (2012). Cell-cycle-regulated expression of STIL controls centriole number in human cells. *J Cell Sci*.125 (Pt 5):1342-52.

Asghar, U., Witkiewicz, A. K., Turner, N. C., & Knudsen, E. S. (2015). The history and future of targeting cyclin-dependent kinases in cancer therapy. *Nature Reviews. Drug Discovery*, *14*(2), 130–146.

Asteriti, I. A., Giubettini, M., Lavia, P. and Guarguaglini, G. (2011). Aurora-A inactivation causes mitotic spindle pole fragmentation by unbalancing microtubule-generated forces. *Mol Cancer,* 10, pp. 131.

Azimzadeh, J., Hergert, P., Delouvee, A., Euteneuer, U., Formstecher, E., Khodjakov, A. and Bornens, M. (2009). hPOC5 is a centrin-binding protein required for assembly of full-length centrioles. *J Cell Biol,* 185(1), pp. 101-14.

Azimzadeh, J., Wong, M. L., Downhour, D. M., Sanchez Alvarado, A. and Marshall, W. F. (2012). Centrosome loss in the evolution of planarians. *Science,* 335(6067), pp. 461-3.

Bader, J. R. and Vaughan, K. T. (2010). Dynein at the kinetochore: Timing, Interactions and Functions. *Semin Cell Dev Biol,* 21(3), pp. 269-75.

Bahe, S., Stierhof, Y. D., Wilkinson, C. J., Leiss, F. and Nigg, E. A. (2005). Rootletin forms centriole-associated filaments and functions in centrosome cohesion. *J Cell Biol,* 171(1), pp. 27-33.

Bahmanyar, S., Kaplan, D. D., Deluca, J. G., Giddings, T. H., Jr., O'Toole, E. T., Winey, M., Salmon, E. D., Casey, P. J., Nelson, W. J. and Barth, A. I. (2008). beta-Catenin is a Nek2 substrate involved in centrosome separation. *Genes Dev,* 22(1), pp. 91-105.

Balch, W. E., Morimoto, R. I., Dillin, A. and Kelly, J. W. (2008). Adapting proteostasis for disease intervention. *Science,* 319(5865), pp. 916-9.

Barboro, P., Ferrari, N. and Balbi, C. (2014). Emerging roles of heterogeneous nuclear ribonucleoprotein K (hnRNP K) in cancer progression. *Cancer Lett,* 352(2), pp. 152-9.

Bartlett, A. I. and Radford, S. E. (2009). An expanding arsenal of experimental methods yields an explosion of insights into protein folding mechanisms. *Nat Struct Mol Biol,* 16(6), pp. 582-8.

Barr, A. R., Kilmartin, J. V., & Gergely, F. (2010). CDK5RAP2 functions in centrosome to spindle pole attachment and DNA damage response. *The Journal of Cell Biology*, *189*(1), 23–39.

Basso, A. D., Solit, D. B., Chiosis, G., Giri, B., Tsichlis, P. and Rosen, N. (2002). Akt forms an intracellular complex with heat shock protein 90 (Hsp90) and Cdc37 and is destabilized by inhibitors of Hsp90 function. *J Biol Chem,* 277(42), pp. 39858-66.

Basto, R., Brunk, K., Vinadogrova, T., Peel, N., Franz, A., Khodjakov, A. and Raff, J. W. (2008). Centrosome amplification can initiate tumorigenesis in flies. *Cell,* 133(6), pp. 1032-42.

Basto, R., Gergely, F., Draviam, V. M., Ohkura, H., Liley, K. and Raff, J. W. (2007) 'Hsp90 is required to localise cyclin B and Msps/ch-TOG to the mitotic spindle in Drosophila and humans', *J Cell Sci,* 120(Pt 7), pp. 1278-87.

Basto, R., Lau, J., Vinogradova, T., Gardiol, A., Woods, C. G., Khodjakov, A. and Raff, J. W. (2006). Flies without centrioles. *Cell,* 125(7), pp. 1375-86.

Baumbach, J., Novak, Z. A., Raff, J. W. and Wainman, A. (2015). Dissecting the function and assembly of acentriolar microtubule organizing centers in Drosophila cells in vivo. *PLoS Genet,* 11(5), pp. e1005261.

Bavetsias, V., & Linardopoulos, S. (2015). Aurora Kinase Inhibitors: Current Status and Outlook. *Frontiers in Oncology*, *5*, 278.

Beisson, J. and Wright, M. (2003). Basal body/centriole assembly and continuity. *Curr Opin Cell Biol,* 15(1), pp. 96-104.

Belham, C., Roig, J., Caldwell, J. A., Aoyama, Y., Kemp, B. E., Comb, M. and Avruch, J. (2003). A mitotic cascade of NIMA family kinases. Nercc1/Nek9 activates the Nek6 and Nek7 kinases. *J Biol Chem,* 278(37), pp. 34897-909.

Berbari, N. F., O'Connor, A. K., Haycraft, C. J. and Yoder, B. K. (2009). The primary cilium as a complex signaling center. *Curr Biol,* 19(13), pp. R526-35.

Bertran, M. T., Sdelci, S., Regue, L., Avruch, J., Caelles, C. and Roig, J. (2011). Nek9 is a Plk1-activated kinase that controls early centrosome separation through Nek6/7 and Eg5. *Embo j,* 30(13), pp. 2634-47.

Bettencourt-Dias, M., Hildebrandt, F., Pellman, D., Woods, G. and Godinho, S. A. (2011). Centrosomes and cilia in human disease. *Trends Genet,* 27(8), pp. 307-15.

Bettencourt-Dias, M., Rodrigues-Martins, A., Carpenter, L., Riparbelli, M., Lehmann, L., Gatt, M. K., Carmo, N., Balloux, F., Callaini, G. and Glover, D. M. (2005). SAK/PLK4 is required for centriole duplication and flagella development. *Curr Biol,* 15(24), pp. 2199-207.

Blachon, S., Gopalakrishnan, J., Omori, Y., Polyanovsky, A., Church, A., Nicastro, D., Avidor-Reiss, T. (2008). Drosophila *asterless* and Vertebrate Cep152 Are Orthologs Essential for Centriole Duplication. *Genetics*, *180*(4), 2081–2094.

Bornens, M. (2012). The centrosome in cells and organisms. *Science,* 335(6067), pp. 422-6.

Boveri, T. (2008). Concerning the origin of malignant tumours by Theodor Boveri. Translated and annotated by Henry Harris. *J Cell Sci,* 121 Suppl 1, pp. 1-84.

Brancati, F., Iannicelli, M., Travaglini, L., Mazzotta, A., Bertini, E., Boltshauser, E., D'Arrigo, S., Emma, F., Fazzi, E., Gallizzi, R., Gentile, M., Loncarevic, D., Mejaski-Bosnjak, V., Pantaleoni, C., Rigoli, L., Salpietro, C. D., Signorini, S.,

Stringini, G. R., Verloes, A., Zabloka, D., Dallapiccola, B., Gleeson, J. G. and Valente, E. M. (2009). MKS3/TMEM67 mutations are a major cause of COACH Syndrome, a Joubert Syndrome related disorder with liver involvement. *Hum Mutat,* 30(2), pp. E432-42.

Breuer, M., Kolano, A., Kwon, M., Li, C. C., Tsai, T. F., Pellman, D., Brunet, S. and Verlhac, M. H. (2010). HURP permits MTOC sorting for robust meiotic spindle bipolarity, similar to extra centrosome clustering in cancer cells. *J Cell Biol,* 191(7), pp. 1251-60.

Brinkley, B. R. (2001). Managing the centrosome numbers game: from chaos to stability in cancer cell division. *Trends Cell Biol,* 11(1), pp. 18-21.

Brodsky, J. L. and Chiosis, G. (2006). Hsp70 molecular chaperones: emerging roles in human disease and identification of small molecule modulators. *Curr Top Med Chem,* 6(11), pp. 1215-25.

Brownlee, C. W. and Rogers, G. C. (2013). Show me your license, please: deregulation of centriole duplication mechanisms that promote amplification. *Cell Mol Life Sci,* 70(6), pp. 1021-34.

Carreno, S., Kouranti, I., Glusman, E. S., Fuller, M. T., Echard, A. and Payre, F. (2008). Moesin and its activating kinase Slik are required for cortical stability and microtubule organization in mitotic cells. *J Cell Biol,* 180(4), pp. 739-46.

Castellanos, E., Dominguez, P. and Gonzalez, C. (2008). Centrosome dysfunction in Drosophila neural stem cells causes tumors that are not due to genome instability. *Curr Biol,* 18(16), pp. 1209-14.

Castiel, A., Visochek, L., Mittelman, L., Dantzer, F., Izraeli, S. and Cohen-Armon, M. (2011). A phenanthrene derived PARP inhibitor is an extra-centrosomes de-clustering agent exclusively eradicating human cancer cells. *BMC Cancer,* 11, pp. 412.

Chan, J. Y. (2011). A clinical overview of centrosome amplification in human cancers. *Int J Biol Sci,* 7(8), pp. 1122-44.

Chang, J., Baloh, R. H. and Milbrandt, J. (2009). The NIMA-family kinase Nek3 regulates microtubule acetylation in neurons. *J Cell Sci,* 122(Pt 13), pp. 2274-82.

Chavali, P. L., Chandrasekaran, G., Barr, A. R., Tatrai, P., Taylor, C., Papachristou, E. K., Woods, C. G., Chavali, S. and Gergely, F. (2016). A CEP215-HSET complex

links centrosomes with spindle poles and drives centrosome clustering in cancer. *Nat Commun,* 7, pp. 11005.

Cheeseman, I. M. and Desai, A. (2008). Molecular architecture of the kinetochore-microtubule interface. *Nat Rev Mol Cell Biol,* 9(1), pp. 33-46.

Chen, J. G. and Horwitz, S. B. (2002). Differential mitotic responses to microtubule-stabilizing and -destabilizing drugs. *Cancer Res,* 62(7), pp. 1935-8.

Chen, Y., Chen, C. F., Riley, D. J. and Chen, P. L. (2011). Nek1 kinase functions in DNA damage response and checkpoint control through a pathway independent of ATM and ATR. *Cell Cycle,* 10(4), pp. 655-63.

Chen, Z., Indjeian VB, McManus M, Wang L, Dynlacht BD. (2002) CP110, a cell cycle-dependent CDK substrate, regulates centrosome duplication in human cells. *Dev Cell*. 3(3):339-50.

Choi, H. J., Lin, J. R., Vannier, J. B., Slaats, G. G., Kile, A. C., Paulsen, R. D., Manning, D. K., Beier, D. R., Giles, R. H., Boulton, S. J. and Cimprich, K. A. (2013). NEK8 links the ATR-regulated replication stress response and S phase CDK activity to renal ciliopathies. *Mol Cell,* 51(4), pp. 423-39.

Cimini, D. (2008). Merotelic kinetochore orientation, aneuploidy, and cancer. *Biochim Biophys Acta,* 1786(1), pp. 32-40.

Cimini, D., Howell, B., Maddox, P., Khodjakov, A., Degrassi, F., & Salmon, E. D. (2001). Merotelic Kinetochore Orientation Is a Major Mechanism of Aneuploidy in Mitotic Mammalian Tissue Cells. *The Journal of Cell Biology*, *153*(3), 517–528.

Clerico, E. M., Tilitsky, J. M., Meng, W. and Gierasch, L. M. (2015). How hsp70 molecular machines interact with their substrates to mediate diverse physiological functions. *J Mol Biol,* 427(7), pp. 1575-88.

Cobrinik, D. (2005). Pocket proteins and cell cycle control. *Oncogene,* 24(17), pp. 2796-809.

Coene, K. L., Mans, D. A., Boldt, K., Gloeckner, C. J., van Reeuwijk, J., Bolat, E., Roosing, S., Letteboer, S. J., Peters, T. A., Cremers, F. P., Ueffing, M. and Roepman, R. (2011). The ciliopathy-associated protein homologs RPGRIP1 and RPGRIP1L are linked to cilium integrity through interaction with Nek4 serine/threonine kinase. *Hum Mol Genet,* 20(18), pp. 3592-605.

Conduit, P. T., Wainman, A. and Raff, J. W. (2015). Centrosome function and assembly in animal cells. *Nat Rev Mol Cell Biol,* 16(10), pp. 611-24.

Crasta, K., Ganem, N. J., Dagher, R., Lantermann, A. B., Ivanova, E. V., Pan, Y., Nezi, L., Protopopov, A., Chowdhury, D. and Pellman, D. (2012). DNA breaks and chromosome pulverization from errors in mitosis. *Nature,* 482(7383), pp. 53-8.

Cunha-Ferreira, I., Rodrigues-Martins, A., Bento, I., Riparbelli, M., Zhang, W., Laue, E., Callaini, G., Glover, D. M. and Bettencourt-Dias, M. (2009). The SCF/Slimb ubiquitin ligase limits centrosome amplification through degradation of SAK/PLK4. *Curr Biol,* 19(1), pp. 43-9.

D'Assoro, A. B., Barrett, S. L., Folk, C., Negron, V. C., Boeneman, K., Busby, R., Whitehead, C., Stivala, F., Lingle, W. L. and Salisbury, J. L. (2002). Amplified centrosomes in breast cancer: a potential indicator of tumor aggressiveness. *Breast Cancer Res Treat,* 75(1), pp. 25-34.

D'Assoro, A. B., Busby, R., Suino, K., Delva, E., Almodovar-Mercado, G. J., Johnson, H., Folk, C., Farrugia, D. J., Vasile, V., Stivala, F. and Salisbury, J. L. (2004). Genotoxic stress leads to centrosome amplification in breast cancer cell lines that have an inactive G1/S cell cycle checkpoint. *Oncogene,* 23(23), pp. 4068-75.

Daugaard, M., Jaattela, M. and Rohde, M. (2005). Hsp70-2 is required for tumor cell growth and survival. *Cell Cycle,* 4(7), pp. 877-80.

Daugaard, M., Rohde, M. and Jaattela, M. (2007). The heat shock protein 70 family: Highly homologous proteins with overlapping and distinct functions. *FEBS Lett,* 581(19), pp. 3702-10.

Davies, J. R., Osmani, A. H., De Souza, C. P., Bachewich, C. and Osmani, S. A. (2004). Potential link between the NIMA mitotic kinase and nuclear membrane fission during mitotic exit in Aspergillus nidulans. *Eukaryot Cell,* 3(6), pp. 1433-44.

Davila, M., Frost, A. R., Grizzle, W. E. and Chakrabarti, R. (2003). LIM kinase 1 is essential for the invasive growth of prostate epithelial cells: implications in prostate cancer. *J Biol Chem,* 278(38), pp. 36868-75.

de Billy, E., Powers, M. V., Smith, J. R. and Workman, P. (2009). Drugging the heat shock factor 1 pathway: exploitation of the critical cancer cell dependence on the guardian of the proteome. *Cell Cycle: Vol. 23*. United States, pp. 3806-8.

de Carcer, G. (2004). Heat shock protein 90 regulates the metaphase-anaphase transition in a polo-like kinase-dependent manner. *Cancer Res,* 64(15), pp. 5106-12.

de Carcer, G., do Carmo Avides, M., Lallena, M. J., Glover, D. M. and Gonzalez, C. (2001). Requirement of Hsp90 for centrosomal function reflects its regulation of Polo kinase stability. *Embo j,* 20(11), pp. 2878-84.

Deckbar, D., Stiff, T., Koch, B., Reis, C., Lobrich, M., Jeggo, P.A. (2010). The limitations of the G1-S checkpoint. *Cancer Research*. 70, 4412-4421.

Deckbar, D., Jeggo, P.A., Lobrich, M., 2011. Understanding the limitations of radiation-induced cell cycle checkpoints. *Critical Reviews in Biochemistry and Molecular Biology*. 46, 271-283.

De Souza, C. P., Osmani, A. H., Wu, L. P., Spotts, J. L. and Osmani, S. A. (2000). Mitotic histone H3 phosphorylation by the NIMA kinase in Aspergillus nidulans. *Cell,* 102(3), pp. 293-302.

Debec, A. (1978). Haploid cell cultures of Drosophila melanogaster. *Nature,* 274(5668), pp. 255-6.

Dell, K. R., Turck, C. W. and Vale, R. D. (2000). Mitotic phosphorylation of the dynein light intermediate chain is mediated by cdc2 kinase. *Traffic,* 1(1), pp. 38-44.

Denu, R. A., Zasadil, L. M., Kanugh, C., Laffin, J., Weaver, B. A. and Burkard, M. E. (2016). Centrosome amplification induces high grade features and is prognostic of worse outcomes in breast cancer. *BMC Cancer,* 16, pp. 47.

Downs, J. A. and Jackson, S. P. (2004). A means to a DNA end: the many roles of Ku. *Nat Rev Mol Cell Biol,* 5(5), pp. 367-78.

Doxsey, S. (2001). Re-evaluating centrosome function. *Nat Rev Mol Cell Biol,* 2(9), pp. 688-98.

Drosopoulos, K., Tang, C., Chao, W. C. and Linardopoulos, S. (2014). APC/C is an essential regulator of centrosome clustering. *Nat Commun,* 5, pp. 3686.

Duensing, S., Lee, B. H., Dal Cin, P. and Munger, K. (2003). Excessive centrosome abnormalities without ongoing numerical chromosome instability in a Burkitt's lymphoma. *Mol Cancer,* 2, pp. 30.

Dujardin, D. L. and Vallee, R. B. (2002). Dynein at the cortex. *Curr Opin Cell Biol,* 14(1), pp. 44-9.

Dumont, J. and Desai, A. (2012). Acentrosomal spindle assembly and chromosome segregation during oocyte meiosis. *Trends Cell Biol,* 22(5), pp. 241-9.

Dunsch, A. K., Hammond, D., Lloyd, J., Schermelleh, L., Gruneberg, U. and Barr, F. A. (2012). Dynein light chain 1 and a spindle-associated adaptor promote dynein asymmetry and spindle orientation. *J Cell Biol,* 198(6), pp. 1039-54.

el-Deiry, W.S., Tokino, T., Velculescu, V.E., Levy, D.B., Parsons, R., Trent, J.M., Lin, D., Mercer, W.E., Kinzler, K.W., Vogelstein, B. (1993). WAF1, a potential mediator of p53 tumor suppression. Cell. 75, 817-825.

Evans, J. E., Snow, J. J., Gunnarson, A. L., Ou, G., Stahlberg, H., McDonald, K. L. and Scholey, J. M. (2006). Functional modulation of IFT kinesins extends the sensory repertoire of ciliated neurons in Caenorhabditis elegans. *J Cell Biol,* 172(5), pp. 663-9.

Fang, G., Zhang, D., Yin, H., Zheng, L., Bi, X. and Yuan, L. (2014). Centlein mediates an interaction between C-Nap1 and Cep68 to maintain centrosome cohesion. *J Cell Sci,* 127(Pt 8), pp. 1631-9.

Faragher, A. J. and Fry, A. M. (2003). Nek2A kinase stimulates centrosome disjunction and is required for formation of bipolar mitotic spindles. *Mol Biol Cell,* 14(7), pp. 2876-89.

Fehon, R. G., McClatchey, A. I. and Bretscher, A. (2010). Organizing the cell cortex: the role of ERM proteins. *Nat Rev Mol Cell Biol,* 11(4), pp. 276-87.

Fewell, S. W., Day, B. W. and Brodsky, J. L. (2001). Identification of an inhibitor of hsc70-mediated protein translocation and ATP hydrolysis. *J Biol Chem,* 276(2), pp. 910-4.

Fielding, A. B., Dobreva, I. and Dedhar, S. (2008a). Beyond focal adhesions: integrin-linked kinase associates with tubulin and regulates mitotic spindle organization. *Cell Cycle,* 7(13), pp. 1899-906.

Fielding, A. B., Dobreva, I., McDonald, P. C., Foster, L. J. and Dedhar, S. (2008b). Integrin-linked kinase localises to the centrosome and regulates mitotic spindle organization. *J Cell Biol,* 180(4), pp. 681-9.

Fielding, A. B., Lim, S., Montgomery, K., Dobreva, I. and Dedhar, S. (2011). A critical role of integrin-linked kinase, ch-TOG and TACC3 in centrosome clustering in cancer cells. *Oncogene,* 30(5), pp. 521-34.

Fletcher, L., Cerniglia, G. J., Yen, T. J. and Muschel, R. J. (2005). Live cell imaging reveals distinct roles in cell cycle regulation for Nek2A and Nek2B. *Biochim Biophys Acta,* 1744(2), pp. 89-92.

Foley, E. A. and Kapoor, T. M. (2013). Microtubule attachment and spindle assembly checkpoint signalling at the kinetochore. *Nat Rev Mol Cell Biol,* 14(1), pp. 25-37.

Forment, J. V., Kaidi, A. and Jackson, S. P. (2012). Chromothripsis and cancer: causes and consequences of chromosome shattering. *Nat Rev Cancer,* 12(10), pp. 663-70.

Fry, A. M., Mayor, T., Meraldi, P., Stierhof, Y. D., Tanaka, K. and Nigg, E. A. (1998a). C-Nap1, a novel centrosomal coiled-coil protein and candidate substrate of the cell cycle-regulated protein kinase Nek2. *J Cell Biol,* 141(7), pp. 1563-74.

Fry, A. M., Meraldi, P. and Nigg, E. A. (1998b). A centrosomal function for the human Nek2 protein kinase, a member of the NIMA family of cell cycle regulators. *Embo j,* 17(2), pp. 470-81.

Fry, A. M., O'Regan, L., Sabir, S. R. and Bayliss, R. (2012). Cell cycle regulation by the NEK family of protein kinases. *J Cell Sci,* 125(Pt 19), pp. 4423-33.

Fujiwara, T., Bandi, M., Nitta, M., Ivanova, E. V., Bronson, R. T. and Pellman, D. (2005). Cytokinesis failure generating tetraploids promotes tumorigenesis in p53-null cells. *Nature,* 437(7061), pp. 1043-7.

Fukasawa, K. (2007). Oncogenes and tumour suppressors take on centrosomes. *Nat Rev Cancer,* 7(12), pp. 911-24.

Fukasawa, K., Choi, T., Kuriyama, R., Rulong, S. and Vande Woude, G. F. (1996). Abnormal centrosome amplification in the absence of p53. *Science,* 271(5256), pp. 1744-7.

Gabai, V. L., Budagova, K. R. and Sherman, M. Y. (2005). Increased expression of the major heat shock protein Hsp72 in human prostate carcinoma cells is dispensable for their viability but confers resistance to a variety of anticancer agents. *Oncogene,* 24(20), pp. 3328-38.

Gabrielli, B., Brooks, K., & Pavey, S. (2012). Defective Cell Cycle Checkpoints as Targets for Anti-Cancer Therapies. *Frontiers in Pharmacology*, *3*, 9.

Ganem, N. J., Cornils, H., Chiu, S. Y., O'Rourke, K. P., Arnaud, J., Yimlamai, D., Thery, M., Camargo, F. D. and Pellman, D. (2014). Cytokinesis failure triggers hippo tumor suppressor pathway activation. *Cell,* 158(4), pp. 833-48.

Ganem, N. J., Godinho, S. A. and Pellman, D. (2009). A mechanism linking extra centrosomes to chromosomal instability. *Nature,* 460(7252), pp. 278-82.

Ganem, N. J. and Pellman, D. (2012). Linking abnormal mitosis to the acquisition of DNA damage. *J Cell Biol,* 199(6), pp. 871-81.

Ganem, N. J., Storchova, Z. and Pellman, D. (2007). Tetraploidy, aneuploidy and cancer. *Curr Opin Genet Dev,* 17(2), pp. 157-62.

Gao, R., Yu, Y., Inoue, A., Widodo, N., Kaul, S. C. and Wadhwa, R. (2013). Heterogeneous nuclear ribonucleoprotein K (hnRNP-K) promotes tumor metastasis by induction of genes involved in extracellular matrix, cell movement, and angiogenesis. *J Biol Chem,* 288(21), pp. 15046-56.

Garrido, C., Brunet, M., Didelot, C., Zermati, Y., Schmitt, E. and Kroemer, G. (2006). Heat shock proteins 27 and 70: anti-apoptotic proteins with tumorigenic properties. *Cell Cycle,* 5(22), pp. 2592-601.

Gentric, G., Desdouets, C. and Celton-Morizur, S. (2012). Hepatocytes polyploidization and cell cycle control in liver physiopathology. *Int J Hepatol,* 2012, pp. 282430.

Gergely, F. and Basto, R. (2008). Multiple centrosomes: together they stand, divided they fall. *Genes Dev,* 22(17), pp. 2291-6.

Giehl, M., Fabarius, A., Frank, O., Hochhaus, A., Hafner, M., Hehlmann, R. and Seifarth, W. (2005). Centrosome aberrations in chronic myeloid leukemia correlate with stage of disease and chromosomal instability. *Leukemia,* 19(7), pp. 1192-7.

Giffin, W., Torrance, H., Rodda, D. J., Prefontaine, G. G., Pope, L. and Hache, R. J. (1996). Sequence-specific DNA binding by Ku autoantigen and its effects on transcription. *Nature,* 380(6571), pp. 265-8.

Glover, D. M. (2005). Polo kinase and progression through M phase in Drosophila: a perspective from the spindle poles. *Oncogene,* 24(2), pp. 230-7.

Godinho, S. A., Kwon, M. and Pellman, D. (2009). Centrosomes and cancer: how cancer cells divide with too many centrosomes. *Cancer Metastasis Rev,* 28(1-2), pp. 85-98.

Godinho, S. A. and Pellman, D. (2014). Causes and consequences of centrosome abnormalities in cancer. *Philos Trans R Soc Lond B Biol Sci,* 369(1650).

Godinho, S. A., Picone, R., Burute, M., Dagher, R., Su, Y., Leung, C. T., Polyak, K., Brugge, J. S., Thery, M. and Pellman, D. (2014). Oncogene-like induction of cellular invasion from centrosome amplification. *Nature,* 510(7503), pp. 167-71.

Goetz, S. C. and Anderson, K. V. (2010). The primary cilium: a signalling centre during vertebrate development. *Nat Rev Genet,* 11(5), pp. 331-44.

Gomez-Ferreria, M.A., Rath, U., Buster, D.W., Chanda, S.K., Caldwell, J.S., et al. (2007). Human Cep192 Is Required for Mitotic Centrosome and Spindle Assembly. *Current Biology*. 17: 1960–1966.

Gonczy, P. (2015). Centrosomes and cancer: revisiting a long-standing relationship. *Nat Rev Cancer,* 15(11), pp. 639-52.

Goshima, G., Wollman, R., Goodwin, S. S., Zhang, N., Scholey, J. M., Vale, R. D., & Stuurman, N. (2007). Genes Required for Mitotic Spindle Assembly in *Drosophila* S2 Cells. *Science (New York, N.Y.)*, *316*(5823), 417–421.

Goshima, G. and Kimura, A. (2010). New look inside the spindle: microtubule-dependent microtubule generation within the spindle. *Curr Opin Cell Biol,* 22(1), pp. 44-9.

Goshima, G., Nedelec, F. and Vale, R. D. (2005). Mechanisms for focusing mitotic spindle poles by minus end-directed motor proteins. *J Cell Biol,* 171(2), pp. 229-40.

Goshima, G., Mayer, M., Zhang, N., Stuurman, N., & Vale, R. D. (2008). Augmin: a protein complex required for centrosome-independent microtubule generation within the spindle. *The Journal of Cell Biology*, *181*(3), 421–429.

Grallert, A., Krapp, A., Bagley, S., Simanis, V. and Hagan, I. M. (2004). Recruitment of NIMA kinase shows that maturation of the S. pombe spindle-pole body occurs over consecutive cell cycles and reveals a role for NIMA in modulating SIN activity. *Genes Dev,* 18(9), pp. 1007-21.

Graser, S., Stierhof, Y. D., Lavoie, S. B., Gassner, O. S., Lamla, S., Le Clech, M. and Nigg, E. A. (2007a). Cep164, a novel centriole appendage protein required for primary cilium formation. *J Cell Biol,* 179(2), pp. 321-30.

Graser, S., Stierhof, Y. D. and Nigg, E. A. (2007b). Cep68 and Cep215 (Cdk5rap2) are required for centrosome cohesion. *J Cell Sci,* 120(Pt 24), pp. 4321-31.

Greaves, M. (2016). Leukaemia 'firsts' in cancer research and treatment. *Nat Rev Cancer,* 16(3), pp. 163-72.

Gruss, O. J. and Vernos, I. (2004). The mechanism of spindle assembly: functions of Ran and its target TPX2. *J Cell Biol,* 166(7), pp. 949-55.

Guderian, G., Westendorf, J., Uldschmid, A. and Nigg, E. A. (2010). Plk4 trans-autophosphorylation regulates centriole number by controlling betaTrCP-mediated degradation. *J Cell Sci,* 123(Pt 13), pp. 2163-9.

Gudimchuk, N., Vitre, B., Kim, Y., Kiyatkin, A., Cleveland, D. W., Ataullakhanov, F. I. and Grishchuk, E. L. (2013). Kinetochore kinesin CENP-E is a processive bi-directional tracker of dynamic microtubule tips. *Nat Cell Biol,* 15(9), pp. 1079-88.

Guerrero, A. A., Martinez, A. C. and van Wely, K. H. (2010). Merotelic attachments and non-homologous end joining are the basis of chromosomal instability. *Cell Div*. England, pp. 13.

Gunaldi, M., Afsar, C. U., Okuturlar, Y., Gedikbasi, A., Kocoglu, H., Kural, A., Akarsu, C., Gunduz, U. and Tiken, E. E. (2015). Elevated serum levels of heat shock protein 70 are associated with breast cancer. *Tohoku J Exp Med,* 236(2), pp. 97-102.

Guo, H. Q., Gao, M., Ma, J., Xiao, T., Zhao, L. L., Gao, Y. and Pan, Q. J. (2007). Analysis of the cellular centrosome in fine-needle aspirations of the breast. *Breast Cancer Res,* 9(4), pp. R48.

Gustafson, L. M., Gleich, L. L., Fukasawa, K., Chadwell, J., Miller, M. A., Stambrook, P. J. and Gluckman, J. L. (2000). Centrosome hyperamplification in head and neck squamous cell carcinoma: a potential phenotypic marker of tumor aggressiveness. *Laryngoscope,* 110(11), pp. 1798-801.

Gutierrez-Caballero, C., Burgess, S. G., Bayliss, R. and Royle, S. J. (2015). TACC3-ch-TOG track the growing tips of microtubules independently of clathrin and Aurora-A phosphorylation. *Biol Open,* 4(2), pp. 170-9.

Gutteridge, R. E. A., Ndiaye, M. A., Liu, X., & Ahmad, N. (2016). Plk1 inhibitors in cancer therapy: *From laboratory to clinics*. *Molecular Cancer Therapeutics*, *15*(7), 1427–1435.

Habedanck, R., Stierhof, Y. D., Wilkinson, C. J. and Nigg, E. A. (2005). The Polo kinase Plk4 functions in centriole duplication. *Nat Cell Biol,* 7(11), pp. 1140-6.

Hall, J., Song, Y., Karplus, P. A. and Barbar, E. (2010). The crystal structure of dynein intermediate chain-light chain roadblock complex gives new insights into dynein assembly. *J Biol Chem,* 285(29), pp. 22566-75.

Hammond, J. W., Cai, D. and Verhey, K. J. (2008), Tubulin modifications and their cellular functions. *Curr Opin Cell Biol,* 20(1), pp. 71-6.

Hanahan, D. and Weinberg, R. A. (2011). Hallmarks of cancer: the next generation. *Cell,* 144(5), pp. 646-74.

Hao, L. and Scholey, J. M. (2009). Intraflagellar transport at a glance. *J Cell Sci,* 122(Pt 7), pp. 889-92.

Haq, T., Richards, M. W., Burgess, S. G., Gallego, P., Yeoh, S., O'Regan, L., Reverter, D., Roig, J., Fry, A. M. and Bayliss, R. (2015). Mechanistic basis of Nek7 activation through Nek9 binding and induced dimerization. *Nat Commun,* 6, pp. 8771.

Hartl, F. U. (1996). Molecular chaperones in cellular protein folding. *Nature,* 381(6583), pp. 571-9.

Hartl, F. U., Bracher, A. and Hayer-Hartl, M. (2011). Molecular chaperones in protein folding and proteostasis. *Nature,* 475(7356), pp. 324-32.

Hatch, E. M., Kulukian, A., Holland, A. J., Cleveland, D. W., & Stearns, T. (2010). Cep152 interacts with Plk4 and is required for centriole duplication. *The Journal of Cell Biology*, *191*(4), 721–729.

Hayward, D. G., Clarke, R. B., Faragher, A. J., Pillai, M. R., Hagan, I. M. and Fry, A. M. (2004). The centrosomal kinase Nek2 displays elevated levels of protein expression in human breast cancer. *Cancer Res,* 64(20), pp. 7370-6.

He, R., Huang, N., Bao, Y., Zhou, H., Teng, J. and Chen, J. (2013). LRRC45 is a centrosome linker component required for centrosome cohesion. *Cell Rep,* 4(6), pp. 1100-7.

Heald, R. and Khodjakov, A. (2015). Thirty years of search and capture: The complex simplicity of mitotic spindle assembly. *J Cell Biol,* 211(6), pp. 1103-11.

Heald, R., Tournebize, R., Blank, T., Sandaltzopoulos, R., Becker, P., Hyman, A. and Karsenti, E. (1996). Self-organization of microtubules into bipolar spindles around artificial chromosomes in Xenopus egg extracts. *Nature,* 382(6590), pp. 420-5.

Helps, N. R., Luo, X., Barker, H. M. and Cohen, P. T. (2000). NIMA-related kinase 2 (Nek2), a cell-cycle-regulated protein kinase localized to centrosomes, is complexed to protein phosphatase 1. *Biochem J,* 349(Pt 2), pp. 509-18.

Hendrick, J. P. and Hartl, F. U. (1995). The role of molecular chaperones in protein folding. *Faseb j,* 9(15), pp. 1559-69.

Heng, H. H., Bremer, S. W., Stevens, J. B., Horne, S. D., Liu, G., Abdallah, B. Y., Ye, K. J. and Ye, C. J. (2013). Chromosomal instability (CIN): what it is and why it is crucial to cancer evolution. *Cancer Metastasis Rev,* 32(3-4), pp. 325-40.

Hensel, M., Zoz, M., Giesecke, C., Benner, A., Neben, K., Jauch, A., Stilgenbauer, S., Ho, A. D. and Kramer, A. (2007). High rate of centrosome aberrations and correlation with proliferative activity in patients with untreated B-cell chronic lymphocytic leukemia. *Int J Cancer,* 121(5), pp. 978-83.

Hoffman, D. B., Pearson, C. G., Yen, T. J., Howell, B. J. and Salmon, E. D. (2001). Microtubule-dependent changes in assembly of microtubule motor proteins and mitotic spindle checkpoint proteins at PtK1 kinetochores. *Mol Biol Cell,* 12(7), pp. 1995-2009.

Holland, A. J., Fachinetti, D., Zhu, Q., Bauer, M., Verma, I. M., Nigg, E. A. and Cleveland, D. W. (2012). The autoregulated instability of Polo-like kinase 4 limits centrosome duplication to once per cell cycle. *Genes Dev,* 26(24), pp. 2684-9.

Hong, D. S., Banerji, U., Tavana, B., George, G. C., Aaron, J. and Kurzrock, R. (2013). Targeting the molecular chaperone heat shock protein 90 (HSP90): lessons learned and future directions. *Cancer Treat Rev,* 39(4), pp. 375-87.

Hood, F. E., Williams, S. J., Burgess, S. G., Richards, M. W., Roth, D., Straube, A., Pfuhl, M., Bayliss, R. and Royle, S. J. (2013). Coordination of adjacent domains mediates TACC3-ch-TOG-clathrin assembly and mitotic spindle binding. *J Cell Biol,* 202(3), pp. 463-78.

Hou, Y., Pazour, G. J. and Witman, G. B. (2004). A dynein light intermediate chain, D1bLIC, is required for retrograde intraflagellar transport. *Mol Biol Cell,* 15(10), pp. 4382-94.

Hsu, L. C., Kapali, M., DeLoia, J. A. and Gallion, H. H. (2005). Centrosome abnormalities in ovarian cancer. *Int J Cancer,* 113(5), pp. 746-51.

Huangfu, D., Liu, A., Rakeman, A. S., Murcia, N. S., Niswander, L. and Anderson, K. V. (2003). Hedgehog signalling in the mouse requires intraflagellar transport proteins. *Nature,* 426(6962), pp. 83-7.

Hunter, K. W. (2004). Ezrin, a key component in tumor metastasis. *Trends Mol Med,* 10(5), pp. 201-4.

Hut, H. M., Kampinga, H. H. and Sibon, O. C. (2005). Hsp70 protects mitotic cells against heat-induced centrosome damage and division abnormalities. *Mol Biol Cell,* 16(8), pp. 3776-85.

Hwang, H. C. and Clurman, B. E. (2005). Cyclin E in normal and neoplastic cell cycles. *Oncogene,* 24(17), pp. 2776-86.

Inamdar, K. V., O'Brien, S., Sen, S., Keating, M., Nguyen, M. H., Wang, X., Fernandez, M., Thomazy, V., Medeiros, L. J. and Bueso-Ramos, C. E. (2008). Aurora-A kinase nuclear expression in chronic lymphocytic leukemia. *Mod Pathol,* 21(12), pp. 1428-35.

Inbar-Rozensal, D., Castiel, A., Visochek, L., Castel, D., Dantzer, F., Izraeli, S. and Cohen-Armon, M. (2009). A selective eradication of human nonhereditary breast cancer cells by phenanthridine-derived polyADP-ribose polymerase inhibitors. *Breast Cancer Res,* 11(6), pp. R78.

Ishikawa, H. and Marshall, W. F. (2011). Ciliogenesis: building the cell's antenna. *Nat Rev Mol Cell Biol,* 12(4), pp. 222-34.

Jackson, S.P. & Bartek, J. (2009). The DNA-damage response in human biology and disease. *Nature*. 461, 1071-1078.

Jakobsen, L., Vanselow, K., Skogs, M., Toyoda, Y., Lundberg, E., Poser, I., Falkenby, L. G., Bennetzen, M., Westendorf, J., Nigg, E. A., Uhlen, M., Hyman, A. A. and Andersen, J. S. (2011). Novel asymmetrically localizing components of human centrosomes identified by complementary proteomics methods. *Embo j,* 30(8), pp. 1520-35.

Jana, S. C., Marteil, G. and Bettencourt-Dias, M. (2014). Mapping molecules to structure: unveiling secrets of centriole and cilia assembly with near-atomic resolution. *Curr Opin Cell Biol,* 26, pp. 96-106.

Janssen, A. and Medema, R. H. (2011). Mitosis as an anti-cancer target. *Oncogene,* 30(25), pp. 2799-809.

Jaspersen, S. L. and Winey, M. (2004). The budding yeast spindle pole body: structure, duplication, and function. *Annu Rev Cell Dev Biol,* 20, pp. 1-28.

Kampinga, H. H. and Craig, E. A. (2010). The HSP70 chaperone machinery: J proteins as drivers of functional specificity. *Nat Rev Mol Cell Biol,* 11(8), pp. 579-92.

Kandli, M., Feige, E., Chen, A., Kilfin, G. and Motro, B. (2000). Isolation and characterization of two evolutionarily conserved murine kinases (Nek6 and nek7) related to the fungal mitotic regulator, NIMA. *Genomics,* 68(2), pp. 187-96.

Karna, P., Rida, P. C., Pannu, V., Gupta, K. K., Dalton, W. B., Joshi, H., Yang, V. W., Zhou, J. and Aneja, R. (2011). A novel microtubule-modulating noscapinoid triggers apoptosis by inducing spindle multipolarity via centrosome amplification and declustering. *Cell Death Differ,* 18(4), pp. 632-44.

Karsenti, E. and Vernos, I. (2001). The mitotic spindle: a self-made machine. *Science,* 294(5542), pp. 543-7.

Kasap, E., Boyacioglu, S. O., Korkmaz, M., Yuksel, E. S., Unsal, B., Kahraman, E., Ozutemiz, O. and Yuceyar, H. (2012). Aurora kinase A (AURKA) and never in mitosis gene A-related kinase 6 (NEK6) genes are upregulated in erosive esophagitis and esophageal adenocarcinoma. *Exp Ther Med,* 4(1), pp. 33-42.

Kawamura, E., Fielding, A. B., Kannan, N., Balgi, A., Eaves, C. J., Roberge, M. and Dedhar, S. (2013). Identification of novel small molecule inhibitors of centrosome clustering in cancer cells. *Oncotarget,* 4(10), pp. 1763-76.

Kearns, W. G., Yamaguchi, H., Young, N. S. and Liu, J. M. (2004). Centrosome amplification and aneuploidy in bone marrow failure patients. *Genes Chromosomes Cancer,* 40(4), pp. 329-33.

Kerketta, L. S., Ghosh, K., Nadkarni, A., Madkaikar, M. and Vundinti, B. R. (2017). Centrosome Aberration Frequency and Disease Association in B-Acute Lymphoblastic Leukemia. *In Vivo,* 31(2), pp. 215-220.

Khodjakov, A. and Rieder, C. L. (2001). Centrosomes enhance the fidelity of cytokinesis in vertebrates and are required for cell cycle progression. *J Cell Biol,* 153(1), pp. 237-42.

Khodjakov, A., Rieder, C. L., Sluder, G., Cassels, G., Sibon, O. and Wang, C. L. (2002). De novo formation of centrosomes in vertebrate cells arrested during S phase. *J Cell Biol,* 158(7), pp. 1171-81.

Kim, S., Lee, K. and Rhee, K. (2007). NEK7 is a centrosomal kinase critical for microtubule nucleation. *Biochem Biophys Res Commun,* 360(1), pp. 56-62.

King, S. J. and Schroer, T. A. (2000). Dynactin increases the processivity of the cytoplasmic dynein motor. *Nat Cell Biol,* 2(1), pp. 20-4.

Kitagawa, D., Vakonakis, I., Olieric, N., Hilbert, M., Keller, D., Olieric, V., Steinmetz, M. O. (2011). Structural Basis of the 9-Fold Symmetry of Centrioles. *Cell*, *144*(3), 364–375.

Kleylein-Sohn, J., Pollinger, B., Ohmer, M., Hofmann, F., Nigg, E. A., Hemmings, B. A. and Wartmann, M. (2012). Acentrosomal spindle organization renders cancer cells dependent on the kinesin HSET. *J Cell Sci,* 125(Pt 22), pp. 5391-402.

Kleylein-Sohn, J., Westendorf, J., Le Clech, M., Habedanck, R., Stierhof, Y. D. and Nigg, E. A. (2007). Plk4-induced centriole biogenesis in human cells. *Dev Cell,* 13(2), pp. 190-202.

Kocsis, J., Meszaros, T., Madaras, B., Toth, E. K., Kamondi, S., Gal, P., Varga, L., Prohaszka, Z. and Fust, G. (2011). High levels of acute phase proteins and soluble 70 kDa heat shock proteins are independent and additive risk factors for mortality in colorectal cancer. *Cell Stress Chaperones,* 16(1), pp. 49-55.

Kohlmaier, G., Loncarek, J., Meng, X., McEwen, B. F., Mogensen, M. M., Spektor, A., Dynlacht, B. D., Khodjakov, A. and Gonczy, P. (2009). Overly long centrioles and defective cell division upon excess of the SAS-4-related protein CPAP. *Curr Biol,* 19(12), pp. 1012-8.

Kollareddy, M., Zheleva, D., Dzubak, P., Brahmkshatriya, P. S., Lepsik, M. and Hajduch, M. (2012). Aurora kinase inhibitors: progress towards the clinic. *Invest New Drugs,* 30(6), pp. 2411-32.

Kollman, J. M., Merdes, A., Mourey, L. and Agard, D. A. (2011). Microtubule nucleation by gamma-tubulin complexes. *Nat Rev Mol Cell Biol,* 12(11), pp. 709-21.

Konopka, J. B., Watanabe, S. M. and Witte, O. N. (1984). An alteration of the human c-abl protein in K562 leukemia cells unmasks associated tyrosine kinase activity. *Cell,* 37(3), pp. 1035-42.

Konotop, G., Bausch, E., Nagai, T., Turchinovich, A., Becker, N., Benner, A., Boutros, M., Mizuno, K., Kramer, A. and Raab, M. S. (2016). Pharmacological Inhibition of Centrosome Clustering by Slingshot-Mediated Cofilin Activation and Actin Cortex Destabilization. *Cancer Res,* 76(22), pp. 6690-6700.

Korzeniewski, N., Hohenfellner, M. and Duensing, S. (2013). The centrosome as potential target for cancer therapy and prevention. *Expert Opin Ther Targets,* 17(1), pp. 43-52.

Korzeniewski, N., Treat, B. and Duensing, S. (2011). The HPV-16 E7 oncoprotein induces centriole multiplication through deregulation of Polo-like kinase 4 expression. *Mol Cancer,* 10, pp. 61.

Korzeniewski, N., Zheng, L., Cuevas, R., Parry, J., Chatterjee, P., Anderton, B., Duensing, A., Munger, K. and Duensing, S. (2009). Cullin 1 functions as a centrosomal suppressor of centriole multiplication by regulating polo-like kinase 4 protein levels. *Cancer Res,* 69(16), pp. 6668-75.

Koutsami, M. K., Tsantoulis, P. K., Kouloukoussa, M., Apostolopoulou, K., Pateras, I. S., Spartinou, Z., Drougou, A., Evangelou, K., Kittas, C., Bartkova, J., Bartek, J. and Gorgoulis, V. G. (2006). Centrosome abnormalities are frequently observed in non-small-cell lung cancer and are associated with aneuploidy and cyclin E overexpression. *J Pathol,* 209(4), pp. 512-21.

Kramer, A., Neben, K. and Ho, A. D. (2002). Centrosome replication, genomic instability and cancer. *Leukemia,* 16(5), pp. 767-75.

Kramer, A., Neben, K. and Ho, A. D. (2005). Centrosome aberrations in hematological malignancies. *Cell Biol Int,* 29(5), pp. 375-83.

Kramer, A., Raab, M. S. and Rebacz, B. (2008). Induction of spindle multipolarity by centrosomal cluster inhibition. *Cell Oncol,* 30(6), pp. 505-6.

Kramer, A., Schweizer, S., Neben, K., Giesecke, C., Kalla, J., Katzenberger, T., Benner, A., Muller-Hermelink, H. K., Ho, A. D. and Ott, G. (2003). Centrosome aberrations as a possible mechanism for chromosomal instability in non-Hodgkin's lymphoma. *Leukemia,* 17(11), pp. 2207-13.

Kraus, W. L. (2008). Transcriptional control by PARP-1: chromatin modulation, enhancer-binding, coregulation, and insulation. *Curr Opin Cell Biol,* 20(3), pp. 294-302.

Kronenwett, U., Huwendiek, S., Castro, J., Ried, T. and Auer, G. (2005). Characterisation of breast fine-needle aspiration biopsies by centrosome aberrations and genomic instability. *Br J Cancer,* 92(2), pp. 389-95.

Krzywicka-Racka, A. and Sluder, G. (2011). Repeated cleavage failure does not establish centrosome amplification in untransformed human cells. *J Cell Biol,* 194(2), pp. 199-207.

Kwon, M., Godinho, S. A., Chandhok, N. S., Ganem, N. J., Azioune, A., Thery, M. and Pellman, D. (2008). Mechanisms to suppress multipolar divisions in cancer cells with extra centrosomes. *Genes Dev,* 22(16), pp. 2189-203.

Lane, H. A. and Nigg, E. A. (1996). Antibody microinjection reveals an essential role for human polo-like kinase 1 (Plk1) in the functional maturation of mitotic centrosomes. *J Cell Biol,* 135(6 Pt 2), pp. 1701-13.

Lange, B. M., Bachi, A., Wilm, M. and Gonzalez, C. (2000). Hsp90 is a core centrosomal component and is required at different stages of the centrosome cycle in Drosophila and vertebrates. *Embo j,* 19(6), pp. 1252-62.

Lanneau, D., de Thonel, A., Maurel, S., Didelot, C. and Garrido, C. (2007). Apoptosis versus cell differentiation: role of heat shock proteins HSP90, HSP70 and HSP27. *Prion,* 1(1), pp. 53-60.

Lapenna, S. and Giordano, A. (2009). Cell cycle kinases as therapeutic targets for cancer. *Nat Rev Drug Discov,* 8(7), pp. 547-66.

Lawo, S., Bashkurov, M., Mullin, M., Ferreria, M. G., Kittler, R., Habermann, B., Tagliaferro, A., Poser, I., Hutchins, J. R., Hegemann, B., Pinchev, D., Buchholz, F., Peters, J. M., Hyman, A. A., Gingras, A. C. and Pelletier, L. (2009). HAUS, the 8-subunit human Augmin complex, regulates centrosome and spindle integrity. *Curr Biol,* 19(10), pp. 816-26.

Leber, B., Maier, B., Fuchs, F., Chi, J., Riffel, P., Anderhub, S., Wagner, L., Ho, A. D., Salisbury, J. L., Boutros, M. and Kramer, A. (2010). Proteins required for centrosome clustering in cancer cells. *Sci Transl Med,* 2(33), pp. 33ra38.

Lee, K. and Rhee, K. (2011). PLK1 phosphorylation of pericentrin initiates centrosome maturation at the onset of mitosis. *J Cell Biol,* 195(7), pp. 1093-101.

Leidel, S., Delattre, M., Cerutti, L., Baumer, K. and Gonczy, P. (2005). SAS-6 defines a protein family required for centrosome duplication in C. elegans and in human cells. *Nat Cell Biol,* 7(2), pp. 115-25.

Letwin, K., Mizzen, L., Motro, B., Ben-David, Y., Bernstein, A. and Pawson, T. (1992). A mammalian dual specificity protein kinase, Nek1, is related to the NIMA cell cycle regulator and highly expressed in meiotic germ cells. *Embo j,* 11(10), pp. 3521-31.

Leu, J. I., Pimkina, J., Frank, A., Murphy, M. E. and George, D. L. (2009). A small molecule inhibitor of inducible heat shock protein 70. *Mol Cell,* 36(1), pp. 15-27.

Levine, M. S., Bakker, B., Boeckx, B., Moyett, J., Lu, J., Vitre, B., Spierings, D. C., Lansdorp, P. M., Cleveland, D. W., Lambrechts, D., Foijer, F. and Holland, A. J. (2017). Centrosome Amplification Is Sufficient to Promote Spontaneous Tumorigenesis in Mammals. *Dev Cell,* 40(3), pp. 313-322.e5.

Li, J., Tan, M., Li, L., Pamarthy, D., Lawrence, T. S. and Sun, Y. (2005). SAK, a new polo-like kinase, is transcriptionally repressed by p53 and induces apoptosis upon RNAi silencing. *Neoplasia,* 7(4), pp. 312-23.

Li, Y., Zhang, T., Schwartz, S. J. and Sun, D. (2009). New developments in Hsp90 inhibitors as anti-cancer therapeutics: mechanisms, clinical perspective and more potential. *Drug Resist Updat,* 12(1-2), pp. 17-27.

Liang, P. and MacRae, T. H. (1997). Molecular chaperones and the cytoskeleton. *J Cell Sci,* 110 (Pt 13), pp. 1431-40.

Liang, Y., Yu, W., Li, Y., Yu, L., Zhang, Q., Wang, F., Yang, Z., Du, J., Huang, Q., Yao, X. and Zhu, X. (2007). Nudel modulates kinetochore association and function of cytoplasmic dynein in M phase. *Mol Biol Cell,* 18(7), pp. 2656-66.

Lienkamp, S., Ganner, A. and Walz, G. (2012). Inversin, Wnt signaling and primary cilia. *Differentiation,* 83(2), pp. S49-55.

Lingle, W. L., Lutz, W. H., Ingle, J. N., Maihle, N. J. and Salisbury, J. L. (1998). Centrosome hypertrophy in human breast tumors: implications for genomic stability and cell polarity. *Proc Natl Acad Sci U S A,* 95(6), pp. 2950-5.

Lingle, W. L. and Salisbury, J. L. (1999). Altered centrosome structure is associated with abnormal mitoses in human breast tumors. *Am J Pathol,* 155(6), pp. 1941-51.

Liu, S., Lu, W., Obara, T., Kuida, S., Lehoczky, J., Dewar, K., Drummond, I. A. and Beier, D. R. (2002). A defect in a novel Nek-family kinase causes cystic kidney disease in the mouse and in zebrafish. *Development,* 129(24), pp. 5839-46.

Liu, X., Lei, M. and Erikson, R. L. (2006). Normal cells, but not cancer cells, survive severe Plk1 depletion. *Mol Cell Biol,* 26(6), pp. 2093-108.

Loffler, H., Bochtler, T., Fritz, B., Tews, B., Ho, A. D., Lukas, J., Bartek, J. and Kramer, A. (2007). DNA damage-induced accumulation of centrosomal Chk1 contributes to its checkpoint function. *Cell Cycle,* 6(20), pp. 2541-8.

Loncarek, J., Hergert, P. and Khodjakov, A. (2010). Centriole reduplication during prolonged interphase requires procentriole maturation governed by Plk1. *Curr Biol,* 20(14), pp. 1277-82.

Loncarek, J., Hergert, P., Magidson, V. and Khodjakov, A. (2008). Control of daughter centriole formation by the pericentriolar material. *Nat Cell Biol,* 10(3), pp. 322-8.

Lu, K. P. and Hunter, T. (1995). Evidence for a NIMA-like mitotic pathway in vertebrate cells. *Cell,* 81(3), pp. 413-24.

Lucas, E. P., & Raff, J. W. (2007). Maintaining the proper connection between the centrioles and the pericentriolar matrix requires *Drosophila* Centrosomin. *The Journal of Cell Biology*, *178*(5), 725–732.

Lukinavicius, G., Reymond, L., D'Este, E., Masharina, A., Gottfert, F., Ta, H., Guther, A., Fournier, M., Rizzo, S., Waldmann, H., Blaukopf, C., Sommer, C., Gerlich, D. W., Arndt, H. D., Hell, S. W. and Johnsson, K. (2014). Fluorogenic probes for live-cell imaging of the cytoskeleton. *Nat Methods,* 11(7), pp. 731-3.

Ma, Z., Izumi, H., Kanai, M., Kabuyama, Y., Ahn, N. G. and Fukasawa, K. (2006). Mortalin controls centrosome duplication via modulating centrosomal localization of p53. *Oncogene,* 25(39), pp. 5377-90.

MacCallum, D. E., Melville, J., Frame, S., Watt, K., Anderson, S., Gianella-Borradori, A., Lane, D. P. and Green, S. R. (2005). Seliciclib (CYC202, R-Roscovitine) induces cell death in multiple myeloma cells by inhibition of RNA polymerase II-dependent transcription and down-regulation of Mcl-1. *Cancer Res,* 65(12), pp. 5399-407.

Macurek, L., Lindqvist, A., Lim, D., Lampson, M. A., Klompmaker, R., Freire, R., Clouin, C., Taylor, S. S., Yaffe, M. B. and Medema, R. H. (2008). Polo-like kinase-1 is

activated by aurora A to promote checkpoint recovery. *Nature,* 455(7209), pp. 119-23.

Mahalingam, D., Swords, R., Carew, J. S., Nawrocki, S. T., Bhalla, K. and Giles, F. J. (2009). Targeting HSP90 for cancer therapy. *Br J Cancer,* 100(10), pp. 1523-9.

Mahoney, N. M., Goshima, G., Douglass, A. D. and Vale, R. D. (2006). Making microtubules and mitotic spindles in cells without functional centrosomes. *Curr Biol,* 16(6), pp. 564-9.

Makhnevych, T. and Houry, W. A. (2013). The control of spindle length by Hsp70 and Hsp110 molecular chaperones. *FEBS Lett,* 587(8), pp. 1067-72.

Malumbres, M. and Barbacid, M. (2005). Mammalian cyclin-dependent kinases. *Trends Biochem Sci,* 30(11), pp. 630-41.

Manandhar, G., Schatten, H. and Sutovsky, P. (2005). Centrosome reduction during gametogenesis and its significance. *Biol Reprod,* 72(1), pp. 2-13.

Mardin, B. R., Lange, C., Baxter, J. E., Hardy, T., Scholz, S. R., Fry, A. M. and Schiebel, E. (2010). Components of the Hippo pathway cooperate with Nek2 kinase to regulate centrosome disjunction. *Nat Cell Biol,* 12(12), pp. 1166-76.

Marthiens, V., Piel, M. and Basto, R. (2012). Never tear us apart--the importance of centrosome clustering. *J Cell Sci,* 125(Pt 14), pp. 3281-92.

Marthiens, V., Rujano, M. A., Pennetier, C., Tessier, S., Paul-Gilloteaux, P. and Basto, R. (2013). Centrosome amplification causes microcephaly. *Nat Cell Biol,* 15(7), pp. 731-40.

Martin, C. A., Ahmad, I., Klingseisen, A., Hussain, M. S., Bicknell, L. S., Leitch, A., Nurnberg, G., Toliat, M. R., Murray, J. E., Hunt, D., Khan, F., Ali, Z., Tinschert, S., Ding, J., Keith, C., Harley, M. E., Heyn, P., Muller, R., Hoffmann, I., Daire, V. C., Dollfus, H., Dupuis, L., Bashamboo, A., McElreavey, K., Kariminejad, A., Mendoza-Londono, R., Moore, A. T., Saggar, A., Schlechter, C., Weleber, R., Thiele, H., Altmuller, J., Hohne, W., Hurles, M. E., Noegel, A. A., Baig, S. M., Nurnberg, P. and Jackson, A. P. (2014). Mutations in PLK4, encoding a master regulator of centriole biogenesis, cause microcephaly, growth failure and retinopathy. *Nat Genet,* 46(12), pp. 1283-92.

Martoglio, A. M., Tom, B. D., Starkey, M., Corps, A. N., Charnock-Jones, D. S. and Smith, S. K. (2000). Changes in tumorigenesis- and angiogenesis-related gene

transcript abundance profiles in ovarian cancer detected by tailored high density cDNA arrays. *Mol Med,* 6(9), pp. 750-65.

Massey, A. J., Williamson, D. S., Browne, H., Murray, J. B., Dokurno, P., Shaw, T., Macias, A. T., Daniels, Z., Geoffroy, S., Dopson, M., Lavan, P., Matassova, N., Francis, G. L., Graham, C. J., Parsons, R., Wang, Y., Padfield, A., Comer, M., Drysdale, M. J. and Wood, M. (2010). A novel, small molecule inhibitor of Hsc70/Hsp70 potentiates Hsp90 inhibitor induced apoptosis in HCT116 colon carcinoma cells. *Cancer Chemother Pharmacol,* 66(3), pp. 535-45.

Mayer, F., Stoop, H., Sen, S., Bokemeyer, C., Oosterhuis, J. W. and Looijenga, L. H. (2003). Aneuploidy of human testicular germ cell tumors is associated with amplification of centrosomes. *Oncogene,* 22(25), pp. 3859-66.

Mayor, T., Stierhof, Y. D., Tanaka, K., Fry, A. M. and Nigg, E. A. (2000). The centrosomal protein C-Nap1 is required for cell cycle-regulated centrosome cohesion. *J Cell Biol,* 151(4), pp. 837-46.

McBride, M., Rida, P. C. and Aneja, R. (2015). Turning the headlights on novel cancer biomarkers: Inspection of mechanics underlying intratumor heterogeneity. *Mol Aspects Med,* 45, pp. 3-13.

Melixetian, M., Klein, D. K., Sorensen, C. S. and Helin, K. (2009). NEK11 regulates CDC25A degradation and the IR-induced G2/M checkpoint. *Nat Cell Biol,* 11(10), pp. 1247-53.

Mellacheruvu, D., Wright, Z., Couzens, A. L., Lambert, J. P., St-Denis, N. A., Li, T., Miteva, Y. V., Hauri, S., Sardiu, M. E., Low, T. Y., Halim, V. A., Bagshaw, R. D., Hubner, N. C., Al-Hakim, A., Bouchard, A., Faubert, D., Fermin, D., Dunham, W. H., Goudreault, M., Lin, Z. Y., Badillo, B. G., Pawson, T., Durocher, D., Coulombe, B., Aebersold, R., Superti-Furga, G., Colinge, J., Heck, A. J., Choi, H., Gstaiger, M., Mohammed, S., Cristea, I. M., Bennett, K. L., Washburn, M. P., Raught, B., Ewing, R. M., Gingras, A. C. and Nesvizhskii, A. I. (2013). The CRAPome: a contaminant repository for affinity purification-mass spectrometry data. *Nat Methods,* 10(8), pp. 730-6.

Mennella, V., Agard, D. A., Huang, B. and Pelletier, L. (2014). Amorphous no more: subdiffraction view of the pericentriolar material architecture. *Trends Cell Biol,* 24(3), pp. 188-97.

Meraldi, P., Honda, R. and Nigg, E. A. (2002). Aurora-A overexpression reveals tetraploidization as a major route to centrosome amplification in p53-/- cells. *Embo j,* 21(4), pp. 483-92.

Merdes, A., Ramyar, K., Vechio, J. D. and Cleveland, D. W. (1996). A complex of NuMA and cytoplasmic dynein is essential for mitotic spindle assembly. *Cell,* 87(3), pp. 447-58.

Meunier, S. and Vernos, I. (2012). Microtubule assembly during mitosis - from distinct origins to distinct functions?. *J Cell Sci,* 125(Pt 12), pp. 2805-14.

Mikami, A., Tynan, S. H., Hama, T., Luby-Phelps, K., Saito, T., Crandall, J. E., Besharse, J. C. and Vallee, R. B. (2002). Molecular structure of cytoplasmic dynein 2 and its distribution in neuronal and ciliated cells. *J Cell Sci,* 115(Pt 24), pp. 4801-8.

Mikeladze-Dvali, T., von Tobel, L., Strnad, P., Knott, G., Leonhardt, H., Schermelleh, L. and Gonczy, P. (2012). Analysis of centriole elimination during C. elegans oogenesis. *Development,* 139(9), pp. 1670-9.

Milunovic-Jevtic, A., Mooney, P., Sulerud, T., Bisht, J. and Gatlin, J. C. (2016). Centrosomal clustering contributes to chromosomal instability and cancer. *Curr Opin Biotechnol,* 40, pp. 113-8.

Mitchison, T. J., Maddox, P., Gaetz, J., Groen, A., Shirasu, M., Desai, A., Salmon, E. D. and Kapoor, T. M. (2005). Roles of polymerization dynamics, opposed motors, and a tensile element in governing the length of Xenopus extract meiotic spindles. *Mol Biol Cell,* 16(6), pp. 3064-76.

Mittal, K., Choi, D. H., Klimov, S., Pawar, S., Kaur, R., Mitra, A. K., Gupta, M. V., Sams, R., Cantuaria, G., Rida, P. C. and Aneja, R. (2016). A centrosome clustering protein, KIFC1, predicts aggressive disease course in serous ovarian adenocarcinomas. *J Ovarian Res,* 9, pp. 17.

Miwa, M. and Masutani, M. (2007). PolyADP-ribosylation and cancer. *Cancer Sci,* 98(10), pp. 1528-35.

Moniz, L., Dutt, P., Haider, N. and Stambolic, V. (2011). Nek family of kinases in cell cycle, checkpoint control and cancer. *Cell Div,* 6, pp. 18.

Moniz, L. S. and Stambolic, V. (2011). Nek10 mediates G2/M cell cycle arrest and MEK autoactivation in response to UV irradiation. *Mol Cell Biol,* 31(1), pp. 30-42.

Moore, J. K., Stuchell-Brereton, M. D. and Cooper, J. A. (2009). Function of dynein in budding yeast: mitotic spindle positioning in a polarized cell. *Cell Motil Cytoskeleton,* 66(8), pp. 546-55.

Morimoto, R. I. (2008). Proteotoxic stress and inducible chaperone networks in neurodegenerative disease and aging. *Genes Dev,* 22(11), pp. 1427-38.

Morris, N. R. (1975). Mitotic mutants of Aspergillus nidulans. *Genet Res,* 26(3), pp. 237-54.

Morrison, D. K. (2009). The 14-3-3 proteins: integrators of diverse signaling cues that impact cell fate and cancer development. *Trends Cell Biol,* 19(1), pp. 16-23.

Mountain, V., Simerly, C., Howard, L., Ando, A., Schatten, G. and Compton, D. A. (1999). The kinesin-related protein, HSET, opposes the activity of Eg5 and cross-links microtubules in the mammalian mitotic spindle. *J Cell Biol,* 147(2), pp. 351-66.

Mullighan, C. G. (2012). Molecular genetics of B-precursor acute lymphoblastic leukemia. *J Clin Invest,* 122(10), pp. 3407-15.

Murata, T., Tanahashi, T., Nishiyama, T., Yamaguchi, K. and Hasebe, M. (2007). How do Plants Organize Microtubules Without a Centrosome?. Journal of Integrative Plant Biology, 49: 1154–1163. doi:10.1111/j.1672-9072.2007.00545.x

Musacchio, A. (2015). The Molecular Biology of Spindle Assembly Checkpoint Signaling Dynamics. *Curr Biol,* 25(20), pp. R1002-18.

Musacchio, A. and Salmon, E. D. (2007). The spindle-assembly checkpoint in space and time. *Nat Rev Mol Cell Biol,* 8(5), pp. 379-93.

Mykytyn, K., Mullins, R. F., Andrews, M., Chiang, A. P., Swiderski, R. E., Yang, B., Braun, T., Casavant, T., Stone, E. M. and Sheffield, V. C. (2004). Bardet-Biedl syndrome type 4 (BBS4)-null mice implicate Bbs4 in flagella formation but not global cilia assembly. *Proc Natl Acad Sci U S A,* 101(23), pp. 8664-9.

Na, Y., Kaul, S. C., Ryu, J., Lee, J. S., Ahn, H. M., Kaul, Z., Kalra, R. S., Li, L., Widodo, N., Yun, C. O. and Wadhwa, R. (2016). Stress chaperone mortalin contributes to epithelial-mesenchymal transition and cancer metastasis. *Cancer Res*.

Nadeau, K., Nadler, S. G., Saulnier, M., Tepper, M. A. and Walsh, C. T. (1994). Quantitation of the interaction of the immunosuppressant deoxyspergualin and analogs with Hsc70 and Hsp90. *Biochemistry,* 33(9), pp. 2561-7.

Nakamura, F., Stossel, T. P. and Hartwig, J. H. (2011). The filamins: organizers of cell structure and function. *Cell Adh Migr,* 5(2), pp. 160-9.

Nassirpour, R., Shao, L., Flanagan, P., Abrams, T., Jallal, B., Smeal, T. and Yin, M. J. (2010). Nek6 mediates human cancer cell transformation and is a potential cancer therapeutic target. *Mol Cancer Res,* 8(5), pp. 717-28.

Neben, K., Giesecke, C., Schweizer, S., Ho, A. D. and Kramer, A. (2003). Centrosome aberrations in acute myeloid leukemia are correlated with cytogenetic risk profile. *Blood,* 101(1), pp. 289-91.

Neben, K., Tews, B., Wrobel, G., Hahn, M., Kokocinski, F., Giesecke, C., Krause, U., Ho, A. D., Kramer, A. and Lichter, P. (2004). Gene expression patterns in acute myeloid leukemia correlate with centrosome aberrations and numerical chromosome changes. *Oncogene,* 23(13), pp. 2379-84.

Neckers, L. and Workman, P. (2012). Hsp90 molecular chaperone inhibitors: are we there yet?. *Clin Cancer Res,* 18(1), pp. 64-76.

Newell-Litwa, K. A., Horwitz, R. and Lamers, M. L. (2015). Non-muscle myosin II in disease: mechanisms and therapeutic opportunities. *Dis Model Mech,* 8(12), pp. 1495-515.

Nguyen, C. L., McLaughlin-Drubin, M. E. and Munger, K. (2008). Delocalisation of the microtubule motor Dynein from mitotic spindles by the human papillomavirus E7 oncoprotein is not sufficient for induction of multipolar mitoses. *Cancer Res,* 68(21), pp. 8715-22.

Nigg, E. A. (2001). Mitotic kinases as regulators of cell division and its checkpoints. *Nat Rev Mol Cell Biol.* 2(1), pp. 21-32.

Nigg, E. A. (2002). Centrosome aberrations: cause or consequence of cancer progression?. *Nat Rev Cancer,* 2(11), pp. 815-25.

Nigg, E. A. (2006). Origins and consequences of centrosome aberrations in human cancers. *Int J Cancer,* 119(12), pp. 2717-23.

Nigg, E. A. and Raff, J. W. (2009). Centrioles, centrosomes, and cilia in health and disease. *Cell,* 139(4), pp. 663-78.

Nigg, E. A. and Stearns, T. (2011). The centrosome cycle: Centriole biogenesis, duplication and inherent asymmetries. *Nat Cell Biol,* 13(10), pp. 1154-60.

Niikura, Y., Ohta, S., Vandenbeldt, K. J., Abdulle, R., McEwen, B. F. and Kitagawa, K. (2006). 17-AAG, an Hsp90 inhibitor, causes kinetochore defects: a novel

mechanism by which 17-AAG inhibits cell proliferation. *Oncogene,* 25(30), pp. 4133-46.

Nishio, S., Tian, X., Gallagher, A. R., Yu, Z., Patel, V., Igarashi, P. and Somlo, S. (2010). Loss of oriented cell division does not initiate cyst formation. *J Am Soc Nephrol,* 21(2), pp. 295-302.

Noguchi, K., Fukazawa, H., Murakami, Y. and Uehara, Y. (2002). Nek11, a new member of the NIMA family of kinases, involved in DNA replication and genotoxic stress responses. *J Biol Chem,* 277(42), pp. 39655-65.

Nonaka, S., Tanaka, Y., Okada, Y., Takeda, S., Harada, A., Kanai, Y., Kido, M. and Hirokawa, N. (1998). Randomization of left-right asymmetry due to loss of nodal cilia generating leftward flow of extraembryonic fluid in mice lacking KIF3B motor protein. *Cell,* 95(6), pp. 829-37.

Nowell, P. C. and Hungerford, D. A. (1960). Chromosome studies on normal and leukemic human leukocytes. *J Natl Cancer Inst,* 25, pp. 85-109.

Nurse, P. (2000). A long twentieth century of the cell cycle and beyond. *Cell,* 100(1), pp. 71-8.

O'Connell, M. J., Krien, M. J. and Hunter, T. (2003). Never say never. The NIMA-related protein kinases in mitotic control. *Trends Cell Biol,* 13(5), pp. 221-8.

O'Regan, L., Blot, J. and Fry, A. M. (2007). Mitotic regulation by NIMA-related kinases. *Cell Div,* 2, pp. 25.

O'Regan, L. and Fry, A. M. (2009). The Nek6 and Nek7 protein kinases are required for robust mitotic spindle formation and cytokinesis. *Mol Cell Biol,* 29(14), pp. 3975-90.

O'Regan, L., Sampson, J. and Fry, A. M. (2015a). Hsp70 proteins in mitosis and disease. *Oncotarget: Vol. 32*. United States, pp. 32293-4.

O'Regan, L., Sampson, J., Richards, M. W., Knebel, A., Roth, D., Hood, F. E., Straube, A., Royle, S. J., Bayliss, R. and Fry, A. M. (2015b). Hsp72 is targeted to the mitotic spindle by Nek6 to promote K-fiber assembly and mitotic progression. *J Cell Biol,* 209(3), pp. 349-58.

Oakley, B. R. and Morris, N. R. (1983). A mutation in Aspergillus nidulans that blocks the transition from interphase to prophase. *J Cell Biol,* 96(4), pp. 1155-8.

Ogden, A., Cheng, A., Rida, P. C., Pannu, V., Osan, R., Clewley, R. and Aneja, R. (2014). Quantitative multi-parametric evaluation of centrosome declustering drugs: centrosome amplification, mitotic phenotype, cell cycle and death. *Cell Death Dis,* 5, pp. e1204.

Ogden, A., Rida, P. C. and Aneja, R. (2012). Let's huddle to prevent a muddle: centrosome declustering as an attractive anticancer strategy. *Cell Death Differ,* 19(8), pp. 1255-67.

Ogden, A., Rida, P. C. and Aneja, R. (2013). Heading off with the herd: how cancer cells might maneuver supernumerary centrosomes for directional migration. *Cancer Metastasis Rev,* 32(1-2), pp. 269-87.

Osmani, A. H., McGuire, S. L. and Osmani, S. A. (1991a). Parallel activation of the NIMA and p34cdc2 cell cycle-regulated protein kinases is required to initiate mitosis in A. nidulans. *Cell,* 67(2), pp. 283-91.

Osmani, A. H., O'Donnell, K., Pu, R. T. and Osmani, S. A. (1991b). Activation of the nimA protein kinase plays a unique role during mitosis that cannot be bypassed by absence of the bimE checkpoint. *Embo j,* 10(9), pp. 2669-79.

Osmani, S. A., Pu, R. T. and Morris, N. R. (1988). Mitotic induction and maintenance by overexpression of a G2-specific gene that encodes a potential protein kinase. *Cell,* 53(2), pp. 237-44.

Osmani, S. A. and Ye, X. S. (1996). Cell cycle regulation in Aspergillus by two protein kinases. *Biochem J,* 317 (Pt 3), pp. 633-41.

Otto, E. A., Trapp, M. L., Schultheiss, U. T., Helou, J., Quarmby, L. M. and Hildebrandt, F. (2008). NEK8 mutations affect ciliary and centrosomal localisation and may cause nephronophthisis. *J Am Soc Nephrol,* 19(3), pp. 587-92.

Ou, G., Stuurman, N., D'Ambrosio, M. and Vale, R. D. (2010). Polarized myosin produces unequal-size daughters during asymmetric cell division. *Science,* 330(6004), pp. 677-80.

Ouyang, X., Wang, X., Xu, K., Jin, D. Y., Cheung, A. L., Tsao, S. W. and Wong, Y. C. (2001). Effect of p53 on centrosome amplification in prostate cancer cells. *Biochim Biophys Acta,* 1541(3), pp. 212-20.

Paintrand, M., Moudjou, M., Delacroix, H. and Bornens, M. (1992). Centrosome organization and centriole architecture: their sensitivity to divalent cations. *J Struct Biol,* 108(2), pp. 107-28.

Palmer, K. J., Hughes, H. and Stephens, D. J. (2009). Specificity of cytoplasmic dynein subunits in discrete membrane-trafficking steps. *Mol Biol Cell,* 20(12), pp. 2885-99.

Panda, D., Rathinasamy, K., Santra, M. K. and Wilson, L. (2005). Kinetic suppression of microtubule dynamic instability by griseofulvin: implications for its possible use in the treatment of cancer. *Proc Natl Acad Sci U S A,* 102(28), pp. 9878-83.

Pannu, V., Rida, P. C., Celik, B., Turaga, R. C., Ogden, A., Cantuaria, G., Gopalakrishnan, J. and Aneja, R. (2014). Centrosome-declustering drugs mediate a two-pronged attack on interphase and mitosis in supercentrosomal cancer cells. *Cell Death Dis,* 5, pp. e1538.

Pannu, V., Rida, P. C., Ogden, A., Clewley, R., Cheng, A., Karna, P., Lopus, M., Mishra, R. C., Zhou, J. and Aneja, R. (2012). Induction of robust de novo centrosome amplification, high-grade spindle multipolarity and metaphase catastrophe: a novel chemotherapeutic approach. *Cell Death Dis,* 3, pp. e346.

Pannu, V., Rida, P. C., Ogden, A., Turaga, R. C., Donthamsetty, S., Bowen, N. J., Rudd, K., Gupta, M. V., Reid, M. D., Cantuaria, G., Walczak, C. E. and Aneja, R. (2015). HSET overexpression fuels tumor progression via centrosome clustering-independent mechanisms in breast cancer patients. *Oncotarget,* 6(8), pp. 6076-91.

Patel, H. and Gordon, M. Y. (2009). Abnormal centrosome-centriole cycle in chronic myeloid leukaemia?. *Br J Haematol,* 146(4), pp. 408-17.

Patury, S., Miyata, Y. and Gestwicki, J. E. (2009). Pharmacological targeting of the Hsp70 chaperone. *Curr Top Med Chem,* 9(15), pp. 1337-51.

Peckham, M. (2016). How myosin organization of the actin cytoskeleton contributes to the cancer phenotype. *Biochem Soc Trans,* 44(4), pp. 1026-34.

Peeper, D. S., van der Eb, A. J. and Zantema, A. (1994). The G1/S cell-cycle checkpoint in eukaryotic cells. *Biochim Biophys Acta,* 1198(2-3), pp. 215-30.

Pelegrini, A. L., Moura, D. J., Brenner, B. L., Ledur, P. F., Maques, G. P., Henriques, J. A., Saffi, J. and Lenz, G. (2010). Nek1 silencing slows down DNA repair and blocks DNA damage-induced cell cycle arrest. *Mutagenesis,* 25(5), pp. 447-54.

Pelletier L, O'Toole E, Schwager A, Hyman AA, Muller-Reichert T. (2006). Centriole assembly in Caenorhabditis elegans. *Nature*. 444(7119):619-23.

Pelletier, L. and Yamashita, Y. M. (2012). Centrosome asymmetry and inheritance during animal development. *Curr Opin Cell Biol,* 24(4), pp. 541-6.

Perucca-Lostanlen, D., Rostagno, P., Grosgeorge, J., Marcie, S., Gaudray, P. and Turc-Carel, C. (2004). Distinct MDM2 and P14ARF expression and centrosome amplification in well-differentiated liposarcomas. *Genes Chromosomes Cancer,* 39(2), pp. 99-109.

Peset, I. and Vernos, I. (2008a). The TACC proteins: TACC-ling microtubule dynamics and centrosome function. *Trends Cell Biol,* 18(8), pp. 379-88.

Piel, M., Meyer, P., Khodjakov, A., Rieder, C. L. and Bornens, M. (2000). The Respective Contributions of the Mother and Daughter Centrioles to Centrosome Activity and Behavior in Vertebrate Cells. *J Cell Biol: Vol. 2*, pp. 317-30.

Pihan, G. A., Purohit, A., Wallace, J., Knecht, H., Woda, B., Quesenberry, P. and Doxsey, S. J. (1998). Centrosome defects and genetic instability in malignant tumors. *Cancer Res,* 58(17), pp. 3974-85.

Pihan, G. A., Purohit, A., Wallace, J., Malhotra, R., Liotta, L. and Doxsey, S. J. (2001). Centrosome defects can account for cellular and genetic changes that characterize prostate cancer progression. *Cancer Res,* 61(5), pp. 2212-9.

Powers, E. T., Morimoto, R. I., Dillin, A., Kelly, J. W. and Balch, W. E. (2009). Biological and chemical approaches to diseases of proteostasis deficiency. *Annu Rev Biochem,* 78, pp. 959-91.

Powers, M. V., Clarke, P. A. and Workman, P. (2008). Dual targeting of HSC70 and HSP72 inhibits HSP90 function and induces tumor-specific apoptosis. *Cancer Cell,* 14(3), pp. 250-62.

Powers, M. V., Jones, K., Barillari, C., Westwood, I., van Montfort, R. L. and Workman, P. (2010). Targeting HSP70: the second potentially druggable heat shock protein and molecular chaperone?. *Cell Cycle,* 9(8), pp. 1542-50.

Prigent, C., Glover, D. M. and Giet, R. (2005). Drosophila Nek2 protein kinase knockdown leads to centrosome maturation defects while overexpression causes centrosome fragmentation and cytokinesis failure. *Exp Cell Res,* 303(1), pp. 1-13.

Prosser, S. L., O'Regan, L. and Fry, A. M. (2016). Novel insights into the mechanisms of mitotic spindle assembly by NEK kinases. *Mol Cell Oncol,* 3(3), pp. e1062952.

Prosser, S. L., Samant, M. D., Baxter, J. E., Morrison, C. G. and Fry, A. M. (2012). Oscillation of APC/C activity during cell cycle arrest promotes centrosome amplification. *J Cell Sci,* 125(Pt 22), pp. 5353-68.

Prosser, S. L., Straatman, K. R. and Fry, A. M. (2009). Molecular dissection of the centrosome overduplication pathway in S-phase-arrested cells. *Mol Cell Biol,* 29(7), pp. 1760-73.

Pu, R. T. and Osmani, S. A. (1995). Mitotic destruction of the cell cycle regulated NIMA protein kinase of Aspergillus nidulans is required for mitotic exit. *Embo j,* 14(5), pp. 995-1003.

Puklowski, A., Homsi, Y., Keller, D., May, M., Chauhan, S., Kossatz, U., Grunwald, V., Kubicka, S., Pich, A., Manns, M. P., Hoffmann, I., Gonczy, P. and Malek, N. P. (2011). The SCF-FBXW5 E3-ubiquitin ligase is regulated by PLK4 and targets HsSAS-6 to control centrosome duplication. *Nat Cell Biol,* 13(8), pp. 1004-9.

Quintyne, N. J., Reing, J. E., Hoffelder, D. R., Gollin, S. M. and Saunders, W. S. (2005). Spindle multipolarity is prevented by centrosomal clustering. *Science,* 307(5706), pp. 127-9.

Quintyne, N. J. and Schroer, T. A. (2002). Distinct cell cycle-dependent roles for dynactin and dynein at centrosomes. *J Cell Biol,* 159(2), pp. 245-54.

Raab, M. S., Breitkreutz, I., Anderhub, S., Ronnest, M. H., Leber, B., Larsen, T. O., Weiz, L., Konotop, G., Hayden, P. J., Podar, K., Fruehauf, J., Nissen, F., Mier, W., Haberkorn, U., Ho, A. D., Goldschmidt, H., Anderson, K. C., Clausen, M. H. and Kramer, A. (2012). GF-15, a novel inhibitor of centrosomal clustering, suppresses tumor cell growth in vitro and in vivo. *Cancer Res,* 72(20), pp. 5374-85.

Raaijmakers, J. A., Tanenbaum, M. E. and Medema, R. H. (2013). Systematic dissection of dynein regulators in mitosis. *J Cell Biol,* 201(2), pp. 201-15.

Rapley, J., Nicolas, M., Groen, A., Regue, L., Bertran, M. T., Caelles, C., Avruch, J. and Roig, J. (2008). The NIMA-family kinase Nek6 phosphorylates the kinesin Eg5 at a novel site necessary for mitotic spindle formation. *J Cell Sci,* 121(Pt 23), pp. 3912-21.

Rappaport, R. (1961). Experiments concerning the cleavage stimulus in sand dollar eggs. *J Exp Zool,* 148, pp. 81-9.

Rathinasamy, K., Jindal, B., Asthana, J., Singh, P., Balaji, P. V. and Panda, D. (2010). Griseofulvin stabilizes microtubule dynamics, activates p53 and inhibits the proliferation of MCF-7 cells synergistically with vinblastine. *BMC Cancer,* 10, pp. 213.

Rauch, A., Thiel, C.T., Schindler, D., Wick, U., Crow, Y.J., Ekici, A.B., et al. (2008). Mutations in the pericentrin (PCNT) gene cause primordial dwarfism. *Science*. 319(5864):816-9.

Rauch, A., Thiel CT, Schindler D, Wick U, Crow YJ, Ekici AB, et al. (2008). Mutations in the pericentrin (PCNT) gene cause primordial dwarfism. Science. 319(5864):816-9.

Rauch A, Thiel CT, Schindler D, Wick U, Crow YJ, Ekici AB, et al. Mutations in the pericentrin (PCNT) gene cause primordial dwarfism. Science. 2008;319(5864):816-9. Epub 2008/01/05. doi: 10.1126/science.1151174. PubMed PMID: 18174396.

Ray, S., Lu, Y., Kaufmann, S. H., Gustafson, W. C., Karp, J. E., Boldogh, I., Fields, A. P. and Brasier, A. R. (2004). Genomic mechanisms of p210BCR-ABL signaling: induction of heat shock protein 70 through the GATA response element confers resistance to paclitaxel-induced apoptosis. *J Biol Chem,* 279(34), pp. 35604-15.

Rebacz, B., Larsen, T. O., Clausen, M. H., Ronnest, M. H., Loffler, H., Ho, A. D. and Kramer, A. (2007). Identification of griseofulvin as an inhibitor of centrosomal clustering in a phenotype-based screen. *Cancer Res,* 67(13), pp. 6342-50.

Reiter, R., Gais, P., Steuer-Vogt, M. K., Boulesteix, A. L., Deutschle, T., Hampel, R., Wagenpfeil, S., Rauser, S., Walch, A., Bink, K., Jutting, U., Neff, F., Arnold, W., Hofler, H. and Pickhard, A. (2009). Centrosome abnormalities in head and neck squamous cell carcinoma (HNSCC). *Acta Otolaryngol,* 129(2), pp. 205-13.

Richards, M. W., O'Regan, L., Mas-Droux, C., Blot, J. M., Cheung, J., Hoelder, S., Fry, A. M. and Bayliss, R. (2009). An autoinhibitory tyrosine motif in the cell-cycle-regulated Nek7 kinase is released through binding of Nek9. *Mol Cell,* 36(4), pp. 560-70.

Riley, R. R., Duensing, S., Brake, T., Munger, K., Lambert, P. F. and Arbeit, J. M. (2003). Dissection of human papillomavirus E6 and E7 function in transgenic mouse models of cervical carcinogenesis. *Cancer Res,* 63(16), pp. 4862-71.

Ring, D., Hubble, R. and Kirschner, M. (1982). Mitosis in a cell with multiple centrioles. *J Cell Biol,* 94(3), pp. 549-56.

Ritossa F. (1962). A new puffing pattern induced by temperature shock and DNP in drosophila. Experientia 18: 571–573. doi: 10.1007/bf02172188

Roberts, A. J., Kon, T., Knight, P. J., Sutoh, K. and Burgess, S. A. (2013). Functions and mechanics of dynein motor proteins. *Nat Rev Mol Cell Biol,* 14(11), pp. 713-26.

Rogers, G. C., Rusan, N. M., Roberts, D. M., Peifer, M. and Rogers, S. L. (2009). The SCF Slimb ubiquitin ligase regulates Plk4/Sak levels to block centriole reduplication. *J Cell Biol,* 184(2), pp. 225-39.

Rohde, M., Daugaard, M., Jensen, M. H., Helin, K., Nylandsted, J. and Jaattela, M. (2005). Members of the heat-shock protein 70 family promote cancer cell growth by distinct mechanisms. *Genes Dev,* 19(5), pp. 570-82.

Roig, J., Groen, A., Caldwell, J. and Avruch, J. (2005). Active Nercc1 protein kinase concentrates at centrosomes early in mitosis and is necessary for proper spindle assembly. *Mol Biol Cell,* 16(10), pp. 4827-40.

Roig, J., Mikhailov, A., Belham, C. and Avruch, J. (2002). Nercc1, a mammalian NIMA-family kinase, binds the Ran GTPase and regulates mitotic progression. *Genes Dev,* 16(13), pp. 1640-58.

Rowley, J. D. (2001). Chromosome translocations: dangerous liaisons revisited. *Nat Rev Cancer,* 1(3), pp. 245-50.

Ruchaud, S., Carmena, M. and Earnshaw, W. C. (2007). Chromosomal passengers: conducting cell division. *Nat Rev Mol Cell Biol,* 8(10), pp. 798-812.

Sabir, S. R., Sahota, N. K., Jones, G. D. and Fry, A. M. (2015). Loss of Nek11 Prevents G2/M Arrest and Promotes Cell Death in HCT116 Colorectal Cancer Cells Exposed to Therapeutic DNA Damaging Agents. *PLoS One,* 10(10), pp. e0140975.

Sahota, N.K. (2010). Cell cycle studies on the human Nek3, Nek5 and Nek11 protein kinases. Unpublished PhD thesis ed. University of Leicester.

Salic, A., Waters, J. C. and Mitchison, T. J. (2004). Vertebrate shugoshin links sister centromere cohesion and kinetochore microtubule stability in mitosis. *Cell,* 118(5), pp. 567-78.

Samuel, J., Jayne, S., Chen, Y., Majid, A., Wignall, A., Wormull, T., Najeeb, H., Luo, J. L., Jones, G. D., Macip, S. and Dyer, M. J. (2016). Posttranscriptional Upregulation of p53 by Reactive Oxygen Species in Chronic Lymphocytic Leukemia. *Cancer Res,* 76(21), pp. 6311-6319.

Sampson, J., and Fry, A. (2016). Monitoring centrosome clustering in cancer cells. In: Dawe H, editor. The centriole: methods and protocols. Volume in press, Methods in Molecular Biology. Spinger; 2016

Santarosa, M., Favaro, D., Quaia, M. and Galligioni, E. (1997). Expression of heat shock protein 72 in renal cell carcinoma: possible role and prognostic implications in cancer patients. *Eur J Cancer,* 33(6), pp. 873-7.

Sato, N., Mizumoto, K., Nakamura, M., Nakamura, K., Kusumoto, M., Niiyama, H., Ogawa, T. and Tanaka, M. (1999). Centrosome abnormalities in pancreatic ductal carcinoma. *Clin Cancer Res,* 5(5), pp. 963-70.

Saurin, A. T., Durgan, J., Cameron, A. J., Faisal, A., Marber, M. S. and Parker, P. J. (2008). The regulated assembly of a PKCepsilon complex controls the completion of cytokinesis. *Nat Cell Biol,* 10(8), pp. 891-901.

Sawada, M., Sun, W., Hayes, P., Leskov, K., Boothman, D. A. and Matsuyama, S. (2003). Ku70 suppresses the apoptotic translocation of Bax to mitochondria. *Nat Cell Biol,* 5(4), pp. 320-9.

Sawin, K. E. and Mitchison, T. J. (1995). Mutations in the kinesin-like protein Eg5 disrupting localisation to the mitotic spindle. *Proc Natl Acad Sci U S A,* 92(10), pp. 4289-93.

Schafer, K. A. (1998). The cell cycle: a review. *Vet Pathol,* 35(6), pp. 461-78.

Schlecht, R., Scholz, S. R., Dahmen, H., Wegener, A., Sirrenberg, C., Musil, D., Bomke, J., Eggenweiler, H. M., Mayer, M. P. and Bukau, B. (2013). Functional analysis of Hsp70 inhibitors. *PLoS One,* 8(11), pp. e78443.

Schmidt, T. I., Kleylein-Sohn, J., Westendorf, J., Le Clech, M., Lavoie, S. B., Stierhof, Y. D. and Nigg, E. A. (2009). Control of centriole length by CPAP and CP110. *Curr Biol,* 19(12), pp. 1005-11.

Schmitt, E., Maingret, L., Puig, P. E., Rerole, A. L., Ghiringhelli, F., Hammann, A., Solary, E., Kroemer, G. and Garrido, C. (2006). Heat shock protein 70 neutralization exerts potent antitumor effects in animal models of colon cancer and melanoma. *Cancer Res,* 66(8), pp. 4191-7.

Schockel, L., Mockel, M., Mayer, B., Boos, D. and Stemmann, O. (2011). Cleavage of cohesin rings coordinates the separation of centrioles and chromatids. *Nat Cell Biol,* 13(8), pp. 966-72.

Schopf, F. H., Biebl, M. M. and Buchner, J. (2017). The HSP90 chaperone machinery. *Nat Rev Mol Cell Biol,* 18(6), pp. 345-360.

Schroer, T. A. (2004). Dynactin. *Annu Rev Cell Dev Biol,* 20, pp. 759-79.

Schultz, S. J., Fry, A. M., Sutterlin, C., Ried, T. and Nigg, E. A. (1994). Cell cycle-dependent expression of Nek2, a novel human protein kinase related to the NIMA mitotic regulator of Aspergillus nidulans. *Cell Growth Differ,* 5(6), pp. 625-35.

Schultz, S. J. and Nigg, E. A. (1993). Identification of 21 novel human protein kinases, including 3 members of a family related to the cell cycle regulator nimA of Aspergillus nidulans. *Cell Growth Differ,* 4(10), pp. 821-30.

Schvartzman, J. M., Sotillo, R. and Benezra, R. (2010). Mitotic chromosomal instability and cancer: mouse modelling of the human disease. *Nat Rev Cancer,* 10(2), pp. 102-15.

Sdelci, S., Bertran, M. T. and Roig, J. (2011). Nek9, Nek6, Nek7 and the separation of centrosomes. *Cell Cycle: Vol. 22*. United States, pp. 3816-7.

Shah, J. V. and Cleveland, D. W. (2000). Waiting for anaphase: Mad2 and the spindle assembly checkpoint. *Cell,* 103(7), pp. 997-1000.

Shaheen, R., Al Tala, S., Almoisheer, A. and Alkuraya, F. S. (2014). Mutation in PLK4, encoding a master regulator of centriole formation, defines a novel locus for primordial dwarfism. *J Med Genet,* 51(12), pp. 814-6.

Shalom, O., Shalva, N., Altschuler, Y. and Motro, B. (2008). The mammalian Nek1 kinase is involved in primary cilium formation. *FEBS Lett,* 582(10), pp. 1465-70.

Signor, D., Wedaman, K. P., Orozco, J. T., Dwyer, N. D., Bargmann, C. I., Rose, L. S. and Scholey, J. M. (1999). Role of a class DHC1b dynein in retrograde

transport of IFT motors and IFT raft particles along cilia, but not dendrites, in chemosensory neurons of living Caenorhabditis elegans. *J Cell Biol,* 147(3), pp. 519-30.

Simizu, S. and Osada, H. (2000). Mutations in the Plk gene lead to instability of Plk protein in human tumour cell lines. *Nat Cell Biol,* 2(11), pp. 852-4.

Singla, V., Romaguera-Ros, M., Garcia-Verdugo, J. M. and Reiter, J. F. (2010). Ofd1, a human disease gene, regulates the length and distal structure of centrioles. *Dev Cell,* 18(3), pp. 410-24.

Sir, J. H., Putz, M., Daly, O., Morrison, C. G., Dunning, M., Kilmartin, J. V. and Gergely, F. (2013). Loss of centrioles causes chromosomal instability in vertebrate somatic cells. *J Cell Biol,* 203(5), pp. 747-56.

Sjoblom, B., Salmazo, A. and Djinovic-Carugo, K. (2008). Alpha-actinin structure and regulation. *Cell Mol Life Sci,* 65(17), pp. 2688-701.

Sjoblom, T., Jones, S., Wood, L. D., Parsons, D. W., Lin, J., Barber, T. D., Mandelker, D., Leary, R. J., Ptak, J., Silliman, N., Szabo, S., Buckhaults, P., Farrell, C., Meeh, P., Markowitz, S. D., Willis, J., Dawson, D., Willson, J. K., Gazdar, A. F., Hartigan, J., Wu, L., Liu, C., Parmigiani, G., Park, B. H., Bachman, K. E., Papadopoulos, N., Vogelstein, B., Kinzler, K. W. and Velculescu, V. E. (2006). The consensus coding sequences of human breast and colorectal cancers. *Science,* 314(5797), pp. 268-74.

Sliutz, G., Karlseder, J., Tempfer, C., Orel, L., Holzer, G. and Simon, M. M. (1996). Drug resistance against gemcitabine and topotecan mediated by constitutive hsp70 overexpression in vitro: implication of quercetin as sensitiser in chemotherapy. *Br J Cancer,* 74(2), pp. 172-7.

Smith, L. A., Bukanov, N. O., Husson, H., Russo, R. J., Barry, T. C., Taylor, A. L., Beier, D. R. and Ibraghimov-Beskrovnaya, O. (2006). Development of polycystic kidney disease in juvenile cystic kidney mice: insights into pathogenesis, ciliary abnormalities, and common features with human disease. *J Am Soc Nephrol,* 17(10), pp. 2821-31.

Sohara, E., Luo, Y., Zhang, J., Manning, D. K., Beier, D. R. and Zhou, J. (2008). Nek8 regulates the expression and localisation of polycystin-1 and polycystin-2. *J Am Soc Nephrol,* 19(3), pp. 469-76.

Sommi, P., Cheerambathur, D., Brust-Mascher, I. and Mogilner, A. (2011). Actomyosin-dependent cortical dynamics contributes to the prophase force-balance in the early Drosophila embryo. *PLoS One,* 6(3), pp. e18366.

Sonnen, K. F., Gabryjonczyk, A. M., Anselm, E., Stierhof, Y. D. and Nigg, E. A. (2013). Human Cep192 and Cep152 cooperate in Plk4 recruitment and centriole duplication. *J Cell Sci,* 126(Pt 14), pp. 3223-33.

Sonnen, K. F., Schermelleh, L., Leonhardt, H. and Nigg, E. A. (2012). 3D-structured illumination microscopy provides novel insight into architecture of human centrosomes. *Biol Open,* 1(10), pp. 965-76.

Sreedhar, A. S., Kalmar, E., Csermely, P. and Shen, Y. F. (2004). Hsp90 isoforms: functions, expression and clinical importance. *FEBS Lett,* 562(1-3), pp. 11-5.

Starita, L. M., Machida, Y., Sankaran, S., Elias, J. E., Griffin, K., Schlegel, B. P., Gygi, S. P. and Parvin, J. D. (2004). BRCA1-dependent ubiquitination of gamma-tubulin regulates centrosome number. *Mol Cell Biol,* 24(19), pp. 8457-66.

Stephens, P. J., Greenman, C. D., Fu, B., Yang, F., Bignell, G. R., Mudie, L. J., Pleasance, E. D., Lau, K. W., Beare, D., Stebbings, L. A., McLaren, S., Lin, M. L., McBride, D. J., Varela, I., Nik-Zainal, S., Leroy, C., Jia, M., Menzies, A., Butler, A. P., Teague, J. W., Quail, M. A., Burton, J., Swerdlow, H., Carter, N. P., Morsberger, L. A., Iacobuzio-Donahue, C., Follows, G. A., Green, A. R., Flanagan, A. M., Stratton, M. R., Futreal, P. A. and Campbell, P. J. (2011). Massive genomic rearrangement acquired in a single catastrophic event during cancer development. *Cell,* 144(1), pp. 27-40.

Sun, Z., Amsterdam, A., Pazour, G. J., Cole, D. G., Miller, M. S. and Hopkins, N. (2004). A genetic screen in zebrafish identifies cilia genes as a principal cause of cystic kidney. *Development,* 131(16), pp. 4085-93.

Taipale, M., Jarosz, D. F. and Lindquist, S. (2010). HSP90 at the hub of protein homeostasis: emerging mechanistic insights. *Nat Rev Mol Cell Biol,* 11(7), pp. 515-28.

Takaoka, M., Saito, H., Takenaka, K., Miki, Y. and Nakanishi, A. (2014). BRCA2 phosphorylated by PLK1 moves to the midbody to regulate cytokinesis mediated by nonmuscle myosin IIC. *Cancer Res,* 74(5), pp. 1518-28.

Tanaka, K. and Nigg, E. A. (1999). Cloning and characterization of the murine Nek3 protein kinase, a novel member of the NIMA family of putative cell cycle regulators. *J Biol Chem,* 274(19), pp. 13491-7.

Tetsu, O. and McCormick, F. (2003). Proliferation of cancer cells despite CDK2 inhibition. *Cancer Cell,* 3(3), pp. 233-45.

Thakur, H. C., Singh, M., Nagel-Steger, L., Prumbaum, D., Fansa, E. K., Gremer, L., Ezzahoini, H., Abts, A., Schmitt, L., Raunser, S., Ahmadian, M. R. and Piekorz, R. P. (2013). Role of centrosomal adaptor proteins of the TACC family in the regulation of microtubule dynamics during mitotic cell division. *Biol Chem,* 394(11), pp. 1411-23.

Thery, M., Racine, V., Pepin, A., Piel, M., Chen, Y., Sibarita, J. B. and Bornens, M. (2005). The extracellular matrix guides the orientation of the cell division axis. *Nat Cell Biol: Vol. 10*. England, pp. 947-53.

Thiel, C., Kessler, K., Giessl, A., Dimmler, A., Shalev, S. A., von der Haar, S., Zenker, M., Zahnleiter, D., Stoss, H., Beinder, E., Abou Jamra, R., Ekici, A. B., Schroder-Kress, N., Aigner, T., Kirchner, T., Reis, A., Brandstatter, J. H. and Rauch, A. (2011). NEK1 mutations cause short-rib polydactyly syndrome type majewski. *Am J Hum Genet,* 88(1), pp. 106-14.

Thornton, G. K. and Woods, C. G. (2009). Primary microcephaly: do all roads lead to Rome?. *Trends Genet,* 25(11), pp. 501-10.

Tissieres, A., Mitchell, H. K. and Tracy, U. M. (1974). Protein synthesis in salivary glands of Drosophila melanogaster: relation to chromosome puffs. *J Mol Biol,* 84(3), pp. 389-98.

Tollenaere, M. A., Mailand, N. and Bekker-Jensen, S. (2015). Centriolar satellites: key mediators of centrosome functions. *Cell Mol Life Sci,* 72(1), pp. 11-23.

Tong, W. M., Yang, Y. G., Cao, W. H., Galendo, D., Frappart, L., Shen, Y. and Wang, Z. Q. (2007). Poly(ADP-ribose) polymerase-1 plays a role in suppressing mammary tumourigenesis in mice. *Oncogene,* 26(26), pp. 3857-67.

Toriello, H. V. and Parisi, M. A. (2009). Cilia and the ciliopathies: an introduction. *Am J Med Genet C Semin Med Genet,* 151c(4), pp. 261-2.

Tsang, W. Y., Spektor, A., Luciano, D. J., Indjeian, V. B., Chen, Z., Salisbury, J. L., Sanchez, I. and Dynlacht, B. D. (2006). CP110 cooperates with two calcium-binding proteins to regulate cytokinesis and genome stability. *Mol Biol Cell,* 17(8), pp. 3423-34.

Tsou, M. F. and Stearns, T. (2006). Mechanism limiting centrosome duplication to once per cell cycle. *Nature,* 442(7105), pp. 947-51.

Turturici, G., Sconzo, G. and Geraci, F. (2011). Hsp70 and its molecular role in nervous system diseases. *Biochem Res Int,* 2011, pp. 618127.

Uehara, R., Nozawa, R. S., Tomioka, A., Petry, S., Vale, R. D., Obuse, C. and Goshima, G. (2009). The augmin complex plays a critical role in spindle microtubule generation for mitotic progression and cytokinesis in human cells. *Proc Natl Acad Sci U S A,* 106(17), pp. 6998-7003.

van der Vaart, B., Manatschal, C., Grigoriev, I., Olieric, V., Gouveia, S. M., Bjelic, S., Demmers, J., Vorobjev, I., Hoogenraad, C. C., Steinmetz, M. O. and Akhmanova, A. (2011). SLAIN2 links microtubule plus end-tracking proteins and controls microtubule growth in interphase. *J Cell Biol,* 193(6), pp. 1083-99.

Vasiliev, J. M., Omelchenko, T., Gelfand, I. M., Feder, H. H. and Bonder, E. M. (2004). Rho overexpression leads to mitosis-associated detachment of cells from epithelial sheets: a link to the mechanism of cancer dissemination. *Proc Natl Acad Sci U S A,* 101(34), pp. 12526-30.

Vaz Meirelles, G., Ferreira Lanza, D. C., da Silva, J. C., Santana Bernachi, J., Paes Leme, A. F. and Kobarg, J. (2010). Characterization of hNek6 interactome reveals an important role for its short N-terminal domain and colocalisation with proteins at the centrosome. *J Proteome Res,* 9(12), pp. 6298-316.

Ventura, R. A., Martin-Subero, J. I., Knippschild, U., Gascoyne, R. D., Delsol, G., Mason, D. Y. and Siebert, R. (2004). Centrosome abnormalities in ALK-positive anaplastic large-cell lymphoma. *Leukemia: Vol. 11*. England, pp. 1910-1.

Vitre, B. D. and Cleveland, D. W. (2012). Centrosomes, chromosome instability (CIN) and aneuploidy. *Curr Opin Cell Biol,* 24(6), pp. 809-15.

Voss, A. K., Thomas, T. and Gruss, P. (2000). Mice lacking HSP90beta fail to develop a placental labyrinth. *Development,* 127(1), pp. 1-11.

Walczak, C. E., Cai, S., & Khodjakov, A. (2010). Mechanisms of chromosome behaviour during mitosis. *Nature Reviews. Molecular Cell Biology*, *11*(2), 91–102.

Wang, W., Eddy, R. and Condeelis, J. (2007). The cofilin pathway in breast cancer invasion and metastasis. *Nat Rev Cancer,* 7(6), pp. 429-40.

Wang, W. J., Soni, R. K., Uryu, K. and Tsou, M. F. (2011). The conversion of centrioles to centrosomes: essential coupling of duplication with segregation. *J Cell Biol,* 193(4), pp. 727-39.

Watts, C. A., Richards, F. M., Bender, A., Bond, P. J., Korb, O., Kern, O., Riddick, M., Owen, P., Myers, R. M., Raff, J., Gergely, F., Jodrell, D. I. and Ley, S. V. (2013). Design, synthesis, and biological evaluation of an allosteric inhibitor of HSET that targets cancer cells with supernumerary centrosomes. *Chem Biol,* 20(11), pp. 1399-410.

Wei, R. R., Al-Bassam, J. and Harrison, S. C. (2007). The Ndc80/HEC1 complex is a contact point for kinetochore-microtubule attachment. *Nat Struct Mol Biol,* 14(1), pp. 54-9.

White, M. C. and Quarmby, L. M. (2008). The NIMA-family kinase, Nek1 affects the stability of centrosomes and ciliogenesis. *BMC Cell Biol,* 9, pp. 29.

Whitesell, L. and Lindquist, S. (2009). Inhibiting the transcription factor HSF1 as an anticancer strategy', *Expert Opin Ther Targets,* 13(4), pp. 469-78.

Whitesell, L. and Lindquist, S. L. (2005). HSP90 and the chaperoning of cancer. *Nat Rev Cancer,* 5(10), pp. 761-72.

Wigley, W. C., Fabunmi, R. P., Lee, M. G., Marino, C. R., Muallem, S., DeMartino, G. N. and Thomas, P. J. (1999). Dynamic association of proteasomal machinery with the centrosome. *J Cell Biol,* 145(3), pp. 481-90.

Wilkie, G. S. and Davis, I. (2001). Drosophila wingless and pair-rule transcripts localise apically by dynein-mediated transport of RNA particles. *Cell,* 105(2), pp. 209-19.

Williams, D. R., Ko, S. K., Park, S., Lee, M. R. and Shin, I. (2008). An apoptosis-inducing small molecule that binds to heat shock protein 70. *Angew Chem Int Ed Engl,* 47(39), pp. 7466-9.

Williamson, D. S., Borgognoni, J., Clay, A., Daniels, Z., Dokurno, P., Drysdale, M. J., Foloppe, N., Francis, G. L., Graham, C. J., Howes, R., Macias, A. T., Murray, J. B., Parsons, R., Shaw, T., Surgenor, A. E., Terry, L., Wang, Y., Wood, M. and Massey, A. J. (2009). Novel adenosine-derived inhibitors of 70 kDa heat shock protein, discovered through structure-based design. *J Med Chem,* 52(6), pp. 1510-3.

Wojcik, E., Basto, R., Serr, M., Scaerou, F., Karess, R. and Hays, T. (2001). Kinetochore dynein: its dynamics and role in the transport of the Rough deal checkpoint protein. *Nat Cell Biol,* 3(11), pp. 1001-7.

Wong, Y. L., Anzola, J. V., Davis, R. L., Yoon, M., Motamedi, A., Kroll, A., … Oegema, K. (2015). Reversible centriole depletion with an inhibitor of Polo-like kinase 4. *Science (New York, N.Y.)*, *348*(6239), 1155–1160.

Woodruff, J. B., Ferreira Gomes, B., Widlund, P. O., Mahamid, J., Honigmann, A. and Hyman, A. A. (2017). The Centrosome Is a Selective Condensate that Nucleates Microtubules by Concentrating Tubulin. *Cell,* 169(6), pp. 1066-1077.e10.

Woodruff, J. B., Wueseke, O. and Hyman, A. A. (2014). Pericentriolar material structure and dynamics. *Philos Trans R Soc Lond B Biol Sci,* 369(1650).

Woodruff, J. B., Wueseke, O., Viscardi, V., Mahamid, J., Ochoa, S. D., Bunkenborg, J., Widlund, P. O., Pozniakovsky, A., Zanin, E., Bahmanyar, S., Zinke, A., Hong, S. H., Decker, M., Baumeister, W., Andersen, J. S., Oegema, K. and Hyman, A. A. (2015). Centrosomes. Regulated assembly of a supramolecular centrosome scaffold in vitro. *Science,* 348(6236), pp. 808-12.

Workman, P., Burrows, F., Neckers, L. and Rosen, N. (2007). Drugging the cancer chaperone HSP90: combinatorial therapeutic exploitation of oncogene addiction and tumor stress. *Ann N Y Acad Sci,* 1113, pp. 202-16.

Wu, J., Mikule, K., Wang, W., Su, N., Petteruti, P., Gharahdaghi, F., Code, E., Zhu, X., Jacques, K., Lai, Z., Yang, B., Lamb, M. L., Chuaqui, C., Keen, N. and Chen, H. (2013). Discovery and mechanistic study of a small molecule inhibitor for motor protein KIFC1. *ACS Chem Biol,* 8(10), pp. 2201-8.

Yamamoto, Y., Matsuyama, H., Furuya, T., Oga, A., Yoshihiro, S., Okuda, M., Kawauchi, S., Sasaki, K. and Naito, K. (2004). Centrosome hyperamplification predicts progression and tumor recurrence in bladder cancer. *Clin Cancer Res,* 10(19), pp. 6449-55.

Yang, J., Adamian, M. and Li, T. (2006). Rootletin interacts with C-Nap1 and may function as a physical linker between the pair of centrioles/basal bodies in cells. *Mol Biol Cell,* 17(2), pp. 1033-40.

Yang, Z., Loncarek, J., Khodjakov, A. and Rieder, C. L. (2008). Extra centrosomes and/or chromosomes prolong mitosis in human cells. *Nat Cell Biol,* 10(6), pp. 748-51.

Yang, Z., Tulu, U. S., Wadsworth, P. and Rieder, C. L. (2007). Kinetochore dynein is required for chromosome motion and congression independent of the spindle checkpoint. *Curr Biol,* 17(11), pp. 973-80.

Yeh, T. Y., Quintyne, N. J., Scipioni, B. R., Eckley, D. M. and Schroer, T. A. (2012). Dynactin's pointed-end complex is a cargo-targeting module. *Mol Biol Cell,* 23(19), pp. 3827-37.

Yin, M. J., Shao, L., Voehringer, D., Smeal, T. and Jallal, B. (2003). The serine/threonine kinase Nek6 is required for cell cycle progression through mitosis. *J Biol Chem,* 278(52), pp. 52454-60.

Yoshioka, K., Foletta, V., Bernard, O. and Itoh, K. (2003). A role for LIM kinase in cancer invasion. *Proc Natl Acad Sci U S A,* 100(12), pp. 7247-52.

Young, J. C., Agashe, V. R., Siegers, K. and Hartl, F. U. (2004). Pathways of chaperone-mediated protein folding in the cytosol. *Nat Rev Mol Cell Biol,* 5(10), pp. 781-91.

Yue, L., Karr, T. L., Nathan, D. F., Swift, H., Srinivasan, S. and Lindquist, S. (1999). Genetic analysis of viable Hsp90 alleles reveals a critical role in Drosophila spermatogenesis. *Genetics,* 151(3), pp. 1065-79.

Zalli, D., Bayliss, R. and Fry, A. M. (2012). The Nek8 protein kinase, mutated in the human cystic kidney disease nephronophthisis, is both activated and degraded during ciliogenesis. *Hum Mol Genet,* 21(5), pp. 1155-71.

Zhang, J., Wang, L., Zhuang, L., Huo, L., Musa, S., Li, S. and Xiang, X. (2008). Arp11 affects dynein-dynactin interaction and is essential for dynein function in Aspergillus nidulans. *Traffic,* 9(7), pp. 1073-87.

Zhou, H., Kuang, J., Zhong, L., Kuo, W. L., Gray, J. W., Sahin, A., Brinkley, B. R. and Sen, S. (1998). Tumour amplified kinase STK15/BTAK induces centrosome amplification, aneuploidy and transformation. *Nat Genet,* 20(2), pp. 189-93.

Zimmermann, M., Nickl, S., Lambers, C., Hacker, S., Mitterbauer, A., Hoetzenecker, K., Rozsas, A., Ostoros, G., Laszlo, V., Hofbauer, H., Renyi-Vamos, F., Klepetko, W., Dome, B. and Ankersmit, H. J. (2012). Discrimination of clinical stages in non-small cell lung cancer patients by serum HSP27 and HSP70: a multi-institutional case-control study. *Clin Chim Acta,* 413(13-14), pp. 1115-20.

Zitouni, S., Nabais, C., Jana, S. C., Guerrero, A. and Bettencourt-Dias, M. (2014). Polo-like kinases: structural variations lead to multiple functions. *Nat Rev Mol Cell Biol,* 15(7), pp. 433-52.